ABSTRACT

Marcoita T. Gilbert. CHANGES IN ZEBRA FINCH CENTRAL NERVOUS SYSTEM MORPHOLOGY ASSOCIATED WITH DEVELOPMENTAL CANNABINOID EXPOSURE. (Under the supervision of Dr. Ken Soderstrom) Interdisciplinary Doctoral Program in Biological Sciences, Brody School of Medicine, East Carolina University, October 2012.

Adolescent CNS development is a highly organized, coordinated process that is both genetically and environmentally influenced, and is characterized by a period of dynamic, activity-dependent changes in synaptic connectivity. Growing evidence suggests that adolescent cannabis use is a risk factor for the development of persistent alterations in brain function. Taeniopygia guttata, the zebra finch, was used as a model of cannabinoid-altered vocal learning. We explored effects of cannabinoid-altered signaling during normal late-postnatal CNS development, as well as lasting morphological changes following exogenous cannabinoid exposure. In these studies, the cannabinoid agonist WIN 55,212-2 was administered to developing male zebra finches during sensorimotor song learning and dendritic spine densities measured following Golgi-Cox impregnation. Within HVC, a region necessary for songbird vocal production, and Area X, a striatal region essential for song learning, dendritic spines were inappropriately elevated by an average of 25% following developmental cannabinoid treatment. Treatments of adults that had already learned song were not associated with spine density changes. Cannabinoid-altered song and neuronal morphology were correlated with changes in levels of proteins related to cell signaling and morphology, including axonal Nf-200 and dendritic MAP2. After sensorimotor

developmental cannabinoid treatment, anti-Nf-200 and -MAP2 antibodies were used to immunohistochemically confirm Golgi-Cox staining results. In the same brain areas where dendritic spines were elevated following CB agonist treatment, Nf-200 and MAP2 immunoreactivity (ir) were also elevated. To investigate mechanisms of cannabinoid-induced changes in neuronal morphology, we measured expression of the cytoskeletal protein Arc in NCM. A single exposure to novel song increased the postsynaptic densities of Arc protein. Two exposures to song were sufficient to produce habituation of this response. Habituation was prevented by pretreatment with WIN. These findings suggest there is a persistent, developmentally-restricted condition during periadolescence, and that cannabinoid agonism interferes with sensory integration and encoding necessary for accurate formation of memories.

CHANGES IN ZEBRA FINCH CENTRAL NERVOUS SYSTEM MORPHOLOGY ASSOCIATED WITH DEVELOPMENTAL CANNABINOID EXPOSURE

A Dissertation

Presented To

The Faculty Associated with the Interdisciplinary Doctoral Program in Biological Sciences

The Brody School of Medicine at East Carolina University

In Partial Fulfillment

of the Requirements for the Degree

Doctor of Philosophy in Interdisciplinary Biological Sciences

By

Marcoita Terreen Gilbert

October 2012

CHANGES IN ZEBRA FINCH CENTRAL NERVOUS SYSTEM MORPHOLOGY FOLLOWING DEVELOPMENTAL CANNABINOID EXPOSURE

by

Marcoita Terreen Gilbert

APPROVED BY:

DIRECTOR OF DISSERTATION:_____

Ken Soderstrom, Ph.D.

COMMITTEE MEMBER:_____

Rukiyah Van Dross-Anderson, Ph.D.

COMMITTEE MEMBER:_____

Kori L. Brewer, Ph.D.

COMMITTEE MEMBER:_____

Mona M. McConnaughey, Ph.D.

COMMITTEE MEMBER:_____

Brian A. McMillen, Ph. D.

DIRECTOR OF IDPBS:_____

Terry L. West, Ph.D.

DEAN OF THE GRADUATE SCHOOL:_____

Paul J. Gemperline, Ph.D.

ACKNOWLEDGEMENTS

Psalms 25.

Isaiah 54:17.

TABLE OF CONTENTS

LIST OF TABLES

LIST OF FIGURES

Figure 3.5. Photomicrographs of Nf-200 staining within caudal song regions of adult male zebra finch telencephalon following 25 days of treatment with either vehicle or WIN (1 mg/kg), using DAB immunohistochemistry.

Figure 3.6. DAB-immunohistochemical staining of Nf-200 protein within rostral song regions lMAN and Area X of adult male zebra finch telencephalon following 25 consecutive days of vehicle treatment or treatment with WIN (1 mg/kg).

Figure 3.7. Representative low and high-power micrographs of Nf-200 staining of adult male zebra finch midbrain thalamic regions Ov and DLM using DAB immunohistochemistry. Animals were subjected to either 25 consecutive treatments with vehicle or WIN (1 mg/kg) after song learning had occurred.

Figure 3.8. Representative images of DAB-immunohistochemical staining of Nf-200 protein within the cerebellum of adult male zebra finches treated with either vehicle or WIN (1 mg/kg) after song learning.

Figure 3.9. Photomicrographs of dendritically associated MAP2 staining within caudal song regions of adult male zebra finch telencephalon following developmental treatment with either vehicle or WIN (1 mg/kg) using DAB immunohistochemistry.

Figure 3.10. DAB-immunohistochemical staining of MAP2 protein within rostral song regions lMAN and Area X of adult male zebra finch telencephalon following developmental vehicle treatment or treatment with WIN (1 mg/kg).

Figure AD1. Electrophoretic analysis of PCR products generated in an effort to clone ZFN1.

LIST OF ABBREVIATIONS

(PC)-AEA	o-phosphorylcholine
^{3}H	Tritium
Amp	Ampicillin
AMPA	2-amino-3-(3-hydroxy-5-methyl-isoxazol-4-yl)propanoic acid
Area X	*Proper name*
BLAST	Basic Local Alignment Search Tool
B_{max}	Maximum saturation
BSA	Bovine Serum Albumin
Bsd	Blasticidin
CB	Cannabinoid
cDNA	Complimentary DNA
CHO	Chinese Hamster Ovary
CI	Confidence interval
Ci	Curie

CIAP	Calf Intestinal Alkaline Phosphatase
CMV	Cytomegalovirus
CNS	Central nervous system
COX-2	Cyclooxygenase-2
CYP450	Cytochrome P450
DEPC	Diethylpyrocarbonate
DLM	Dorsolateral nucleus of medial hypothalamus
DMEM	Dulbecco’s Modified Eagle Medium
DMSO	Dimethyl Sulfoxide
DNA	Deoxyribonucleic acid
DNase	Deoxyribonuclease
dNTP	Deoxyribonucleotide Triphosphate
E. Coli	Escherichia coli
EcoRI	E. coli restriction enzyme 1

EDTA	Ethylenediaminetetraacetic Acid
EtOH	Ethanol
F12-K	F12 Kaighns
FAAH	Fatty acid amide hydrolase
FBS	Fetal bovine serum
FITC	Fluorescein Isothiocyanate
GABA	γ-aminobutyric acid
GF/C	Glass Microfiber Filter type C
GPCR	G-protein coupled receptor
GPR55	G-protein coupled receptor 55
HEK	Human epithileal kidney
HI	Heat-inactivated
HindIII	Haemophilus influenza deoxyribonuclease III
HIV	Human Immunodeficiency Virus

HSP70	Heat-shock protein 70
HVC	*Proper name*
IM	Intramuscular
K_d	Dissociation constant
kDa	Kilodalton
LB broth	Luria-Bertani Broth
lMAN	Lateral magnocellular nucleus of the anterior neostriatum
LOX	lipoxygenase
MAG-L	Monoacylglycerol lipase
$MgCl_2$	Magnesium chloride
NaOAc	Sodium acetate
NAPE	N-acyl phosphatydilethanolamine
NMDA	N-methyl-D-aspartic acid
OEA	N-oleoyl ethanolamine

ORF	Open reading frame
Ov	Nucleus Ovoidalis
P/S	Penicilin-Streptomycin Solution, 100X
PC12	Pheochromocytoma line 12
PCR	Polymerase chain reaction
PGH2	Prostoglandin H2
PGP	P-glycoprotein
PLD	Phospholipase D
PLL, PDL	Poly-L-Lysine, Poly-D-Lysine
PND	Postnatal day
QS	Quantity Sufficient
RA	Robust nucleus of the Arcopallium
RACE	Rapid Amplification of cDNA Ends
RNA	Ribonucleic acid

RNase	Ribonuclease
RPM	Revolutions per minute
RPMI	Roswell Park Memorial Institute
S.O.C medium	Super Optimal broth with Catabolite repression medium
TAG	Triacylglicerol
Taq	Thermus aquaticus
Tris	hydoxymethylaminomethane
TRPV1	Transient receptor potential vanilloid 1
V_d	Volume of distribution
VEH	Vehicle
Vent	Deep-vent polymerase
WIN	WIN 55,212-2
X-Gal	5-bromo-4-chloro-indolyl-β-D-galactopyranoside
Δ^9-THC	Δ^9-Tetrahydrocannabinol

CHAPTER 1: INTRODUCTION

The History of Cannabis Usage

Trends in Marijuana Consumption: Before 1800

Cannabis Indica, Cannabis Sativa, Cannabis Americanus, Indian hemp and marihuana are names that all refer to the same plant: marijuana. While its sharp rise in popularity and usage has occurred over the past couple of decades, marijuana has been known since antiquity, and used as a medicinal and recreational agent since ancient times. Some of the first recorded medicinal uses of marijuana occurred around 3000 B.C., with the Chinese emperor Shen Nung prescribing *Cannabis* tea and seedling preparations for the treatment of malaria, rheumatism, gout, female reproductive issues, intestinal constipation, and even poor memory (Russo, 2007). As a result, these practices were recorded in the world's oldest pharmacopeia, the Pen T's-aoChing, which was compiled in the first century of this era (Lambert, 2001; Zuardi, 2006). At the turn of the first millennium (A.D. 110 – 207), preparations of marijuana compounds mixed with wine were frequently used as an anesthetic during surgical operations (Li, 1973). Evidence suggests that in ancient India, marijuana was widely used as a medicine and as an agent for achieving euphoria as well. It is speculated that within this society, the medical and recreational use of marijuana began around 1000 B.C. (Touw, 1981). In many regions, cannabis usage maintained a close association with religious rituals, which often assigned sacred virtues to the plant. For example, the Atharvaveda, a sacred text of Hinduism, mentions cannabis as one of five sacred plants used as a "source of happiness, donator of joy, and bringer of freedom" (Mikuriya, 1969). In Assyria (1000 B.C) and Persia (650 B.C), many also knew about the

psychoactive effects of marijuana, and the plant was burned as a medicinal incense for analgesia, and used as a hypnotic tranquilizer (Mikuriya, 1969). However, in the 12th and 13th centuries, ancient Arabs documented very cruel but unsuccessful attempts made by the local authorities to suppress recreational consumption (Walton, 1938). For a more thorough review of this topic, please refer to (Fernberger, 1939).

Trends in Marijuana Consumption: 19th Century Pioneers

Before the 19th century, marijuana use was often described in both the literature and pharmacopeia as being a physical and mental health benefit; however, in the decades following, religious and medical views towards excessive consumption began to change. Investigation into the properties of marijuana began in this era, following a major trend in pharmacological research at the time that centered on the isolation of natural active compounds (Kogan and Mechoulam, 2007). In the 19th century, interest in use of cannabis as a therapeutic agent was intensified by the works of William Brooke O'Shaughnessy, a British pharmacologist working as a Professor of medicinal chemistry and Material Medica in Calcutta, India. He brought a large supply of cannabis over to England, and provided samples to physicians in the form of Squire's Extract, a concentrated alcoholic extract of Indian hemp. After testing several cannabis preparations on animals, he decided the compounds were safe, and beneficial for human medicinal use. As a result, in his published 1839 account of his experiments, he describes several successful attempts to treat general pain symptoms, rheumatism, and even muscular spasms resulting from rabies (Zuardi, 2006). In this publication, he perceptively alludes to the fact that "In the popular medicine of [other] nations, we find it extensively employed for a multitude of affections. But in Western Europe, its use either

as a stimulant or as a remedy is unequally unknown" (original documents reproduced by (Mikuriya, 1973). In 19th century France, however, cannabis was used with a very different purpose: as a psychoactive agent. Dissatisfied with the inability to locate a physiological cause for mental illnesses, early French psychiatrists such as Jacques Joseph Moreau eventually began to focus on gross and molecular brain function. As an assistant physician at the Charenton Asylum near Paris, one of his duties was to accompany patients to the Far East, in the then eclectic practice of "therapeutic travel". During these trips, he both observed and participated in hashish usage, and was able to experience effects first-hand. Upon returning to France, he proceeded to experiment with a slew of cannabis preparations on himself and his students, and published his findings in *Du Hachisch et de l'Alienation Mentale: Etudies Psychologiques*, (which was later translated in to English as *Hashish and Mental Illness*) known to be one of the most complete descriptions of the acute effects of cannabis ever written (Moreau, 1973; Nahas, 1984). In these writings, he proposed an organic basis of insanity; he theorized that since cannabis elicited some of the same psychoactive effects as what were observed in patients with mental illnesses, then psychopathy most likely stemmed from a persistent disruption of brain function that led to imbalance. As a result of his work, Moreau revolutionized Western European medicine by being one of the first to employ herbal pharmacology in the systematic treatment of mental illnesses (Abel, 2005).

Trends in Marijuana Consumption: The 20th Century and Beyond

As the years progressed into the early 20th century, interest in using marijuana as a medicine and euphoric agent began to decline, and, usage in the clinical setting rapidly came to a halt. Consequently, when cannabis was dropped from the British and

American Pharmacopeia in 1932 and 1941, respectively, its original illegalization was barely challenged (Kalant, 2001). This lack of enthusiasm occurred for many reasons, namely because the shelf-life of the plant was very short and unpredictable. In addition, caregivers faced the predicament that since cannabis was a natural raw product, different samples of the many species of cannabis varied widely in both efficacy and potency. Due to the fact that these synthesized preparations (used in the form of tinctures or extracts whose power was dependent on origin, age, and method of preparation) almost always contained different proportions of flower, stem, plant and seed, it was virtually impossible to achieve medicinal/psychoactive effects that were replicable (Kalant, 1971). Furthermore, the introduction of the hypodermic needle, and faster acting, more water-soluble drugs (such as opioids) became more readily available, and replaced cannabis as an analgesic (Mikuriya, 1969). Narcotics such as chloral hydrate, paraldehyde, various barbiturates and synthetic drugs replaced cannabis as a sedative (Bennett, 1974; Zuardi, 2006). However, interest in marijuana piqued again in the 1930's, when scientific experiments were conducted in which isolated crude cannabinoid compounds (which contained cannabidiol and various tetrahydrocannabinoids) were shown to be solely responsible for the psychoactive effects experienced. Accordingly, this body of work is at the nexus of modern-day recreational cannabinoid use (Adams et al., 1941; Pertwee, 2006a).

In several ways, the insufficient amount of concrete knowledge available regarding cannabinoid effects on neurophysiology is the consequence of two main issues: 1) our inability to understand and isolate pure cannabinoid compounds until the mid-20th century, and 2) the long and complicated legal history of marijuana usage in

this country. In the early 1900's, an explosion of marijuana consumption occurred for hedonistic purposes in the United States. During this time, usage was mostly restricted to minorities, Mexican immigrant rural workers, musicians/artists, and individuals of a low socioeconomic status. The use of cannabis continued to spread in the United States in these populations, mostly in the southern and southwestern states until the late 1920's (Mikuriya, 1969). However, laws were passed in 27 states between 1915 and 1937 to discourage use (Musto, 1972). Many speculate these actions were largely based on hysteria engendered by law enforcement officials and other alarmist groups at the time, (many felt great hostility toward the individual populations that used it, and others feared that cannabis would be used as a substitute for other narcotics banned by the 1914 Harrison Tax Act) and medical ignorance (little was known about active constituents, and many believed that other addictive substances would lead to cannabis addiction), and as such, the events during this time period have resulted in a slow progression in the field of cannabinoid research (Grotenhermen, 2007; Hollister, 1969; Kaplan, 1969; Mikuriya, 1969; Mikuriya, 1973). As a finale to the growing state legislation trends, the Marijuana Tax Act of 1937 was passed in an effort to regulate marijuana.

Despite restrictive legislation, the use of marijuana among individuals, especially adolescents for recreational purposes has quickly spread throughout the U.S. over the past couple of decades. As stated previously, crude cannabis compounds were indeed isolated in the 1930's and 1940's, however the chemical structure of Δ^9-THC has only been known since 1964 (Gaoni and Mechoulam, 1964), and thus neither purification of natural compounds, nor production of synthetic compounds was possible (Figure 1.1).

In this country, the historical percentage of adolescents reported to have used cannabis at least once went from 5% in 1967, to 44%, 49%, 68%, and 64% in 1971, 1975, 1980, and 1982 respectively (Kandel, 1984; Lipton et al., 1979; Zuardi, 2006). This startling trend that still continues today, which has severely magnified its societal importance, has heightened the need to understand the chemical composition of drugs within this class, and the physiological and psychoactive effects conferred upon the central nervous system.

Adolescents and Cannabis Use

Illicit drug consumption among adolescents is steadily increasing, and reportedly, usage occurs the most frequently among individuals in their teens and early twenties than at any other age (Figure 1.2). This increase is mostly due to the rising popularity of marijuana and new synthetically derived cannabis-like substances. Monitoring the Future is an ongoing study that obtains data from 50,000 8^{th}, 10^{th}, and 12^{th} graders regarding illicit drug, alcohol and tobacco use. This research is conducted yearly by a series of National Institute on Drug Abuse (NIDA, a division of the National Institute of Health)-funded investigators. The following statistics are reported from this source. In addition, more details and supplemental information on this subject can be found at (available 1 October 2012) http://www.monitoringthefuture.org/, and http://www.drugabuse.gov/drugs-abuse/marijuana. In 2010, more than 29 million Americans (11.5%) aged 12 or older reported abusing marijuana within the past year; this is an enormous increase over rates reported each year from 2002-2008. Apparently, a consistent decline in marijuana use began in the mid-1990's and continued into the early 2000s, but since then, this downward trend has completely

Figure 1.1. The relationships between crude cannabis products and pure cannabinoids. Cpds = compounds; THC = Tetrahydrocannabinol [Adapted from (Kalant, 2001)].

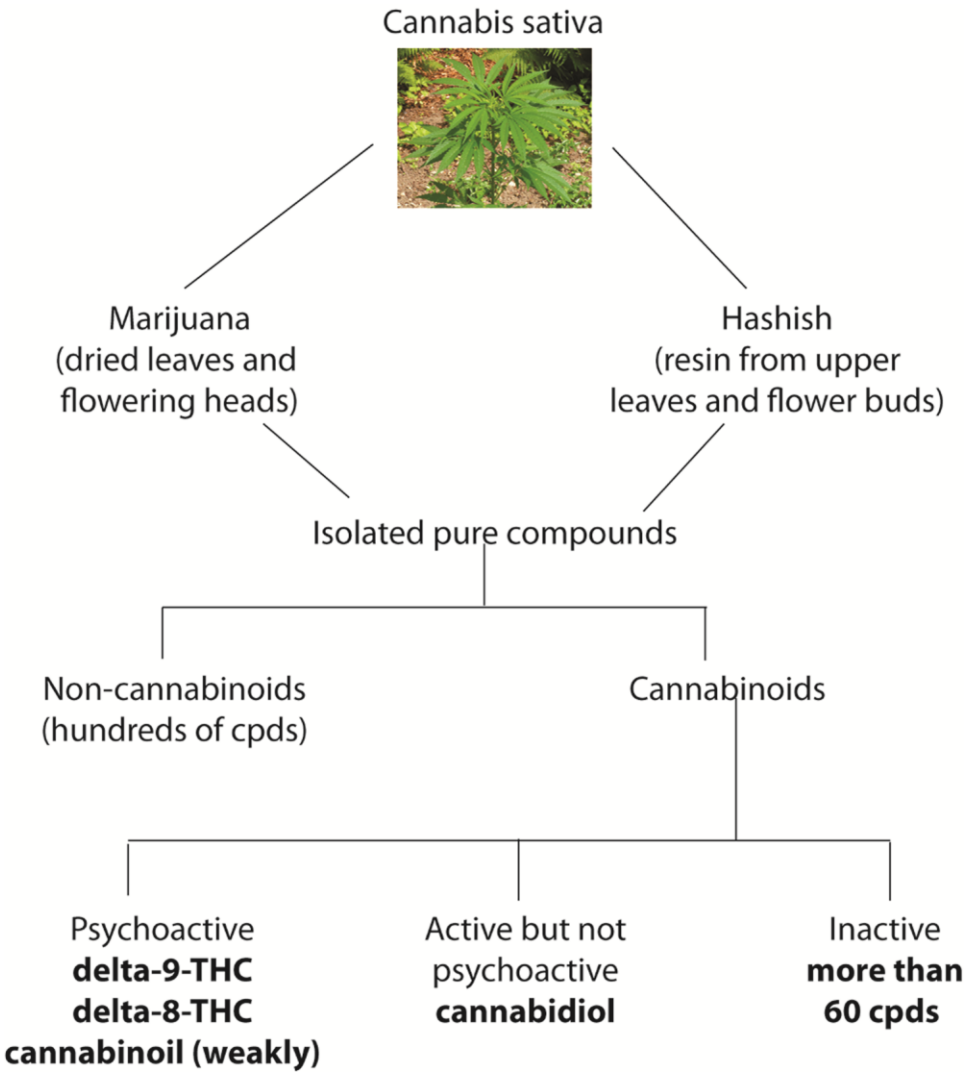
Cannabis sativa
Marijuana
(dried leaves and
flowering heads)
Hashish
(resin from upper
leaves and flower buds)
Isolated pure compounds
Non-cannabinoids
(hundreds of cpds)
Cannabinoids
Psychoactive
delta-9-THC
delta-8-THC
cannabinoil (weakly)
Active but not
psychoactive
cannabidiol
Inactive
more than
60 cpds

reversed itself. These results show a significant rise among older adolescents, (both 10th and 12th graders) in daily, current, and past-year marijuana use. In 2011, 7.2% of 8th graders, 17.6% of 10th graders, and 22.6% of 12th graders were reported to have used marijuana in the past month, compared to 5.7%, 14.2%, and 18.8% respectively, in 2007. Daily use in 12th graders also increased: 6.6% used marijuana at least once a day, compared to only 5% in the previous decade. This year (2012), 12.5% of 8th graders, 28.8% of 10th graders, and 36.4% of 12th graders reported past-year marijuana use (Figure 1.2).

Even though there were no significant increases between 2010 and 2011, it appears that using marijuana continues to far exceed cigarette use in adolescents—a quite surprising trend. In 2011, 22.6% (almost 1 in 4) of high school seniors were reported to have used marijuana in the past month compared with 18.7% who smoked cigarettes. In addition, for the first time, the 2012 study captured the use of synthetic marijuana among teenage groups, as these drugs have seen a spike in popularity over the past year. The results are startling: 11.4% (that is almost 1 in 9) of high school 12th graders reported using these agents in the past year (Johnston, 2012).

Why is this drug class so popular among adolescents and young adults? Superficially, these trends seem somewhat inexplicable, however upon closer inspection; the reasoning behind this is pretty straightforward. Historically speaking, as the perception of risks associated with using a particular drug goes down, the use of that drug goes up. The inverse of this statement is true as well: As perception of risks goes up, usage goes down. Adolescents are likely having less of an issue with

Figure 1.2.Drug use is highest among people in their late teens and twenties. In 2010, 23.1 percent of 18- to 20-year-olds reported using an illicit drug in the past month. [taken with permission from drugabuse.gov/drugs-abuse/marijuana]

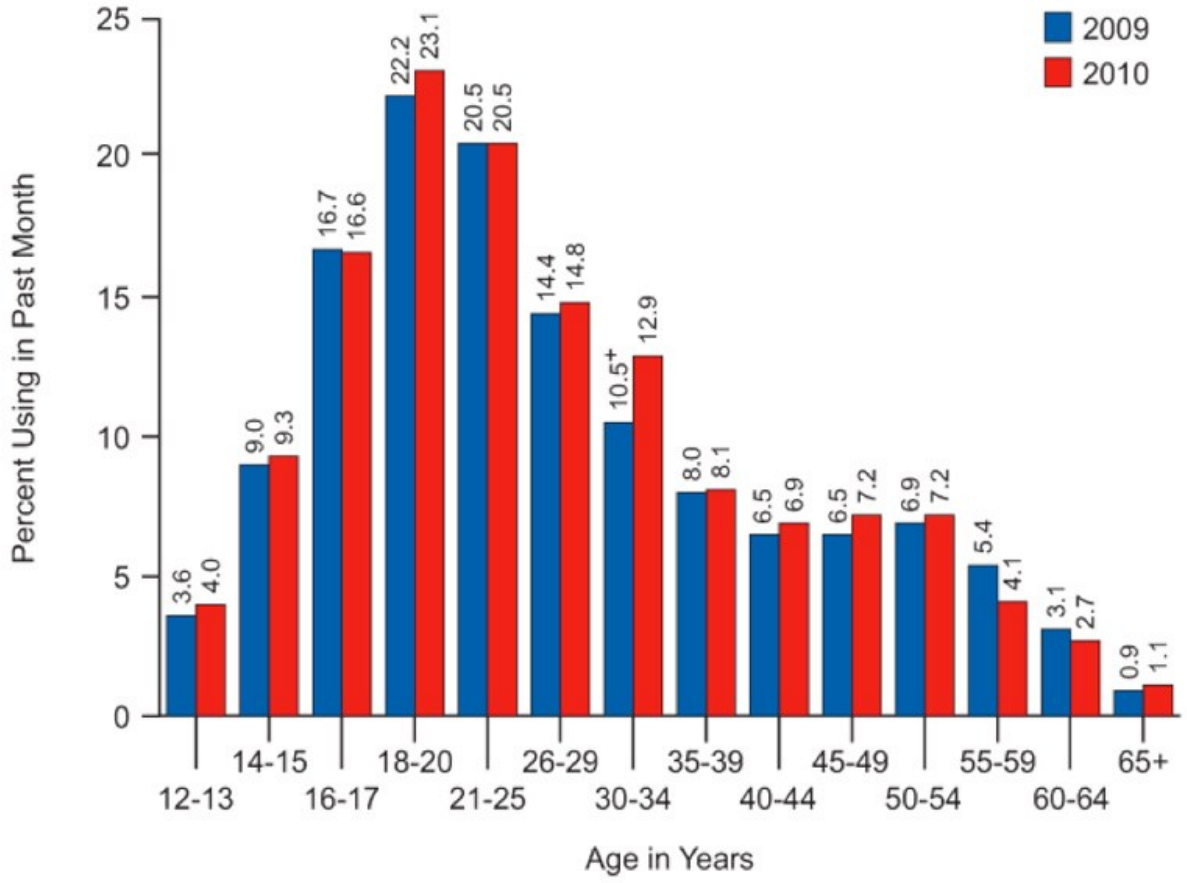
2009
2010
Percent Using in Past Month
25
20
15
10
5
0
3.6
4.0
9.0
9.3
16.7
16.6
22.2
23.1
20.5
20.5
14.4
14.8
10.5+
12.9
8.0
8.1
6.5
6.9
6.5
7.2
6.9
7.2
5.4
4.1
3.1
2.7
0.9
1.1
12-13
14-15
16-17
18-20
21-25
26-29
30-34
35-39
40-44
45-49
50-54
55-59
60-64
65+
Age in Years

marijuana use, and therefore a perception that the drug is less dangerous. This attitude likely reflects recent discussions and legislation involving cannabis use for medical reasons. Furthermore, many believe that because most cannabis products are naturally derived, they pose less of a health risk than those agents that are not produced in nature. In addition, users report that they have a greater availability of cannabis products, based on use among their friends within their social group (Ausems et al., 2003; Brown, 2005; Marroyo Gordo et al., 2012). Finally, cannabis is more attractive to teenagers because compared to other illicit substances; the legal ramifications of possession are less harsh.

What Are Cannabinoids?

Cannabinoids are traditionally known as a diverse class of structurally-related chemical constituents of cannabis that bind to the cannabinoid receptor. The system that these compounds belongs to is one of the most evolutionarily conserved in nature, and subsequently, an enormous variety of these agents exist within both plants and animals (Chang et al., 1993; Elphick, 2002; Elphick and Egertova, 2001a). In the last few years, a cohort of “non-cannabinoid” plant constituents have been shown to bind to and functionally activate cannabinoid receptors (Gertsch et al., 2010), however these results will not be reviewed in this text. Cannabinoids are traditionally divided into three main groups: these include phytocannabinoids (cannabinoids derived from plant sources), endocannabinoids (endogenously produced cannabinoids), and synthetically-derived cannabinoids.

Phytocannabinoids

According to Gertsch et al. phytocannabinoids are defined as those plant-derived natural products capable of either directly interacting with cannabinoid receptors, sharing chemical similarity with cannabinoids, or both. Phytocannabinoids have been identified in a large number of plant species, namely the well-characterized *Cannabis sativa, Cannabis indica, Echinacea purpurea, Echinacea pallida, Echinacea angustifolia*, and others (ElSohly, 2006; Woelkart et al., 2008). As a general rule, most phytocannabinoids are 21-carbon compounds, but are known to vary in the number of carbons in the side chain attached to the aromatic ring. So far over 85 different types of cannabinoids have been isolated from cannabis plants, and 25 identified in Echinacea plants. These phytocannabinoids are divided into nine distinct subclasses. One of these subclasses, Δ^9-THC- type (also referred to as THC in this text), is the principal psychoactive constituent of marijuana, and is thus one of the more well-known phytocannabinoids of this group (ElSohly, 2006; Hemphill et al., 1980; Iversen, 2003; Turner et al., 1973).

Δ^9-THC

The pharmacokinetics of THC involve different absorption rates through various routes of administration, and from different drug formulations (e.g. tablet vs. cigarette). As an aromatic terpenoid, THC has a very low solubility in aqueous solutions but is soluble in organic preparations, especially lipids and alcohols. Smoking is the principal route of THC administration, due to the fact that inhalation delivers the drug rapidly from the lungs to the brain, resulting in almost immediate CNS drug exposure. Recent studies have demonstrated that intravenous injection of THC results in only slightly

higher peak concentrations than what is achieved after smoking (Ohlsson et al., 1980). The bioavailability of THC following smoking varies widely (2% - 56%); due to differences in smoking methods, plasma concentrations vary from subject to subject. There have been fewer studies conducted on the oral absorption of THC compared to smoking; however this route is generally preferred for therapeutic applications, as most experts believe the advantages of THC inhalation are offset by the harmful effects of cannabis smoke. Accordingly, Marinol® (dronabinol) preparations are usually administered orally or rectally. Orally, THC is readily absorbed, due to its high alcohol/water *P* (partition coefficient, 9 X 10^6 (Harder and Rietbrock, 1997)) however absorption is slower than other routes when ingested, resulting in low, more delayed peak concentrations (bioavailability of ~20 %, (Grotenhermen, 2003; Law et al., 1984). Although THC is typically not abused through intravenous injection, pharmacologists often employ this technique in the lab. A study was conducted in which 0, 2.5 and 5 mg of THC was administered to healthy individuals with a history of cannabis use in the past. (Assuming these individuals weighed 70 kg, concentrations were 0, 0.35, and 0.7 mg/kg, respectively). After 10 minutes, plasma [THC] = 82 ± 87.4 and 119.2 ± 166.5 ng/ml for 0.35 and 0.7 mg/kg THC, respectively (D'Souza et al., 2004). THC is distributed rapidly into tissues after administration. Due to its high lipophilicity, THC is distributed and retained in fatty tissue as opposed to less-fatty tissue in a 64:1 ratio after about a month's exposure (Kreuz and Axelrod, 1973). In addition, THC is taken up by other organs that are highly perfused such as the liver, brain, heart, and lung. This substance is also known to rapidly distribute into the placenta and breast milk, and is greatest within these areas in early pregnancy (Atkinson et al., 1988; Perez-Reyes and

Wall, 1982). Surprisingly, even though THC is 95% – 99% protein bound in the blood (mostly to lipoproteins), V_d of THC is quite large, 101 L/kg (Huestis, 2007). Metabolism of THC has been known to occasionally occur in the intestines, however for the most part, it undergoes hepatic biotransformation. Phase I reactions include allylic and aliphatic hydroxylations at C (9) by CYP 450, leading to the metabolite 11-OH-THC, originally thought to be the true psychoactive constituent of cannabis, and oxidation of alcohols, β-oxidation, and degradation of the pentyl side-chain. Phase II reactions involving THC include glucuronidation, and sometimes sulfation (Huestis, 2007; Iribarne et al., 1996; Lemberger et al., 1970). Lastly, it has been demonstrated that within five days, almost all of THC is excreted out of the body as a hydroxylated metabolite. THC is mostly eliminated in the feces (65% of a total dose), followed by the urine (20%). Most of the glucuronic acid-conjugated metabolites are excreted through the urine, as the Phase II glucuronidation step increases their solubility in water. 11-OH-THC is primarily eliminated in the feces (Wall et al., 1983; Williams and Moffat, 1980).

Other Phytocannabinoids

THC is known as the most potent psychoactive phytocannabinoid from *Cannabis sativa*, but there are several other structurally related cannabinoids that interact with cannabinoid receptors. Cannabigerols (CBG), were the very first cannabinoids identified, cannabichromenes (CBC), are non-psychoactive C5 cannabinoid analogs, cannabidiols (CBD), are psychoactive agents which constitute the most abundant cannabinoid found in hemp, representing about 40% of its extracts, Δ^8-THC- type, exist as the more thermodynamically stable, 20% less active artifacts of Δ^9-THC, and cannabicyclols (CBL), are heat-generated artifacts of CBC. Other subclasses include

cannabielsoins (CBE), which are byproducts formed from CBD, and cannabinols (CBN), mildly psychoactive substances synthesized by degradation (oxidation) of Δ^8- or Δ^9-THC, and of which concentrations in cannabis vary widely with age and storage conditions. Lastly, there are cannabitroils (CBT), which have no known pharmacological characteristics at this time (ElSohly, 2006; Hemphill et al., 1980; Turner et al., 1973).

Endocannabinoids

After researchers determined that the human body actually possessed receptors that selectively bind cannabinoids, they soon realized that the presence of these receptors could only be explained by the presence of endogenous ligands that were key to its use. Hence, they soon discovered that mammalian tissues were able to both synthesize endogenous agonists, and release them retroactively onto various receptors (Devane et al., 1992; Mechoulam et al., 1995; Sugiura et al., 1995). Endogenous cannabinoids, or "Endocannabinoids", are the terms for these polyunsaturated fatty acids which are synthesized and released in response to rises in intracellular calcium (Basavarajappa, 2007; Maccarrone and Finazzi-Agro, 2002). Endocannabinoids are derivatives of arachidonic acid and conjugated with ethanolamine or glycerol, which closely resemble other lipid-based neuromodulators (eicosanoids, such as leukotirenes and prostaglandins, (Rodriguez de Fonseca et al., 2005). Produced on demand from components of the phospholipid bilayer, these lipid messengers rapidly influence cellular dynamics in response to both the subtlest and most robust changes in physiology. Endocannabinoids play neuromodulatory roles in a number of physiological processes, but most notably, these lipids appear to be critically involved in the maintenance of homeostasis and physiological stress recovery (Pagotto et al., 2006). It

is important to note that endocannabinoids are extremely labile and undergo almost instant cellular hydrolysis after production (Murphy et al., 2012), thus much of the information gathered about these substances has been obtained from enzyme inhibitor studies. At the present time, five endocannabinoids have been isolated and characterized, and all five have been found in the brain, plasma, and peripheral tissues.

AEA

In 1992, the amide of arachadonic acid and ethanolamine was identified in porcine brain, and named anandamide (AEA, or arachidonylethanolamide, (Devane et al., 1992)). Although the chemical structure of AEA is different from other cannabinoids (namely THC), it has been shown to possess very similar pharmacological properties (Romero et al., 1995; Smith et al., 1994). AEA is widely distributed throughout the brain, with levels varying by a factor of 4-6 within different regions, with the lowest amounts in the cerebellum and cortex, and the highest levels in the striatum and brainstem (Basavarajappa, 2007). It has become increasingly clear that the relative abundance of AEA in the brain does not correlate with the distribution of cannabinoid receptors, and therefore may serve a purpose within the CNS apart from the cannabinoid system (Basavarajappa, 2007). Unlike classic peptide and transmitter ligands, AEA is not stored in intracellular compartments or vesicles, but is synthesized almost instantaneously, and released from neurons immediately afterwards. AEA is formed by cleavage of its phospholipid precursor NAPE, by the action of PLD (phospholipase D). To review the synthesis of AEA, please refer to Figure 1.3. Once AEA is formed, it can either exert effects on the same cell from which it was produced, or diffuse backwards through the extracellular fluid to reach targets with the help of lipocalins and/or albumin (Piomelli,

2003). Generally speaking, two mechanisms are present within our organ systems that aid to eliminate AEA signal; uptake and enzymatic degradation. Uptake of AEA is accomplished by the actions of the following intracellular transport proteins: fatty acid binding protein 5/7, HSP 70, albumin, and FAAH-like AEA transporter protein (Fowler, 2012). The most common method of AEA degradation within the cell is via hydrolysis by FAAH, but alternative processes do exist. In addition to being hydrolyzed, AEA is readily metabolized by COX-2, LOX, and CYP450, and in the absence of FAAH, is converted to (PC)-AEA in the CNS (Basavarajappa, 2007).

2-AG

Soon after the discovery of AEA, scientists isolated a second arachidonic acid derivative that functions as an endocannabinoid, 2-arachidonoylglycerol (2-AG, (Mechoulam et al., 1995). In contrast to being a product of membrane phospholipid cleavage like AEA, 2-AG, a monoacylglycerol, is a metabolic intermediate in lipid metabolism. In the brain, the distribution of the two endocannabinoids is similar, however the concentration of 2-AG is 200 fold higher than AEA, and is therefore considered the most abundant endocannabinoid. Even so, researchers have yet to determine the full role of this messenger in the body. Not only is information regarding tissue levels of 2-AG sparse, but there are no correlations between regional 2-AG concentrations and cannabinoid receptor distributions in the brain (Sugiura et al., 2002). The biosynthesis of 2-AG is very different from AEA; since 2-AG is a monoglyceride, its formation is based on the metabotropic receptor-dependent activation of PLC, which mediates the breakdown of triacylglycerols. PLC-mediated hydrolysis of TAG in turn

Figure 1.3. The biosynthesis and inactivation of endocannabinoids. Endocannabinoids are membrane-derived local neuromodulators that are synthesized on demand. They can, in principle, be released from pre-and postsynaptic nerve terminals [taken with permission from (Di Marzo et al., 1998)].

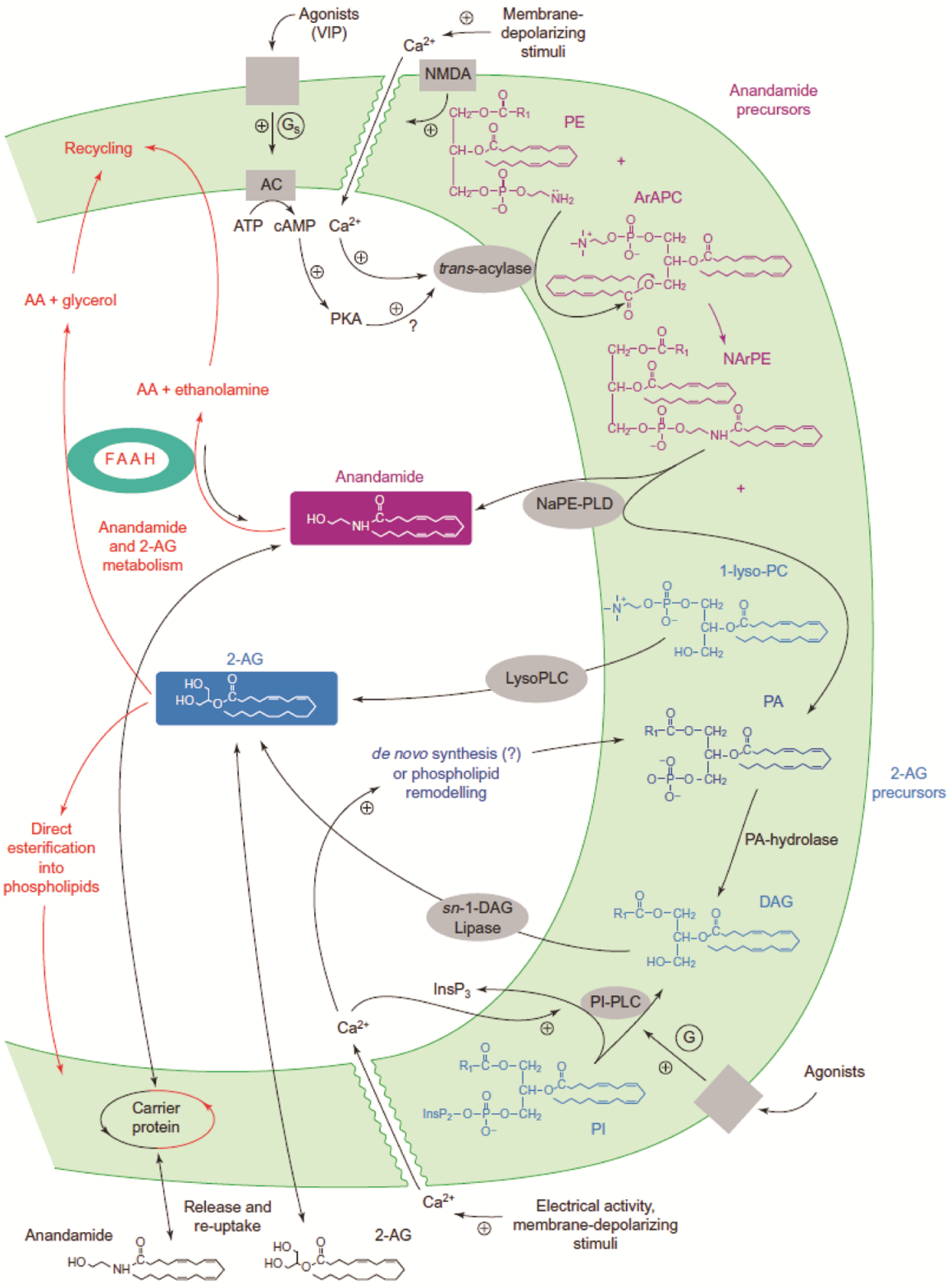
Agonists (VIP)
Membrane-depolarizing stimuli
Ca2+
NMDA
Anandamide precursors
PE
Recycling
Gs
AC
ATP
cAMP
Ca2+
ArAPC
trans-acylase
PKA
?
AA + glycerol
NArPE
AA + ethanolamine
FAAH
Anandamide
NaPE-PLD
Anandamide and 2-AG metabolism
1-lyso-PC
2-AG
LysoPLC
PA
de novo synthesis (?) or phospholipid remodelling
2-AG precursors
Direct esterification into phospholipids
PA-hydrolase
sn-1-DAG Lipase
DAG
InsP3
PI-PLC
Ca2+
G
Agonists
Carrier protein
PI
Release and re-uptake
Anandamide
2-AG
Ca2+
Electrical activity, membrane-depolarizing stimuli

produces DAG, which is converted into 2-AG by the enzyme DAGL-α (Siguria et al. 1995). Thus, unlike the previously discussed endocannabinoid, 2-AG is heavily dependent on postsynaptic Ca^{2+} release. For a review of 2-AG biosynthesis, please refer to Figure 1.3. Similar to AEA, once synthesized, 2-AG is immediately released from the cell plasmalemma, targets receptors, and is metabolized (Rodriguez de Fonseca et al., 2005). 2-AG signal is tightly regulated in tissues by rapid elimination. Like AEA, this includes transport into cells, and hydrolysis by enzymatic systems. 2-AG is eliminated by the AEA membrane transporter (known to be widely distributed throughout the brain) in an energy-dependent fashion (Beltramo et al., 1997). In certain cases, 2-AG is metabolized by enzymatic oxygenation (COX-2) into PGH_2 glycerol esters (Basavarajappa, 2007). It has been demonstrated that fatty acid amide hydrolase (FAAH) can also inactivate 2-AG (this enzyme is widely distributed throughout the body, but concentrated in the brain), however the main enzyme responsible for its degradation is monoacylglycerol lipase (MAGL), located in the presynaptic terminal (Dinh et al., 2002).

Other endocannabnoids

Since the discovery of these compounds, three other endocannabinoids have been identified. The third type of endocannabinoid, an ether derivative of 2-AG (2-arachidonylglycerol ether, or noladin ether), was isolated from porcine CNS, and displays pharmacological properties similar to that of AEA. The fourth endocannabinoid, virodhamine (OEA), is an arachidonic acid and ethanolamine joined by an ester link, instead of an amide linkage like AEA. This molecule is mostly found peripheral of the central nervous system. N-arachidonoyl-dopamine (NADA), which also binds to TRPV1

vannilloid receptors, has just been recently identified as an endocannabinoid; researchers are currently working to investigate its pharmacological properties (Basavarajappa, 2007).

Synthetically-Derived Cannabinoids

The history of the development of synthetic Δ^9-THC, and other synthetic cannabinoid analogs can provide some insight into why cannabinoid-based illicit drugs are emerging as the most popular drugs of choice these days. Once the structure and function of phytocannabinoids became more clear in the mid- 20th century, laboratory synthesis of cannabinoid derivatives were produced and tested in a variety of applications (Gaoni and Mechoulam, 1964; Reggio, 2008). From a historical perspective, these agents were mainly produced to be used either in medications such as Dronabinol, Sativex, Nabilone, and Rimonabant, or to be used in experiments that determined relationships between the structure and function (activity) of cannabinoid compounds. Subsequently, this class of cannabinoids made their appearance into mainstream medicine. Unfortunately, for almost every beneficial use identified, these synthetic substances exerted many more undesirable physiological and behavioral side effects, which greatly limited their therapeutic use (Carroll et al., 2012).

Synthetic Cannabinoid Agonist: WIN55,212-2

In the present day, most of the newer synthesized cannabinoids are not related to phytocannabinoids, or based on the structure of endocannabinoids. Members of the aminoalkylindole group of cannabinoid agonists have structures that differ greatly from those of classical cannabinoids. The best known, and most widely utilized member of this group is: R-(+)-[2,3-dihydro-5-methyl-3-(4-morpholinylmethyl)pyrrolo[1,2,3-*de*]-1,4-

benxozazin-6-yl]-1-napthalenylmethanone mesylate, or WIN55,212-2 (which is usually shortened even further: WIN). The pharmacokinetics of WIN resemble the kinetics of THC in rodents (Agurell et al., 1986), but besides this information, there has been very little research on the metabolism of WIN and other analogs, either in vitro or in vivo. However, because of the vast structural difference between WIN and other cannabinoids, many predict that WIN undergoes biotransformations that differ from classical cannabinoid metabolic patterns, and still possess functional metabolites that contribute its efficacy (Zhang et al., 2002). WIN produces physiological effects similar to that of THC, but offers a great advantage in larger scale experimental studies, as it is much more potent, more soluble in aqueous solutions, and is easier to obtain in a laboratory setting (Pertwee, 2006a). WIN is unscheduled in many countries, including the United States, as it has not yet been approved for human consumption. For this reason, the addictive potential of WIN is currently unknown.

Synthetic Cannabinoid Antagonist: SR141716a

One other major advance made by those in the field of cannabinoid research was the development of selective cannabinoid receptor antagonists. These ligands are useful in experiments that examine the necessity of cannabinoid function, as they block agonist-induced activation of cannabinoid receptors in a competitive manner, yet lack the capability to activate cannabinoid receptors when administered alone. That having been said, a plethora of evidence exists that within some cannabinoid receptor-containing tissues and systems, these substances are able to induce physiological responses in the opposite direction of those elicited by an agonist (“inverse cannabinoid agonism”, reviewed in later sections); this reflects an ability of these compounds to

decrease the spontaneous coupling of cannabinoid receptors to their effector mechanisms that sometimes occur in the absence of exogenously added, or endogenously released agonists (Pertwee, 2006a; Pertwee et al., 2010). The diarylpyrazole SR141716a (Rimonabant, or SR), along with its structural derivatives AM251 and AM281 are some of the most commonly used cannabinoid antagonists in the laboratory setting. With the exception of SR for a brief period of time, these agents have not been approved for human consumption. The pharmacokinetics of SR were described as dose-proportional up to 20 mg in humans. Rimonabant is not a P-glycoprotein (PGP) substrate, inhibitor, or inducer, however it does cross the BBB and is psychoactive, nevertheless, its absolute bioavailability in humans is not currently known. Since SR is an water soluble compound, V_d is proportional to body weight, with more obese organisms having a higher distribution volume, and taking a much longer time to reach a steady state. In vitro, SR's protein binding in plasma is very similar to that of phytocannabinoids, approximately 99%. SR is hepatically metabolized by CYP3A, and its metabolites do not contribute to its pharmacodynamic effects. Approximately 90% of SR is excreted in the feces as unchanged drug (Samat et al., 2008).

Designer Cannabinoid Drugs

Throughout the drug discovery process, research labs, pharmaceutical companies, and other institutions publish data in manuscripts, books and patents, most of which is freely accessible by the public. As stated before, this information is used to understand the nature of drug abuse, develop the therapeutic potential of cannabinoids, and to investigate related mechanisms of action. Unfortunately, many times this

information is used by “sketchball chemists” for lack of a better term, to copy what has been produced in the medical community to manufacture an endless variety of analog designer drugs. This class of cannabinoid drugs has proven to be very dangerous; most have not been approved for human consumption or use. Furthermore, many of these compounds are so new that researchers and other professionals rarely get an opportunity to fully examine these drugs in mechanistic or functional studies in order to characterize pharmacokinetics and side effects. Because of a lack of legal controls and adequate detection methods (mass spectometry, immunoassays, etc.,) the number of derivatives has rapidly multiplied (Carroll et al., 2012). The synthetic cannabinoid agonists HU-210 and JWH-018 are examples of THC analogs that have very slight modifications, yet are significantly more potent (1999).

Cannabinoid Receptors

In the early to mid-1980’s, studies conducted in Allyn Howlett’s laboratory elucidated the existence of cannabinoid receptors by demonstrating that 1) psychotropic cannabinoids have the ability to inhibit adenylyl cyclase by acting through G_i proteins, and that 2) unlabeled cannabinoid possessed the ability to displace [^{3}H]-CP55940, from a receptor site, an effect that was coupled with the G_i-inhibition of adenylyl cyclase, and the production of cannabimimetic behavioral responses (Howlett, 2005; Johnson et al., 1988; Pertwee, 2006a). This was confirmed in 1990, when the rat CB_1 receptor was cloned (Matsuda et al., 1992). Since the discovery of these receptors, much has become known about their structure and signal transduction, as well as their regulation, distribution, and roles within the body. To date, two absolute cannabinoid receptors exist: CB_1, found predominantely at the terminals of CNS neurons, and CB_2, found

predominately on immune cells. Within recent years, some have classified the lysophosphatidylinositol-sensitive receptor GPR55 as a putative cannabinoid receptor, however it presently remains a contentious issue (Ross, 2009). Since almost all of the behavioral effects of cannabinoids are mediated through the CB_1 receptors, this receptor is discussed with more detail. For a review of the CB_2 receptor system, refer to (Pertwee et al., 2010).

Structure

The coding sequence of cannabinoid receptor 1 (CNR1) is approximately 1.5KB, and in its translated form, has a molecular mass of approximately 60 kDa. As mentioned previously, the CB_1 receptor is highly conserved in vertebrates, with most other vertebrates, sharing at least an 85% sequence homology to humans (Soderstrom and Johnson, 2001). The CB_1 receptor is a well-defined, but dynamic protein, as this receptor is subject to post-translational modifications that contribute to its pharmacological properties (especially receptor binding). These changes include nitrosylation, phosphorylation, and most commonly, glycosylation (Bosier et al., 2010). In addition, CB_1 receptors can exist as homodimers, and have been shown to heterodimerize with other GPCRs, existing in such forms as $A_{2A}CB_1$, $Orexin_1CB_1$, and CB_1D_2 (Pertwee, 2006b). Cannabinoid receptors are rhodopsin-like members of the super family of GPCRs, and as such, are classified as heptahelical receptors. Like other GPCRs in this class, they couple to guanine-nucleotide-binding proteins, possess an extracellular amino terminal, an intracellular carboxy terminal, and thread through the membrane seven times. These receptors are associated with the inhibitory proteins $G_{i/O}$ through the intracellular loops of the protein (Howlett, 2005). The results of structure-

activity relationship studies have helped researchers identify a number of amino acid moieties that are key to CB_1 receptor binding and function (Pertwee, 2006b; Pertwee et al., 2010; Razdan, 1986). Within the third transmembrane region (TM3) of CB_1, Lys_{192} is an important residue for ligand binding. Not only is this residue homologous to other key amino acids essential for agonist binding in rhodopsin receptors, Lys_{192} is essential for binding of [^{3}H]-CP55940 and subsequent intracellular signaling response as demonstrated by site-directed mutagenesis studies (Chen et al., 1998; Song and Bonner, 1996). It was hypothesized that Lys_{192} serves as a hydrogen bond donor to a phenolic hydroxyl shown to be critical for agonist binding (Reggio, 1987). Similar to other GPCRs, the CB_1 receptor interacts with G proteins on the cytoplasmic domain. In pertussis toxin sensitivity studies, it was demonstrated that the juxtamembrane C-terminal of CB_1 is critical for recognizing and facilitating the activation G_i proteins, the actions of which are promoted by changes in its seventh transmembrane region. Additionally, the third intracellular loop (C3) is important for directing G protein signal transduction (Howlett, 2000). Just beside the C3 loop lays a Ser_{317} which is responsible for the cannabinoid agonist-regulation of ion channels (Garcia et al., 1998). For an illustration of CB_1 receptor structure, please see Figure 1.4.

Signaling

Under certain conditions with certain agonists, the CB_1 receptor may couple to G_S and Gq, but mainly signals through $G_{i/O}$. Subsequently, the consequences of the CB_1 receptor activation are mediated through three main signal transduction pathways: 1) the inhibition of adenylyl cyclase, 2) the modulation of various ion channels, and 3) the

Figure 1.4. The rat CB1 receptor in two-dimensional representation. Three extracellular (E1, E2, and E3) and intracellular (C1, C2, and C3) regions are represented. The most conserved residues within each helix is indicated by an arrow. The palmitoylation of a C-terminal cys residue is depicted as a membrane attachment locus. Amino acid residues mentioned in the text are depicted in bold type. Putative intrahelical interactions are denoted by lines drawn between amino acid residues proposed to be associated by hydrogen bonding interactions. [Taken with permission from (Howlett, 2000)].

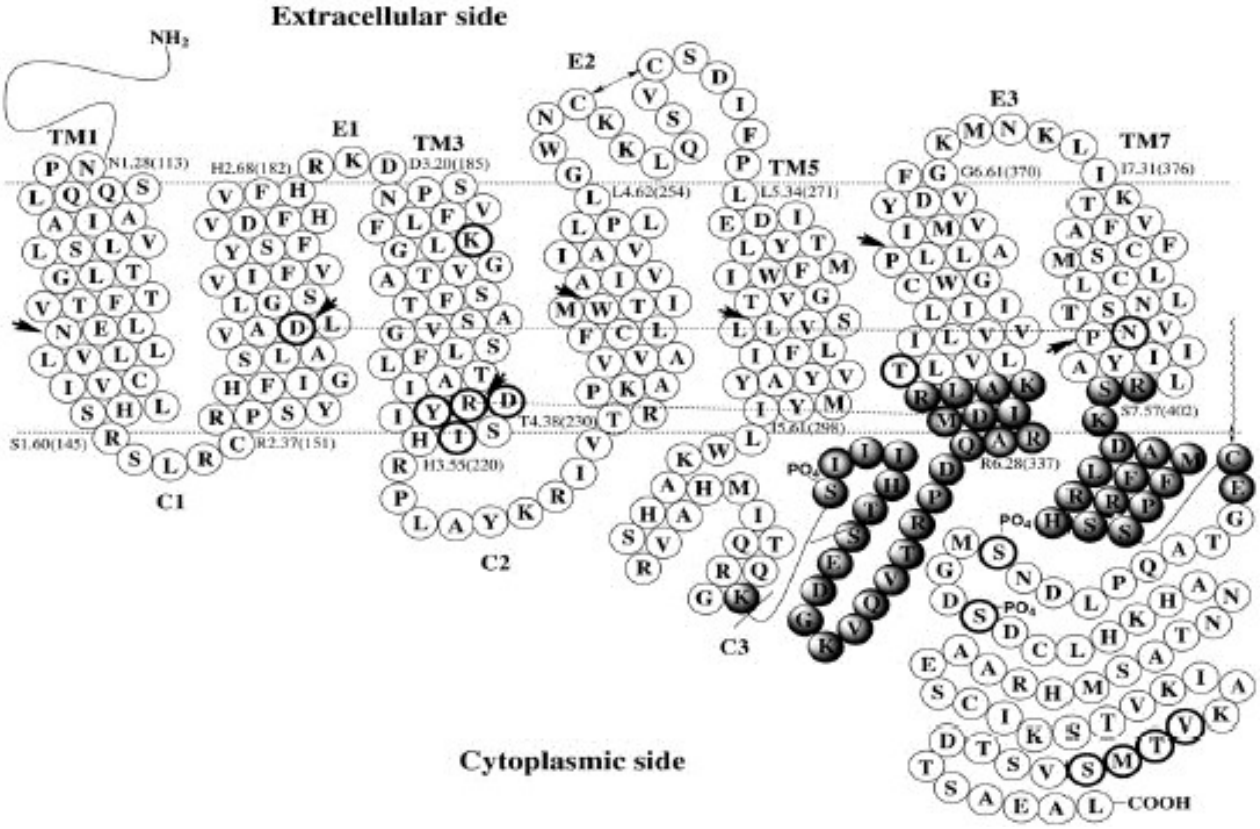
Extracellular side
NH2
TM1
E1
TM3
E2
TM5
E3
TM7
N1.28(113)
H2.68(182)
D3.20(185)
L4.62(254)
L5.34(271)
G6.61(370)
I7.31(376)
S1.60(145)
R2.37(151)
T4.38(230)
H3.55(220)
I5.61(298)
R6.28(337)
S7.57(402)
C1
C2
C3
PO4
PO4
PO4
Cytoplasmic side
COOH

regulation of mitogen-activated protein kinase (MAPK) pathways (Demuth and Molleman, 2006).The inhibition of adenylyl cyclase was the first CB_1 signaling pathway characterized (see Figure 1.5). Since Allyn Howlett's laboratory demonstrated that micomolar concentrations of THC blocked cAMP production in N18TG2 neuroblastoma cells (an effect reversed by pertussis toxin), the functional inhibition of the cAMP cascade was shown in a number of studies. CB_1-mediated adenylyl cyclase inhibition can be observed both centrally and peripherally, as well as in cells overexpressing functional CB_1 receptors (Howlett, 2005). Specifically, cannabinoids have displayed an attenuation of cAMP production in CHO cells heterologously expressing CB_1 receptors; an effect that can be reversed by both pertussis toxin and SR. (Matsuda et al., 1992). Many have repeatedly shown that brain regions that contain the highest concentrations of cannabinoid binding sites are the areas in which cannabinoids are the most effective in inhibiting adenylyl cyclase activity. Therefore, it is no surprise that WIN, AEA, and CP55940 were demonstrated to be potent inhibitors of cAMP in cerebellum, striatum, hippocampus, and cortex (Childers and Deadwyler, 1996).

The modulation of Ca^{2+} and G-protein inwardly-rectifying potassium (GIRK) channels is thought to underlie the inhibition of neurotransmitter release from presynaptic nerve terminals. In this context, cAMP, serving as a second messenger to outward GIRK channels is inhibited, thereby prolonging the duration of the hyperpolarizing GIRK currents. Simultaneously, activation of CB_1 receptors directly inhibits Ca^{2+} entry through L, N, and P/Q type inward Ca^{2+} channels, which are required for neurotransmitter vesicle fusion and exocytosis (Demuth and Molleman, 2006; Turu

and Hunyady, 2010). These mechanisms synergistically shorten the duration and strength of presynaptic action potentials.

In general, stimulation of GPCRs leads to activation of MAPK pathways (Demuth and Molleman, 2006). Accordingly, CB_1 signal transduction mechanisms involving MAPK have not been fully clarified. Some have proposed that CB_1 stimulation indirectly regulates MAPK activity through its modulation of cAMP, and consequently PKA activity (Melck et al., 1999). This cannabinoid induced activation of MAPK expression has been linked to the mediation of immediate-early gene expression in a number of studies (Bouaboula et al., 1995; Patel et al., 1998).

Characterizing the dynamics of cannabinoid receptor signaling is key to understanding the functional properties of cannabinoids. It is worthy to note that in recent years, many studies have demonstrated that cannabinoid receptors adopt multiple conformations and affinity states (Pertwee et al., 2010), which lead to a number of entirely different signaling cascades. Each of these different conformations is subject to stabilization by a number of cannabinoids, leading to a situation where the transduction of a particular signal pathway is contingent upon the individual type of ligand bound. In this situation, the signal transduction pathway elicited defines the agonistic/antagonistic properties of the ligand, as the same cannabinoid can act as an agonist in one pathway, and an antagonist in an entirely different pathway (Kenakin, 2007).

Distribution

The development of high-affinity synthetic cannabinoid agonists (as discussed earlier) has allowed researchers to map CB_1 receptor distribution throughout the CNS

Figure 1.5. Schematic illustration of signal transduction mechanisms stimulated by CB_1 receptor in a presynaptic nerve terminal. [Taken with permission from (Yamamoto and Takada, 2000)

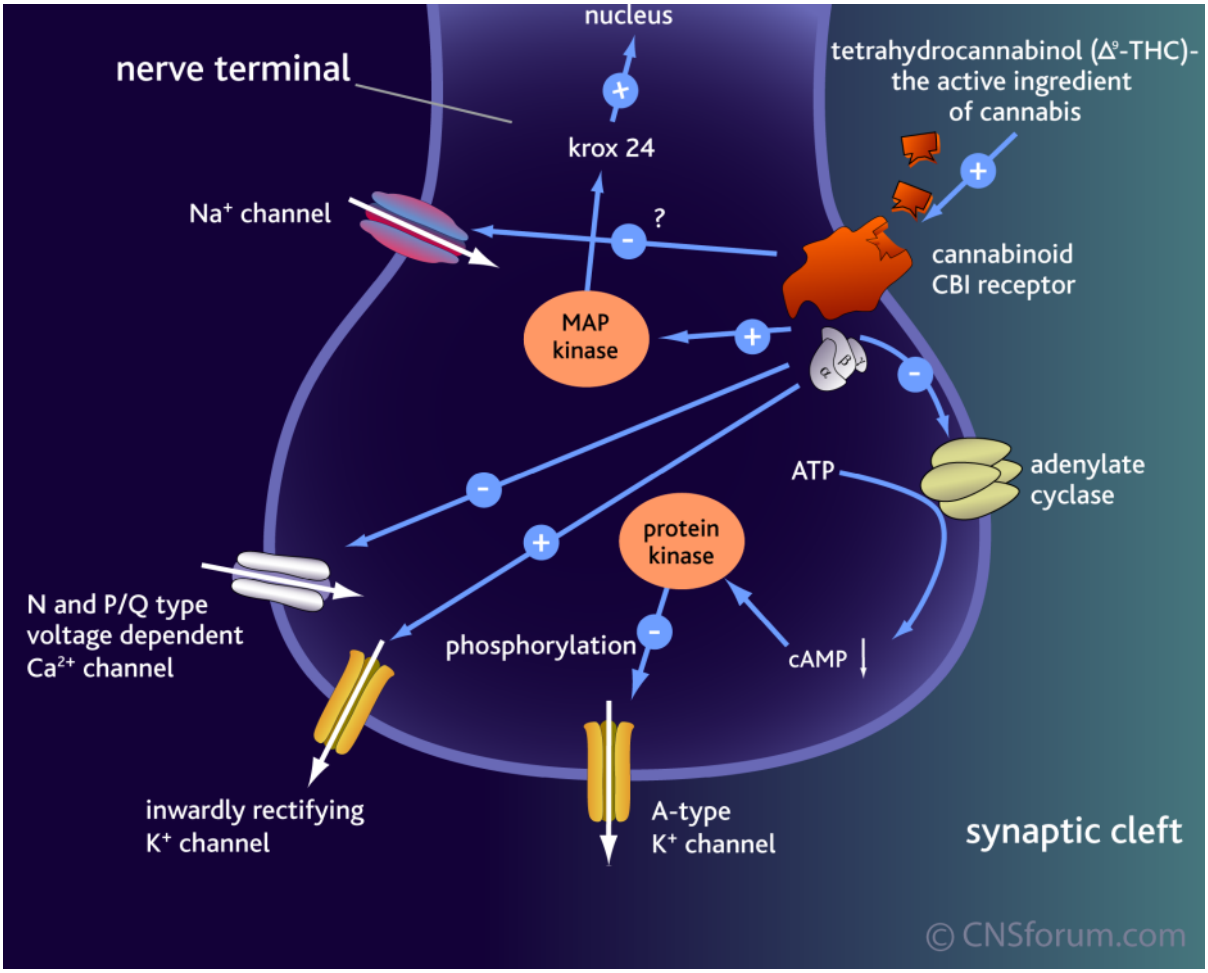
nucleus
nerve terminal
tetrahydrocannabinol (Δ⁹-THC)-
the active ingredient
of cannabis
krox 24
Na⁺ channel
?
cannabinoid
CBI receptor
MAP
kinase
adenylate
cyclase
ATP
protein
kinase
N and P/Q type
voltage dependent
Ca²⁺ channel
phosphorylation
cAMP
inwardly rectifying
K⁺ channel
A-type
K⁺ channel
synaptic cleft
© CNSforum.com

and periphery (Reggio, 2008). Much of what is currently known about receptor localization has been determined through in situ hybridization, quantitative autoradiography, and immunohistochemistry. The in situ hybridization studies spawned from the first cloning of CB_1 demonstrated that receptor expression in neurons was dichotomized; for example, in the forebrain, hippocampus, and striatum, a very small number of specialized neurons express CB_1 receptors on a large scale, while most other neurons express CB_1 on a much smaller scale (Mackie, 2005). Autoradiographic studies performed by Herkenham and colleagues (Herkenham et al., 1991; Herkenham et al., 1990) demonstrated that the brain regions that expressed CB_1 were those same regions expected to be influenced by the psychoactive effects of THC (such as the hippocampus), and that receptor expression was low in areas that were responsible for effects that weren't altered by cannabinoids (such as the medulla). These studies also provided researchers with an accurate quantitation of CB_1 receptor expression levels, and interestingly, they determined that cannabinoid receptors are among the most abundant GPCRs in the body, and the most abundant GPCR in the brain. The results of these receptor binding experiments in combination with in situ hybridization demonstrated that CB_1 receptors are mostly localized to presynaptic axon terminals, and that very few are located on proximal axons, dendrites, or the cell body. Immnunohistochemistry experiments allow for very precise mapping of receptor expression, and demonstrate that CB_1 receptors are densely expressed on CCK-containing basket cells (a subset of GABAergic interneurons in the forebrain), and sparsely expressed on glutamatergic terminals (Bodor et al., 2005). For a more detailed review of this subject, please refer to (Mackie, 2008).

CB_1 receptors are expressed most densely in the CNS, and the receptor distribution pattern within the CNS correlates with the characteristic behavioral effects of CB_1 agonists, such as their ability to produce anxiolysis, hypokinesia and catalepsy, and to induce various psychoactive effects (Abood, 2005; Grotenhermen, 2003). CB_1 receptor expression was detected in the cortical regions besides the GABAergic interneurons of the hippocampus (neocortex, amygdale), some subcortical regions (hypothalamus, basal ganglia, thalamus) , the granular layer of cerebellum, brainstem, and interneurons of the dorsal horn (Pagotto et al., 2006). Although sparse, CB_1 receptors were also found in a number of peripheral tissues. Among these organs and tissues are endocrine glands, leukocytes, spleen, heart, and parts of the urinary, reproductive and GI tracts (Pertwee, 1997). A series of recent studies reported receptor expression on adipocytes, liver, pancreas, and skeletal muscle. It has been hypothesized that these play a role in metabolism, however results are inconclusive (Cavuoto et al., 2007; Cota, 2007; Osei-Hyiaman et al., 2005).

Pharmacodynamic Properties of Cannabinoid Agonism

The main action of cannabinoid receptor activation is to decrease the probability of depolarization and neurotransmitter release from the presynaptic terminus and decrease transmitter reaching the postsynaptic neuronal membrane. In non-human primates, cannabinoid agonism decreases locomotor activity, and impairs learning and memory recall by governing mechanisms of long-term and short-term depression. In rodents, CB_1 agonism is known to produce a tetrad of characteristic pharmacological effects. These include hypothermia, sedation, catalepsy, and antinociception (Martin et al., 1991). In humans, activation of CB_1 receptors leads to a number of physiological

effects, most of which are psychoactive. A number of cannabinoid drugs were tested in humans for subjective perceptions of “highness”, as well as more objective measures such as tachycardia; and compatible doses of SR were able to block both responses (Razdan, 1986). In addition, activation of CB_1 receptors inhibits gastrointestinal mobility, contributes to hemorrhagic cardiovascular hypertension, and increases lipogenesis in the liver (Osei-Hyiaman et al., 2005; Varga et al., 1998). A more detailed description of the central and peripheral consequences of cannabinoid agonism can be found in Table 1.1.

Within a system, different cannabinoids activate the CB_1 receptor to a different degree, and consequently, the magnitude of the behavioral and physiological effects conferred upon on the system vary as well. Cannabinoids that are full CB_1 agonists, such as HU-210, CP55940, and AM-2201, which possess relatively low K_i values for the CB_1 receptor (0.06 nM, 0.5 nM, and 1 nM respectively), favor an active receptor conformation. In contrast, partial cannabinoid agonists like THC (K_i = 5 nM) favor both active and inactive receptor states. As a result, generally speaking, a dose of the full CB_1 agonist will elicit more intense cannabimimetic responses than the same dose of partial agonist. For a list of relative cannabinoid K_i values for CB_1, please refer to (Pertwee et al., 2010). There are exceptions to this rule however; occasionally, the difference between the efficacy of a full and partial agonist lies in the relationship between the percent of cannabinoid receptors occupied and the responses evoked. Consider the scenario where the same dose of HU-210 and THC was administered to a system: If CB_1 receptors within that system are few, then the effects of THC would

expectedly be much less than that of HU-210. However, if the system or tissue densely expressed CB_1 receptors, (like in the case of the hippocampus), the biological effects

Table 1.1. Physiological effects of cannabinoids. These dose-dependent effects have been observed in clinical studies, in vivo, or in vitro. [Taken from (Grotenhermen, 2003)

Body system	Effects
Psyche and perception	Fatigue, euphoria, enhanced well-being, dysphoria, anxiety, reduction of anxiety, depersonalisation, increased sensory perception, heightened sexual experience, hallucinations, alteration of time perception, aggravation of psychotic states, sleep
Cognition and psychomotor performance	Fragmented thinking, enhanced creativity, disturbed memory, unsteady gait, ataxia, slurred speech, weakness, deterioration or amelioration of motor coordination
Nervous system	Analgesia, muscle relaxation, appetite stimulation, vomiting, antiemetic effects, neuroprotection in ischaemia and hypoxia
Body temperature	Decrease of body temperature
Cardiovascular system	Tachycardia, enhanced heart activity, increased output, increase in oxygen demand, vasodilation, orthostatic hypotension, hypertension (in horizontal position), inhibition of platelet aggregation
Eye	Reddened conjunctivae, reduced tear flow, decrease of intraocular pressure
Respiratory system	Bronchodilation
Gastrointestinal tract	Hyposalivation and dry mouth, reduced bowel movements and delayed gastric emptying
Hormonal system	Influence on luteinising hormone, follicle-stimulating hormone, testosterone, prolactin, somatotropin, thyroid-stimulating hormone, glucose metabolism, reduced sperm count and sperm motility, disturbed menstrual cycle and suppressed ovulation
Immune system	Impairment of cell-mediated and humoral immunity, immune stimulation, anti-inflammatory and antiallergic effects
Fetal development	Malformations, growth retardation, impairment of fetal and postnatal cerebral development, impairment of cognitive functions
Genetic material and cancer	Antineoplastic activity, inhibition of synthesis of DNA, RNA and proteins

would not be limited by the number of bound CB_1 receptors, and thus maximal responses to CB_1 receptor agonism by these two drugs could be exactly the same.

Thus, the effects of partial cannabinoid agonists like THC and 2-AG depend on the properties of each particular signaling system (e.g. the amount of proteins available in a signaling cascade). For a review of these topics, please refer to (Mackie, 2008; Pertwee et al., 2010; Turu and Hunyady, 2010).

The Neurobiology of Cognition

One of the central questions in the cannabinoid neurobiology field is how the cannabinoid system contributes to cognitive development and function under normal conditions, and how this architecture disintegrates in cannabinoid abuse. It is becoming increasingly clear that subjective clinical studies are no longer sufficient; the need to understand the physiological basis of cognition as it relates to cannabinoid signaling is urgent.

Dendritic Spines

The brain as a whole is a very complex structural and functional network that is dramatically modified by our sensory experiences during early postnatal life. How do we process sensory information that eventually results in the formation of a memory? The bases of these modifications are various forms of synaptic plasticity that contribute to learning and memory acquisition (Clem et al., 2008). The dendritic spine is a structure specialized for synaptic transmission, and the locus of long-term synaptic plasticity associated with the storage of information in the brain. These door knob-like protrusions are often thought of as a stable structural extension of the synapse. These

entities process and retain sensory information by mechanistically undergoing long term and short term morphological changes. Receptor and protein turnover is rapid within the spine, which allows neurons to keep up with the fast flow of information through the brain on a minute-to-minute basis (Segal, 2005). Once information is processed through the neuron, spines are either formed *de novo*, or from an existing dendritic shaft. In the case of de novo synthesis, filipodia shoot out of the dendrite in search of a presynaptic axon complement, makes contact, and pulls it in close to the dendritic synapse, from which it later forms a spine. This mechanism is proposed to occur mostly during early postnatal development, as few filipodia are found in studies that examine mature neurons (Woolley and McEwen, 1993). Conversely, with the help of adhesion molecules, and proteins located in the postsynaptic density (PSD-95), existing dendritic shafts protrude out to nearby presynaptic terminals, and then collapse to become a short mature spine that is typically 1-2 μm long (Dailey and Smith, 1996; Harris and Kater, 1994). Rapid local spine morphing is essential to learning and memory formation, as it is proposed to be involved in the diffusion of molecules through the plasma membrane into the spine. In addition, a recent study showed that this mechanism aids in the rapid delivery of AMPA receptors into the postsynaptic density, a process that is accelerated during memory acquisition (Richards et al., 2004). Spine pruning, an active, ongoing process which requires the acute activation of NMDA receptors, occurs simultaneously with spine formation. When neurons are activated with extracellular glutamate, spines disappear rapidly, and reappear just as quickly in the same location when the stimulus is removed (Hasbani et al., 2001).

How Does the Brain Learn and Memorize Information?

The interaction between dendritic spine densities and the ability to form new memories from sensory experiences has been a hot topic for decades. In the past, it has been proposed that dendritic spine densities and learning/memory formation are positively correlated, that is to say, that memory formation was thought to always result in an increase in dendritic spine densities (Airey et al., 2000; Moser, 1999). This theory presents a conundrum, however. If memory formation results in a higher spine density, then this suggests that when new memories are formed, they will either reside on independent spines of the same neuron, or on a totally different neuron altogether. If this is so, then our memory storage capacity would be limited to how many spines could fit on a neuron, or how many neurons could reside in our brain. This would also suggest that the number of neurons within the brain (around one billion) increases significantly with time, and that all synaptic connections are of the same strength, but research has repeatedly demonstrated that this is not true (Jones, 1994). Furthermore, what would be the purpose of simultaneous synaptic pruning during learning? This scenario is highly unlikely, as it is counterintuitive to the brain's tendency to conserve energy and resources (e.g. sensory habituation, optical illusions). A more reasonable theory for the physiological basis of learning is that early on during the first years of development, neurons undergo synaptogenesis, a massive spontaneous overproduction of synapses between neurons. A main reason for this is because early postnatal sensory systems are not yet cross-modally differentiated (Kozorovitskiy et al., 2012). In other words, as the efficiency of neural activity and amount of sensorimotor experience increases, some synaptic connections selectively strengthen and stabilize, while other, less used

connections are subsequently eliminated. This process known as selective stabilization (Figure 1.6) is the basis of much of the learning and memory acquisition that occurs within the brain (Allport, 1985; Changeux et al., 1973; Landmesser, 1998; Xu et al., 2009). The most direct links between memory and spine densities have been shown in songbirds. For example, Wallhausser-Franke and colleagues report that in a CNS region essential for vocal learning, social, song-tutored zebra finches have dendritic spine densities 41% lower than that of learning-deprived animals (Wallhausser-Franke et al., 1995). For more examples of this well-documented phenomenon in songbirds, please refer to chapter 1.

Long-Term Potentiation

One of the main neuronal processes that is correlated with spine maintenance, and thought to underline learning and memory, is the modulation of synaptic transmission either in an upward or a downward direction. The synaptic plasticity and memory hypothesis states that “activity-dependent synaptic plasticity is induced at appropriate synapses during memory formation, and is both necessary and sufficient for the information storage underlying the type of memory mediated by the region in which plasticity is observed” (Martin et al., 2000). Long-term potentiation (LTP) is a long-lasting increase in the synaptic strength of an excitatory afferent following high-frequency stimulation. This phenomenon can be induced either by strong stimulation of one solitary pathway to a synapse, or through the weaker, simultaneous stimulation of many pathways that converge upon a synapse (McNaughton, 2003). The end result of this process is the enhancement of signal transmission between two neurons; synapses that have undergone LTP have much stronger chemical/electrical responses to stimuli

Figure 1.6. Stabilization of dendritic spines. (a) Synaptic activity, including adhesive contact between pre- and postsynaptic compartments and trophic signaling between the two compartments, enhances dendritic spine stability. (b) Synaptic support maintains the integrity of dendritic architecture over time. The loss of this support results in destabilization of dendritic spines followed by dendritic simplification.

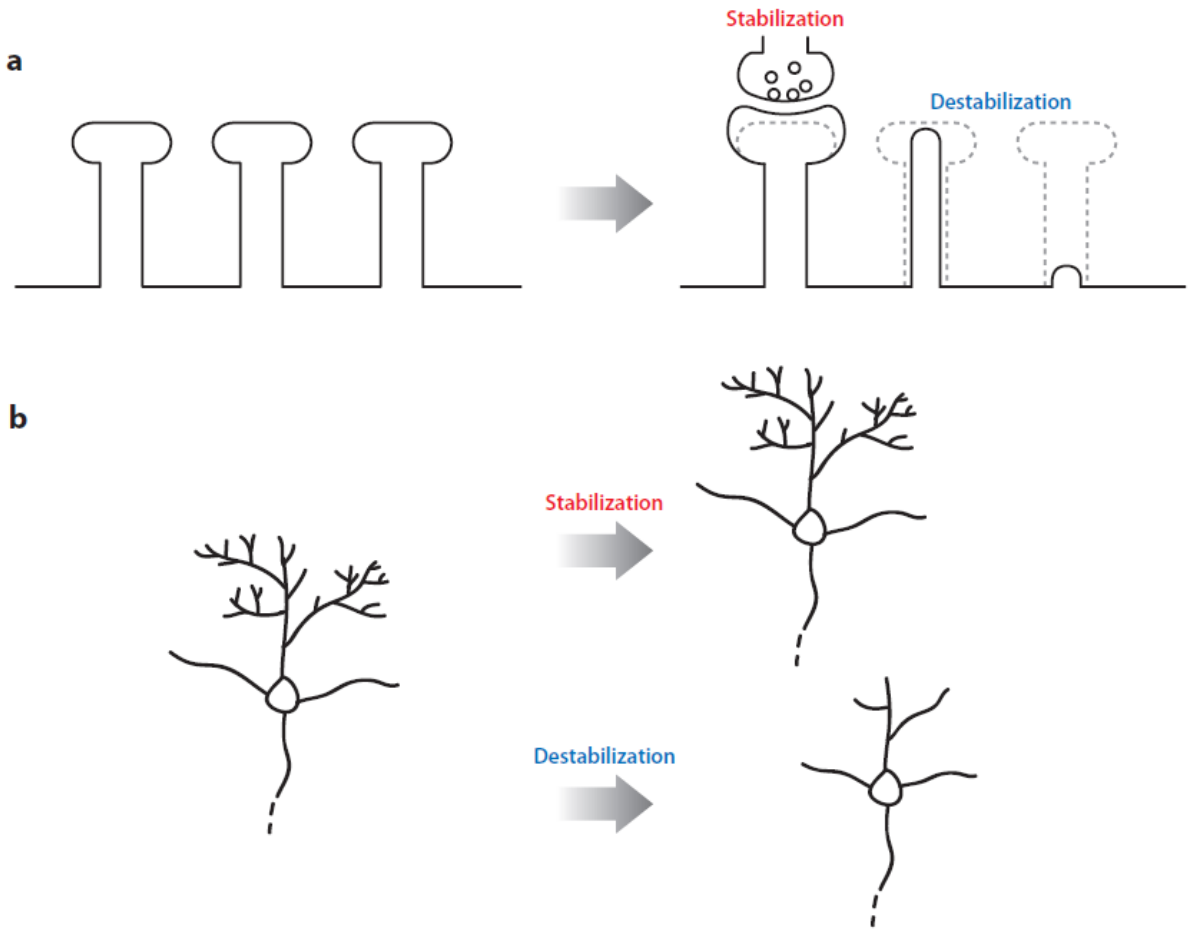
a
Stabilization
Destabilization
b
Stabilization
Destabilization

than those that have not undergone LTP (Welberg, 2008). In general, most regions display Hebbian LTP (under the Hebb's rule that "cells that fire together, wire together", LTP ensues when both the presynaptic and postsynaptic membrane are depolarized at the same time, (Wigstrom and Gustafsson, 1986)) and is therefore the focus here. One of the main mediators of LTP is Ca^{2+}, which is required in order for potentiation to occur (Kapur et al., 1998). Most forms of LTP are glutamatergic, and involve the activation of the NMDA receptor. Recent studies have shown that the NMDA receptor is involved in mediating LTP at synapses, however continued activation acts to suppress synaptic strengthening after prolonged stimulation, in a process called LTP occlusion (a physiological method in which the brain stabilizes memory encoding (Martin et al., 2000). Additionally, these same studies demonstrated that the mGluR is also involved in LTP, as it can counteract the synaptic occlusion mediated by the NMDA receptor, and maintain synaptic plasticity (Clem et al., 2008). This mechanism underlies learning-related neuroplasticity in compulsive drug seeking and addiction (Bellone and Mameli, 2012).

Long-Term Depression

If dendritic spine formation and maintenance can be correlated with LTP, then dendritic spine retraction is, perhaps, correlated with Long-term depression (LTD) and/or depotentiation (DP). LTD is a lasting decrease in synaptic strength resulting from prolonged, low frequency neurotransmission, and DP is an activity-dependent reversal (depression) of a long-term potentiated synapse. Like LTP, LTD is induced by an increase in the concentration of Ca^{2+} within the postsynaptic dendritic spine, but the sources of Ca^{2+} are very different. In LTP, Ca^{2+} influx is NMDA/mGluR receptor-

dependent, whereas LTD requires mGluR activation paired with influx through L-type voltage-gated Ca^{2+} channels. Other differences lie in the synaptic environments: LTP is due to an increase in either transmitter release or to an increased postsynaptic response to glutamate, whereas LTD usually results from a long-lasting decrease in presynaptic neurotransmitter release, coupled with a decrease in postsynaptic receptor densities (Bolshakov and Siegelbaum, 1994). It is thought that LTD functionally dampens LTP in an effort to make constructive use of the enhancement of signal transmission resulting from LTP. This mechanism is necessary in order to prevent synapses from reaching a plateau in efficiency, which would retard sensory encoding of information (Purves, 2011). LTD can also be classified in regards to Hebb's rule: Homeosynaptic LTD is restricted to individual synapses, and is activity dependent (requires simultaneous presynaptic and postsynaptic activation). However heterosynaptic LTD, in contrast, occurs at a synapse that is not potentiated; postsynaptic activity is driven by other afferents that converge upon the dendritic spine (Massey and Bashir, 2007).

The cannabinoid system is heavily involved in both short and long-term synaptic plasticity, especially in LTD in many memory-related CNS regions, such as the amygdala, hippocampus, striatum, neocortex, and cerebellum (Izumi and Zorumski, 2012; Massey and Bashir, 2007). Most agree that the endocannabinoids AEA and 2-AG act as retrograde messengers through activation of CB_1 receptors, and modify neural circuits through two main mechanisms: 1) by long-term regulation of GABA release, and 2) Depolarization-induced suppression of excitation (DSE)/(inhibition, DSI). By regulating presynaptic GABA release, endocannabinoids profoundly impact circuit

processing by indirectly decreasing the inducibility of LTP (Azad et al., 2004; Carlson et al., 2002). DSI and DSE are transient forms of neurotransmitter-mediated synaptic depression in which cannabinoid signaling causes a temporary reduction in inhibitory or excitatory input into the postsynaptic cell (Diana and Marty, 2004). Because the cannabinoid system is so widely distributed throughout the brain, this is the most common method by which LTD is induced (Diana and Marty, 2004).

In general, learning and memory processing by LTP and LTD is network-specific. What gets encoded, and the way it gets encoded is heavily dependent on the region/type of network where the plasticity takes place, not just the mechanisms that happen at the synapse. For example, hippocampus and cortically-encoded memories are vastly different from those processed in the amygdala (Martin et al., 2000).

Immediate Early Genes and Memory Acquisition

Neurons can also display adaptability in response to sensorimotor perception of the external environment by coupling extracellular cues with changes in transcription and translation. Behavioral changes that lead to altered synaptic activity or changes in neurotransmitter levels can lead to rapid activation of immediate-early gene (IEG) expression despite not having any proteins yet translated. Neuronal IEGs function at the synapse to encode cytoskeletal proteins, transcription factors, proteins, and metabolic enzymes involved in signal transduction cascades (Lanahan and Worley, 1998). Most typically, they function as part of a network of constitutively expressed proteins, and their regulation provides a means of controlling neuronal function. IEGs such as Arc and Egr-1 are highly correlated with sensory-evoked neuronal activity, facilitate the maintenance of LTP and LTD (Guzowski et al., 2000) and are required for both

encoding and consolidation of sensory memories (Okuno, 2011). IEGs are activity regulated, and thus mark very recent changes in neuronal activity (Bramham et al., 2010).

The Endocannabinoid System in Developing Individuals: How is This System Influenced by Cannabinoid Abuse?

Postnatal Development of the Endocannabinoid System

The endocannabinoid system plays a number of vital roles in developing individuals, a number of which have been discussed above (see Endocannabinoids section). It is because of this that concern continually grows about adverse psychological and neurophysiological effects produced by these agents, which are significantly more pronounced among those who use cannabinoids at an early age, mainly during mid-adolescence (Arseneault et al., 2004; Fernandez-Ruiz et al., 1999; Hall, 2006; Verdurand et al., 2011). Unfortunately, limited information is available regarding mechanisms underlying the role of the endocannabinoid system in late-postnatal development. Several autoradiographic studies have examined the density of cannabinoid receptor binding sites in telencephalic regions from early postnatal development through adulthood, and show that CB_1 receptors are steadily increased during a critical time window: the transition from early to late-postnatal development. Rodriguez and colleagues found a region-specific increase in CB_1 receptor binding in rats, which rose starting from PND 10, and plateaued around an average PND of 35. This was followed by a decrease during the transition into adulthood (Rodriguez de Fonseca et al., 1993). This pattern is very interesting, namely because it is the opposite of what is seen with patterns of most other neuroreceptor systems, which have usually

already tapered off during this time period (Verdurand et al., 2011). In humans, researchers demonstrated an increase in CB_1 receptor density between childhood (average of 4 years of age) and adulthood (average of 37.5 years old) in the hippocampus, frontal cortex, and cerebellum (Mato et al., 2003). Interestingly, studies have shown that mRNA expression can be detected within the CNS as early as PND 3, however these levels remain roughly the same throughout adulthood. One rationale for this discrepancy is that the transcriptional information for the CB_1 receptor is consistently present at high levels within the cell, but the message remains mostly untranslated into receptor protein. The increase in CB_1 receptor binding in autoradiographic studies might reflect the number of CB_1 receptors that are functionally mature at that time in life (Schneider, 2008). In addition to the restricted increase in CB_1 receptors during postnatal development, research has shown that levels of AEA increase correlatively during this period (Wenger et al., 2002).

Persistent Behavioral and Neurphysiological Effects Following Adolescent Cannabinoid Exposure

The cannabinoid system is most active during the onset of late postnatal development, which makes adolescents particularly vulnerable to the negative neurophysiological effects of cannabinoids. Chronic treatment of animals with WIN leads to persistent alterations in adult learned behavior that differ significantly with comparable treatments with vehicle (Schneider and Koch, 2003; Soderstrom and Johnson, 2003). In humans, cannabinoid consumption produces lasting morphological changes in teenagers that are absent after identical exposures of adults (Ehrenreich et al., 1999). As cannabinoid signaling is involved in altering neural circuit modulation and

maturation, it can be expected that these changes will manifest in behavioral alterations. Behavioral abnormalities following cannabinoid exposure during adolescence, but not in adults, are known for several vertebrate species. Deficits in learning (Cha et al., 2007) memory (Moore et al., 2010; Rubino et al., 2009b), and cognitive function, including increases in anxiety and depressive phenotypes (Rubino et al., 2009a), with correlates to results of human studies, have been documented (Dekker et al., 2010; Hanson et al., 2010; Kristensen and Cadenhead, 2007; Solowij and Michie, 2007) (Realini et al., 2011) For a review, please see (Soderstrom and Gilbert, 2012).

Songbird Models Provide Powerful Models for Studying Cannabinoid-Altered CNS Learning and Development

Cannabinoid-altered cognition studies in humans are useful in rectrospectively underscoring the consequences of adolescent cannabis use on adult CNS function, and how this issue relates to human health and performance, but several limitations unfortunately exist. Firstly, many studies fail to provide information about the manner in which cannabinoids were consumed early on, like whether this usage was persistent or occasional. Furthermore, the type of cannabinoid used, abstinence patterns, and the route of administration vary widely in human studies. Lastly, the diminished ability to obtain anatomical/morphological information about the brains of human cannabinoid users in real time is a hindrance. Keeping in mind the limitations of each individual experimental system, animal models may offer many advantages, namely experimentation within a controlled environment.

Songbirds present a useful model to study how abused substances influence CNS physiology and cognition, as well as natural behavioral and neuromolecular

mechanisms that underlie developmental learning, processing, and memorizing vocal communication systems. Vocal learning is an extremely rare ability: songbirds are one of the few species of animals (besides bats, cetaceans, and humans) who have evolved a natural capacity to acquire a concatenate system for communication, and offer a unique advantage over other learning models that often involve some type of reinforcement conditioning (Fee and Scharff, 2010). Songbird expert Richard Mooney points out that "one of the greatest similarities between human speech and birdsong is that both processes are under executive control of the telencephalon, as opposed to the brainstem-mediated control of vocalizations seen in most other vertebrates, including non-human primates" (Mooney, 2009a). Similar to humans, the act of songbird auditory learning is a complex behavior that is essential for accomplishing such tasks as memorizing the correct song of an adult tutor during sensorimotor learning, mate recognition, and distinguishing between conspecific vocalizations and those of heterospecific threats. This includes the ability to detect and localize vocal signals, discrimination between target signal and noise, categorize and represent distinct functional units of vocal communication, such as calls, motifs and songs, as well as individual vocal recognition (for a review, see (Knudsen and Gentner, 2010)). Thus, the songbird model enables the characterization of specialized brain areas responsible for learning and memorizing information, explore relationships between neural circuitry and the production/function of sequential behaviors, identify genetic and protein targets that underlie learned communication such as FoxP2,egr-1, Arc, etc. (Fee and Scharff, 2010; Soderstrom and Luo, 2010).

The Zebra Finch

Song Learning

Young male zebra finches learn to sing (females do not sing) during a sensitive period that is critical for vocal learning (Figure 1.7). Experts usually divide this critical period into two distinct phases: sensory learning, and sensorimotor learning. Both of these periods depend heavily on auditory sensory experience. The sensory learning period generally takes place during the first couple of months of life, ranging from day 20 to around day 65, significantly overlapping with sensorimotor learning (Mooney, 1999). During sensory learning, young animals listen to one or more songs of their father, or another conspecific adult, which is referred to as tutor song. Soon after, these birds begin to memorize the spectral and temporal qualities of the tutor song template. Interestingly, zebra finches that have been experimentally deafened, or raised in auditory isolation sing much simpler (isolate) songs as adults than those that were tutored (Marler and Tamura, 1964). The termination of sensory learning is dependent upon both the age of the bird and the amount of tutor song exposure. Nottebohm and colleagues determined that zebra finches raised in auditory isolation until adulthood (>100 days) are able to learn a new tutor song, in spite of already having memorized an isolate song (Marler and Tamura, 1964).

Before discussing the dynamics of zebra finch sensorimotor learning, it may prove helpful to evaluate a couple of key points regarding what is necessary of these young zebra finches in order to produce a high-fidelity copy of his father's song:

1. The ability to control the vocal/respiratory organs with great precision

Figure 1.7 Birdsongs consist of ordered, often highly stereotyped strings of sounds separated by brief silent intervals. Sound energy is plotted as a function of frequencyand time. Syllables are indicated by letters, and form a repeated ‘motif’. a, Adult zebra finch song. b, Song of a zebra finch, tutored by the bird in a, at an early stage of sensorimotor learning. c, Song of the same bird close to song ‘crystallization’. Note the similarities between this bird’s song and that of its tutor. d, Song of a zebra finch raised in acoustic isolation. Note the overall simplicity of this song, but its general similarity of structure to other zebra finch songs. [Taken with permission from Brainard and Doupe, 2002]

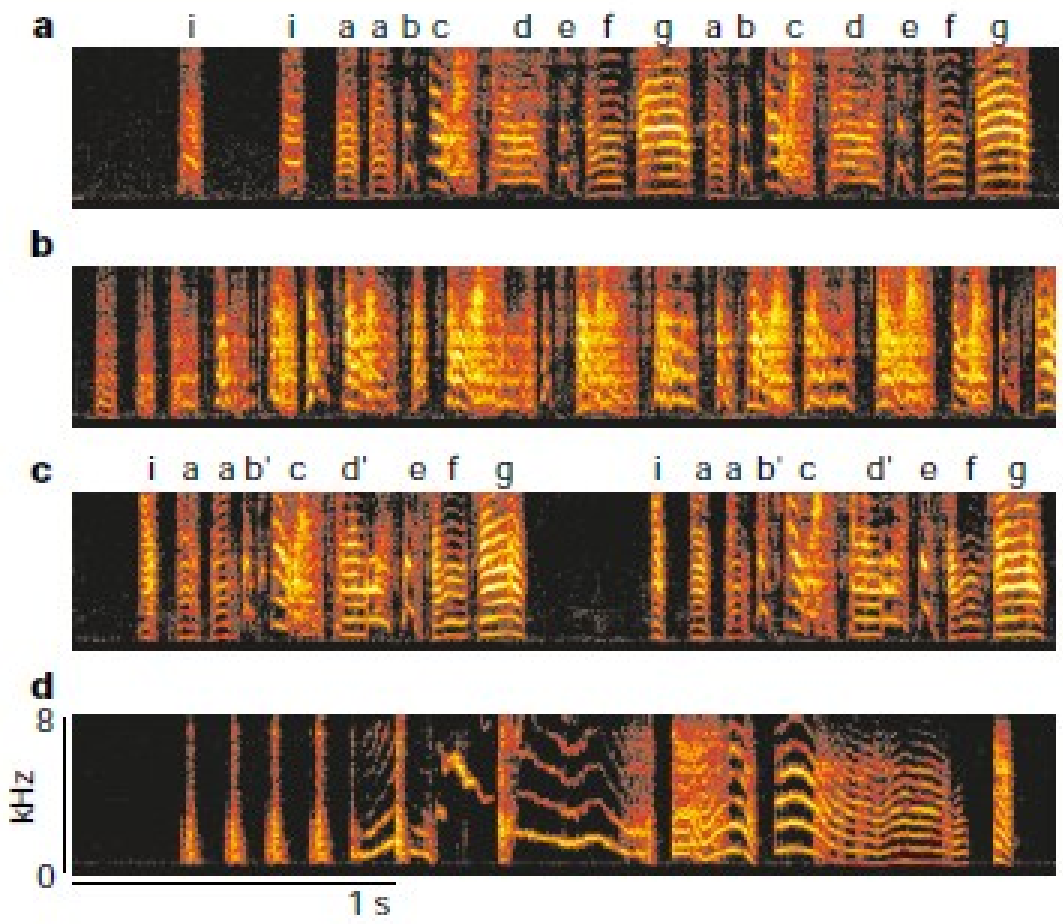
a
i i a a b c d e f g a b c d e f g
b
c
i a a b' c d' e f g i a a b' c d' e f g
d
8
kHz
0
1 s

2. The ability to compare their vocalizations to that of the tutor song memory, using auditory feed-back in order to detect vocal errors
3. When these mistakes are detected, the ability to (accurately) correct them by modifying produced song (adapted from (Mooney, 2009b))

During sensorimotor learning, young birds gradually match their own song to the memorized tutor song. This phase of learning is comprised of several stages. Subsong, which is the equivalency of babbling in babies, bears very little resemblance to that of the tutor song. As young zebra finches grow older, they begin to produce notes and syllables that are recognizable from the tutor's song, but greatly vary in structure and syntax from one song to the next. This is referred to as plastic song. After many weeks of singing practice, the bird's song undergoes crystallization changes that render songs that are extremely high in fidelity (but not always a 100 % copy, as birds are prone to making mistakes just like everything else in nature). Thus, the song produced during this period contains notes and sequence structures that vary greatly in the beginning, but gradually crystallizes with the onset of adulthood. Auditory feedback is essential for evaluating differences between its song and the template, as juvenile zebra finches deafened after song tutoring subsequently develop low-stereotypy (a high variability in syllable production and order) songs (Mooney, 2009b). Thus, sensorimotor learning exhibits a great deal of striking features, two of which are sensory encoding of the tutor song, and a cooperation of sensory and motor learning guided by auditory feedback (Mooney, 2009b).

Functional Anatomy of Song Learning

In zebra finches, song acquisition involves a group of interconnected brain regions that are specialized for learning and producing song called the song system (Figure 1.8). The song system is divided into two separate pathways, one that is required throughout a zebra finch's life for producing normal song (song motor pathway), and one that resembles the mammalian basal ganglia pathways that is involved in juvenile song learning (anterior forebrain pathway) (Nottebohm et al., 1990; Nottebohm et al., 1982). The song motor pathway spans from the telencephalon to the brainstem vocal respiratory organs. HVC and the robust nucleus of the archistriatum (RA) are the main nuclei that comprise this pathway. HVC, the apex of the song motor pathway, projects to RA, and is where auditory information merges with song-motor representations in the brain. Additionally, HVC is important in generating time signals for song (Mooney, 2009b). Recurrent pathways from the brainstem to HVC also contribute to song patterning (Ashmore et al., 2005). RA directly innervates the brainstem vocal/respiratory system, thus neurons in this area generate signals that drives related neurons (e.g. X II ts motor neurons) during singing. In contrast to the slow-firing neurons that project from HVC to RA, neurons within RA fire up to 10 times per song motif. Experts hypothesize that the RA transforms the timing signals generated from HVC into a more specific signal that parallels more with the acoustic features of the bird's song (Leonardo and Fee, 2005). The AFP, on the other hand, bisects the telencephalon and striatum, and is comprised of two regions: lateral magnocellular nucleus of the anterior neostriatum (lMAN) and Area X. lMAN, which projects to Area X, is responsible for integrating different sensory modalities that strengthen song learning; specifically, lMAN

Figure 1.8. Auditory and vocal pathways of the songbird brain within the context of the new consensus view of avian brain organization. Only the most prominent and/or most studied connections are indicated. a) The auditory pathway. Most of the hindbrain connectivity is extrapolated from non-songbird species. For clarity, reciprocal connections in the pallial auditory areas are not indicated. b) The vocal pathways. Black arrows show connections of the posterior vocal pathway (or vocal motor pathway), white arrows indicate the anterior vocal pathway (or pallial–basal ganglia–thalamic–pallial loop) and dashed lines show connections between the two pathways. [Taken with permission from Jarvis et al., 2005].

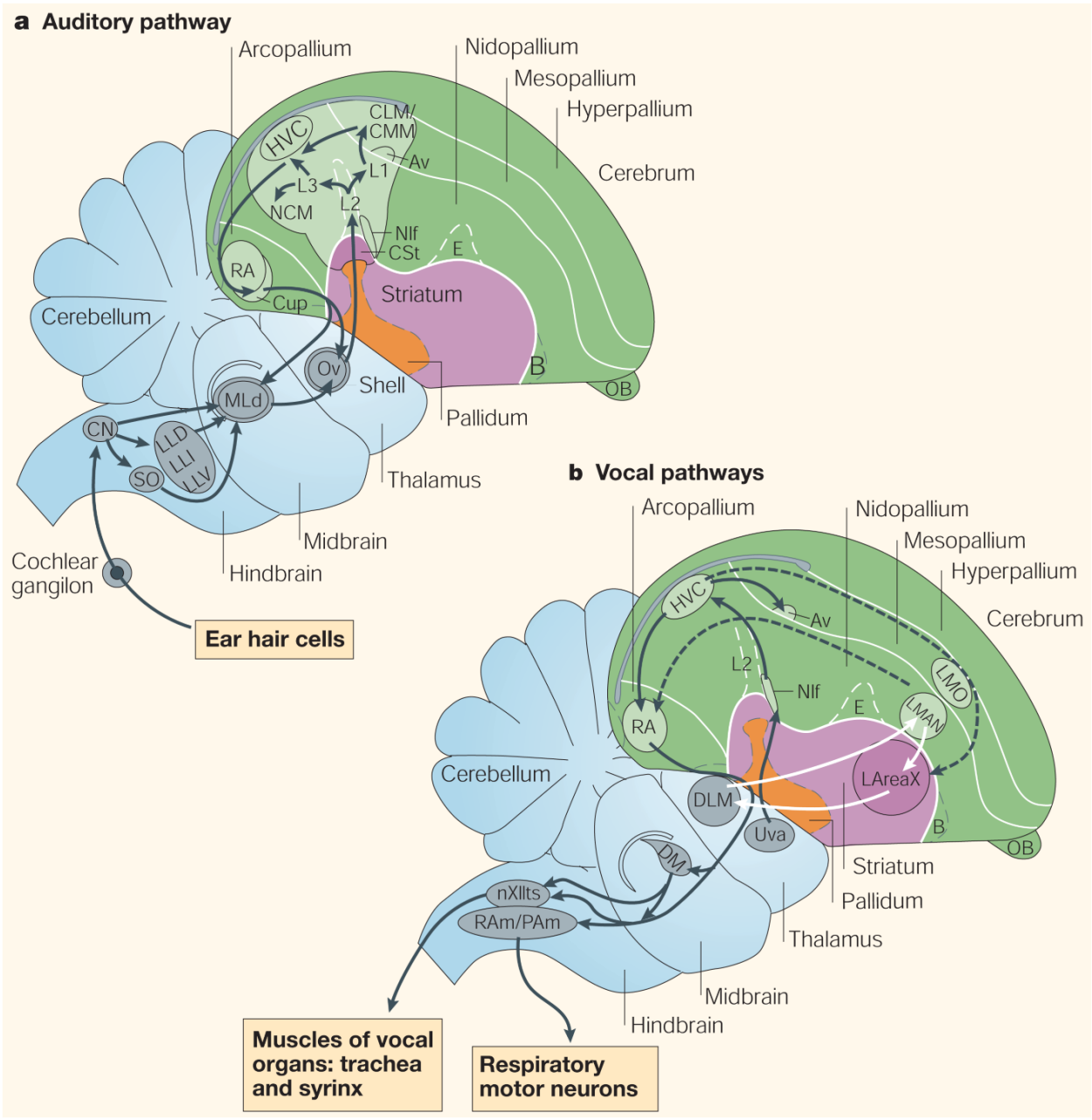
a Auditory pathway
Arcopallium
Nidopallium
Mesopallium
Hyperpallium
Cerebrum
HVC
CLM/
CMM
Av
L1
L3
L2
NCM
Nlf
CSt
E
RA
Cup
Striatum
Cerebellum
Ov
Shell
B
OB
MLd
Pallidum
CN
LLD
LLI
LLV
SO
Thalamus
Midbrain
Hindbrain
Cochlear
gangilon
Ear hair cells
b Vocal pathways
Arcopallium
Nidopallium
Mesopallium
Hyperpallium
Cerebrum
HVC
Av
L2
Nlf
LMO
E
LMAN
RA
Cerebellum
LAreaX
DLM
Uva
B
OB
DM
Striatum
nXIIts
Pallidum
RAm/PAm
Thalamus
Midbrain
Hindbrain
Muscles of vocal
organs: trachea
and syrinx
Respiratory
motor neurons

aids in producing auditory-dependent song plasticity during vocal learning, and has been implicated in the socialization aspects of song learning. lMAN lesions during sensorimotor development result in perpetual state of plastic song, whereas adult lMAN lesions do not affect song integrity after crystallization (Bottjer et al., 1984a). A few researchers suggest that lMAN projects to RA in order to provide instructive signals to the brain, based on the bird's evaluation of its vocalizations during song learning (Mooney, 2009b). Area X is the mammalian basal ganglia analog within the songbird telencephalon, and has been shown to be necessary for proper song learning, however many other aspects of its function remain unclear at present. Fee and colleagues hypothesize that during learning, medium spiny neurons within Area X receive a global, extremely fast afferent signal that conveys the quality of ongoing song, and then this region computes and generates, based on singing performance, a premotor signal that is transmitted through an AFP accessory region, to produce premotor bias in lMAN. They also hypothesis that since mammalian dopaminergic neurons are responsible for encoding discrepancies between anticipated and actual outcomes, and then sending signals to the basal ganglia that influence plasticity, these neurons may play a vital role in Area X function as well (Fee and Goldberg, 2011).

Neural Representations of Song Memories

In addition to the song system, other accessory auditory regions are important for vocal learning, and memorization of song template. Auditory feedback is relayed to HVC from a thalamic Nucleus Ovoidalis (Ov), to Field L, a primary auditory region, to the caudal medial nidopallium (NCM), a site of experience-dependent plasticity which provides an indirect source of auditory input to the song system. NCM is believed to be

the site of song template storage, as conspecific, novel song can induce IEG expression that negatively correlates with how well the bird recognizes the song (Mello et al., 1992).

Preliminary Observations

In a physiological profile similar to humans, in the past our lab confirmed the expression of CB_1 receptors within analogous areas of the zebra finch telencephalon. This study used male birds reared in naturally-tutored environments; we observed low density CB_1 receptor staining within the four song system regions, accessory auditory regions, subcortical regions and cerebellum during the first 25 days of life, which represents the time at which sensory learning ensues (Figure 1.9). This pattern of receptor expression persists within these regions, but gradually increases in density, and peaks at the onset of sensorimotor learning (from 46 days to 78 days old). As animals reach adulthood and songs crystallize, receptor densities wane significantly. These experiments provided us with crucial information to develop the following hypotheses: 1) The receptor distribution and expression patterns observed throughout vocal development indicate that cannabinoid signaling likely plays a role in sensory perception and learning-related synaptic plasticity, 2) this system is the most active during late postnatal development, and 3) the administration of exogenous cannabinoid agonists during this vulnerable time in development will most likely lead to persistent learning-related disruptions in behavior (Soderstrom and Tian, 2006).

Following these experiments, we tested the third hypothesis, and demonstrated that this phenomenon indeed does occur. Using sibling pairs of young male zebra finches tutored by the same adult male as each other's control,

Figure 1.9. Images (12.5X) of immunohistochemical staining of zebra finch brain with anti-zebra finch CB1 receptor antibody. Sections shown were reacted together. A–D: Parasaggital sections representplanes about 2.5 mm lateral from the midline. Rostral is to the left. [Taken with permission from Soderstrom and Tian, 2006].

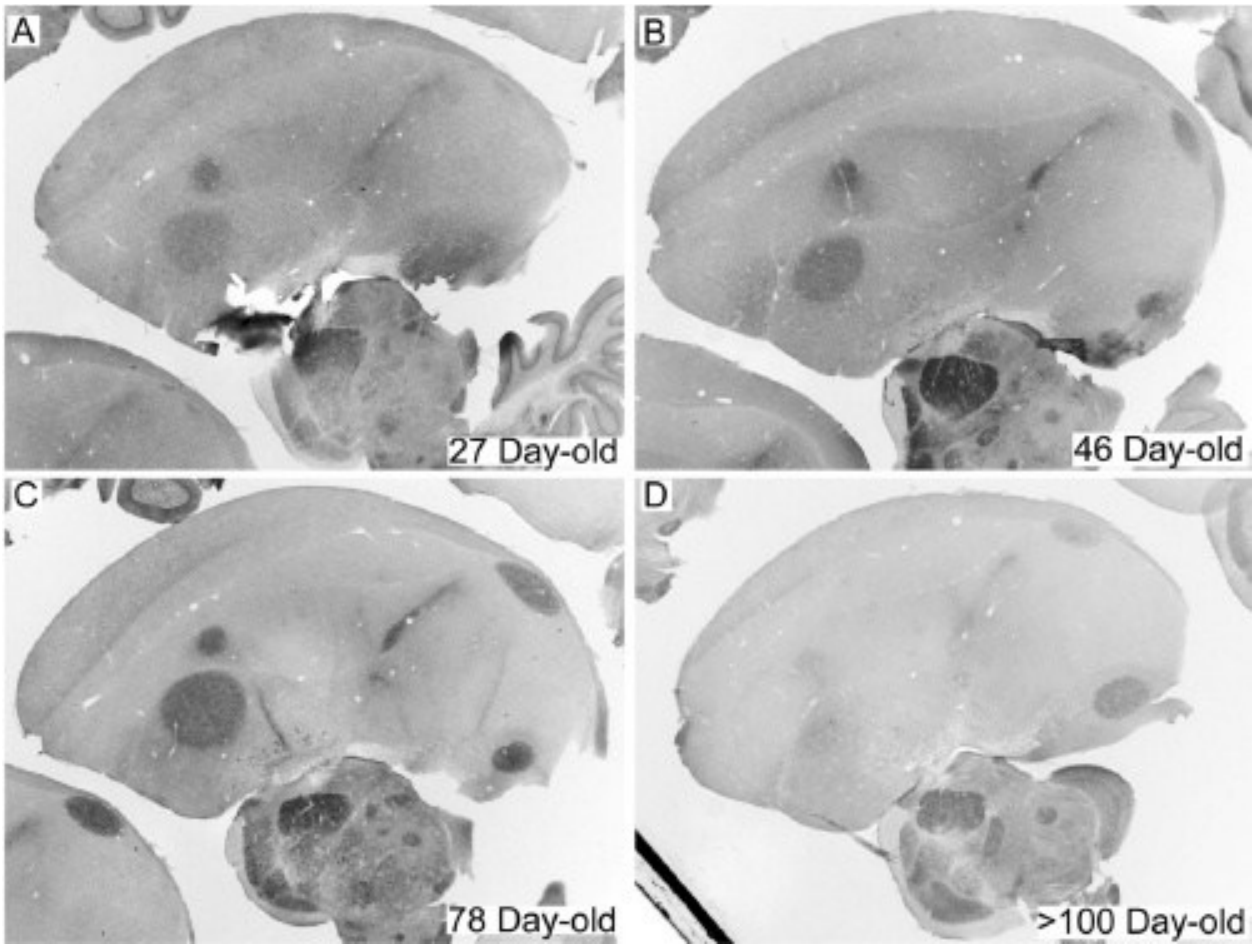
A
27 Day-old
B
46 Day-old
C
78 Day-old
D
>100 Day-old

Figure 1.10. Representative adult song patterns produced by a sibling pair. (a) Vehicle-treated animal B379 and (b) WIN55212-2-treated animal B379. Shown are sonograms produced at 110 days of age. Introductory notes are indicated by ‘i’. Song notes are indicated alphabetically according to order of production by the control animal. A unique note type (with similarities to notes ‘h’ and ‘f’) produced by the WIN55212-2-treated animal is indicated by ‘*’. Evident are fewer note types and decreased stereotypy in the song pattern produced by the WIN55212-2-treated sibling.

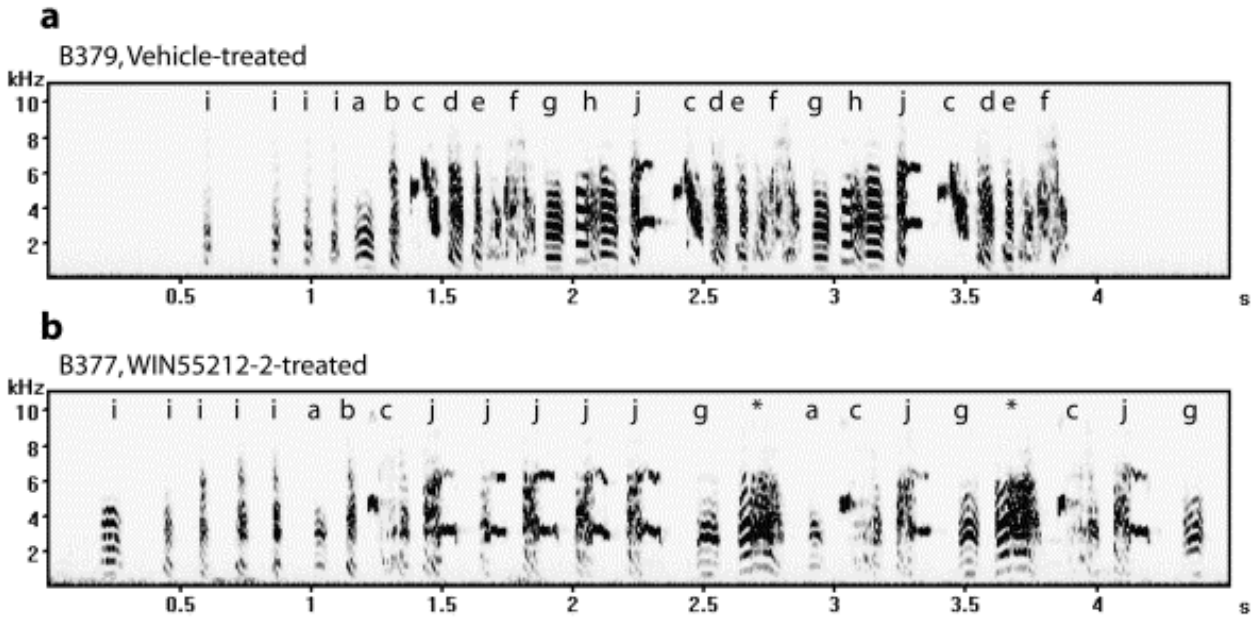
a
B379, Vehicle-treated
kHz
10
8
6
4
2
i i i i a b c d e f g h j c de f g h j c de f
0.5
1
1.5
2
2.5
3
3.5
4
s
b
B377, WIN55212-2-treated
kHz
10
8
6
4
2
i i i i i a b c j j j j j g * a c j g * c j g
0.5
1
1.5
2
2.5
3
3.5
4
s

administeration once daily doses of WIN (1mg/kg) to young zebra finches during sensorimotor development persistently altered the quality of learned song produced in adulthood, specifically via a reduction in the number and order of learned notes produced). Similar to what is seen in humans and rats, and correlating with the previously observed patterns of receptor expression during this time, treatment of adult males that were administered identical treatments of WIN after song learning occurred were rendered ineffective at producing learning-related behavioral effects (Soderstrom 2003).

The Purpose of this Study

As this literature review has shown, adolescent cannabinoid abuse is a great health concern, as regular consumption could potentially hinder the cognitive and physiological development of the brain in manners that persist throughout life. There is a desperate need to understand the molecular mechanisms underlying cannabinoid-interference with the neural growth and rewiring that occurs exclusively during late postnatal development, and how these drugs alter signaling pathways involved in normal processes of learning and memory. The goals of this study are threefold:

- To identify distinct and persistent physiological changes associated with inappropriate CB_1 receptor activation during periadolescent development
- To begin to identify structural proteins and cell signaling involved in these specific changes

These goals were met by pursuing the following specific questions:

1. To what extent does cannabinoid signaling control dendritic spine morphology?

2. Is there a correlation between the behavioral/morphological effects of cannabinoid receptor activation and changes in levels of proteins related to cell signaling and morphology?
3. Can we provide a physiological mechanism by which cannabinoid administration disrupts mechanisms directly related to synaptic plasticity, thus potentially contributing to the altered song learning effect seen?

These questions were answered in the experiments described below

CHAPTER 2: LATE-POSTNATAL CANNABINOID EXPOSURE PERSISTENTLY ELEVATES DENDRITIC SPINE DENSITIES IN AREA X AND HVC SONG REGIONS OF ZEBRA FINCH TELENCEPHALON

ABSTRACT:

Centrally acting cannabinoids are well known for their ability to impair functions associated with both learning and memory but appreciation of the physiological mechanisms underlying these actions, particularly those that persist through life, remains incomplete. Our earlier studies have shown that song stereotypy is persistently reduced in male zebra finches that have been developmentally exposed to cannabinoids. In the present work, we examined the extent to which changes in neuronal morphology (dendritic spine densities and soma size) within brain regions associated with zebra finch vocal learning are affected by late-postnatal cannabinoid agonist exposure. We found that daily treatment with the cannabinoid agonist WIN55212-2 (WIN, 1 mg/kg IM) is associated with 27 % and 31 % elevations in dendritic spine densities in the song regions Area X and HVC, respectively. We also found an overall increase in cell diameter within HVC. Changes in dendritic spine densities were only produced following developmental exposure; treatments given to adults that had completed vocal learning were not effective. These findings have important implications for understanding how repeated cannabinoid exposure can produce significant, lasting alteration of brain morphology, which may contribute to altered development and behavior.

INTRODUCTION

We and others have used zebra finches as an animal model to study neurophysiological processes underlying vocal development because like humans zebra finches undergo vocal learning; the ability to modify vocalizations as a result of experience (Doupe and Kuhl, 1999). This sensorimotor song learning occurs from about 35-75 days of age, a period of late-postnatal development that approximates adolescence. Zebra finch songs are relatively simple and highly stereotyped once crystallized, rendering them easy to analyze and compare across developmental manipulations.

We have previously found that when young zebra finches are exposed to modest dosages of the cannabinoid agonist WIN55212-2 (WIN) during sensorimotor learning, stereotypy of adult song is significantly reduced (Soderstrom and Johnson, 2003; Soderstrom and Tian, 2004). Interestingly, this altered song persists through adulthood, and is not produced following cannabinoid treatment of adults that have already learned song. Currently we are working to identify neurophysiological changes produced by early cannabinoid exposure that are responsible for persistently altered vocal behavior. Developmental periods for learning are often marked by gradual refinements of neural features that reflect both activity-and experience-driven synaptic changes. Earlier studies indicate that songbird vocal learning involves distinct changes in neuronal cell morphology in a number of brain regions; for example, developmental decreases in lMAN dendritic spine densities have been shown to occur between post-hatch day 35 and post-hatch day 65 in male zebra finches raised in normal environments (Changeux, 1997; Changeux and Dehaene, 1989). Furthermore, Rausch and Scheich report that in

young mynah birds trained to imitate human speech, vocal learning is accompanied by significant reductions in spine densities, enlargement of remaining spine heads, lengthened dendrites, as well as gradual increases in perikaryon diameter in HVC (Rausch and Scheich, 1982). Proper vocal learning and processing of sensory information depends upon developmental changes within a number of brain regions (Airey et al., 2000; Devoogd et al., 1985; Lauay et al., 2005), including telencephalic regions lMAN, Area X, HVC and RA that distinctly and densely express CB_1 cannabinoid receptors (Soderstrom and Tian, 2006). Thus, we hypothesized that cannabinoid-altered vocal learning may involve effects on spine densities and neuron size within these song learning and control regions. This hypothesis was tested through the experiments described below.

MATERIALS AND METHODS

Materials

Except where noted, all materials and reagents were purchased from Sigma (St. Louis, MO), or Fisher Scientific (Pittsburgh, PA). The synthetic cannabinoid agonist WIN55212-2 (WIN) used for injections was suspended in vehicle from concentrated DMSO stocks (10 mM). Vehicle consisted of a suspension of 1:1:18 DMSO:Alkamuls EL-620 (Rhodia, Cranberry, NJ):saline.

Animals

The subjects used in these experiments were male zebra finches that were raised in our breeding aviaries. Birds were caged with free access to grit, water, mixed seeds (Sunseed VitaFinch), and cuttlebone, and provided multiple perches. Animals

were maintained in visual isolation on a 14:10 light/dark cycle, and ambient temperature was maintained at 78° F. Birds were housed from 25-50 days of age with an adult male tutor. Birds were cared for and experiments conducted according to protocols approved by East Carolina University's Animal Care and Use Committee.

Treatments

Once daily 50 µl injections of vehicle or 1 mg/kg WIN were administered into the pectoralis muscle in the morning, 30 minutes before lights on for 25 consecutive days, starting at 50 days of age, and ending at 75 days. It has previously been shown that these cannabinoid treatments given during the zebra finch sensorimotor period from 50-75 days permanently alter vocal development (Soderstrom and Johnson, 2003). Following the completion of treatments, animals were allowed to mature to at least 110 days of age in visual isolation. After maturation, animals were killed by Equithesin overdose, and brains prepared for Golgi-Cox impregnation as described below. After analyzing results of this developmental experiment and determination of a significant treatment effect, a second, independent experiment was done using adult animals in order to assess the developmental dependence of treatment effects. This adult experiment was done employing the same regimen of 25 daily treatments given to adult animals (>110 days of age) that had already learned song.

Golgi-Cox Treatments

A mixture containing 5 volumes of 5 % potassium dichromate solution, 5 volumes of 5 % mercuric chloride, and 4 volumes of 5 % potassium chromate solution was prepared and allowed to ripen in the dark five days before use. Following Equithesin overdose, birds were transcardially perfused with phosphate-buffered saline (PBS, pH =

7.4), brains removed and rinsed briefly with ice-cold distilled water, and immersed in a filtered (0.45 micron) aliquot of Golgi-Cox supernatant for 14 days in the dark at room temperature. The brains were then transferred to an ice-cold 30 % sucrose solution for five days. Following sucrose treatment, brains were blocked down the midline, and left hemispheres were sectioned parasagittally on a vibrating microtome. 200 micron sections of zebra finch brain were then gold-toned in order to preserve staining as follows. The sections were exposed to chilled solutions of 80, 60, 40, and 20 % glycerol, rinsed with water, then transferred to a 0.05 % ice-cold gold chloride solution for 80 minutes. After being briefly transferred to an ice-cold 0.2 % oxalic acid solution for two minutes, sections were immersed in 1 % sodium thiosulfate for a total of 60 minutes. The sections were reduced in a 7 % ammonium hydroxide solution at room temperature, in the dark for thirty minutes, followed by further processing in Kodak Fixer. Sections were then mounted and dehydrated on glass slides, and neurons within song regions assessed for dendritic spine densities and average cell diameters as a function of treatment. Tissue was stained and processed in multiple batches; however, in order to eliminate possible variance associated with reaction conditions, each of the treatment groups were represented in each batch.

Light Microscopy

Staining was examined in lMAN, HVC, RA, and Area X at 1000 X with an Olympus BX51 microscope. Images were captured with a Spot Insight QE digital camera and Image-Pro Plus software (Media Cybernetics, Silver Spring MD). Using Image-Pro Plus software, ten grayscale images of individual neurons were captured within each brain region of interest per subject (n = 8 per treatment group). All spines

associated with all visible primary and secondary dendrites emanating from each imaged neuron were counted. Neurons suitable for counting were not obtained within Area X of two animals, reducing the total neurons counted from a planned 1280 to 1260. Average cell diameters and dendritic spine densities of selected neurons were determined as described below.

Measurement of Dendritic Spine Densities

Dendritic spine densities, presented as the average number of spines per length (μm) of each dendrite, were analyzed based on criteria adapted from Norrholm, et al (Norrholm and Ouimet, 2001). Spines along the entire length the primary and secondary dendrites of 10 neurons per each of the 4 representative brain regions of animals treated with both WIN and vehicle (n = 8 for each age group) were counted from captured images. Measurements included all spines observable in each image. Neurons were that were selected for measurement were fully impregnated, intact, located in areas of tissue free of debris and other imperfections, and possessed dendritic processes greater than 20 microns in length. Note that spines within the z-axis were not visible, and therefore were not counted. Thus, our spine density measures are qualitative and not quantitative and therefore only useful for relative comparisons.

Measurement of Cell Body Major Diameters.

The same neurons that were employed for analysis of spine densities were also used to obtain measurements of mean cell body diameter (10 measurements per each of the 4 song regions, for both WIN-and vehicle-treated groups). Given that some neurons tend to be amorphous in shape, mean cell diameter measurements composed of a measured average of both the widest vertical length, and the greatest horizontal

width of each soma. These measures were calculated from the same calibrated, grey-scale images used for counting dendritic spines using Image-Pro Plus analysis software.

Statistical Analyses.

Data analyses were performed using SigmaStat, GraphPad Prism, and Microsoft Excel PC software. Relationships between mean cell diameters, dendritic spine densities and drug treatments were determined through two-way ANOVA with treatment (1 mg/kg WIN vs. vehicle) and brain region (lMAN, HVC, RA, Area X) as factors. Only results relevant to the hypotheses tested (that treatment would affect spine densities and cell diameters) were considered, and all statistics presented refer to effects of treatment only. Following ANOVA determination that dendritic spine densities and cell diameters significantly differed across treatments ($p \leq 0.05$), Student-Newman-Keuls post-tests were performed.

RESULTS

Dendritic Spine Densities.

Two-way ANOVA revealed that developmental treatment with the cannabinoid agonist WIN resulted in a significant difference in mean dendritic spine densities compared to controls ($F(1,632) = 19.52$; $p \leq 0.01$) Student-Newman-Keuls post-tests revealed that spine densities were significantly higher within Area X (from vehicle control mean = 0.61 ± 0.04 to 0.77 ± 0.05 spines/micron in WIN-treated animals, $q = 4.10$, $p \leq 0.01$) and HVC (from vehicle control mean = 0.36 ± 0.03 to 0.46 ± 0.04 spines/micron in WIN-treated animals, $q = 2.75$, $p \leq 0.05$, see Figure 2.2 A and C).

Spine density differences were not found within the other two song regions examined (lMAN, RA, see Figure 2.2 A and D). In adults, cannabinoid treatment did not result in a significant difference in dendritic spine densities ($F(1,612) = 0.99$; $p \leq 0.01$). The adult dendritic spine densities are summarized in Figure 2.3.

Cell Body Diameters

We found that developmental treatment with WIN resulted in significantly larger average soma sizes as compared to control groups ($F(1,632) = 13.70$; $p \leq 0.01$, see Figure 2.4 panel B); post-hoc analyses further revealed that differences lie within HVC (from vehicle control mean = 9.77 ± 0.50 to 11.80 ± 0.43 microns in WIN-treated animals, $q = 3.58$, $p \leq 0.01$). No differences were observed in other song regions examined (lMAN, RA, Area X, refer to Figure 2.4 panel A, C and D). Interestingly, WIN treatment produced a decrease in mean adult cell diameters within HVC (from vehicle control mean = 12.64 ± 1.17 to 10.22 ± 0.40 microns in WIN-treated animals, $q = 2.85$, $p \leq 0.05$), but was ineffective in lMAN, Area X and RA. The average cell diameters following treatment of adults are summarized in Figure 2.5.

DISCUSSION

Dendritic spines are thought to modulate synaptic signaling by regulating the volume and biochemical content of postsynaptic terminals (reviewed by (Koch and Zador, 1993). Densities of dendritic spines generally decrease with age (reviewed by (Dickstein et al., 2007). For example, in macaque monkeys, spine densities on neurons projecting from temporal to prefrontal cortex were 25 % greater in adolescents (10 – 12 year olds) than adult monkeys (24 – 25 year olds, (Duan et al., 2003). This is in reasonable agreement with the magnitude of persistent cannabinoid-related spine

density elevations that we report here (27 % in Area X and 31 % in HVC). Age-related decreases in spine density appear to be under cellular regulation, and therefore may be considered part of normal late-postnatal development(Lieshoff and Bischof, 2003). This implies that the cannabinoid-related elevation of spine densities that we found within Area X and HVC of adult animals may involve a disregulation of normal development. This contention is further supported by the fact that cannabinoid treatments only maintained elevated dendritic spine densities following developmental exposure; treatments administered to adults were ineffective.

The dynamics of dendritic spine formation and loss in vertebrate brain change over the course of development (Bhatt et al., 2009). During normal development, growth factors (BDNF and NT4/5) stimulate proliferation of spiny dendrites (Wirth et al., 2003). A fraction of these spines are subject to elimination during late-postnatal CNS development, a process that is completed prior to adulthood. Adulthood is associated with increased stability of dendritic spine number (Zuo et al., 2005). The mechanisms for these dynamic, developmental activity-dependent changes are not completely understood, but increasing evidence points to effects of calcium and related kinase signaling cascades (reviewed by (Bloodgood and Sabatini, 2007). The CB_1 cannabinoid receptor (that is likely responsible for the effects reported herein) is thought to be primarily coupled to $G_{i/o}$ G-protein subtypes that inhibit adenylyl cyclase, reducing intracellular concentrations of cAMP, that, in turn reduces activity of cAMP-dependent protein kinase (PKA). In neurons, PKA is known to activate ryanodine receptor channels that release calcium from intracellular stores (Zhuang et al., 2005). Thus, the established intracellular signaling pathways associated with cannabinoid agonism are

well-positioned to disregulate the calcium-dependent signaling involved in spine regulation. The emerging view is that a finite range of calcium concentrations promote spine maintenance; disregulation to levels outside this range, either greater or less than, results in resorption or pruning (Dur et al., 2011; Holthoff et al., 2002; Segal et al., 2000). Thus, it seems reasonable to suggest that activation of a potential postsynaptic population CB_1 receptors, and resulting inhibition of calcium release from intracellular stores, may inappropriately maintain spines that would normally be pruned due to elevated intracellular calcium. It may also be the case that a presynaptic population of CB_1 receptors is responsible for the elevated spine densities observed, as cannabinoids are established to act presynaptically to inhibit transmitter release in many other systems (Elphick and Egertova, 2001b). Reduced transmitter release may alter signaling patterns and potentially disrupt activity-dependent spine regulation.

Because spine dynamics are tied to altered synaptic activity, including long-term potentiation (LTP) and depression (LTD, (Feldman, 2009), they are implicated in cellular mechanisms of learning and memory. Thus, cannabinoid-altered vocal development may follow disregulation of memory retrieval of song templates, or impaired sensorimotor consolidation caused by inappropriately elevated dendritic spine densities. Selective maintenance of elevated spine densities within a subset of telencephalic song regions may provide insight into the mechanism of cannabinoid-altered vocal development. Within rostral striatum, Area X is clearly critical for song learning (Bottjer et al., 1984b), but not necessary for production of adult song that has already been learned (Scotto-Lomassese et al., 2007; Sohrabji et al., 1990). This implies that activity within Area X is necessary for forming the long-term memory or ‘template’ of the tutor’s

song that is accessed and practiced during sensorimotor development. Because the treatments in our experiments were administered after tutoring was complete, it's unlikely that altered template encoding was involved. Thus, if disregulation of Area X development is involved in cannabinoid-altered vocal development, the mechanism is more likely related to real-time sensorimotor comparison of practiced song with the previously memorized template; a process involving both memory retrieval and sensory integration. The importance of Area X in this process is suggested by a correlation of the amount of singing during sensorimotor learning with distinct expression of the vocal development-critical transcription factor, FoxP2 (Teramitsu et al., 2010). HVC, on the other hand, is necessary both for learning and motor production of song and links the rostral vocal motor pathway to the anterior forebrain pathway that is critical for song learning (Margoliash, 1997). Ablation studies involving HVC have demonstrated that this region is essential for production of a stereotyped song (Thompson and Johnson, 2007) and HVC clearly contributes to both temporal and spatial aspects of song (Margoliash, 1997). Thus, differences in neuronal activity associated with persistently increased dendritic spine densities within HVC suggest a mechanism by which developmental cannabinoid exposure alters vocal learning and decreases song stereotypy through adulthood.

Each of the telencephalic regions that we have studied have been the subject of other spine density studies, although ours is the only one to include all four as part of a single study. For example, in eastern marsh wrens, spine densities within HVC, but not RA, are directly related to the complexity of song repertoires learned. Lower HVC spine densities are associated with smaller repertoires (Airey et al., 2000). Thus, the elevated

spine densities that we have measured following cannabinoid treatment are consistent with the learning of high-complexity songs, which seems to contrast with the characteristic reduction in the number of notes learned by cannabinoid-treated zebra finches (Soderstrom and Johnson, 2003). This apparent conflict may indicate that there is a "correct" density of spines that should be maintained to properly learn a particular vocal pattern. Inappropriate densities, either greater or less than those necessary for learning a particular song, may result in impairment.

Other regions, including lMAN, have received attention in the context of sex differences, as lMAN is a song region readily detectable in females. Normal development in males is associated with a decrease in dendritic spine densities within lMAN (Nixdorf-Bergweiler, 2001), while males raised without exposure to a tutor during development maintain high spine densities (Wallhausser-Franke et al., 1995), suggesting that the process of learning a particular song is associated with decreased spine densities. Because we did not detect a treatment effect within lMAN, this suggests that cannabinoid-altered song is mechanistically distinct from that following isolation.

Vocal developmental-related changes in dendritic spine densities within Area X have been studied by others in the context of FoxP2-dependent reductions (Schulz et al., 2010). This recent report demonstrates that shRNA-inhibition of FoxP2 expression in Area X is associated with a premature decrease of dendritic spine densities. FoxP2 is normally upregulated during periods of sensorimotor learning (e.g. 50 days, see (Haesler et al., 2004), a developmental period that is also associated with distinctly high-level CB_1 receptor expression (Soderstrom and Tian, 2006). We have found

previously that FoxP2 expression within zebra finch striatum is persistently increased, through adulthood, following the same cannabinoid treatment regimen used in our current report (Soderstrom and Luo, 2010). Therefore it seems reasonable that cannabinoid-induced persistently-increased FoxP2 expression may play a role in the elevated dendritic spine densities within Area X reported herein.

Another recent and particularly elegant 2-photon imaging study has measured the turnover rate of dendritic spines within HVC as a function of tutor song exposure (Roberts et al., 2010). As discussed above, spine dynamics change during development, with maturation associated with reduced turnover (Zuo et al., 2005). Thus it appears that tutor exposure, and the associated memorization of a song template, induces a stabilization of dendritic spine densities early in auditory vocal development. Assuming that Area X- and lMAN-like decreases in spine densities also occur within HVC following the sensorimotor stage of song learning through adulthood, a second pruning stage must follow spine stabilization associated with auditory learning. If this is the case then (as indicated above for lMAN) cannabinoid-altered vocal development must be mechanistically distinct from effects produced by social isolation, as lack of a tutor decreases HVC spine densities measured in adults (by 24 %, (Lauay et al., 2005). Combined with our findings, this suggests that normal vocal development is associated with finite range of dendritic spine densities within HVC, as both increased and decreased densities are associated with altered song learning.

Developmental changes in neuronal cell diameters have not received a great deal of experimental attention. In hamsters and mice, telecncephalic neuron diameters increase from birth through approximately adolescence, after which a plateau is

reached that lasts through adulthood (Haddara, 1956; Ptacek and Fagan-Dubin, 1974). Thus, our finding of cannabinoid-related increased cell diameters within HVC may represent an extension of normal developmental increases and/or inhibition of initiating the plateau phase. The HVC-selectivity of this effect suggests that it isn't attributable to elevated spine densities, as these also occurred within Area X (e.g. compare Figure 2.2 B and C with Figure 2.4 B and C). Selective cannabinoid effects within song regions of caudal telencephalon (HVC and RA) and not rostral regions (lMAN and Area X) have been previously reported in the context of c-fos expression (Soderstrom and Tian, 2008), and suggest distinct cell-signaling roles for the population of CB_1 receptors present within each region. Decreased mean HVC cell diameter was the only persistent effect that we observed following adult treatments and represents an interesting contrast to effects produced following developmental treatments. We know that the developmental treatment regimen employed persistently reduces anti-CB_1 receptor immunoreactivity within HVC, while the same treatment in adults increases it (see(Soderstrom et al., 2011)). Therefore, the differential efficacy of developmental vs. adult treatments on HVC cell diameters may involve distinct receptor expression densities.

In summary, repeated exposure to modest dosages of a cannabinoid agonist during periods of sensorimotor vocal development results in elevated dendritic spine densities within two song regions of zebra finch telencephalon: Area X and HVC, brain regions important to vocal learning and production. Additional effects to increase neuronal cell diameters within HVC were noted. These persistent physiological changes may contribute to the reduced stereotypy and note numbers produced by zebra finches

treated with cannabinoids during the sensorimotor stage of vocal development (Soderstrom and Johnson, 2003; Soderstrom and Tian, 2004). Because these effects were only observed following treatment of animals in sensorimotor stages of development, our results contribute to accumulating evidence for distinct, late-postnatal cannabinoid sensitivity within the developing CNS that may alter developmental course. This underscores the problem of cannabis abuse among adolescents, and provides insight to mechanisms that may underlie associated persistent alterations of learning and other behaviors.

Figure 2.1. Representative image of Golgi-Cox impregnated spiny dendrites used for analysis within HVC of birds developmentally treated from 50 - 75 days of age with WIN (A), or vehicle (B). Animals were allowed to mature to adulthood (> 110 days), and brains were dissected and stained with Golgi-Cox solution (see Methods). Bar = 10 microns. (C) Representative high power image of a typical HVC neuron used for analysis. Measurements pertaining to cell diameters and corresponding dendrites were made for 10 randomly selected neurons for each of the 4 representative song regions of both WIN and vehicle-treated animals. Bar = 30 microns.

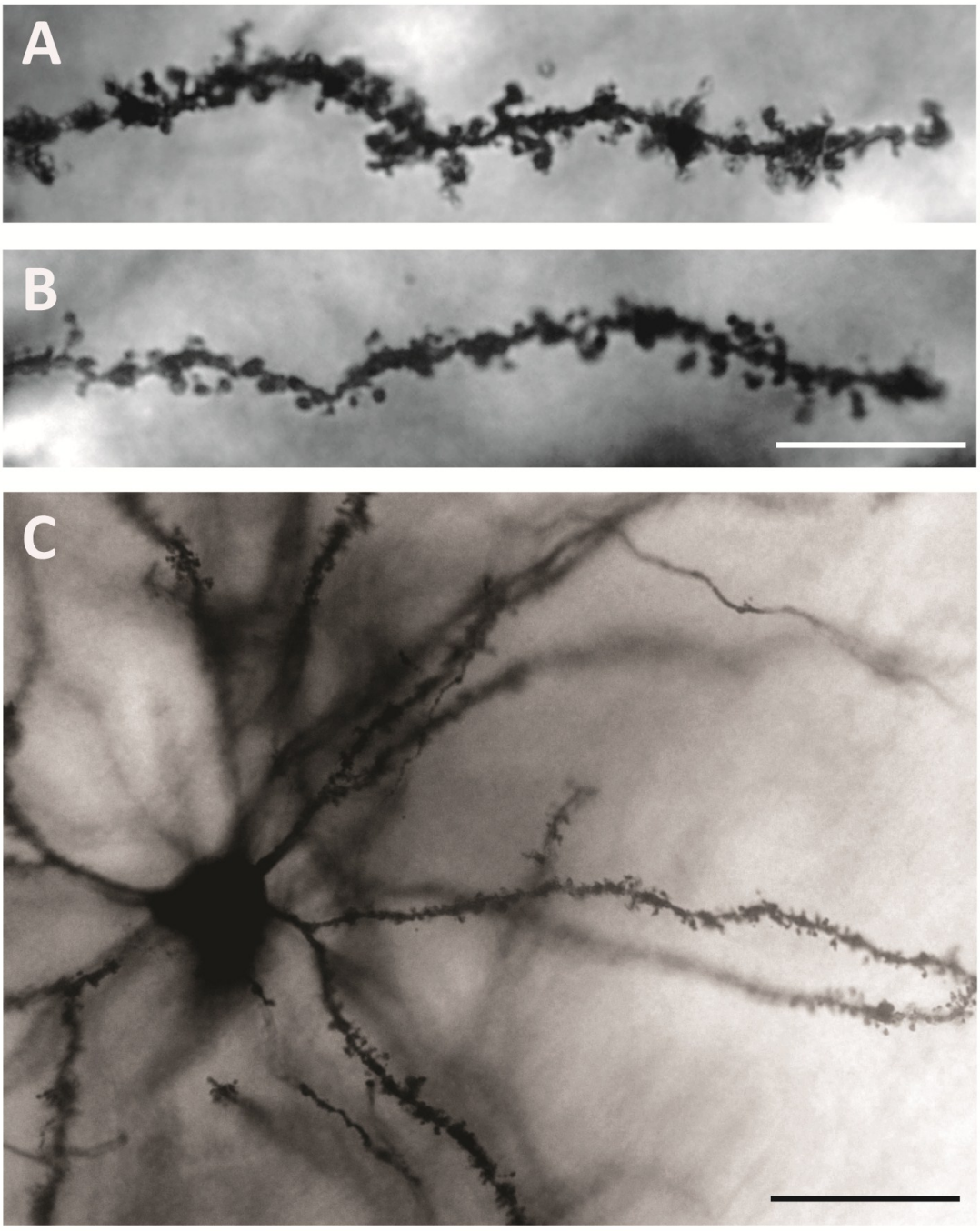
A
B
C

Figure 2.2. Effect of developmental treatments from 50 – 75 days on song region spine densities at adulthood (n = 8). Developmental WIN treatment resulted in significantly elevated dendritic spine densities within Area X and HVC but not lMAN or RA. ($p \leq 0.05$).

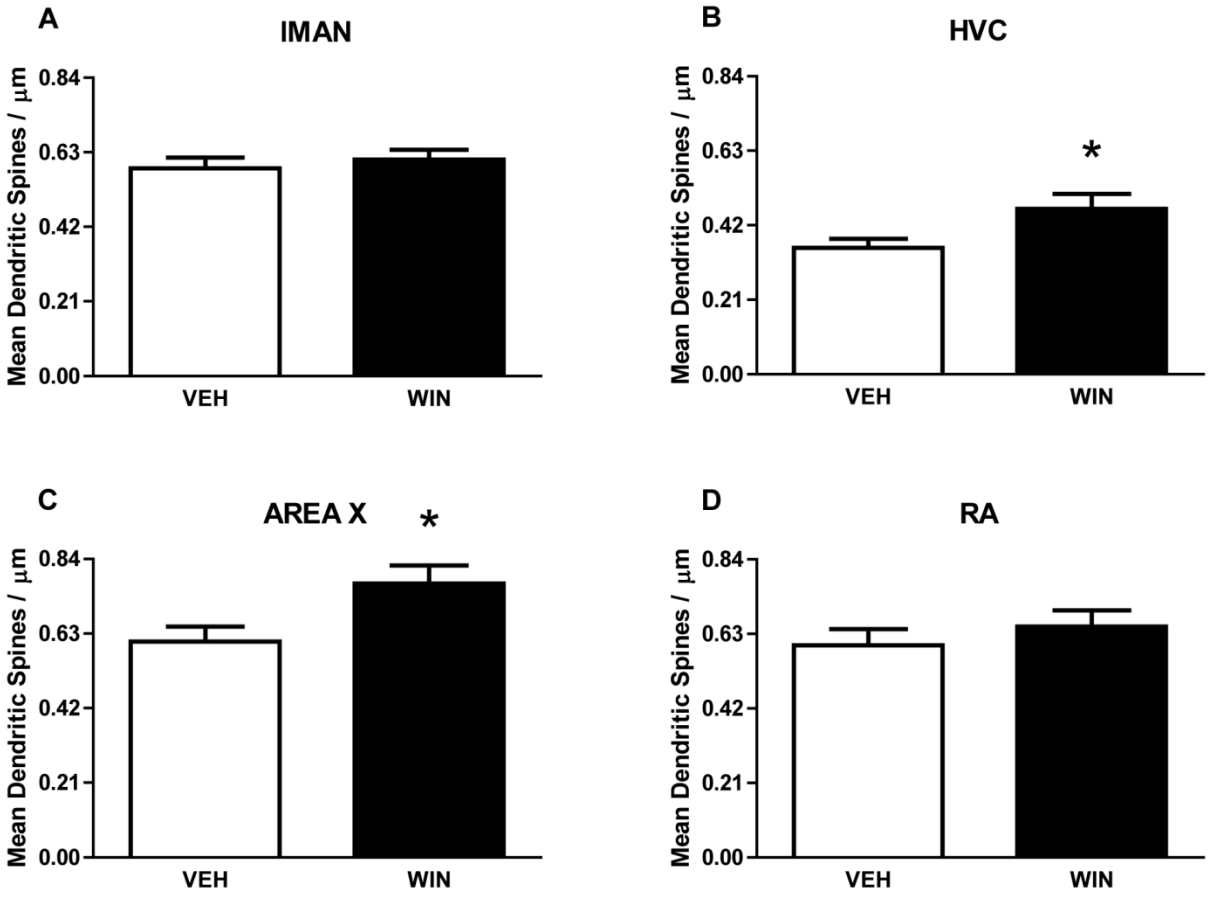
Adult Spine Densities After Developmental WIN Treatment From 50 - 75 Days
A
IMAN
B
HVC
C
AREA X
D
RA
Mean Dendritic Spines / µm
0.84
0.63
0.42
0.21
0.00
VEH
WIN
*

Figure 2.3. Effect of treatments given to adults for 25 days on song region spine densities (n = 8). WIN (1 mg/kg/day) did not result in a significant change in dendritic spine densities in the four song regions of adult males which had already learned song.

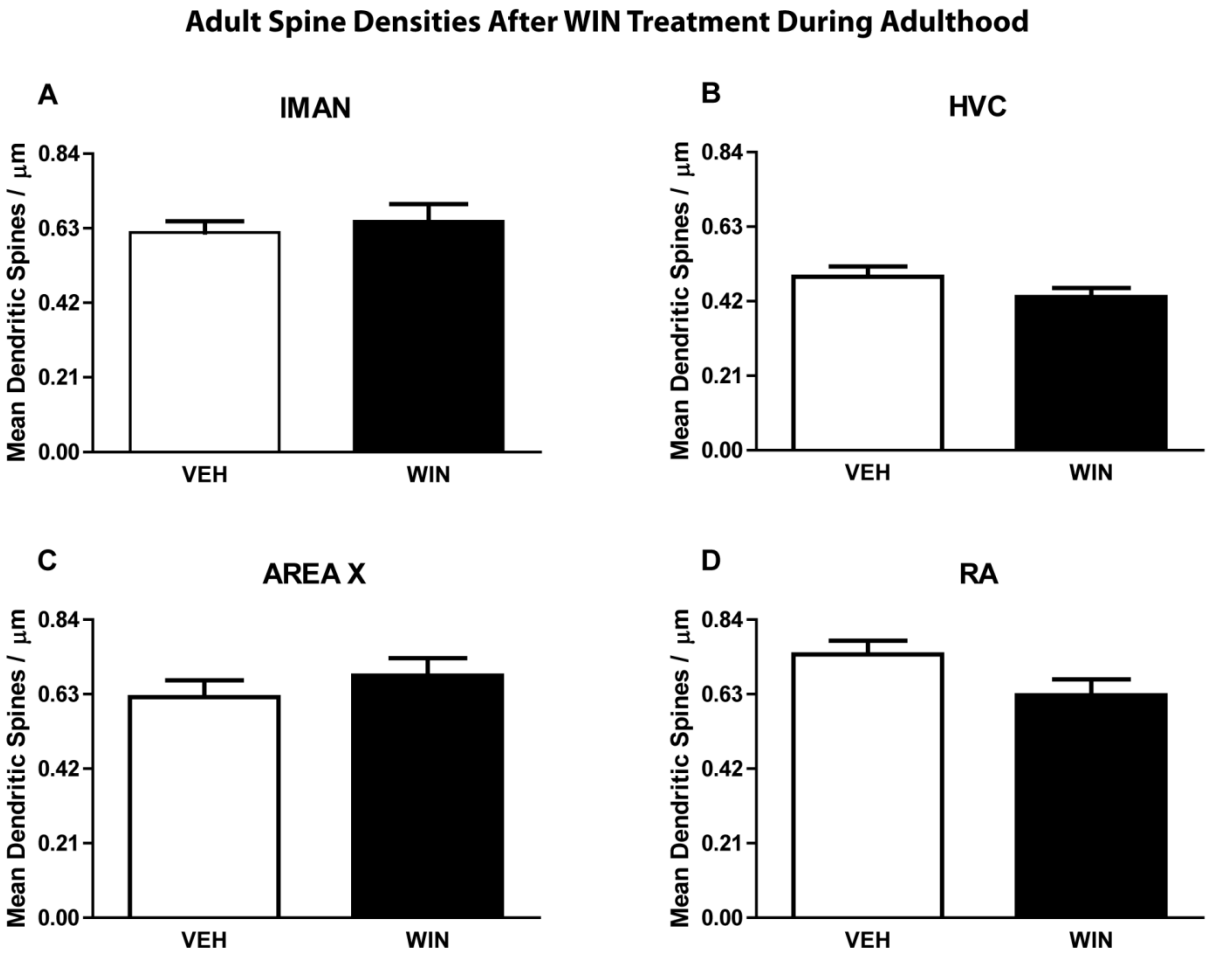
Adult Spine Densities After WIN Treatment During Adulthood
A
lMAN
B
HVC
C
AREA X
D
RA
Mean Dendritic Spines / µm
0.84
0.63
0.42
0.21
0.00
VEH
WIN

Figure 2.4. Effect of developmental treatments from 50 – 75 days on song region average cell diameter at adulthood (n = 8). Developmental WIN treatment (1 mg/kg/day) resulted in significantly increased average cell diameter within HVC, but not other regions (lMAN, Area X, HVC, $p \leq 0.05$).

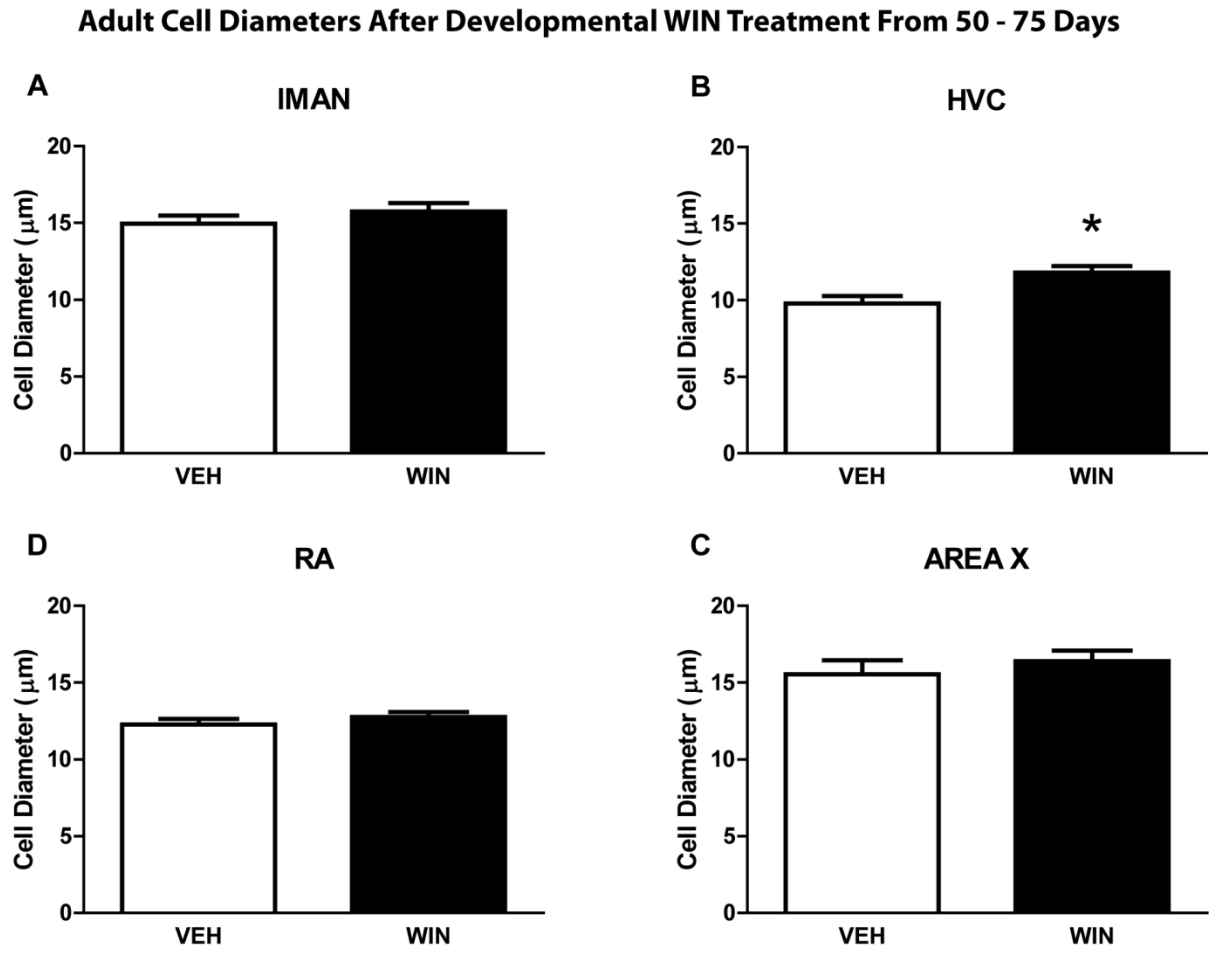
Adult Cell Diameters After Developmental WIN Treatment From 50 - 75 Days
A
IMAN
B
HVC
D
RA
C
AREA X
Cell Diameter (μm)
0
5
10
15
20
VEH
WIN
*

Figure 2.5. Effect of treatments given to adults for 25 days on song region average cell diameter at adulthood (n = 8). Despite a trend for decreased cell diameter within HVC, significant differences were not found.

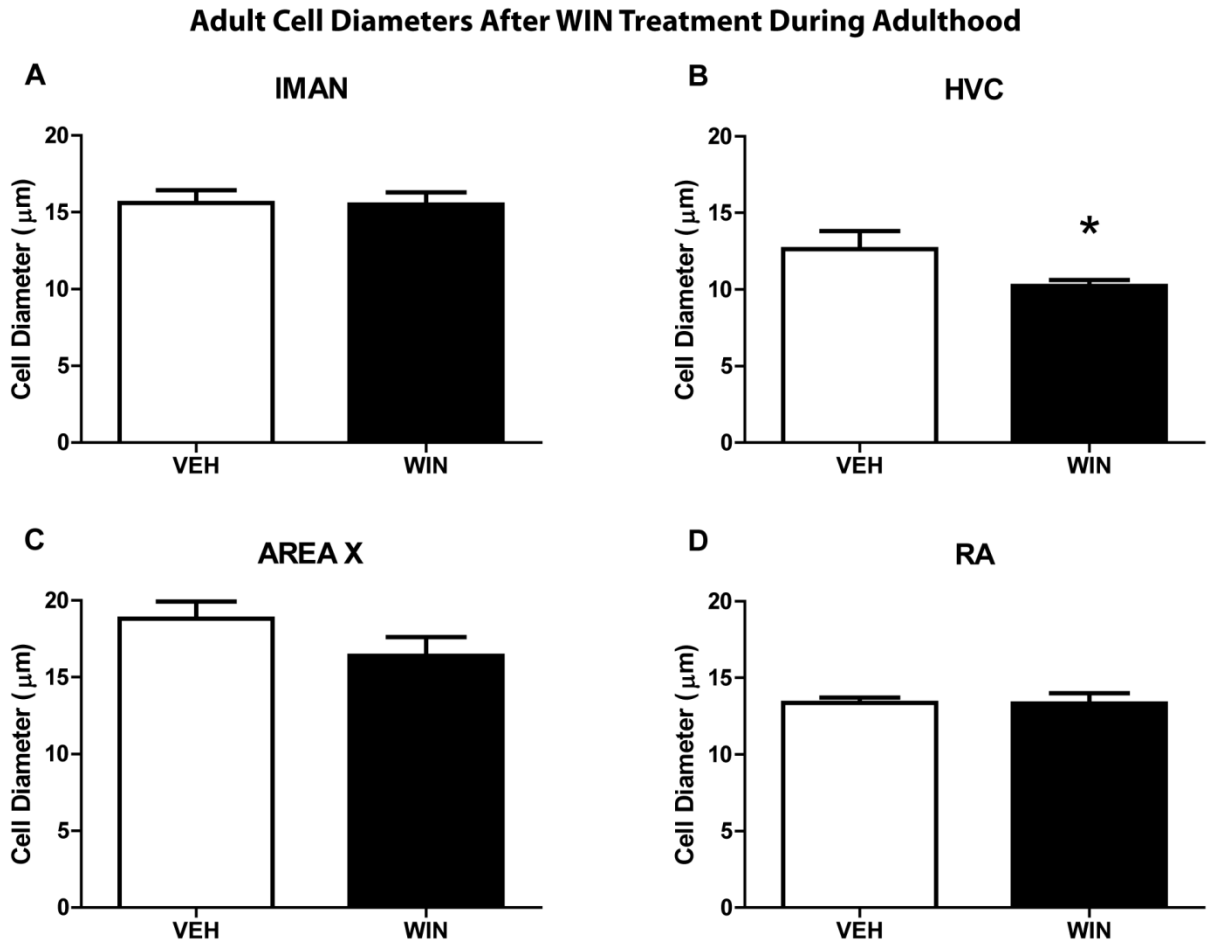
Adult Cell Diameters After WIN Treatment During Adulthood
A
IMAN
B
HVC
C
AREA X
D
RA
Cell Diameter (μm)
0
5
10
15
20
VEH
WIN
*

CHAPTER 3: CANNABINOID TREATMENT DURING ADOLESCENT DEVELOPMENT PERSISTENTLY ALTERS AXONAL PHOSPHORYLATED NF-200 AND DENDRITIC MAP2 EXPRESSION IN BRAIN REGIONS IMPORTANT FOR VOCAL LEARNING

ABSTRACT:

The contributions of cannabinoid signaling to learning and memory are multifarious, making it difficult to pinpoint underlying mechanisms responsible. Previously, we demonstrated that developmental cannabinoid administration impairs vocal learning and reduces the expression of neural correlates of long-term potentiation, memory formation and perception in the zebra finch song learning model. These alterations are associated with elevated dendritic spine densities that suggest lack of plastic changes associated with learning in a subset of brain regions important to vocal learning and control, and where the CB_1 receptor is expressed in high density. In this study, gross morphological and densitometric changes in axonal marker Nf-200 and dendritic marker MAP2 were analyzed following developmental treatment with the $CB_{1,2}$ agonist WIN55,212-2 (WIN), with the hypothesis that developmental cannabinoid treatment is associated with an increased expression of both phosphorylated Nf-200 and MAP2. Following WIN treatment, significantly elevated Nf-200 densities were observed within three of four song control regions (HVC, RA, Area X) as opposed to vehicle treatments, but not in the midbrain, indicating a persistent telencephalic misaccumulation of axonal protein within these areas. Developmental treatment with WIN led to robust increases in MAP2 expression and irregular morphology in Area X, HVC, RA, IMAN as well as midbrain region DLM, indicative of disregulated CNS development and altered dendritic function. Cannabinoid treatments administered to

adult control animals that previously learned song were ineffective. These results further support our previous data and hypothesis that cannabinoids persistently alter gross neuronal morphology, and contribute to altered vocal learning, memory and developmental effects seen.

INTRODUCTION

The 2012 world drug report by the United Nations Office on Drugs and Crime states that cannabinoids, specifically marijuana, are the most widely used illicit drug in the world (Nations, 2012). Cannabinoid receptors are the most abundant G-protein coupled receptor in the brain, and consequences of their activation vary from pleasurable subjective effects such as increased sensations of tranquility, analgesia, euphoria, and anxiolysis along with altered memory formation, respiratory function, sensory perception, and coordinated movement (Ameri, 1999; Herkenham et al., 1990; Pini et al., 2012). Moreover, the cognitive impairments produced by cannabinoids and other drugs (alcohol, cocaine) were reported to be additive (Schulze et al., 2012). Changes in behavior and function are often preceded by morphological change. Given the ubiquity of these agents and receptors within the brain and other body systems, the overwhelming effects that cannabinoids have on cognition and behavior, and the wide usage amongst periadolescents and adults, more research is needed in order to better clarify the specifics of cannabinoid-altered physiology.

Our previous work has demonstrated that when young male zebra finches are administered a once-daily dose of the cannabinoid agonist WIN 55,212-2 (WIN, 1.0 mg/kg) during the developmental period in which they learn song, the stereotyped order in which these learned notes are produced during adulthood is persistently disrupted

(Soderstrom and Johnson, 2003; Soderstrom and Tian, 2004). This altered pattern of song production is not seen in adults that had previously learned song. These observations are correlated with inappropriate maintenance of dendritic spine densities within song regions HVC and Area X, which normally occur during learning (Gilbert and Soderstrom, 2011). These regions (including but not limited to lMAN, RA, Ov, and cerebellum) distinctly and robustly express CB_1 receptors during sensorimotor learning (Soderstrom and Tian, 2006). However, the current understanding of the role(s) of cannabinoid signaling is limited: clearly, a vast neurochemical system involving CB_1 receptor activity exists within the developing brain, but to what degree does this influence CNS neuronal morphology, and ultimately behavior? Moreover, what are the physiological features and processes under the control of cannabinoid signaling during this period? We argue that persistent deficits in song learning and production seen during cannabinoid-altered vocal development involves cannabinoid-altered disruption of protein expression vital for proper neuronal cytoarchitecture and function, specifically phosphorylated 200 kDa neurofilaments (Nf-200) and microtubule-associated protein 2 (MAP2). This contention is consistent with our hypothesis that endogenous cannabinoid signaling is not only a part of, but is essential to normal CNS development and function.

MATERIALS AND METHODS

Materials

Except where noted, all materials and reagents were purchased from Sigma (St. Louis, MO), or Fisher Scientific (Pittsburgh, PA). Immunochemicals were purchased from Vector Laboratories (Burligame, CA). The primary anti-phosphorylated Nf-200 and MAP2 monoclonal antibodies were purchased from Sigma (St. Louis, MO). Equithesin

was prepared from reagents (40% propylene glycol, 10% ETOH, 5% chloral hydrate, 1% pentobarbital). The synthetic cannabinoid agonist WIN 55212-2 was suspended in vehicle from concentrated DMSO stocks (10 mM). Vehicle consisted of a suspension of 1:1:18 DMSO:Alkamuls EL-620 (Rhodia, Cranberry, NJ):phosphate-buffered saline. Dose was corrected for the free base form of the drug

Animals

Both juvenile and adult male zebra finches bred and raised in our aviary were used as subjects in these experiments. Young birds were tutored by an adult male. After tutoring, birds were removed to visual isolation to prevent possible cross tutoring. From three days prior to the start of experiments until the end of experiments, birds were housed singly in visual isolation with free access to grit, water, mixed seeds (Sunseed Vita Finch), and cuttlebone, and provided multiple perches. Animals were maintained on a 14:10 light/dark cycle, and ambient temperature was maintained at 78° F. All experiments were approved by the Institutional Animal Care and Use Committee of East Carolina University.

Treatments

Once daily drug treatments of either vehicle or WIN 55,212-2 were administered via 50µl IM injections into either the right or left pectoralis muscle for 25 consecutive days, 30 minutes before lights on, starting at 50 days of age, and ending at 75 days. Injection sites were alternated daily (eg. day 1 right muscle, day 2 left muscle) in an effort to minimize damage to the skin, protect the administration route, and minimize discomfort. This cannabinoid treatment given during the zebra finch sensorimotor period from 50 to 75 days will permanently alter song learning and vocal development (Gilbert

and Soderstrom, 2011, Soderstrom and Johnson, 2003). Following the completion of treatments, animals were allowed to mature to at least 110 days of age in visual isolation.

Western Blotting

The presence of phosphorylated Nf-200 and MAP2 protein was detected within the zebra finch brain by using mouse monoclonal antibodies targeting phosphorylated Nf-200 and MAP2, respectively. To assess the selectivity of these antibodies against zebra finch protein, western blotting experiments were performed. Protein extraction protocols were adapted from methods described by Schafer and colleagues, (1998). Adult male zebra finches, subjected to song stimulation procedures described above, were killed by Equithesin overdose. Brains were removed, homogenized with a polytron in an ice-cold extraction buffer containing 1 M Tris-HCl, pH = 7.0, 0.6 M KCl, 0.5 mM ATP, 1 mM DTT, 0.5 mM $MgCl_2$, along with a cocktail of protease inhibitors (0.25 M sucrose/1 mM EDTA/4 mM phenylmethylsulfonyl fluoride/1 mM 4-amino benzamidine/0.1 % w/v bacitracin), and briefly micro-centrifuged at *1000 x g.* Supernates were stirred on ice for 30 min, collected and centrifuged at *24,000 x g*. Following this, protein preps were ultra-centrifuged at *100,000 x g* for 1 hour. Pellets were discarded and supernatants were filtered through cheesecloth to remove traces of excess lipid, and dialyzed against 10 L of ice-cold distilled water for 4 hours at 4º C. The fractions were then dialyzed overnight against two changes of ice-cold extraction buffer containing 10 mM Tris-HCl, pH 8.0, 0.2 mM $CaCl_2$, 0.5 mM ATP, 0.1 mM DTT, 100 mM KCl, and 0.1 mM phenylmethylsulfonyl fluoride. Samples were spun a final time at 24,000 x *g* at 4º C to remove trace precipitate. Supernatants were collected and protein

concentrations determined using the Bradford method. 30 µg of soluble protein was loaded into a 10 % polyacrylamide gel, separated by SDS-PAGE, and blotted onto a PVDF membrane. Blots were blocked with a non-mammalian blocking reagent (Odyssey Blocking Buffer, LI-COR Biosciences, Lincoln, NE) and incubated overnight at 4º C in a 1:1500 dilution of the phosphorylated Nf-200 or MAP2 antibodies in Odyssey Blocking Buffer. The next day, the blots were washed three times with 1X PBS-T (Phosphate-Buffered Saline [pH = 7.4] with 0.05 % Tween-20), and incubated in secondary antibody solutions containing an infrared anti-mouse secondary antibody at 1:25,000 (IR Dye 800CW Goat α mouse IgG (H + L), LI-COR Biosciences # 926-32210)) and 0.02 % SDS for 2 hours at room temperature in the dark. The blots were washed 4 times with 1X PBS (Phosphate-Buffered Saline [pH = 7.4]) for 10 minutes each, and visualized using the LI-COR Odyssey Infrared Imaging System. Masses of infrared bands were determined via standard curves fit to distances migrated by molecular weight standards using GraphPad Prism 5.0 software (GraphPad Software, San Diego, CA, USA).

Immunohistochemistry

The immunohistochemical methods used in this study were adapted from Soderstrom and colleagues (2006). After the birds reached either maturation of at least 110 days, or the end of experiments, animals were killed by Equithesin overdose (50 µl), PBS transcardially perfused, followed by phosphate-buffered 4% paraformaldehyde [pH = 7.0]. Brains were immersed in 4% paraformaldehyde overnight, and then transferred to an ice-cold 20% sucrose solution the next morning, in preparation for histological analyses. Once tissues sank in the sucrose solution, brains were blocked

down the midline and sectioned parasagittaly, using a vibrating microtome (Leica VT 1000s, Leica Microsystems Inc., Buffalo Grove IL. Tissue was briefly rinsed in 1X PBS for 10 minutes followed by incubation in 1% H_2O_2 for 30 minutes, in an effort to quench endogenous peroxidase activity. The sections were again rinsed 3 times with 1X PBS, and then blocked with 5% normal goat serum for 35 minutes. Following blocking, sections were incubated overnight at room temperature in a solution containing primary antibody (1:5000 dilution), 1% normal goat serum, 0.01% sodium azide, and 0.3% Triton-X 100 in PBS. The following day, tissues were rinsed three times in PBS and incubated in a biotinylated anti-mouse antiserum for 60 minutes followed by a preassembled avidin-biotin complex solution (VECTASTAIN ABC Elite kit, Vector Laboratories Inc., Burlingame, CA). Specific antibody labeling was revealed using a 3, 3-diaminobenzidine (DAB) solution in the presence of hydrogen peroxide. DAB solution was inactivated by three washes in 1X PBS. Tissue sections were mounted on glass slides coated with 0.3 % gelatin. After sections on slides were allowed to dry overnight, sections were dehydrated with graded concentrations of ethanol (70 %, 95 %, and 100 % respectively), cleared with xylenes, and coverslipped with Permount (Fisher).

Optical Density Measurements

Immunohistochemical staining was examined in various brain regions at 40, 100, and 1000 X using an Olympus BX51 microscope with Nomarski DIC optics. For measurements, images were captured at 100 X using a Spot Insight QE digital camera and Image-Pro Plus 5.0 software (MediaCybernetics, Silver Spring, MD) under identical, calibrated exposure conditions. All images were background-corrected, and converted to 8-bit grey scale; borders that outlined brain regions of interest were traced manually.

Two dimensional optical density measurements of both labeled processes from areas enclosed within traced areas were performed on images without knowledge of treatment condition for each brain region of interest. With the exception of cerebellum, (Figures 4.4, 4.8, 4.12, and 4.16) all intact sections containing brain regions of interest were included for analysis, and analyzed using Image-Pro Plus 5.0 software. Mean optical densities (within brain region counts of stained nuclei and neuropil/area of the region) were compared across each treatment group using two-way ANOVA as described below.

Statistical Methods

All data are expressed as means ± SEM. Statistically significant differences between groups were assessed by the Student's t-test; relationships between optical densities and drug treatments were assessed through two-way ANOVA with brain region (HVC, RA, lMAN, Area X, DLM, Ov) and treatment (vehicle vs. 1 mg/kg WIN) as factors. Statistical significance was defined as a two-tailed probability of less than 0.05. Results pertaining to the hypothesis tested (that drug treatment would alter phosphorylated Nf-200 and/or MAP2 protein expression) were presented in our analysis of data. After a significant treatment effect was determined by two-way ANOVA, Student-Newman-Keuls post-hoc tests were performed. All statistical analyses were performed using GraphPad Prism 5.0, SigmaStat, and Microsoft Excel PC software.

RESULTS

Western Blotting

Western blotting was performed in an effort to assess the selectivity of the antibodies against the two neurocytoskeletal proteins assessed in immunohistochemistry experiments. SDS-PAGE separation of 30 µg of brain cytoskeletal fractions revealed the presence of a single predominant band of approximately 200 kDa labeled by the anti-phosphorylated Nf-200 antibody; SDS-PAGE separation of 30 µg of brain cytoskeletal fractions revealed the presence of two predominant protein bands likely representing the high-molecular weight isoforms of MAP2 (MAP2a and MAP2b, at approximately 230 kDa), and the lower molecular weight isoforms of MAP2 (MAP2c and MAP2d, at approximately 70 kDa), labeled by the anti-MAP2 antibody used. The sizes of these selectively labeled proteins was consistent with that reported from other mammalian species, including mouse, rat, horse and human (Alexanian et al., 2008; Lin et al., 2010; Russo et al., 2012; Saraceno et al., 2012).

Phosphorylated Nf-200 Optical Densities

In this study, two-way ANOVA revealed that developmental treatment with the cannabinoid agonist WIN during sensorimotor learning resulted in a significant increase in phosphorylated NF-200 protein expression as compared to vehicle-treated groups ($F(1,393) = 31.070$, $p < 0.001$). Further Student Newman-Keuls post-hoc analyses revealed that these differences lie within the caudal regions HVC (from vehicle control mean = 0.0569 ± .004 to 0.099 ± 0.010 in WIN-treated subjects, $q = 4.343$, $p = 0.002$, Figure 3.1I), RA (from vehicle control mean 0.062 ± 0.010 to 0.107 ± 0.010 in animals

treated with WIN, q = 4.602, p = 0.001, Figure 3.1J), rostral region Area X (from vehicle-treated control mean 0.083 ± 0.010 to 0.132 ± 0.014, WIN-treated mean, q = 4.945, p < 0.001) and midbrain thalamic regions Ov (from vehicle-treated control mean 0.089 ± 0.010 to 0.113 ± 0.012 WIN-treated mean, q = 4.836, p < 0.001) and DLM (from vehicle-treated control mean 0.103 ± 0.009 to 0.130 ± 0.013, WIN-treated mean, q = 4.906, p < 0.001).

Distinct, dense staining patterns of phosphorylated Nf-200 were observed within HVC, as opposed to surrounding tissue (see Figure 3.1A-B) of adult groups treated with vehicle during development. At 1000X, the presence of long, thin neuronal processes was detected with the phosphorylated Nf-200 antibody used. We observed very little pericellular phosphorylated Nf-200 staining, therefore separate protein strands measuring approximately 0.5 – 1 μm in diameter were easier to detect (Figure 3.1C). In WIN-treated HVC, Nf-200 protein appeared to be increasingly denser, and more darkly stained. Within these treated regions, it was difficult to distinguish distinct cell bodies from masses of neuropil (Figure 3.1B, D).

In caudal region RA, however, morphological differences in phosphorylated Nf-200 staining between both developmentally treated groups were grossly apparent. Thick axonal projections emanating from HVC appear to terminate in different subregions within RA (data not shown). Positive phosporylated Nf-200 staining was noted within the entire arcopallium, however staining was generally heavier, and more distinct within RA (see Figure 3.1E-F, 4.5E-F). Light perisomal phosphorylated Nf-200 expression was evident within vehicle-treated RA regions (see Figure 3.1E, G and Figure 3.5E, G), however in animals treated developmentally with WIN, Nf-200 appears

thick and grossly accumulated within the soma. Within RA, axons emanating from the cell body appear to contain large amounts of phosphorylated Nf-200 at the point at which projections radiate, indicative of an unfavorable state of massive protein misaccumulation within the cell. For an illustration, please refer to Figure 3.1F, H.

In lMAN, phosphorylated Nf-200 staining was apparent, but not restricted to the boundaries of this region. Staining was diffuse throughout axons and around somata, giving the region an overall “scratched” appearance. WIN exposure during development resulted in a noticeable, but not statistically significant increase in phosphorylated Nf-200 protein within lMAN (Figure 3.2B, D) as opposed to vehicle treatments (Figure 3.2A, C). Rostral-ventral regions including Area X and surrounding striatum were positive for phosphorylated Nf-200 staining. At 1000X under vehicle control conditions, phosphorylated Nf-200 morphology appears to parallel that of HVC; distinctly long, thin processes, light perisomatic expression, and very little neuropil staining were frequently noted (see Figure 3.2E, G). However, as summarized in Figure 3.2F, and 2H, developmental WIN treatment was associated with significantly increased phosphorylated Nf-200 within the neuropil, and thicker, more fragmented axons.

General staining patterns of midbrain regions Ov and DLM are similar to HVC in that phosphorylated Nf-200 expression is distinctly expressed within these regions as opposed to a more general staining. Within Ov, under vehicle control conditions, neuropil staining is hardly discernible above background, and long, thinner axonal process emanating from round, moderately-sized neurofilament-lined cell bodies are clearly seen (Figure 3.3A, dashed box, Figure 3.3C). Administration of WIN across development results in increased protein expression throughout Ov neuropil and

processes. Many thicker, irregularly-stained fibers surround unstained somata, giving the axons within the matrix a matted, tangled appearance (Figure 3.3B, dashed box, Figure 3.3D). Additionally, we found that neuronal morphology within DLM is very similar to Ov under vehicle control conditions, in that phosphorylated Nf-200 is densely labeled within axons and around somata; however the axon projections themselves are sparse (Figure 3.3A, solid box, Figure 3.3E).

Because of the robust pattern of heavy anti-CB_1 immunoreactivity identified within the cerebellum of zebra finches and other vertebrate species (Egertova and Elphick, 2000; Herkenham et al., 1991; Pettit et al., 1998), we hypothesized that CB_1 agonism may presynaptically disregulate axonal morphology within this area as well. However, due to an insufficient number of tissue sections available to quantify from a number of treatment groups, this data was not included in our statistical analysis. Nevertheless, similar to what is described within other regions, phosphorylated Nf-200 expression appeared to be elevated in animals developmentally treated with cannabinoids. Specifically, three layers of cerebellum (molecular, Purkinje, and granular layers) were stained positively with anti-phosphorylated Nf-200 antibody under vehicle-treated conditions (Figure 3.4A, C), but phosphorylated Nf-200 expression appears to vary considerably within terminals in the dense granular layer, and within the axons emanating from Purkinje cells after developmental WIN treatment (Figure 3.4B). Upon closer inspection (at 1000X), phosphorylated Nf-200 expression also appears thicker, darker, and more irregular around Purkinje cell bodies (Figure 3.4D). This was previously reported for Nf-200 staining within cerebellums of periadolescent rats

chronically-treated with WIN, and is in harmony with patterns reported for CB_1 receptor staining in zebra finch cerebellum (Soderstrom and Tian, 2006; Tagliaferro et al., 2006).

There were no interactions to report between phosphorylated Nf-200 staining in the brain regions evaluated and drug treatments administered. The results of this experiment are summarized in Figures 3.1-2, I-J, and Figure 3.3G-H. After analyzing results of the developmental experiment, and determination of significant treatment effects, a second, independent experiment was performed using adult animals in order to assess the developmental dependence of treatment effects. The results of this experiment are found in Figures 3.5-6, I-J, and Figure 3.7G-H. Accordingly, daily cannabinoid treatment did not produce significant differences in adult phosphorylated Nf-200 staining ($F(1,384) = 0.049$, $p = 0.825$) within any of the analyzed telencephalic areas or midbrain regions DLM and Ov. At high power, the morphology of these regions (regardless of treatment regimen) is extremely similar to adults that received vehicle treatments during development, further validating earlier observations made in our lab (Gilbert and Soderstrom, 2011; Soderstrom and Tian, 2008). For illustrations and data, please refer to Figures 3.5-7.

MAP2 Optical Densities

Comparison of vehicle-control groups and those treated with WIN during development revealed a significant increase in MAP2 immunoreactivity ($F (1,384) = 48.097$, $p < 0.001$). These differences were found within all four of the telencephalic song regions (HVC, from 0.065 ± 0.0007 to 0.130 ± 0.010, RA, from 0.049 ± 0.010 to 0.085 ± 0.010, Area X, from 0.710 ± 0.007 to 0.104 ± 0.008, and lMAN, from 0.064 ± 0.007 to 0.089 ± 0.010, results summarized in Figures 3.9-10). MAP2 staining within

DLM was decreased by WIN treatment (from vehicle-control mean 0.648 ± 0.009 to 0.094 ± 0.010 in treated animals), but not within Ov. A graphical representation of these data can be found in Figure 3.11. There were no interactions found between the variables tested; the intensity of staining observed within each brain region is contingent upon the treatment administered. Differences in MAP2 immunoreactivity between those adults treated with vehicle for 25 days and those that were administered consecutive treatments of WIN daily for 25 days were not statistically significant (see Figures 3.13-15).

In general, we noted a great deal of similarity in MAP2 staining patterns between different telencephalic regions analyzed under vehicle-treated conditions, regardless of whether treatment occurred during development or as adults. Compared to surrounding areas, MAP2 immunoreactivity was present, but presented in a virtually negative staining pattern to that of phosphorylated Nf-200 (for an example, compare Figure 3.11A, E to Figure 3.9A, E). Upon closer inspection, we noted that in these regions, no staining was observed within or around somata, however, MAP2 expression was prominent throughout dendritic processes, and occasionally detected within neuropil (Figure 3.9C). In some regions, namely Ov and HVC, small, stable bundles of MAP2 protein were noticeable within dendrites. Staining patterns observed in control birds are region-specific, but much lighter in intensity compared to surrounding areas, whereas chronic developmental cannabinoid administration results in overall staining patterns that are heavier and more concentrated in dendritic processes located within distinct regions. This very pronounced morphological consequence of drug treatment was surprising. In HVC regions of developmentally WIN-treated adult brain tissue, MAP2

antibodies show intense labeling of thick dendritic processes, and the boundaries of neuronal cell bodies (Figure 3.9B, D). In contrast to most other regions observed, HVC MAP2 neuropil staining intensities do not seem to vary with developmental cannabinoid treatment. However, denser, more numerous MAP2 bundles are easily observed at 1000X (Figure 3.9D). Some of the most drastic changes in MAP2 morphology and expression with developmental drug treatment lie within caudal region RA. Developmental WIN administration significantly increases the presence of MAP2 protein within RA in addition to the surrounding arcopallium (Figures 3.9F, H). It appears as though a change in the densities of dendrites per area is only partially responsible for the increase in MAP2 expression observed: neurites within WIN-treated RA are considerably thicker in diameter and appear more irregular than vehicle-treated controls.

In lMAN, immunostaining for MAP2 was limited to the neuropil in both control and WIN-treated animals, so therefore it was not possible to render visual analyses of the staining within labeled processes within this region (see Figure 3.10A-D). Nevertheless, heavier MAP2 staining was present within the tissue matrices of those developmentally exposed to WIN. The pattern of immunoreactivity within Area X closely mirrored that of lMAN in respect to neuropil staining, however this region displayed considerably more positive dendritic staining that varied with drug treatment.

Again, the overall light diffuse MAP2 staining observed in both Ov and DLM under control conditions presented as negative images surrounded by more distinct immunoreactivity in surrounding areas (Figure 3.11A). This pattern was drastically altered within both Ov and DLM in WIN-treated groups (compare Figure 3.11A to Figure

3.11B). In DLM, developmental cannabinoid treatment resulted in very intense MAP2 labeling within neuropil and around neuronal cell bodies (Figure 3.11B, solid box, Figure 3.11F). Within DLM, positive staining was limited to a very small number of dendrites within the matrix. Nonetheless, these processes were observed to be very thick, wavy, and irregular (Figure 3.11F). The method of image analysis employed in this study failed to detect any significant differences between MAP2 staining intensities in developmentally-treated vehicle control Ov and developmental WIN-treated Ov regions (see Figure 4.11C-D, G). These results are consistent with other studies performed, that demonstrated that although CB_1 receptors are abundantly expressed in Ov, neither the presentation of novel song stimuli, nor acute cannabinoid treatment alters the expression of Arc, another dendritic and synaptically-associated protein that upon synaptic activation, interestingly triggers dendritic remodeling by interacting with MAP2 (Chapter 5, (Fujimoto et al., 2004; Soderstrom and Tian, 2006).

Likewise, MAP2 immunoreactivity within the cerebellum was restricted to light staining of dendritic processes and more pronounced staining of cell bodies within the granular layer. However, due to an insufficient number of tissue sections available to quantify from a number of treatment groups, data pertaining to the cerebellum was not included in our statistical analysis (For illustrations, see Figure 3.12).

There were no interactions between MAP2 staining in the brain regions evaluated and drug treatments administered. The results of this experiment are summarized in Figures 3.9-10 I-J, and Figure 3.11G-H. After analyzing results of the developmental experiment, and determination of significant treatment effects, a second, independent experiment was performed using adult animals in order to assess the

developmental dependence of treatment effects. The results of this experiment are found in Figures 3.13-14, I-J, and Figure 3.15G-H. Daily cannabinoid treatment did not produce significant differences in adult MAP2 staining ($F(1,419) = 0.546$, $p = 0.580$) within any of the analyzed telencephalic areas or midbrain regions DLM and Ov

DISCUSSION

The results of the experiments conducted in this study indicate that repeated developmental exposure to cannabinoids during critical periods for sensorimotor learning leads to persistent, abnormal gross morphological disruptions in the expression of axonal marker Nf-200, and dendritic marker MAP2. This study was conducted within songbird CNS regions previously shown to express CB_1 cannabinoid receptors in high levels: HVC, RA, lMAN, AreaX, Ov, DLM, and cerebellum (Soderstrom and Tian, 2006). Increases in receptor activation significantly alter the morphological and likely functional dynamics of neurons located within these regions critical for zebra finch development of stereotyped song. This work represents the first attempt to identify enduring neurocytoskeletal morphological correlates within zebra finch song regions of the brain that parallel developmental cannabinoid treatments known to cause persistent disruptions in adult singing behavior.

The functional characteristics of dendrites and axons are conferred to them by their distinct morphological attributes: On average, dendritic processes are relatively short, have multiple degrees of arborization, and tend to taper off in diameter. The growth of both types of neurites involves rapid, highly coordinated cytoskeletal reorganization and membrane trafficking (Farah and Leclerc, 2008; Ye et al., 2007). Both microtubule-associated proteins and neurofilaments constitute major elements of

the neuronal cytoskeleton, and aberrant misaccumulations of these macromolecules within cells have long been speculated to be a major underlying contributor to neurodegenerative conditions.

Neurofilament H, or Nf-200, named for its molecular weight of 200 kDa, is the largest subunit of the three polymers that compose the axon, and so is essential for maintaining correct axonal caliber. Recent advances made in understanding neurofilament molecular biology and transgenic mouse models have established a vital role for these proteins in myelinated motor and sensory axonal radial growth, thus regulating conduction velocity, axonal mobility, and interactions with other cytoskeletal elements (Q. Ashton Acton). The precise consequences of neurofilament misaccumulation within cortical areas are less clear, although traditionally, most critical functions of neurofilaments within the axon have been strongly correlated with the degree to which phosphorylation occurs. Irregular accumulation of hyperphosphorylated neurofilament is often used as a biomarker of axonal injury, and an indicator for a slew of neurodegenerative diseases, including Alzheimer's disease, Multiple Sclerosis, Parkinson's disease and amyotrophic lateral sclerosis (Boylan et al., 2009; Collard et al., 1995; Julien and Mushynski, 1998; Shaw et al., 2005). In these conditions, perikaryal phosphorylation of neurofilament leads to a state of somal misaccumulation without protein transfer to the axon. This scenario eventually leads to the formation of neurofibrillary tangles and inclusions that ultimately result in neurodegeneration and loss (Takahashi and Ishizuka, 2012).

In a similar respect over the past half-century, new mechanisms underlying the involvement of microtubule-associated proteins in dendritic morphology have rapidly

accumulated. Microtubule-associated proteins were first characterized as rod-like anti-parallel dimers that bind longitudinally along the length of microtubule protofilaments (Kim et al., 1979). Isolation of MAP2 from brain tissue revealed that this protein stimulates the rate and extent to which microtubules assemble by reducing the dissociation rate for tubulin. Rapid regulation of MAP2 dynamics is essential for governing microtubule growth, signaling, and transport, molecular associations, as well as cell migration (Kapitein et al., 2010). In a recent study involving non-neuronal cells, overexpression of MAP2 promotes microtubule formation and stabilization also (Weisshaar et al., 1992). MAP2, one of the most abundant microtubule-associated proteins in dendrites, possesses a biological activity (binding capacity) heavily dependent upon the degree to which it is phosphorylated within the dendrite (Brugg and Matus, 1991; Lindwall and Cole, 1984; Sanchez et al., 2000). The levels of MAP2 expression are correlated with the degree to which it stabilizes elements within the cytoskeleton, and altering expression patterns leads dendritic malformation on virtually every level, spanning from irregular neurite morphology and branching, to a lack of microtubule entry into dendritic spines (Chamak et al., 1987; Ruiz-Canada et al., 2004). Indeed, one could expect that if environmental conditions became favorable for such action, dendritic microtubules would likely extend uncontrollably, or erroneously lose characteristics of dynamic instability when neurons are continuously exposed to drugs that induce microtubule polymerization (such as cannabinoids). This is a phenomenon that is tightly regulated by the expression levels and conformation states of MAPs.

Most neuronal cytoskeletal proteins are linked one another in some fashion: Nf-200 binds to microtubules and MAP2 binds to Nf-200 (Heerlein and Richter, 1991). In

addition, MAP2 and Nf-200 are known to share common epitopes.Furthermore, these proteins are often found bound together in a conglomerated state in diseased states, in the form of neurofibrillary tangles and plaques, suggesting normal interactive roles for these proteins in neuritogenesis not previously identified (Galloway et al., 1990). Given this information, it is possible that heavy exogenous cannabinoid consumption produces a similar pattern of pathology within the neuron: cannabinoid-induced protein overexpression or inappropriate lack of protein turnover likely results in an abnormal promotion of synaptic and dendritic maintenance.

Cannabinoids are widely known to modulate various aspects of cognition, specifically the acquisition, processing, and maintenance of sensory information. Other laboratories have demonstrated that cannabinoid signaling plays a significant role in governing neuronal plasticity as well as generation, stabilization, and maintenance of synaptic connections (Katona and Freund, 2012; Kim et al., 2008; Oudin et al., 2011). Our hypothesis is that chronic cannabinoid agonism with WIN inappropriately alters the excitability of neurons affected within these songbird CNS regions, resulting in either a stagnation, or early termination of plastic changes in axonal and dendritic protein expression that should occur during developmental learning. We theorize that these actions likely occur through a number of mechanisms: First, cannabinoid inhibition of presynaptic N and P/Q-type calcium channels (the channels largely responsible for presynaptic calcium entry within this context), resulting in altered calcium flux in response to the action potential (Daniel et al., 2004; Diana et al., 2002). Indeed, exposure to either THC or WIN directly inhibits presynaptic calcium release, which prevents synaptic density loss in rat primary hippocampal neurons in a concentration-

dependent manner (Kim et al., 2008). Second, CB1 receptor modulated direct activation of G-protein coupled inwardly-rectifying (GIRK) and ATP-sensitive K^+ channels results in a rise in ion conductance, and a hyperpolarized presynaptic membrane that reduces neuronal firing rate and plastic changes (Lovinger, 2008; Turu and Hunyady, 2010). These data are in agreement with other noted observations, in which WIN exposure was observed to potently induce K^+ currents in AtT20 cells stably transfected with rat CB_1 receptor (Mackie et al., 1995). And third, another potential mechanism whereby abnormal CNS cannabinoid receptor activation results in a change in neuronal excitability and leads to reduced plasticity is that CB_1 receptor agonism alters the frequency of vesicular fusion with the presynaptic membrane. Furthermore, cannabinoid signaling plays a role in depolarization-induced suppression of excitation (DSE), and depolarization-induced suppression of inhibition (DSI), two closely related forms of short-term synaptic plasticity that directly mediate the firing rate of presynaptic cells (Diana and Marty, 2004).

Many important CNS developmental events (such as those governing neurite maintenance and axonal growth needed to innervate correct targets) heavily involve cannabinoid signaling (Anavi-Goffer and Mulder, 2009). In mice, genetic deletion of the CB_1 receptor is associated with a rapid accumulation of neurocytoskeletal defects, increased activation of caspase cell death pathways, and a significant loss of Nf-200 within axons (Jackson et al., 2005). The steady-state enzyme regulator of the endocannabinoid 2-AG (DAGL-α)-dependent endocannabinoid signaling through the CB_1 receptor is essential and sufficient for developmental axonal growth, and functions by driving calcium influx into growth cones (Gao et al., 2010; Oudin et al., 2011). With a

developmental expression pattern almost paralleling that of MAP2, DAGL-α is expressed in very high levels early during neuronal differentiation and axonal development, but eventually diminishes within axons but *not* somatodendritically, as the system allows for a functional switch between a state of growth and guidance within axons to a state of retrograde synaptic signaling at functional synapses (Galloway et al., 1990). Likewise, cannabinoid activation aids in neuronal migration, and synapse generation (Galve-Roperh et al., 2006; Mulder et al., 2008). As a result of these aforementioned facts, we believe endogenous cannabinoid signaling is a part of, and essential to normal CNS development and function. Thus, one may presume that with periadolescent cannabinoid exposure as observed in our zebra finch developmental learning model, prolonged exogenous cannabinoid administration inapproriately perpetuates the activated period of the CB_1 receptors within distinct CNS regions, and perhaps hijacks normal endocannabinoid signals to evoke molecular and protein rearrangements, ultimately leading to erroneous wiring of neuronal networks.

Similar to humans, songbird adolescent development involves active synaptic remodeling and plasticity, and as such, this phase of growth is particularly vulnerable to the effects of exogenous pharmacological challenges. A substantial increase in both phosphorylated Nf-200 and MAP2 protein densities occurs with once daily periadolescent cannabinoid exposure (see Figures 3.1-4, 9-12). Within all song regions analyzed, excluding lMAN, developmental cannabinoid administration produced striking increases in the overall content of phosphorylated Nf-200 expression per neurite within both telencephalic and midbrain relay regions. Differences in MAP2 densities do not appear to occur within Ov as a function of developmental cannabinoid treatment

although this region expresses CB_1 receptors in high levels. It is possible that Ov-localized cannabinoid expression possesses a function unrelated to vocal learning and production, the specifics of which are not currently known at this time. Not only does this critical data indicate that cannabinoid sensitivity to changes in neuronal cytoarchitecture is restricted to higher-order information processing regions, but it strongly suggests that cannabinoid signaling is likely an important governor of specialized sensory/integrative systems in which neurons may employ as needed.

Taken together, with the exception of Ov, developmental cannabinoid exposure leads to significantly increased MAP2 densities within all regions analyzed. This data is in harmony with previous developmental anatomical studies conducted within our laboratory that show similar trends, and is likely indicative of an unintended consequence of prolonged exogenous cannabinoid agonism: decreases in plasticity and the overall dynamic instability within neurites, a process that is absolutely essential for synaptic reorganization during developmental learning (DeLuca, 2010; Gilbert and Soderstrom, 2011; Soderstrom and Johnson, 2003; Yenjerla et al., 2010).

In contrast with patterns observed in adults treated with cannabinoid across development, we have repeatedly demonstrated that the same consecutive systemic treatments administered to adults in control studies are rendered ineffective in producing significant changes in phosphorylated Nf-200 or MAP2 expression. The reduced sensitivity to WIN treatments during adulthood is likely due to the fact that early in development, song stereotypy in non-seasonal songbirds requires a certain level of congruence between stored tutor song memories and its vocal production. This congruence is heavily dependent on constant auditory feedback, a process essential for

learning and maintenance of vocal behaviors (Brainard and Doupe, 2000; Tschida and Mooney, 2012). The inability of WIN to alter adult phosphorylated Nf-200 and MAP2 protein densities within song regions is associated with a decrease in an adult songbird's ability to alter previously learned song repertoires. Indeed, the absence of song crystallization does not allow for new song motif learning in adulthood (Funabiki and Funabiki, 2009; Zevin et al., 2004). The lack of morphological disruption in densities of phosphorylated Nf-200 and MAP2 protein within neuronal processes is perhaps due to a more complete maturation of synaptic connections in adulthood (Gilbert and Soderstrom, 2011; Soderstrom and Johnson, 2003).

In summary, the results of this study are the first to provide direct evidence for a neurocytoskeletal system heavily influenced by developmental exposure to a cannabinoid agonist. Novel strategies are needed to understand cannabinoid involvement in mechanisms governing neurite growth and maintenance, as we hypothesize that abnormal cannabinoid signaling inappropriately promotes region-specific neurite survival at the great cost of a reduced strength and participation in the synaptic network.

Figure 3.1. Photomicrographs of Nf-200 staining within caudal song regions of adult male zebra finch telencephalon following postnatal developmental treatment with either vehicle (panels A, C, E, G) or WIN (1 mg/kg, panels B, D, F, H) using DAB immunohistochemistry. Panel A with C inset depict normal distribution of Nf-200 protein within axons of HVC; protein has significantly accumulated within this region as a result of developmental cannabinoid administration (Panel B with D inset). In RA, a similar developmental pattern of Nf-200 staining ensues as what is seen within HVC over the course of normal brain development (Panel E with G inset). However, developmental administration of WIN results in a significant, persistent misaccumulation of protein within axons (Panel F with H inset). I-J: Optical density measurements of Nf-200 staining in both HVC (I) and RA (J) after vehicle and WIN administration, respectively. In both regions, protein increases by approximately twofold are observed following daily WIN treatment. 100X scale bar = 300 μm, 1000X scale bar = 30 μm.

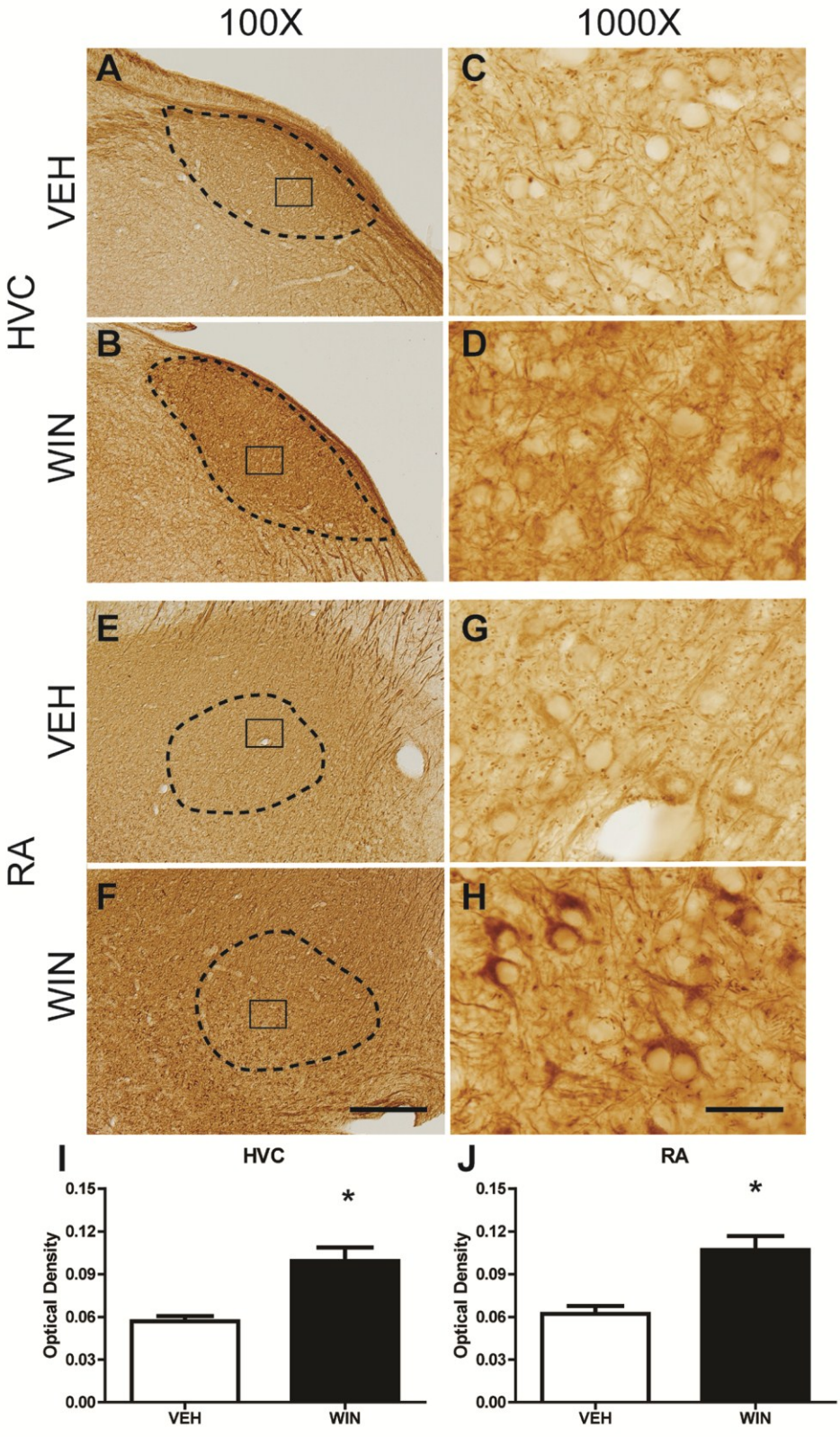
100X
1000X
A
C
VEH
HVC
B
D
WIN
E
G
VEH
RA
F
H
WIN
I
HVC
J
RA
Optical Density
0.15
0.12
0.09
0.06
0.03
0.00
*
VEH
WIN

Figure 3.2. DAB-immunohistochemical staining of Nf-200 protein within rostral song regions lMAN and Area X of adult male zebra finch telencephalon following developmental vehicle treatment (panels A, C, E, G) or treatment with WIN (1 mg/kg, panels B, D, F, H). Developmental WIN exposure results in a noticable, but not statistically significant increase in Nf-200 protein within lMAN (Panel B with D inset) as opposed to vehicle treatments (Panel A with C inset). Significant differences between Nf-200 staining of vehicle-treated striatal Area X (Panel E with G inset) and cannabinoid-treated Area X (Panel F with H inset) were noted. I-J: Optical density measurements of Nf-200 staining in both adult lMAN (I) and Area X (J) after developmental vehicle and WIN administration, respectively. 100X scale bar = 300 μm, 1000X scale bar = 30 μm.

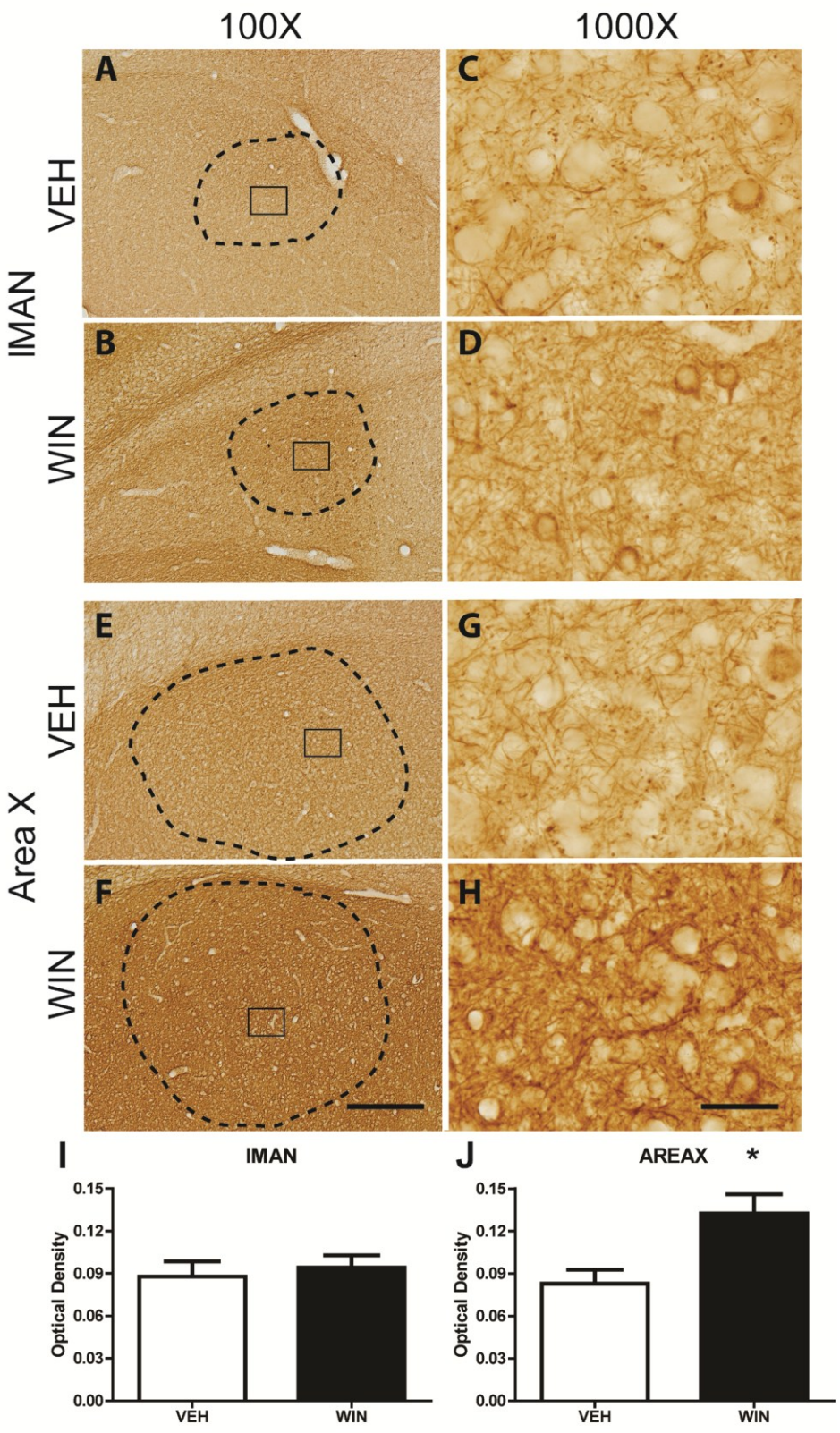
100X
1000X
A
C
B
D
E
G
F
H
IMAN
VEH
WIN
Area X
VEH
WIN
I
IMAN
J
AREAX
*
Optical Density
0.15
0.12
0.09
0.06
0.03
0.00
VEH
WIN
Optical Density
0.15
0.12
0.09
0.06
0.03
0.00
VEH
WIN

Figure 3.3. Representative low and high-power micrographs of Nf-200 staining of adult male zebra finch midbrain thalamic regions Ov and DLM using DAB immunohistochemistry. Animals were subjected to either developmental treatment with vehicle (Panel A, insets C, E) or WIN (1 mg/kg, Panel B, insets D, F) and brain tissue processed at adulthood. Axonal staining within Ov (Panel A-B, bottom left corner) and DLM (Panel A-B, top right corner) is clearly visible within these distinct areas. Daily administration of WIN during sensorymotor development (Panel B, insets D, F) results in a significant increase in Nf-200 staining and altered neuronal morphology within both Ov and DLM that persists well into adulthood. G-H: Optical density measurements of Nf-200 staining within thalamic areas Ov and DLM. 100X scale bar = 300 μm, 1000X scale bar = 30 μm.

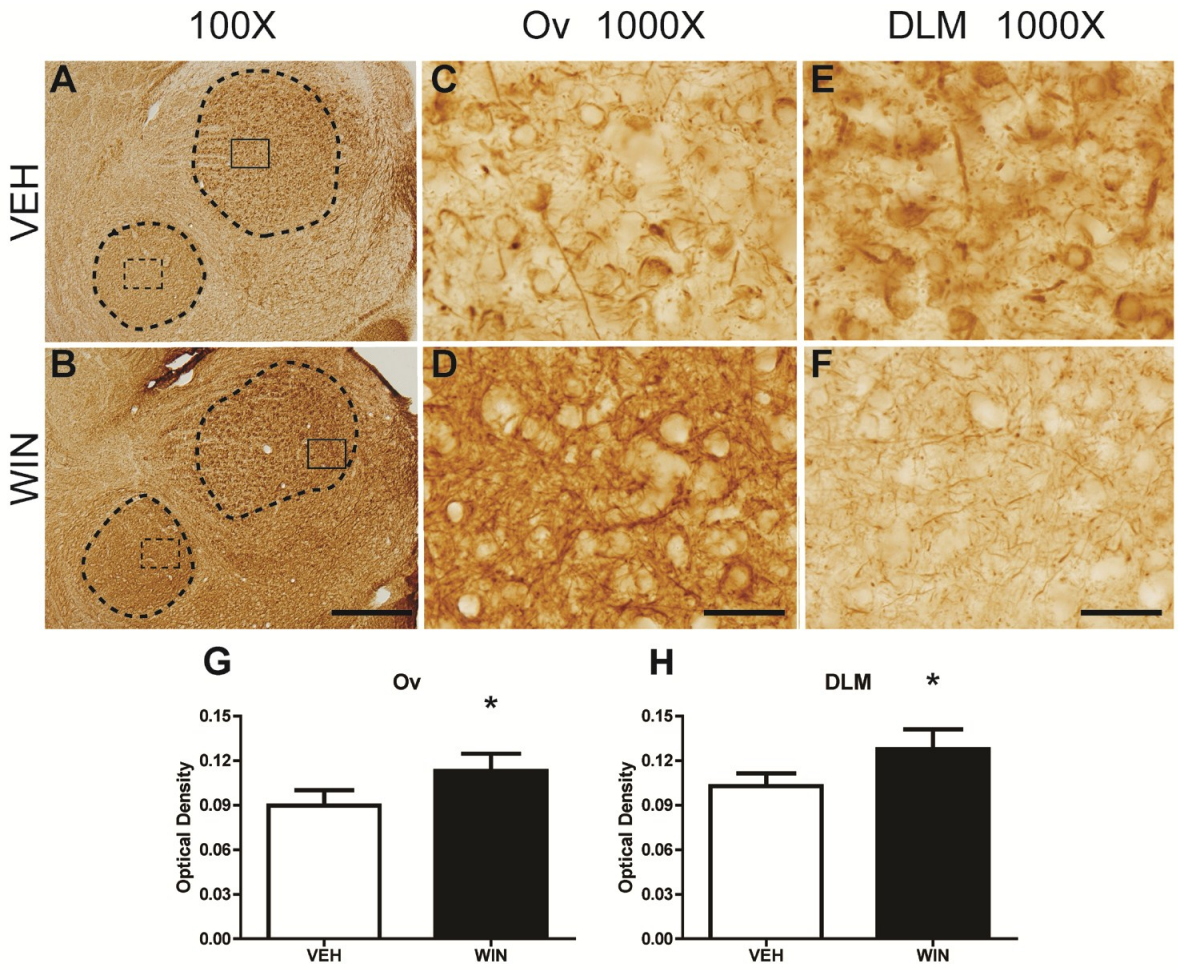
100X
Ov 1000X
DLM 1000X
VEH
WIN
A
B
C
D
E
F
G
Ov
*
Optical Density
0.15
0.12
0.09
0.06
0.03
0.00
VEH
WIN
H
DLM
*
Optical Density
0.15
0.12
0.09
0.06
0.03
0.00
VEH
WIN

Figure 3.4. Representative images of DAB-immunohistochemical staining of Nf-200 protein within the cerebellum of adult male zebra finches developmentally treated with either vehicle (Panel A, inset C) or WIN (1 mg/kg, Panel B, inset D). The number of tissue sections available from each treatment group was not sufficient for statistical analysis, however distinct treatment differences can still be observed. Nf-200 staining within both the molecular and Purkinje cell layer is uncharacteristically denser after developmental cannabinoid treatment (Panel B, inset D) as opposed to vehicle treatment (Panel A, inset C). 100X scale bar = 300 μm, 1000X scale bar = 30 μm.

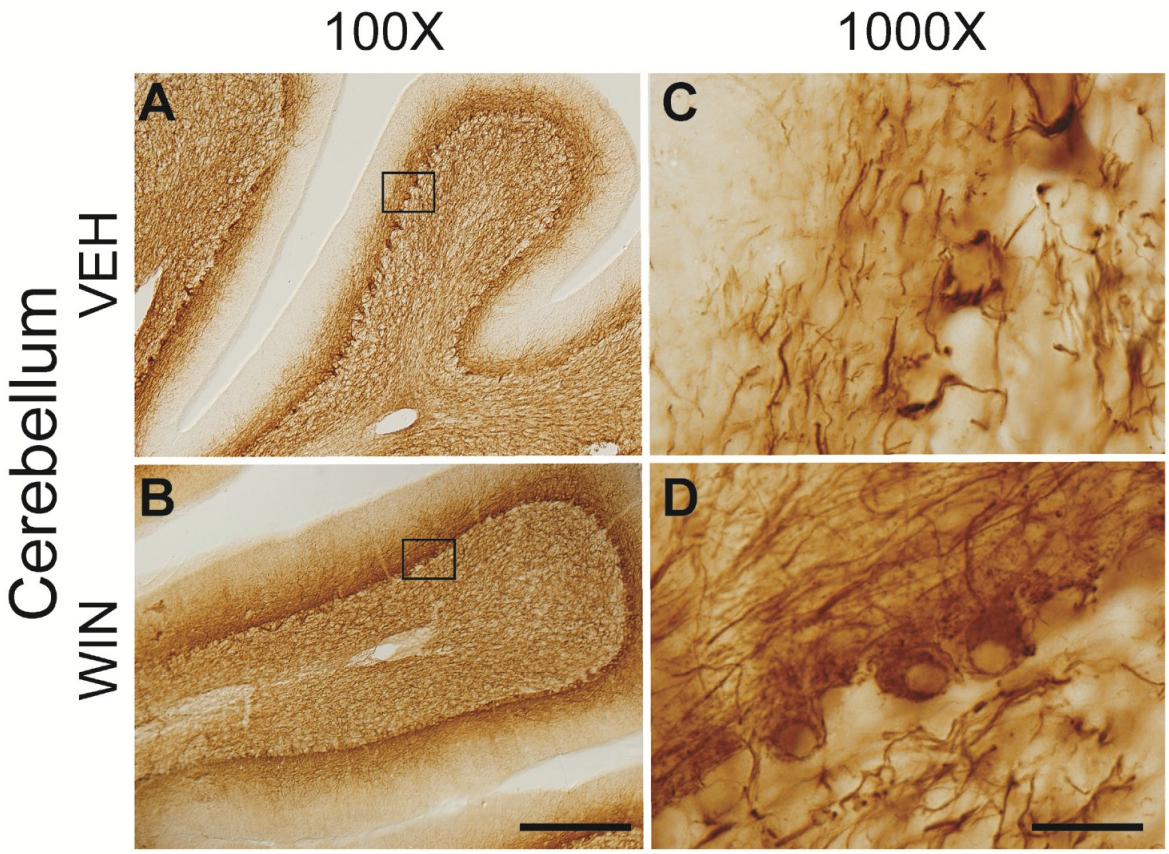
100X
1000X
Cerebellum
VEH
WIN
A
B
C
D

Figure 3.5. Photomicrographs of Nf-200 staining within caudal song regions of adult male zebra finch telencephalon following 25 days of treatment with either vehicle (panels A, C, E, G) or WIN (1 mg/kg, panels B, D, F, H), using DAB immunohistochemistry. No significant treatment differences were observed within HVC or RA of these adults which previously learned song. 100X scale bar = 300 μm, 1000X scale bar = 30 μm

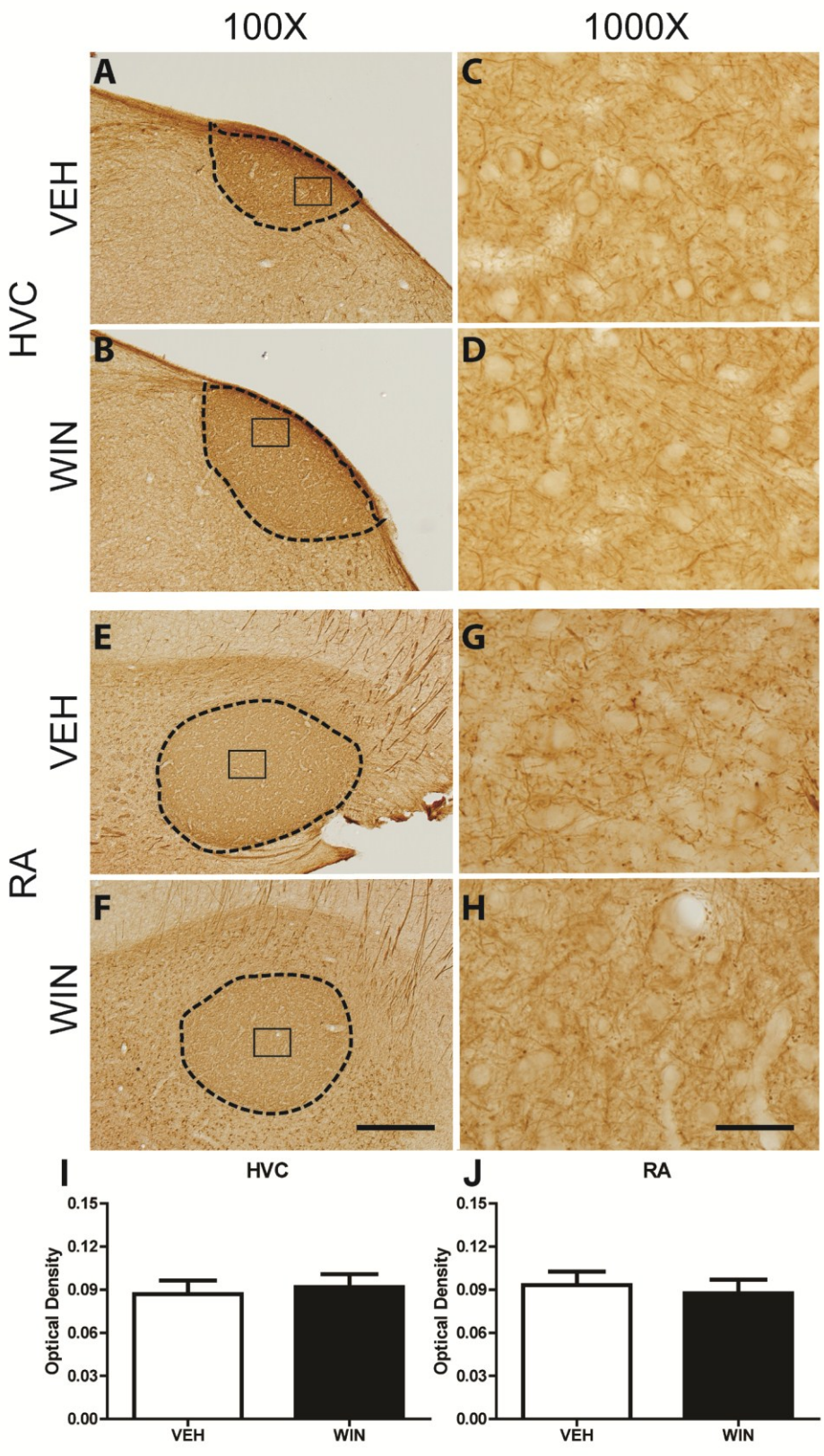
100X
1000X
A
C
B
D
E
G
F
H
HVC
RA
VEH
WIN
VEH
WIN
I
HVC
J
RA
Optical Density
0.15
0.12
0.09
0.06
0.03
0.00
VEH
WIN

Figure 3.6. DAB-immunohistochemical staining of Nf-200 protein within rostral song regions lMAN and Area X of adult male zebra finch telencephalon following 25 consecutive days of vehicle treatment (panels A, C, E, G) or treatment with WIN (1 mg/kg, panels B, D, F, H). WIN treatment did not result in significant elevations in Nf-200 within either region as compared to vehicle-treated counterparts. I-J: Optical density measurements of Nf-200 staining in both adult lMAN (I) and Area X (J) after vehicle and WIN administration, respectively. 100X scale bar = 300 μm, 1000X scale bar = 30 μm.

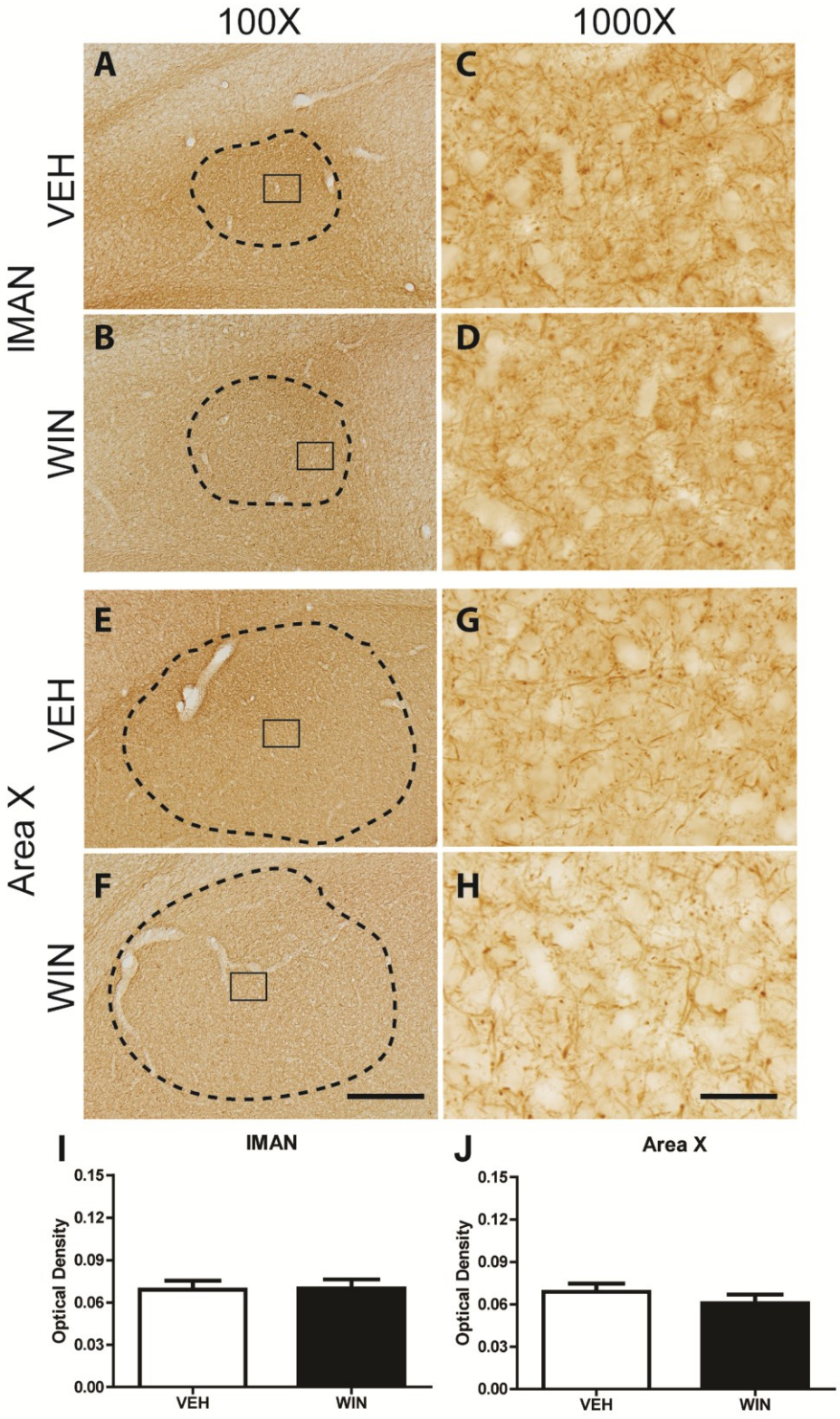
100X
1000X
A
C
IMAN
VEH
B
D
WIN
E
G
Area X
VEH
F
H
WIN
I
IMAN
J
Area X
Optical Density
0.15
0.12
0.09
0.06
0.03
0.00
VEH
WIN

Figure 3.7. Representative low and high-power micrographs of Nf-200 staining of adult male zebra finch midbrain thalamic regions Ov and DLM using DAB immunohistochemistry. Animals were subjected to either 25 consecutive treatments with vehicle (Panel A, insets C, E) or WIN (1 mg/kg, Panel B, insets D, F) after song learning had occurred. Axonal staining within Ov (Panel A-B, bottom left corner) and DLM (Panel A-B, top right corner) is clearly visible within these areas. Daily administration of WIN during sensorymotor development (Panel B, insets D, F) did not lead to a significant increase in Nf-200 staining within either Ov or DLM. G-H: Optical density measurements of Nf-200 staining within thalamic areas Ov and DLM. 100X scale bar = 300 μm, 1000X scale bar = 30 μm.

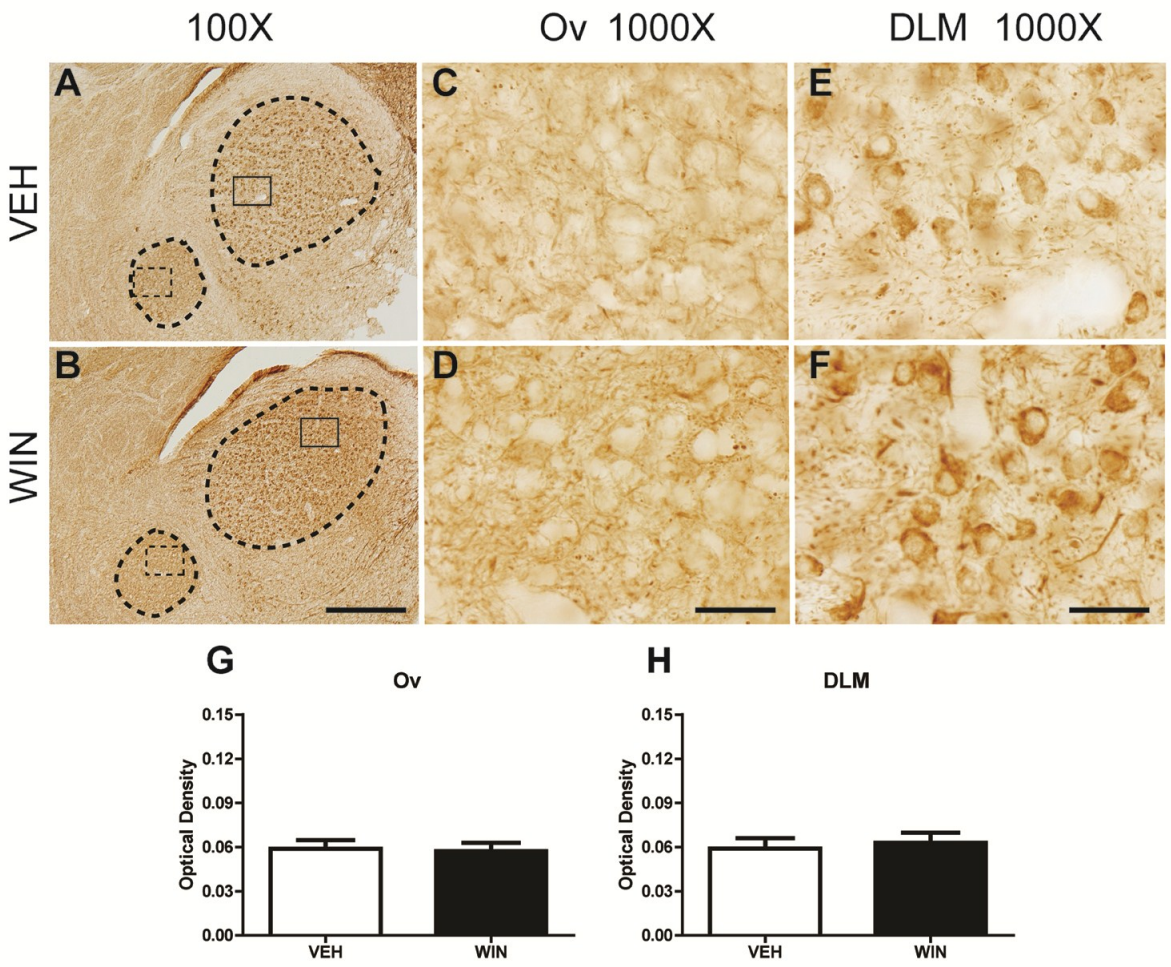
100X
Ov 1000X
DLM 1000X
VEH
WIN
A
B
C
D
E
F
G
Ov
Optical Density
0.15
0.12
0.09
0.06
0.03
0.00
VEH
WIN
H
DLM
Optical Density
0.15
0.12
0.09
0.06
0.03
0.00
VEH
WIN

Figure 3.8. Representative images of DAB-immunohistochemical staining of Nf-200 protein within the cerebellum of adult male zebra finches treated with either vehicle (Panel A, inset C) or WIN (1 mg/kg, Panel B, inset D) after song learning. The number of tissue sections available from each treatment group was not sufficient for statistical analysis. Upon observation, the Purkinje cell layer of adult animals treated with WIN possesses a more sparse density of Nf-200 than that of their vehicle-treated counter parts. 100X scale bar = 300 μm, 1000X scale bar = 30 μm.

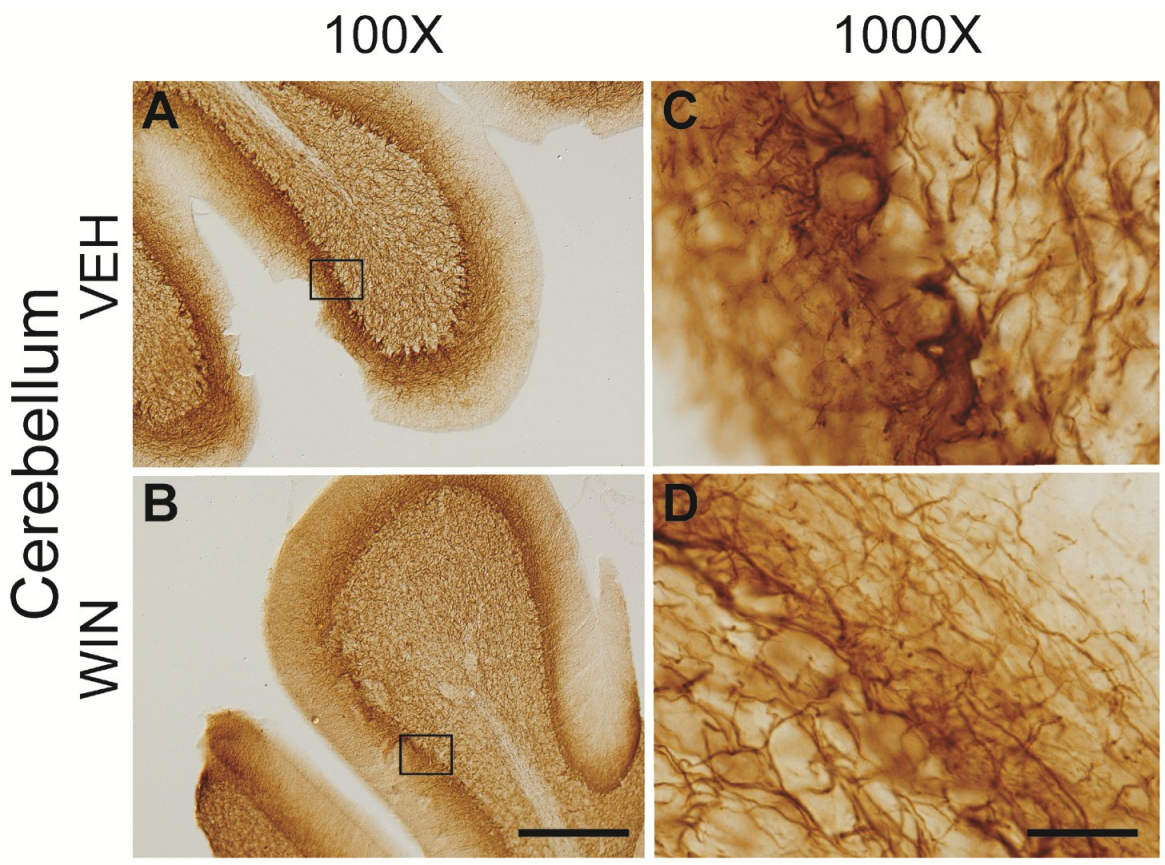
100X
1000X
Cerebellum
VEH
WIN
A
B
C
D

Figure 3.9. Photomicrographs of dendritically associated MAP2 staining within caudal song regions of adult male zebra finch telencephalon following developmental treatment with either vehicle (panels A, C, E, G) or WIN (1 mg/kg, panels B, D, F, H) using DAB immunohistochemistry. Panel A with C inset depict normal distribution of MAP2 protein within HVC dendrites; protein has significantly accumulated within this region as a result of developmental cannabinoid administration (Panel B with D inset). In RA, a similar developmental pattern of MAP2 staining ensues as what is seen within HVC over the course of normal brain development (Panel E with G inset). However, developmental administration of WIN results in a significant, persistent amassing of dendritic protein (Panel F with H inset) within this area. I-J: Optical density measurements of MAP2 staining in both HVC (I) and RA (J) after vehicle and WIN administration, respectively. In both regions, protein increases are observed following daily WIN treatment, however the cannabinoid effect appears to be more robust within HVC. 100X scale bar = 300 μm, 1000X scale bar = 30 μm.

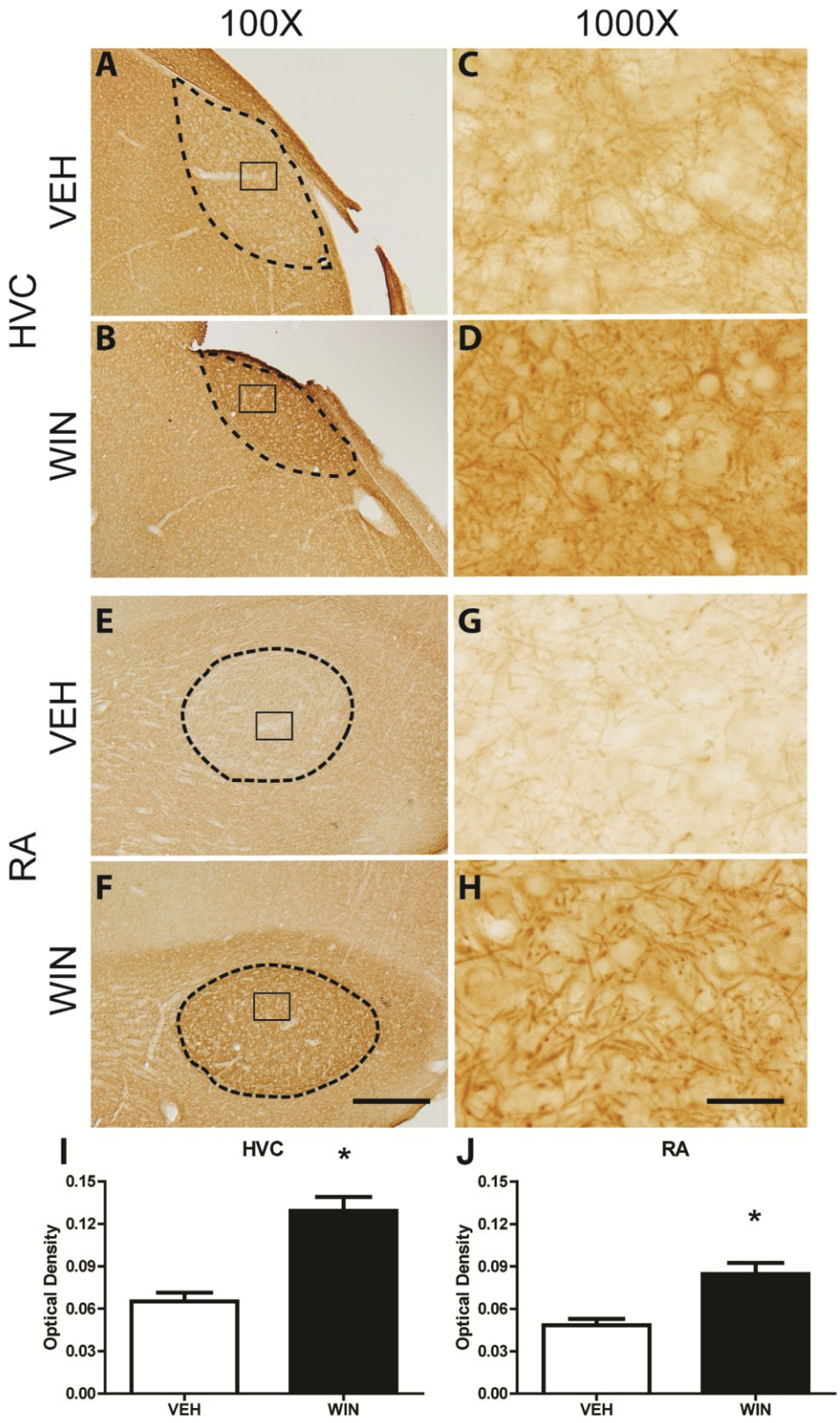
100X
1000X
A
C
B
D
E
G
F
H
HVC
RA
VEH
WIN
VEH
WIN
I
HVC
*
J
RA
*
Optical Density
0.15
0.12
0.09
0.06
0.03
0.00
VEH
WIN

Figure 3.10. DAB-immunohistochemical staining of MAP2 protein within rostral song regions lMAN and Area X of adult male zebra finch telencephalon following developmental vehicle treatment (panels A, C, E, G) or treatment with WIN (1 mg/kg, panels B, D, F, H). Developmental WIN exposure results in a statistically significant increase in MAP2 protein accumulation within lMAN (Panel B with D inset) as opposed to vehicle treatments (Panel A with C inset). Significant differences between MAP2 staining of vehicle-treated striatal Area X (Panel E with G inset) and cannabinoid-treated Area X (Panel F with H inset) were also noted. I-J: Optical density measurements of MAP2 staining in both adult lMAN (I) and Area X (J) after developmental vehicle and WIN administration, respectively. 100X scale bar = 300 μm, 1000X scale bar = 30 μm.

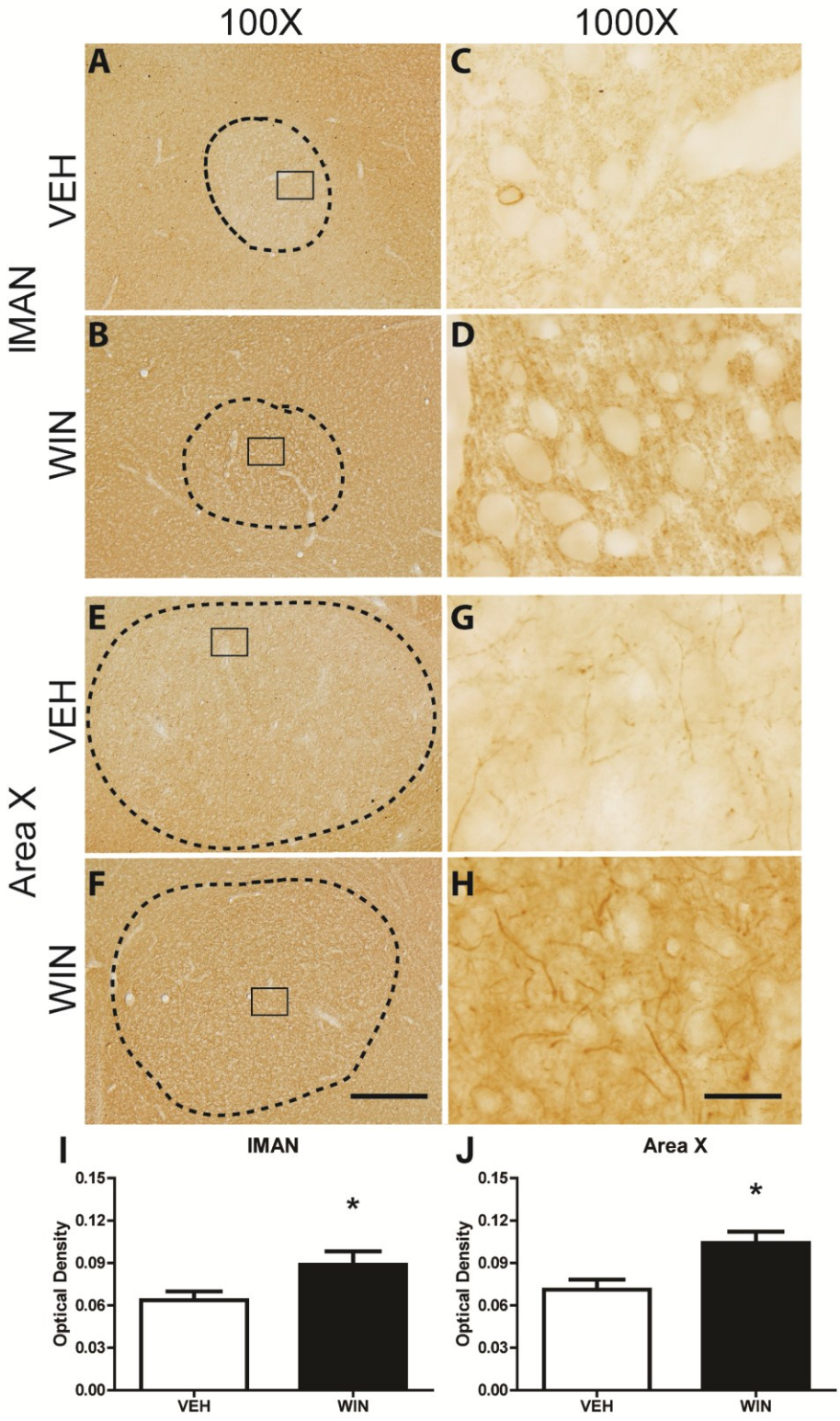
100X
1000X
A
C
VEH
IMAN
B
D
WIN
E
G
VEH
Area X
F
H
WIN
I
IMAN
J
Area X
Optical Density
0.15
0.12
0.09
0.06
0.03
0.00
*
VEH
WIN

Figure 3.11. Representative low and high-power micrographs of MAP2 staining of adult male zebra finch midbrain thalamic regions Ov and DLM, using DAB immunohistochemistry. Animals were subjected to either developmental treatment with vehicle (Panel A, insets C, E) or WIN (1 mg/kg, Panel B, insets D, F) and brain tissue processed at adulthood. Staining within Ov (Panel A-B, bottom left corner) and DLM (Panel A-B, top right corner) is less intense, but visible within these distinct areas. Daily administration of WIN during sensorymotor development (Panel B, inset, F) results in a significant increase in MAP2 staining and altered cellular morphology within DLM; however no significant differences are observed in Ov as a result of cannabinoid treatment(Panel B, inset E). G-H: Optical density measurements of MAP2 staining within thalamic areas Ov and DLM. 100X scale bar = 300 μm, 1000X scale bar = 30 μm.

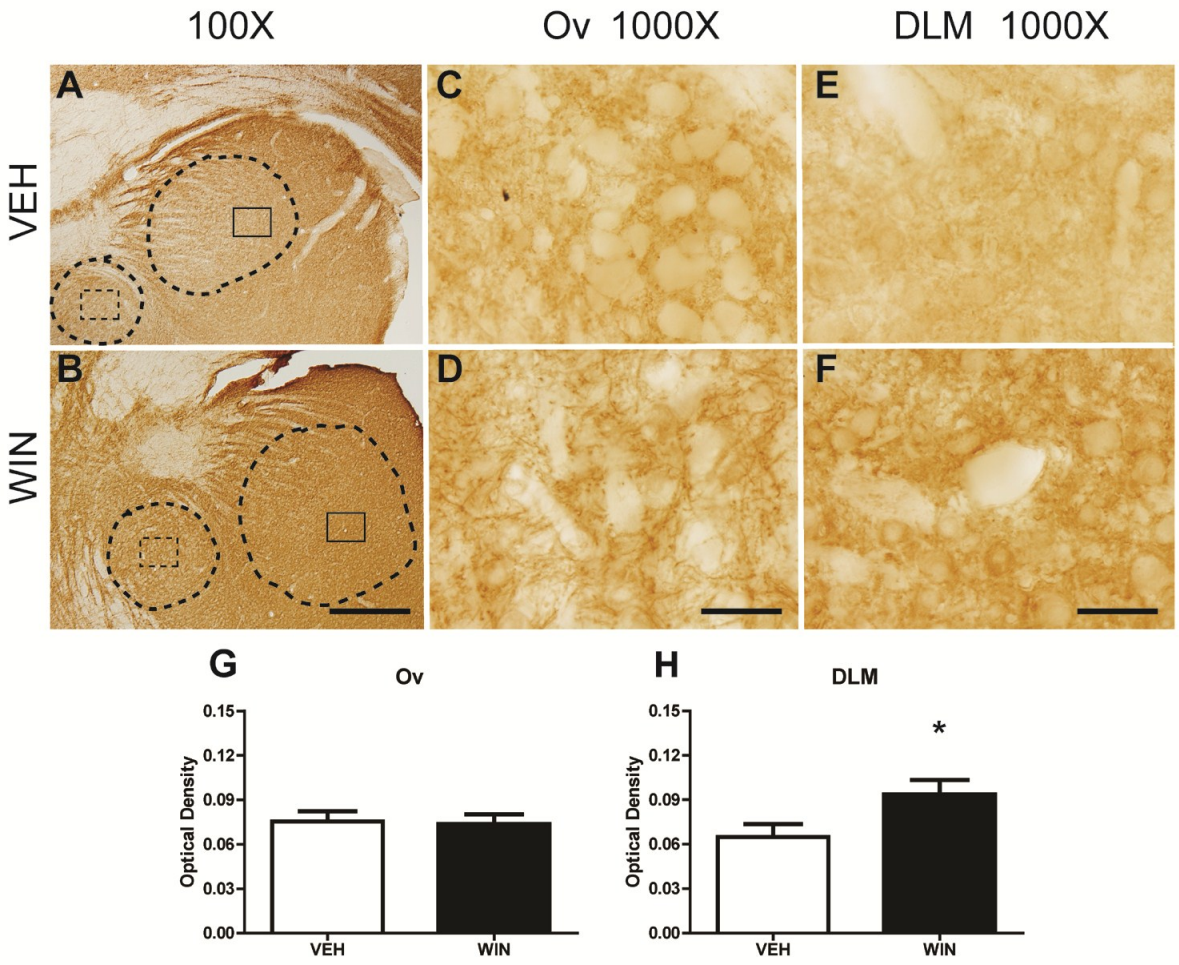
100X
Ov 1000X
DLM 1000X
VEH
WIN
A
B
C
D
E
F
G
Ov
Optical Density
0.15
0.12
0.09
0.06
0.03
0.00
VEH
WIN
H
DLM
*
Optical Density
0.15
0.12
0.09
0.06
0.03
0.00
VEH
WIN

Figure 3.12. Representative images of DAB-immunohistochemical staining of MAP2 protein within the cerebellum of adult male zebra finches developmentally treated with either vehicle (Panel A, inset C) or WIN (1 mg/kg, Panel B, inset D). The number of tissue sections available from each treatment group was not sufficient for statistical analysis, however distinct treatment differences can still be observed. MAP2 staining within the granular layer is considerably less dense after developmental cannabinoid treatment (Panel B, inset D) as opposed to vehicle treatment (Panel A, inset C). 100X scale bar = 300 μm, 1000X scale bar = 30 μm.

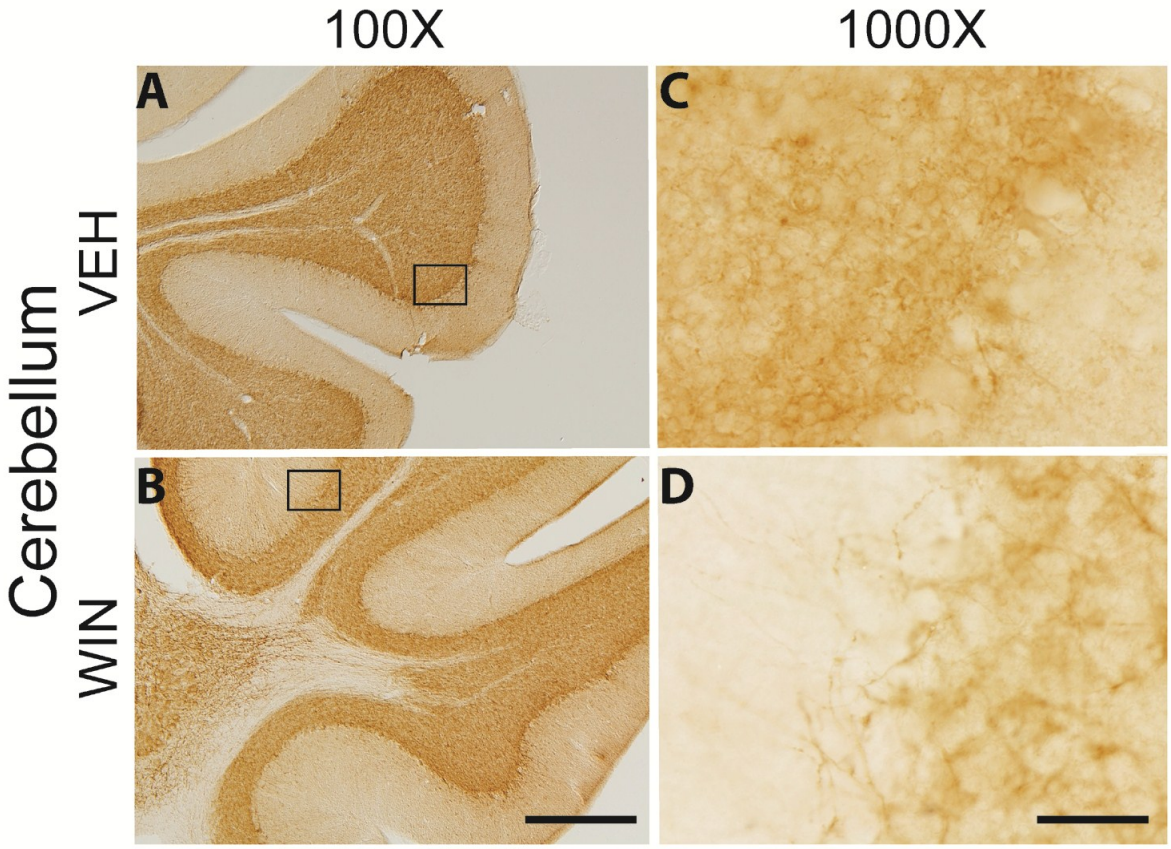
100X
1000X
Cerebellum
VEH
WIN
A
B
C
D

Figure 3.13. Photomicrographs of MAP2 staining within caudal song regions of adult male zebra finch telencephalon following 25 days of treatment with either vehicle (panels A, C, E, G) or WIN (1 mg/kg, panels B, D, F, H), using DAB immunohistochemistry. No significant treatment differences were observed within HVC or RA of these adults which previously learned song. 100X scale bar = 300 μm, 1000X scale bar = 30 μm.

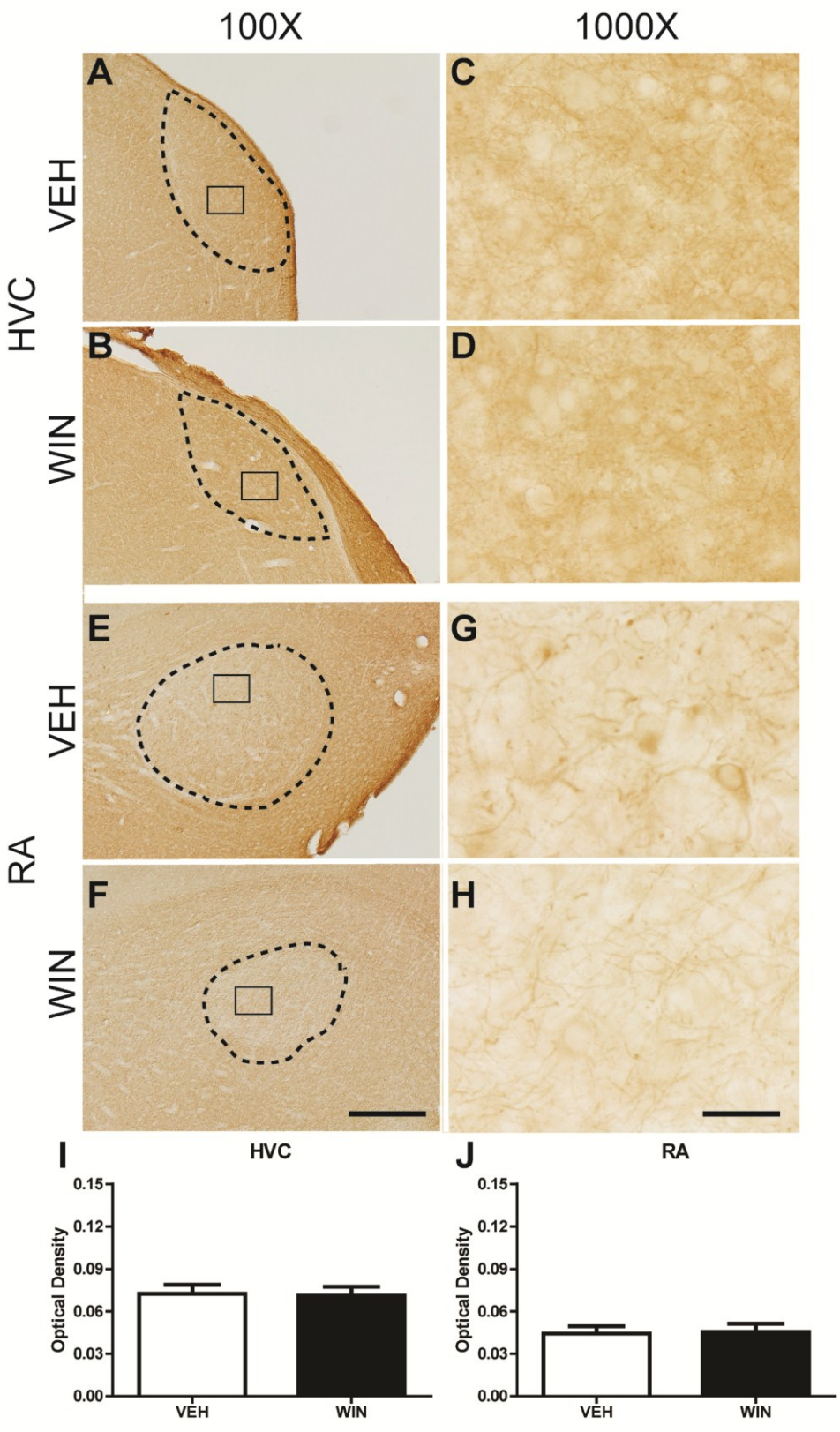
100X
1000X
A
C
VEH
HVC
B
D
WIN
E
G
VEH
RA
F
H
WIN
I
HVC
J
RA
Optical Density
0.15
0.12
0.09
0.06
0.03
0.00
VEH
WIN

Figure 3.14. DAB-immunohistochemical staining of MAP2 protein within rostral song regions lMAN and Area X of adult male zebra finch telencephalon following 25 consecutive days of vehicle treatment (panels A, C, E, G) or treatment with WIN (1 mg/kg, panels B, D, F, H). WIN treatment did not result in significant elevations in MAP2 within either region as compared to vehicle-treated counterparts. I-J: Optical density measurements of MAP2 staining in both adult lMAN (I) and Area X (J) after vehicle and WIN administration, respectively. 100X scale bar = 300 μm, 1000X scale bar = 30 μm.

Figure 3.15. Representative low and high-power micrographs of MAP2 staining of adult male zebra finch midbrain thalamic regions Ov and DLM using DAB immunohistochemistry. Animals were subjected to either 25 consecutive treatments with vehicle (Panel A, insets C, E) or WIN (1 mg/kg, Panel B, insets D, F) after song learning had occurred. Dendritic staining within Ov (Panel A-B, bottom left corner) and DLM (Panel A-B, top right corner) is sparse, but visible within these areas. Daily administration of WIN during sensorymotor development (Panel B, insets D, F) did not lead to a significant increase in MAP2 staining within either Ov or DLM. G-H: Optical density measurements of MAP2 staining within thalamic areas Ov and DLM. 100X scale bar = 300 μm, 1000X scale bar = 30 μm.

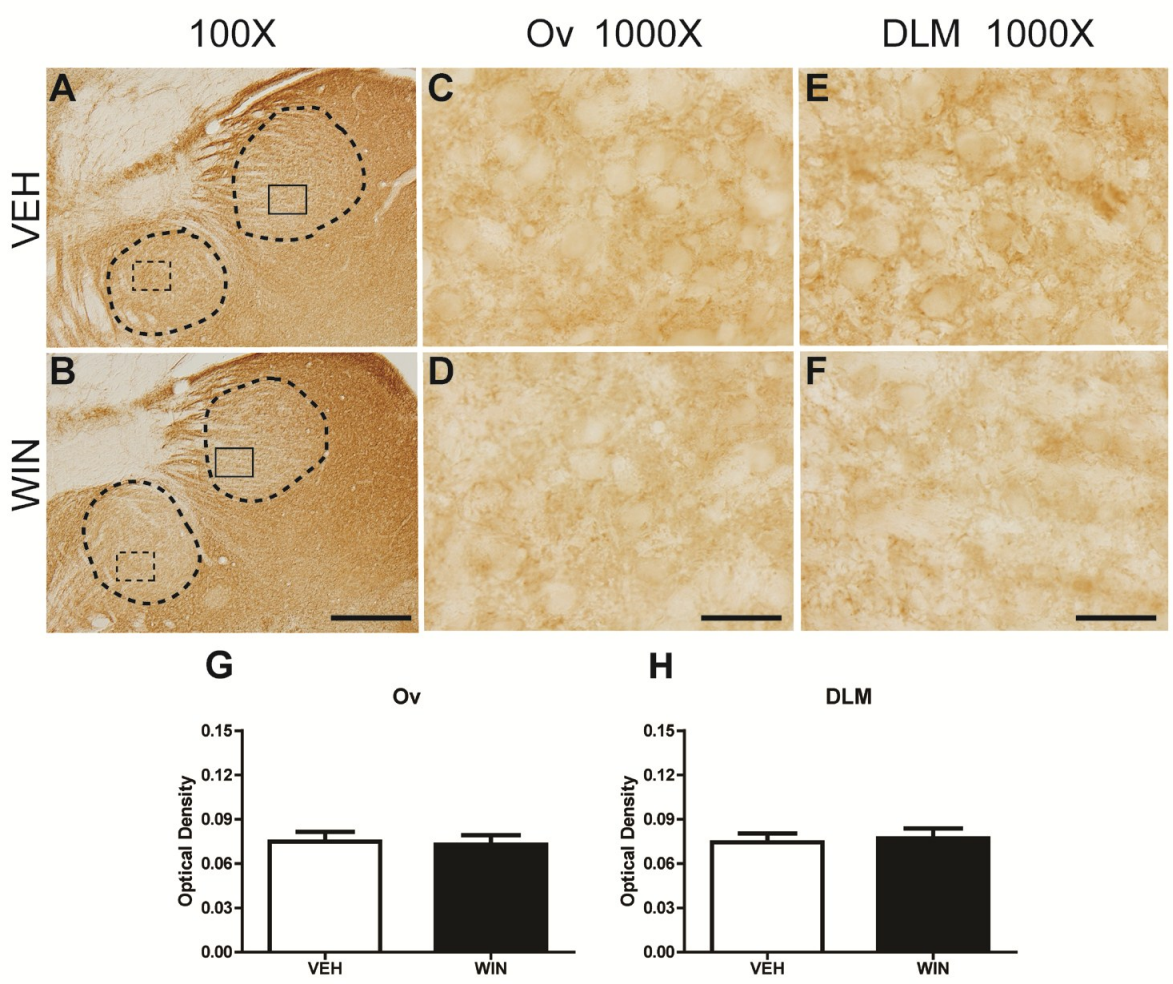
100X
Ov 1000X
DLM 1000X
A
B
C
D
E
F
VEH
WIN
G
Ov
H
DLM
Optical Density
0.15
0.12
0.09
0.06
0.03
0.00
VEH
WIN

Figure 3.16. Representative images of DAB-immunohistochemical staining of MAP2 protein within the cerebellum of adult male zebra finches treated with either vehicle (Panel A, inset C) or WIN (1 mg/kg, Panel B, inset D) after song learning. The number of tissue sections available from each treatment group was not sufficient for statistical analysis. 100X scale bar = 300 μm, 1000X scale bar = 30 μm.

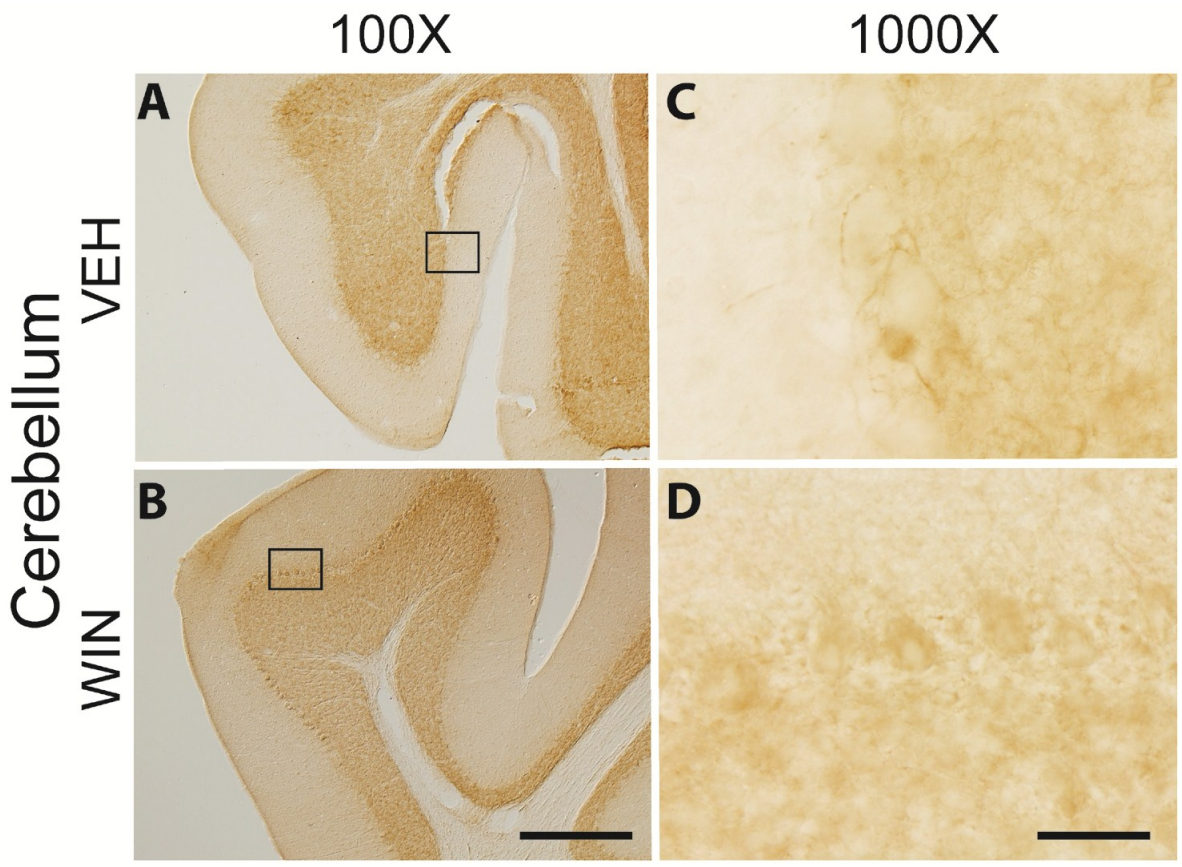
100X
1000X
Cerebellum
VEH
WIN
A
B
C
D

CHAPTER 4: CANNABINOID DISRUPTION OF NOVEL SONG-STIMULATED ARC/ARG 3.1 EXPRESSION IN ZEBRA FINCH AUDITORY TELENCEPHALON: NEURAL CORRELATES OF AUDITORY STIMULATION AND RECOGNITION

ABSTRACT:

Cannabinoids produce an array of cognitive effects; however an understanding of the physiological mechanisms responsible remains incomplete. Arc, an immediate-early gene (IEG) product involved in dendritic spine dynamics and necessary for plasticity changes such as long-term potentiation, is rapidly induced within zebra finch caudal medial nidopallium (NCM) following novel song perception, a response that habituates after repeated stimuli. Arc appears unique in its rapid dendritic expression and is induced postsynaptically following excitatory input. Previously, we found that vocal development-altering cannabinoid treatments are associated with elevated dendritic spine densities. Given Arc's dendritic morphological role, we hypothesized that cannabinoid-altered spine densities may involve Arc-related signaling. To test this, we examined the ability of the cannabinoid agonist WIN 55,212-2 (WIN) to: (1) acutely disrupt song-induced Arc expression; (2) interfere with auditory recognition memory and; (3) alter dendritic spine densities associated with learning. We found that WIN (3 mg/kg) acutely reduced Arc expression within both NCM and Field L2. WIN also blocked Arc habituation in an antagonist-reversible manner. WIN did not alter Arc expression in the thalamic auditory relay Nucleus Ovoidalis (Ov), which suggests the cannabinoid system is important for higher-order sensory processing. Novel song stimulation rapidly increased dendritic spine densities within integrative auditory

telencephalon, an effect blocked by WIN pretreatments. Taken together, cannabinoid inhibition of both Arc induction and its habituation to repeated stimuli implicates this protein in the mechanism underlying cannabinoid-altered spine densities, and reduced ability to encode/consolidate auditory information that is essential for sensorimotor learning.

INTRODUCTION

The cannabinoid system has an important role in many central nervous system functions including (but not limited to) increased feeding behaviors, analgesia, antiemesis, as well as an array of psychoactive effects (Cocchetto et al., 1981; Guindon and Hohmann, 2009; Soderstrom et al., 2004). Cannabinoid chemicals (both naturally and synthethically derived), are known to modulate the degree of neurotransmission between synapses through primary activation of the cannabinoid receptor: particularly, the central actions of these compounds are attributed to activation of the cannabinoid receptor 1 (CB_1). CB_1 receptors are localized in high concentrations in certain brain areas, including the cerebellum, hippocampus, frontal cortex, and basal ganglia, which correlates with well-documented influences on locomotor coordination, anxiolysis, and increases in reward-like behaviors present in models of drug addiction (El Manira and Kyriakatos, 2010; Fernandez-Ruiz et al., 2010; Kinsey et al., 2011). Less well understood are the physiological effects cannabinoids have on the neural aspects of learning and memory acquisition. We previously demonstrated that in zebra finches, a once daily administration of the cannabinoid agonist WIN 55,212-2 is associated with an inappropriate maintenance of dendritic spine densities in regions critical for both sensorimotor learning and production of stereotyped song. Changes in dendritic spine

densities are only produced following developmental exposure; treatments given to adults that had completed vocal learning are not effective (Gilbert and Soderstrom, 2011). It is postulated that cannabinoid diminution of activity within the neuron disrupts the acquisition and consolidation of sensory stimuli, and ultimately cognition, though the specifics remain unclear. Recent observations have led to the hypothesis that the dendritically located immediate early gene product Arc/Arg3.1 (Arc) plays a role in at least one form of cannabinoid-induced disruption of cognitive function.

The vertebrate brain is truly remarkable, in that it is capable of converting sensory experiences of the world around us into discrete physiological changes in both synaptic activity and connectivity. This intricate process involves activity-dependent presynaptic membrane depolarization and subsequent calcium influx into selective neurons within a specific circuit (Bramham et al., 2010; Shepherd and Bear, 2011). These actions often result in the transcription of a wide array of activity-induced genes distinctly expressed within the neuron that can be classified into two groups: classic immediate-early genes (such as *c-fos, egr-1, and c-jun*) which encode for transcription factors that indirectly influence neuronal activity before any new proteins can be synthesized, and "effector" immediate early genes (*BDNF, Homer 1, Neuritin* and particularly *Arc*) which encode for effector proteins that *directly* regulate axonal outgrowth and plasticity at the synapse (Fosnaugh et al., 1995; Rickhag et al., 2007; Tischmeyer and Grimm, 1999). The immediate-early gene *Arc,* also known as activity-regulated cytoskeleton-associated protein, or activity-regulated gene 3.1, is a single copy gene whose mRNA is trafficked directly to dendritic spines and undergoes rapid, local translation (Bramham et al., 2010; Bramham et al., 2008). Recent studies

demonstrated that *Arc*, in its translated form (also referred to as Arc), co-precipitates with polymerized F-actin, shares a near identical intracellular distribution as actin in dendritic spines, and is a necessary component of actin-dependent neuronal structures (Guzowski et al., 2005; Lyford et al., 1995). Furthermore, *Arc* mRNA and protein are both highly conserved within the vertebrate species, and their induction during behavioral learning is so robust, distinct, and reproducible that it is often used as an indicator for neural circuitry that underlies learning and memory (Guzowski et al., 2001; Guzowski et al., 2005). *Arc* has been identified as a key component of protein synthesis-dependent long-term potentiation, and is necessary for the consolidation of synaptic plasticity and formation of long term memories (Bramham et al., 2008; Pastuzyn et al., 2011; Plath et al., 2006; Ploski et al., 2008). In particular, reductions in Arc mRNA/ protein are strongly correlated with reduced performances in spatial memory and fear conditioning in mammals (Guzowski et al., 2000; Zhang et al., 2011). Accordingly, inappropriate activation of the CB_1 receptor is linked to marked reductions in memory consolidation and performances of the very *same* tasks (Abush and Akirav, 2010; Mackowiak et al., 2009). Thus, given the essential roles that both Arc and the CB_1 receptor play in this component of learning and memory, it is reasonable to postulate that these two elements have a relationship that culminates in the disruption of dendritic spine plasticity, the specifics of which currently remain unknown.

Auditory perception provides an excellent example of the importance of sensory experience to cognitive processing. Songbirds, similar to other vertebrates, possess an ascending pathway that conducts auditory information to higher-order integrative brain regions. Interestingly, within the caudomedial region of the zebra finch telencephalon, a

circuit of pallial regions comprise a domain that is homologous to the mammalian primary and secondary auditory cortex (Pinaud and Terleph, 2008). Auditory information enters the avian cochlea, and then travels via a series of projections to a midbrain nucleus of the auditory pathway, the dorsal lateral nucleus of the mesencephalon (MLd, homologous to the mammalian inferior colliculus). This area then projects to a thalamic relay region between it and the auditory cortex, referred to as Nucleus Ovoidalis (Ov, avian homolog of the mammalian medial geniculate nucleus (Krutzfeldt et al., 2010)). Projections from Ov then reach the telencephalon through the primary auditory projection area, Field L, and finally target a region specialized for perceiving conspecific vocal signals, caudal medial nidopallium (NCM, homologous to mammalian supragranular layers (Jarvis et al., 2005; Mello and Clayton, 1994; Mello et al., 2004; Terleph et al., 2007; Zaretsky, 1978)). For an illustration of these regions, see Figure 4.1. Young songbirds must hear, experience, and memorize the stereotyped song of an adult male tutor by use of both auditory feedback and sensory integration, during a critical period known as sensorimotor learning (Tschida and Mooney, 2012). This process involves constant communication between these auditory regions and areas that comprise the passerine song system. In a number of studies, this laboratory has examined the impact of daily developmental cannabinoid exposure on the quality of song learning and recall later on in adulthood, and found that these animals have significant reductions in stereotypy in comparison to the song of their tutors (Soderstrom and Tian, 2004; Soderstrom and Tian, 2008). Presumably, the diminished ability to produce quality song in adulthood is attributed to cannabinoid modulation of sensory

input within auditory and song regions by altering the normal dendritic spine plasticity known to occur during vocal learning.

In effect, when utilized in conjunction with other methods, immediate-early gene expression analysis within passerines can yield significant insights, particularly regarding the spatial organization of the brain's response to sensory stimulation. Because immediate-early genes are activity-dependent, are not induced in the absence of stimulation, and are robustly expressed in response to stimulation leading to cellular depolarization, they are very sensitive indicators of neuronal activation (Sagar et al., 1988; Sheng and Greenberg, 1990). Accordingly, most accept the expression of immediate-early genes within a given neuron reflects previous activation of said neuron by the stimulus under study (Mello et al., 2004). In songbirds, many genomic regulatory events corresponding to the brain's response to sensory stimuli have been elucidated; perhaps one of the most studied targets has been an immediate-early gene referred to as *zif-268, egr-, NGFI-A, Krox-24,* or "*zenk"*. In early experiments, it was determined that *zenk* was strongly induced in NCM in response to a short period of novel, conspecific song; however it was induced at a significantly lower level after exposure to song of a heterospecific species, and none at all in response to tone bursts (Mello and Clayton, 1994; Mello et al., 1992). Since then, a multitude of studies have evaluated the induction of a number of immediate-early genes and their translated products in response to sensory stimulation in many different scenarios. For example, Velho and colleagues (2005) not only established that *Arc* is significantly induced in auditory forebrain areas in response to novel birdsong, but that it is co-expressed with many other immediate-early genes and effectors that are activated by the same natural

sensory experience, namely *zenk* and *c-fos* (Mello et al., 2004; Velho et al., 2005). Furthermore, CB_1 receptor activation with WIN 55,212-2 selectively inhibited novel zenk protein expression within NCM, a result suggesting a role for cannabinoids in influencing cognition at the perceptual level (Whitney et al., 2003). Here, we used behavioral, pharmacological, and, histological methods in order to examine the role of WIN 55,212-2 to acutely disrupt song-induced Arc expression, interfere with auditory recognition memory of a song stimulus, and alter dendritic spine densities normally associated with learning.

MATERIALS AND METHODS

Materials

Except where noted, all materials and reagents were purchased from Sigma (St. Louis, MO), or Fisher Scientific (Pittsburgh, PA). Immunochemicals were purchased from Vector Laboratories (Burligame, CA), and the primary anti-Arc/Arg3.1 antibody was purchased from Abcam (Cambridge MA, Catalog # AB85656). Equithesin was prepared from reagents (40 % propylene glycol, 10 % ETOH, 5 % chloral hydrate, 1 % pentobarbital). The synthetic cannabinoid agonist WIN and inverse agonist SR141716A were suspended in vehicle from concentrated DMSO stocks (10 mM). Vehicle consisted of a suspension of 1:1:18 DMSO:Alkamuls EL-620 (Rhodia, Cranberry, NJ):phosphate-buffered saline.

Animals

Animals were cared for and experiments conducted according to protocols approved by East Carolina University's Animal Care and Use Committee. Adult male

zebra finches bred and raised in our aviary were used as subjects in these experiments. Prior to the start of experiments, birds were housed singly with free access to grit, water, mixed seeds (Sunseed VitaFinch), and cuttlebone, and provided multiple perches. Animals were maintained on a 14:10 light/dark cycle, and ambient temperature was maintained at 78° F.

Acute/Chronic Treatments

Twenty-four hours prior to the start of experiments, animals were housed singly in visual and auditory isolation, in recording chambers, based on a design developed by engineering personnel in the Florida State University Neuroscience Program (Whitney et al., 2003). The method developed to induce Arc protein expression in the zebra finch auditory telencephalon was adapted from protocols used for *Arc* and *Zenk* mRNA co-induction, and Zenk protein expression (Lonergan et al., 2010; Mello and Ribeiro, 1998; Velho et al., 2005). Birds were exposed to a tape recording of 15 s of novel conspecific song, followed by 45 s of silence, repeated 30 times. The novel song consisted of a collection of five second song bouts from three adult males from an outside aviary. Song playbacks were presented in a fifteen second medley, followed by forty five seconds of silence, for a total of a one minute. This procedure was repeated a total of thirty times. Unstimulated control groups were only exposed to silence. Following these 30 minute stimulus periods, birds were left in silence for an additional 90 minutes to reach peak protein expression.

In experiments that involved drug treatments, injections were given thirty minutes prior to the beginning of the song stimulus procedure. A well-established protocol was used in order to determine whether WIN treatment would disrupt

habituation of Arc induction following repeated presentation of the same song stimulus (Whitney et al., 2003). Animals were exposed to the same 30 minute song playbacks for three days. On two consecutive days, birds received an intramuscular injection of WIN (3 mg/kg), SR141716A (6 mg/kg), or vehicle 30 minutes before the start of song playbacks. Silent controls not exposed to song were given either a single intramuscular injection of WIN (3 mg/kg) or vehicle for two days. On the third day of song exposure, all groups were given a single injection of vehicle. At the end of experiments on the third day, animals were given an overdose of Equithesin (100 µl), and brain tissue was processed for immunolabeling of Arc protein.

Western Blotting

The presence of Arc protein was detected in the zebra finch brain by using a rabbit polyclonal antibody targeting the internal sequence of amino acids 288-337 of Human Arg 3.1 (LDLPQKQGEP LDQFLWRKRD LYQTLYVDAD EEEIIQYVVG TLQPKLKRFL.) This epitope was compared to the zebra finch sequence, and found to differ by a single residue (LDLPQKEGEP LDQFLWRKRD LYQTLYVDAD EEEIIQYVVG TLQPKLKRFL, Genbank accession number XP_002186861). To assess the selectivity of the Arc antibody against zebra finch protein, western blotting experiments were done. Protein extraction protocols were adapted from methods described by Schafer et al., 1998. Adult male zebra finches, subjected to song stimulation procedures described above, were killed by Equithesin overdose. Brains were removed, homogenized with a polytron in an ice-cold extraction buffer containing 1 M Tris-HCl, pH = 7.0, 0.6 M KCl, 0.5 mM ATP, 1 mM DTT, 0.5 mM $MgCl_2$, along with a cocktail of protease inhibitors (0.25 M sucrose/1 mM EDTA/4 mM phenylmethylsulfonyl fluoride/1 mM 4-amino

benzamidine/0.1% w/v bacitracin), and briefly micro-centrifuged at 1000 x *g*. Supernatants were stirred on ice for 30 minutes, collected and centrifuged at 24,000 x *g*. Following this, protein preps were ultra-centrifuged at 100,000 x *g* for 1 hour. Pellets were discarded and supernatants were filtered through cheesecloth to remove traces of excess lipid, and dialyzed against 10 L of ice-cold distilled water for 4 hours at 4º C. The fractions were then dialyzed overnight against two changes of ice-cold extraction buffer containing 10 mM Tris-HCl, pH 8.0, 0.2 mM $CaCl_2$, 0.5 mM ATP, 0.1 mM DTT, 100 mM KCl, and 0.1 mM phenylmethylsulfonyl fluoride. Samples were spun a final time at 24,000 x *g* at 4º C to remove trace precipitate. Supernatants were collected and protein concentrations determined using the Bradford method. 30 µg of soluble protein were loaded into a 10% polyacrylamide gel, separated by SDS-PAGE, and blotted onto a PVDF membrane. Blots were blocked with a non-mammalian blocking reagent (Odyssey Blocking Buffer, LI-COR Biosciences, Lincoln, NE) and incubated overnight at 4º C in a 1:1000 dilution of the Arc antibody in Odyssey Blocking Buffer. The next day, the blot was washed three times with 1X PBS-T (Phosphate-Buffered Saline [pH = 7.4] with 0.05% Tween-20), and incubated in a secondary antibody solution containing an infrared anti-rabbit secondary antibody (LI-COR Biosciences # 926-68021, 1:25,000) and 0.02% SDS for 2 hours at room temperature in the dark. The blot was washed 4 times with 1X PBS (Phosphate-Buffered Saline [pH = 7.4]) for 10 minutes each, and visualized using the LI-COR Odyssey Infrared Imaging System. Masses of infrared bands were determined standard curves fit to distances migrated by molecular weight standards using GraphPad Prism 5.0 software (GraphPad Software, SanDiego, CA,

USA). Separate experiments where primary antibody was preabsorbed with 20 □M of the immunizing peptide were performed as a negative control (Abcam, Cambridge, MA).

Additional western blotting experiments were performed with synaptosomal membrane preparation isolated from caudal telencephalon (containing NCM and Field L2) following drug treatments and song exposure procedures as described above. After behavioral experiments, animals were quickly anesthetized, decapitated, and brains rapidly dissected on ice. Brain sections containing regions NCM and Field L2 were placed into a glass and Teflon grinder containing 25 volumes of ice-cold 0.32 M sucrose in 5 mM Tris, pH = 7.4, and ground to homogeneity. Following this, homogenates were centrifuged at *1000 x g* at 4º C for 15 minutes. Pellets were discarded; supernatant was removed and placed into a fresh centrifuge tube on ice, and centrifuged at *30,000 x g* at 4º C for 60 minutes. Pellets were then snap-frozen at -80º C overnight, and resuspended in 150 volumes of 50 mM Tris, 10 mM EDTA, pH = 7.4. Membrane fractions were incubated at 4º C for 2 hours in an effort to chelate endogenous cations and dissociate endogenous ligands from receptors. These fractions were again centrifuged at *30,000 x g* at 4º C for 60 minutes, after which pellet fractions were collected. Pellets were washed by homogenizing with a glass and Teflon grinder in 150 volumes of 50 mM Tris, 5 mM $MgCl_2$, pH = 7.4. Homogenates were centrifuged at *30,000 x g* at 4º C for 60 minutes and resuspended in 50 mM Tris, 5 mM $MgCl_2$, pH = 7.4 a final time, and protein concentrations determined by the Bradford method. In addition to anti-Arc detection, these blots were also probed with an antibody directed against □-actin as an internal control (Sigma # A3853). Relative intensities of Arc and

actin bands were determined and compared across treatment conditions. Potential treatment effects were assessed using t-tests.

Immunohistochemistry

Immediately following the end of song exposure procedures described above, animals were killed by Equithesin overdose (100 µl) and transcardially perfused with PBS, followed by phosphate-buffered 4% paraformaldehyde [pH = 7.0]. Brains were immersed in 4% paraformaldehyde overnight, and then transferred to an ice-cold 20% sucrose solution the next morning. Once tissues sank in the sucrose solution, brains were blocked down the midline and sectioned parasagittaly, using a Leica VT 1000 vibrating microtome. For experiments that required capture of NCM and Field L2, consecutive free-floating sections were collected from the midline (0.0mm) to 2.0 mm lateral of the midline. All tissue was processed using a standard immunohistochemical procedure adapted from (Whitney et al., 2000). Tissue was briefly rinsed in 1X PBS for 10 minutes followed by incubation in 1% H_2O_2 for 30 minutes, to quench endogenous peroxidase. The sections were again rinsed 3 times with 1X PBS, and then blocked with 5% normal goat serum for 35 minutes. Following blocking, sections were incubated overnight at room temperature in a solution containing anti-Arc antibody (1:3000 dilution), 1% normal goat serum, 0.01% sodium azide, and 0.3% Triton-X 100 in PBS. The following day, tissue was rinsed three times in PBS and incubated in a biotinylated anti-rabbit antiserum followed by an avidin-biotin complex from a kit following the manufacturer's instructions (VECTASTAIN ABC Elite kit, Vector Laboratories Inc., Burlingame, CA). Antibody labeling was developed using a 3,3-diaminobenzidine (DAB) solution in the presence of hydrogen peroxide followed by three washes in 1X

PBS. Tissue sections were mounted on glass slides coated with 0.3 % gelatin. After sections on slides were allowed to dry overnight, sections were dehydrated with graded concentrations of ethanol (70 %, 95 %, and 100 % respectively), cleared with xylenes, and coverslipped with Permount (Fisher).

Golgi-Cox Impregnation

A mixture containing 5 volumes of 5% potassium dichromate solution, 5 volumes of 5% mercuric chloride, and 4 volumes of 5% potassium chromate solution was prepared and allowed to ripen in the dark five days before use. After the end of song exposure procedures described above, birds were killed by Equithesin overdose and transcardially perfused with PBS, brains removed and rinsed briefly with ice-cold distilled water, and immersed in a filtered (0.45 micron) aliquot of Golgi-Cox supernatant for 14 days in the dark at room temperature. The brains were then transferred to an ice-cold 30 % sucrose solution for five days. Following sucrose treatment, brains were blocked down the midline, and left hemispheres were sectioned parasagittally on a vibrating microtome. 125-micron sections of zebra finch brain were then gold-toned in order to preserve staining as follows. The sections were exposed to chilled solutions of 80, 60, 40, and 20% glycerol, rinsed with water, then transferred to a 0.05% ice-cold gold chloride solution for 80 minutes. After being briefly transferred to an ice-cold 0.2% oxalic acid solution for two minutes, sections were immersed in 1 % sodium thiosulfate for a total of 60 minutes. The sections were developed in a 7 % ammonium hydroxide solution at room temperature, in the dark for 30 minutes, followed by further processing in Kodak Fixer. Sections were then mounted and dehydrated on glass slides, and neurons of zebra finch auditory nuclei assessed for dendritic spine densities and as a

function of treatment. Tissue was stained and processed in multiple batches; however, in order to eliminate possible variance associated with reaction conditions, each of the treatment groups were represented in each batch.

Optical Density Measurements

Immunohistochemiscal staining was examined in various brain regions at 40, 100, and 1000 X using an Olympus BX51 microscope with Nomarski DIC optics. Images were captured using a Spot Insight QE digital camera and Image-Pro Plus 5.0 software (MediaCybernetics, Silver Spring, MD) under identical, calibrated exposure conditions. All images were background-corrected, and converted to 8-bit grey scale; borders that outlined brain regions of interest were traced manually. Two dimensional optical density measurements of both labeled nuclei and neuropil from areas enclosed within traced areas were performed on images without knowledge of treatment condition for each brain region of interest. For measurements pertaining to NCM and Field L2, All intact sections containing NCM brain regions from the midline (0.0 mm to 2.0 mm from the midline per animal were included for analysis), and analyzed using Image-Pro Plus 5.0 software. Field L2 regions between the midline and 0.5 mm from the midline were not included for analysis. Mean optical densities (within brain region counts of stained nuclei and neuropil/area of the region) were compared across each treatment group using one-way ANOVA as described below.

Measurement of Dendritic Spine Densities

Dendritic spines were visualized at 100 X and 1000 X under oil immersion using a Zeiss AxioImager M2 microscope with QIClick digital CCD optics, and analyzed using

Neurolucida 3D reconstruction imaging software (MBF Bioscience, Williston VT). Dendritic spine densities, expressed as the mean number of dendritic spines per length (μm) of each dendrite, were analyzed based on criteria adapted from Norrholm, et al. (Norrholm and Ouimet, 2001). Neurons that were selected for measurement were fully impregnated, intact, located in areas of tissue free of debris and other imperfections, and possessed dendritic processes greater than 20 microns in length. In order to ensure random sampling, all neurons that fit the criteria above were assigned a number, and 5 neurons were randomly selected from each of 5 separate tissue sections containing NCM for each treatment. 3-D serial reconstructions were created for each neuron directly from slides, and quantitative morphometric analyses were conducted for each neuron (cell body, dendrites, and dendritic spines), and data pertaining to each outline was exported into Microsoft Excel Spreadsheet. All observable spines along the entire length of dendrites of 25 randomly selected neurons per each NCM brain region of animals in each representative treatment group (vehicle + novel song exposure, WIN + novel song exposure, and un-stimulated silence control groups, n = 4 for each treatment group) were analyzed.

RESULTS

Anti-Arc Antibody Selectivity

In an effort to capture Arc protein expression at its maximum levels, brains of male animals exposed to novel song were used for the following experiments. Western blotting was performed to assess selectivity of the anti-Arc antibody used. SDS-PAGE separation of 30 μg of brain protein revealed the presence of a single predominant band of approximately 55 kDa labeled by the anti-Arc antibody. The size of this labeled

protein is consistent with that reported from other mammalian species, including mouse, rat and human (see Figure 4.2A, and Bramham et al., 2008). Anti-Arc immunoreactivity was eliminated following preabsorption of antisera with the immunizing peptide (see Figure 4.2A).

To determine the cellular localization of anti-Arc binding within neurons, images of double immunofluorecence labeling of dendritically-associated MAP2 (Figure 4.3B, red) with activity-stimulated arc protein within NCM (Figure 4.3B, green) were captured at 630 X and 1000 X, via confocal laser scanning microscopy. There was considerable spatial overlap between the dendrite-associated protein MAP2 (Figure 4.3B, red) and the Arc protein, that appears present both somatically and dendritically (see Figure 4.3B, yellow merge). Note the robust expression of Arc protein both within dendrites (Figure 4.3B, solid arrows), and cell bodies (Figure 4.3B, dashed arrows).

Cannabinoid Inhibition of Novel Song-Stimulated Arc Expression

Arc mRNA expression within zebra finch auditory telencephalon following novel conspecific song stimulation has been previously characterized (Velho et al., 2005). Auditory information enters the avian cochlea and travels to a midbrain nucleus of the auditory pathway, the dorsal lateral nucleus of the mesencephalon (MLd, homologous to the mammalian inferior colliculus) then passes a thalamic relay region between it and the auditory cortex, referred to as Nucleus Ovoidalis (Ov, avian homolog of the mammalian medial geniculate nucleus (Krutzfeldt et al., 2010). From here, stimuli reaches telencephalon through the primary auditory Field L2, and finally targets a region specialized for perceiving conspecific vocal signals the caudal medial nidopallium (NCM, homologous to mammalian supragranular layers (Jarvis et al., 2005; Mello and

Clayton, 1994; Mello et al., 2004; Terleph et al., 2007; Zaretsky, 1978). Therefore we began our study of Arc protein expression within these previously-studied areas through a series of immunohistochemistry experiments followed by optical density measurements of anti-Arc staining from 100X grayscale images. As prior dose-response experiments indicated that 3 mg/kg of the cannabinoid agonist, WIN was the lowest fully-effective dosage for inhibition of song-stimulated Zenk expression, we employed this dosage in the current experiments (Whitney et al., 2003).

We found that levels of Arc expression varied significantly within both NCM and Field L2 as a function of treatment: ($F(2,252) = 48.22$; $p < 0.001$) and ($F(2,226) = 23.77$; $p < 0.005$) for NCM and Field L2, respectively. Tukey's post hoc analyses further revealed that within NCM, there were significant differences across all three treatment groups (Vehicle + Silence, Vehicle + Song, WIN + song). Basal levels of Arc expression following periods of silence were low within NCM and Field L2 (see Figure 4.4A-C). Thirty minutes of novel song significantly elevated levels of Arc expression within both NCM and Field L2 relative to control groups (see Figure 4.4D-F). For NCM, average optical densities were significantly increased in novel song exposed animals (0.091 ± 0.004) versus animals treated with vehicle and only exposed to silence (0.049 ± 0.003, $q = 13.28$, $p < 0.05$). In the case of Arc expression within Field L2, average optical densities were significantly increased in novel song exposed animals (0.093 ± 0.005) versus animals treated with vehicle and only exposed to silence (0.051 ± 0.003, $q = 9.63$, $p < 0.05$). In striking contrast to vehicle treatments, acute pretreatment with WIN before song stimulation resulted in significantly reduced magnitude of arc protein expression within both NCM and Field L2 relative to vehicle-treated controls (see Figure

4.4G-I). Within NCM, mean optical densities were significantly reduced by WIN from 0.059 ± 0.002 to 0.049 ± 0.003 ($q = 3.414$, $p < 0.05$). Within Field L2 mean optical densities were significantly reduced from 0.068 ± 0.005 to 0.050 ± 0.003 ($q = 3.922$, $p < 0.05$). These results are summarized in Figures 4.4J-K. In order to confirm that cannabinoid effects on novel stimulus-induced Arc expression were specific to higher-order telencephalic regions and not due to a general stimulation, we examined optical densities of Arc staining within the midbrain thalamic relay region, Ov. Interestingly, optical densities of Arc labeled cells within this thalamic auditory relay region did not vary as a function of novel song exposure or cannabinoid treatment ($F(2,105 = 0.1118$; $p > 0.05$), see Figure 4.5A-F; the optical densities within Ov for each treatment group are summarized in Figure 4.5G).

WIN Prevents Habituation of Arc Expression Following Repeated Auditory Stimulation

Prior work demonstrates that Zenk expression is decreased following habituation to sequential presentations of the same conspecific song, supporting a relationship between Zenk expression and novel song recognition (Mello et al., 1992; Whitney et al., 2003). Similar patterns of Arc expression within auditory telencephalon led us to test whether Arc also habituates following repeated presentation of the same song, and whether this habituation is influenced by CB_1 receptor activation.

As reported by others for Zenk (Mello et al, 1992; Whitney et al., 2003), repeated presentation of the same conspecific song resulted in habituation of Arc expression within both NCM and Field L2 (compare Figure 4.6A-C to Figure 4.6 G-I, and Figure 4.6 P, Vehicle + Silence to Vehicle + Song). One-way ANOVA confirmed treatment differences in Arc immunoreactivity ($F(4,247) = 31.68$; $p < 0.0001$) and ($F(4,143) =$

13.14; $p < 0.0001$) for areas NCM and Field L2, respectively. Further analysis revealed that pretreatment with WIN prior to the first two song presentations prevented this habituation from occurring in response to the same song on the third day within NCM (compare Figure 4.6 G-I to Figure 4.6 J-L, and Figure 4.6 P Vehicle + Song to Day 1-2 WIN, Day 3 Vehicle, from 0.139 ± 0.033 to 0.199 ±0.063 ($q = 11.56$, $p < 0.0001$). Habituation was also prevented by WIN treatment within Field L2 where mean optical densities were significantly elevated from 0.129 ± 0.027 to 0.165 ± 0.0239 ($q = 7.892$, $p < 0.0001$). Importantly, in both NCM and Field L2, agonist-induced prevention of habituation was reversed by pretreatment with the CB_1-selective inverse agonist, SR141716A, demonstrating CB_1 mediation of the effect (compare Figure 4.6J-L to Figure 4.6M-O, and Figure 4.6P Day 1-2 WIN, Day 3 Vehicle to Day 1-2 WIN /SR141716A, Day 3 Vehicle).

WIN Disrupts Auditory Perception-Induced Increased Dendritic Spine Densities within NCM

We previously demonstrated that developmental cannabinoid treatment persistently elevates dendritic spine densities within telencephalic regions essential for song learning and production (Gilbert and Soderstrom, 2011). In addition, others have shown that activity-induced Arc expression is essential for maintenance of LTP, and is positively correlated with various forms of learning and memory, and is required for more durable forms of synaptic plasticity (Chowdhury et al., 2006; Guzowski et al., 2000; Guzowski et al., 1999; Plath et al., 2006). These observations, combined with the findings above for cannabinoid inhibition of Arc expression that is a molecular correlate of auditory recognition, suggests a potential physiological mechanism by which

exogenous cannabinoid exposure may disregulate synaptic plasticity that takes place during learning (Roberts et al., 2010). As our prior experiments investigated effects of chronic cannabinoid exposure, we have extended these results to assess potential acute influences of novel song on dendritic spine densities, and potential cannabinoid modulation of this effect.

Novel song stimulation of vehicle-treated animals resulted in a robust and rapid increase in dendritic spine densities within NCM (Figure 4.7C). WIN administration 30 minutes prior to novel song stimuli reversed these song-stimulated spine increases to levels not significantly different from non-song stimulated, vehicle-treated controls (Compare Figures 4.7B and 4.7D, $F(2, 1053) = 53.67$; $p < 0.0001$).

DISCUSSION

In addition to demonstrating for the first time that sensory perception- and integration-related Arc expression (within Field L2 and NCM, respectively) is mitigated by CB_1 receptor activation, our results importantly demonstrate that these cannabinoid effects on Arc are associated with rapidly-altered dendritic spine densities that suggests a role in processes important to learning and memory. Such a role is consistent with that observed within mammalian hippocampus where Arc is critical for memory-related neuronal plasticity, including LTP and LTD (reviewed by Bramham et al., 2008). Equally significant, we have demonstrated the specific contributions of cannabinoid receptor agonism to disrupting the portion of Arc protein expression exclusively located within functional nerve terminals (see Figure 4.3). Endocannabinoid signaling is directly involved in short-term synaptic plasticity changes (depolarization induced suppression of inhibition [DSI] and –excitation [DSE]) as well more persistent LTD, with a modulatory

role in LTP (reviewed by Chevaleyre et al., 2006). Together, clear involvement of both Arc expression and endogenous cannabinoid signaling in long-term forms of synaptic plasticity suggest that CB_1-altered Arc expression may be a general mechanism critical for regulating changes in synaptic strength. The current report is the first to demonstrate a relationship between memory-essential Arc and CB_1 activation.

Evidence demonstrating the importance of Arc signaling to neural plasticity has rapidly accumulated. For example, Arc co-precipitates and shares nearly identical intracellular distribution with F-actin in dendritic spines, and is a necessary component of actin-dependent morphological change (Bramham et al., 2010; Bramham et al., 2008; Guzowski et al., 2005; Lyford et al., 1995). Both *Arc* mRNA and protein sequences are highly conserved across vertebrates, and their expression during learning is so robust, distinct, and reproducible that it is used as an indicator of neural circuitry that underlies learning and memory (Guzowski et al., 2001; Guzowski et al., 2005). Arc has been identified as a key component of protein synthesis-dependent LTP, and is necessary for the consolidation of synaptic plasticity and formation of long term memories (Bramham et al., 2008; Pastuzyn et al., 2011; Plath et al., 2006; Ploski et al., 2008). Reductions in Arc mRNA and protein are associated with reduced performance in fear conditioning and spatial memory tasks (Guzowski et al., 2000; Zhang et al., 2011). Interestingly, inappropriate activation of CB_1 receptors is linked to impaired memory consolidation and performance in the very *same* tasks (Abush and Akirav, 2010; Mackowiak et al., 2009).

In other systems, Arc is associated with AMPA receptor expressing, calmodulin kinase-positive neurons (Vazdarjanova et al., 2006). As cannabinoid receptors are largely expressed presynaptically (Elphick and Egertova, 2001), this suggests that

effects reported herein are likely attributable to receptor activation on glutamatergic terminals within both NCM and Field L2, that will effectively reduce excitatory glutamatergic signaling. If confirmed, this arrangement has similarities to the circuitry between CB_1–expressing, CA3-emanating Schaeffer collaterals that synapse on dendrites of pyramidal neurons within the CA1 region of mammalian hippocampus (Hoffman et al., 2010), and further implicates nidopallial regions in formation of novel, auditory-related memories. This is further supported by evidence demonstrating potent WIN inhibition of auditory sensory gating activity in rat CA3 (Dissanayake et al., 2008). Our results also provide additional insight into the memory-related, hippocampus-like function of songbird nidopallium that accumulating evidence suggests retains the song "template" memorized during early, auditory stages of vocal development (Gobes et al., 2010; Terpstra et al., 2004; Thompson and Gentner, 2010).

The pattern of novel song-stimulated Arc protein expression that we observed differs from that of mRNA expression previously reported. Specifically, song-stimulated expression of Arc mRNA appears distinctly higher within NCM than within Field L2 (Velho et al., 2005). In contrast we have found similar levels of protein expression within these regions. This suggests that Arc expression is differentially-controlled within regions of primary and integrative auditory telencephalon, with possible temporal differences in mRNA regulation. Our experiments included a 90 minutes post-stimulation period to capture peak protein expression within NCM. The prior *in situ* hybridization studies prepared tissue earlier, and immediately following the period of song-stimulation (see Figure 4.4).

The similar efficacy of cannabinoid-decreased Arc expression within both Field L2 and NCM may be unexpected given distinct differences in the magnitude of CB_1 densities in the regions; much higher level expression is present within Field L2 than within surrounding nidopallium (Soderstrom and Tian, 2006). High-density Field L2 expression includes several features; staining is present within cell bodies, neuropil and within distinct, small puncta that may represent terminal fields. Almost exclusive punctual staining is observed within NCM, implicating it in the Arc inhibition observed within both regions. This suggests that the non-punctal staining present within Field L2 is involved in additional, endocannabinoid-mediated processes that are yet to be established. This also illustrates that relatively low-level cannabinoid receptor expression is capable of significant physiological efficacy. It is important to note that neither song stimulation nor WIN administration changed Arc expression within the thalamic auditory relay region, Ov that is also associated with distinct and dense CB_1 receptor expression. This clearly demonstrates a selective role for Arc in perceptual (Field L2) and integrative (NCM) processes, that it is not simply attributable to general neuronal activation.

Conclusion

In summary, our results demonstrate that Arc is induced by perception of novel auditory stimuli in a manner inhibited by CB_1 receptor activation. Stimulation of Arc expression within auditory telencephalon is associated with rapid increases in dendritic spine densities, a process that is also acutely cannabinoid-reduced. Taken together, these results suggest an Arc-dependent mechanism involved in cannabinoid-modulated processes of auditory perception, integration and memory. These findings may extend

and provide insight to endocannabinoid signaling in other sensory systems, and CB_1-related roles in memory extinction, stress responses and deleterious effects following exogenous cannabinoid exposure, particularly during CNS development.

Figure 4.1. Simplified schematic representation of the avian auditory brain regions studied. The thalamic region nucleus ovoidalis (Ov) transmits primary auditory sensory information to thalamorecipient Field L2 (L2, shown in light grey), which projects to caudal medial neostriatum (NCM, shown in darker grey).

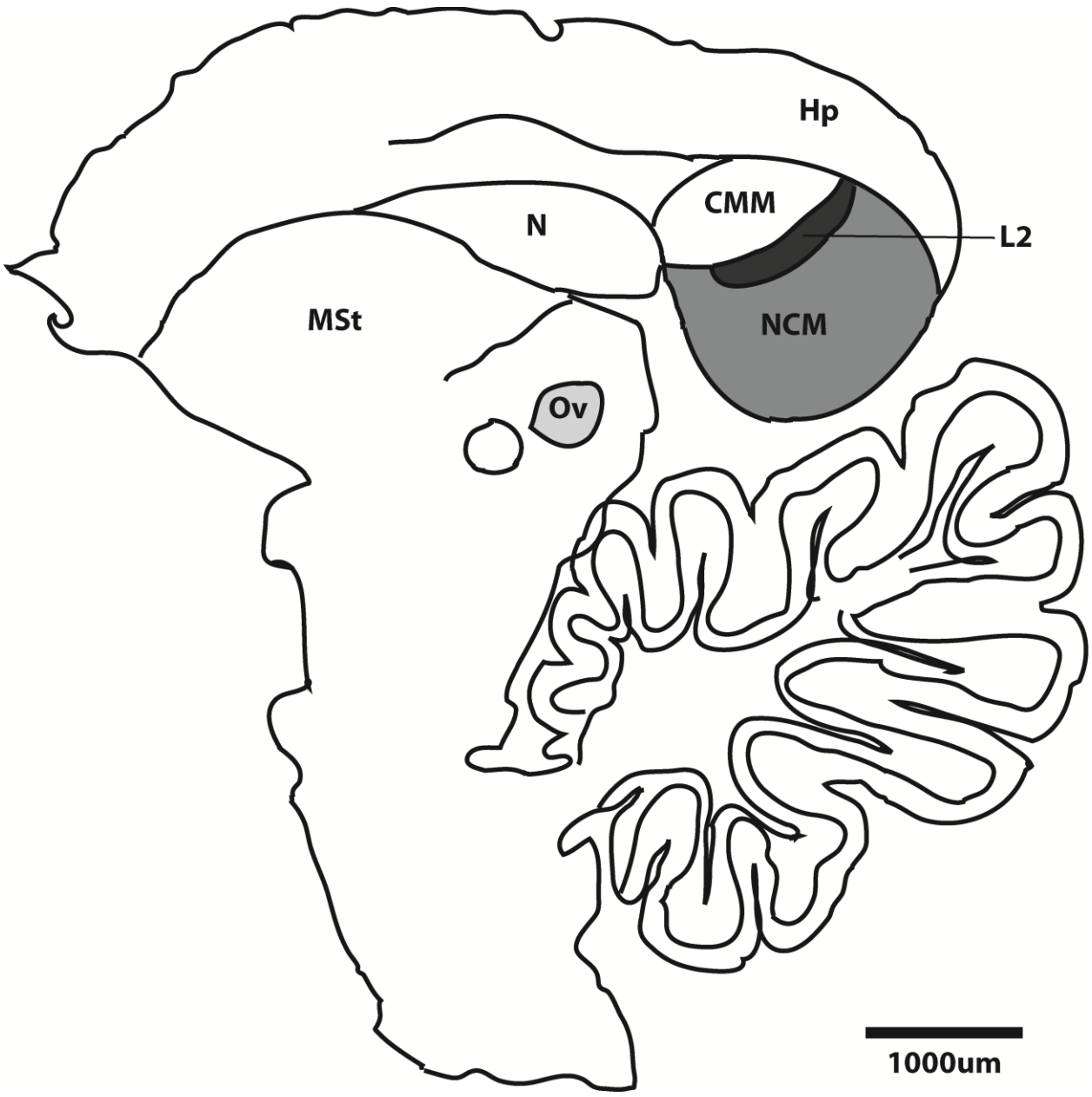
Hp
CMM
N
L2
MSt
NCM
Ov
1000um

Figure 4.2. (A) Representative Western blot of the soluble fraction of protein isolated from male NCM brain homogenates. Similar to other species, the anti-Arc antibody labels a single predominant band of about 55 kDa (left lane). Staining is abolished by preabsorption with 20 μM of the immunizing peptide (right lane**)**. (B) Novel song stimulation increases Arc protein levels in zebra finch caudal telencephalon that contains auditory regions NCM and Field L2 (compare Silence to Song). This stimulation was prevented by pretreatment with the cannabinoid agonist WIN (WIN + Song). Blots were reprobed with an antibody directed against β-actin as an internal control. (C) Summary of the relative intensities of Arc:β-actin bands. Shown are means +/- SEM of five pooled experiments. Novel song stimulation (Song) increased Arc expression over that of silence-exposed controls (Silence). WIN treatment prior to novel song exposure (Song + WIN) reduced Arc expression. Asterisk indicates significant difference from Silence group, dagger indicates difference from Song group ($p < 0.05$, 1-tailed t-test).

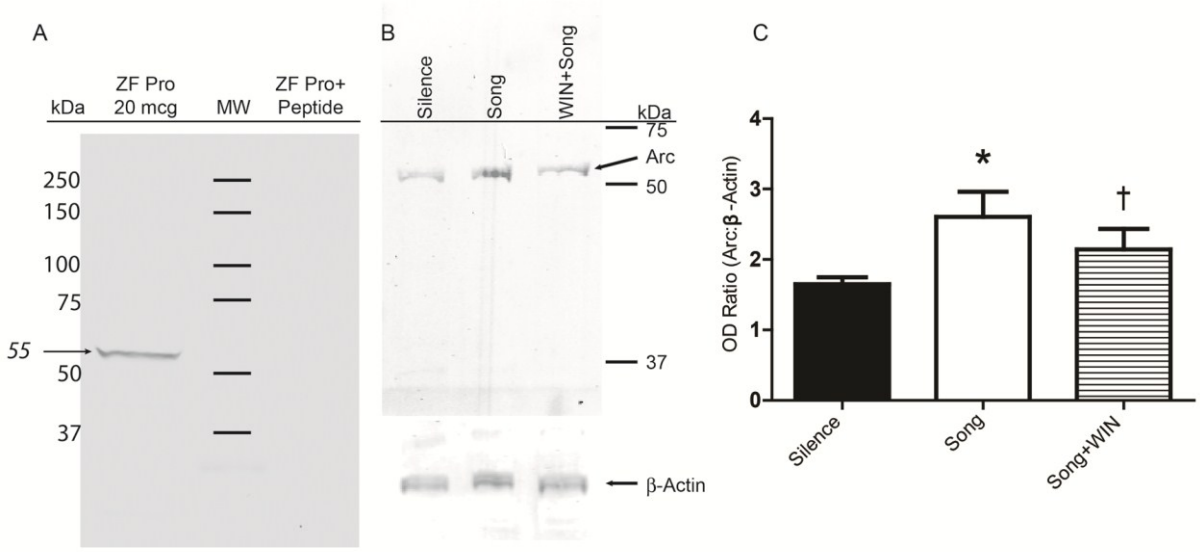
A
kDa
ZF Pro
20 mcg
MW
ZF Pro+
Peptide
250
150
100
75
55
50
37
B
Silence
Song
WIN+Song
kDa
75
Arc
50
37
β-Actin
C
OD Ratio (Arc:β-Actin)
4
3
2
1
0
*
†
Silence
Song
Song+WIN

Figure 4.3. Double immunofluorescence labeling of Arc protein with dendritically-associated MAP2 (630,1000X), visualized via confocal laser scanning microscopy. In an effort to capture Arc protein expression at its maximum level, brains of male animals exposed to novel song were used for these experiments. Images demonstrating Arc distribution alone (green), and colocalized with MAP2 (yellow, image overlays) show both cellular and dendritic distribution of protein. Bar = 20 μm.

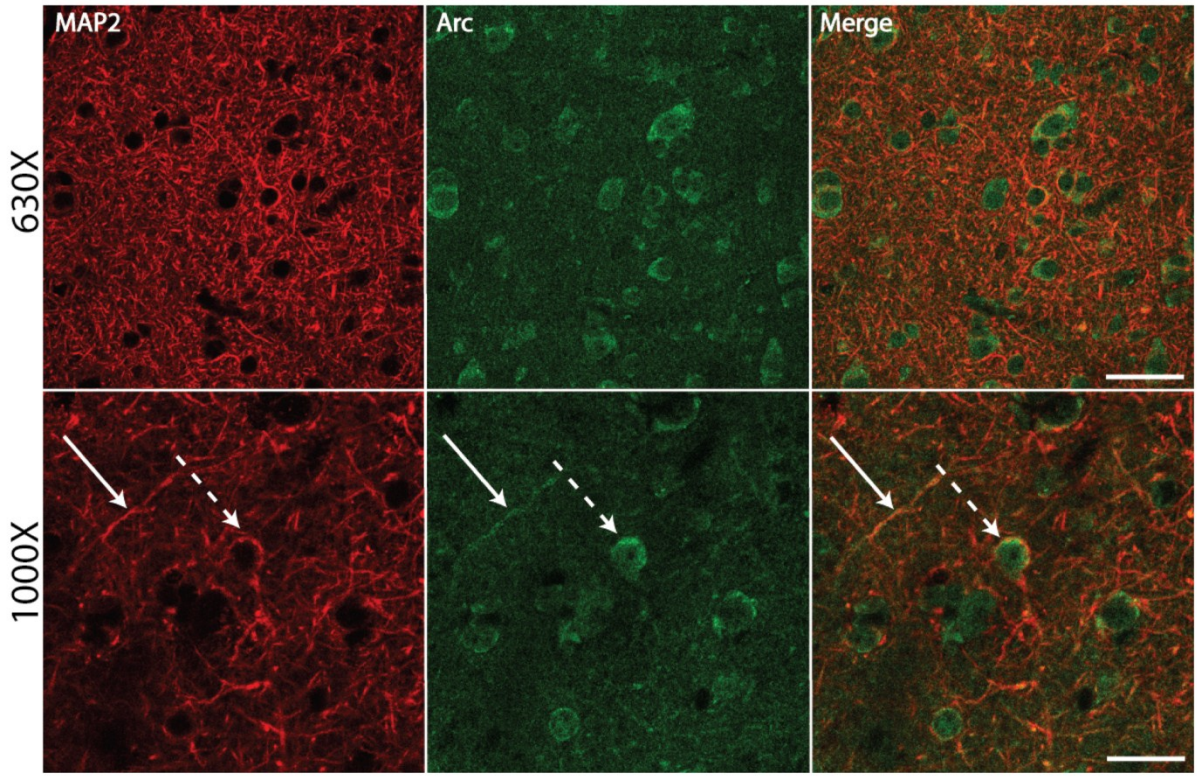
MAP2
Arc
Merge
630X
1000X

Figure 4.4. Immunohistochemical staining of NCM (solid boxes in A,D,G) and Field L2 (dashed boxes in A,D,G) with Arc antibody. Animals were exposed to either vehicle (D-F) or WIN pretreatment (G-I) 30 minutes before novel song exposure. Unstimulated control animals (A-C) received only silence.. At 1000X magnification, novel song stimultion increases cellular and neuropil Arc expression within both NCM (E) and Field L2 (F). J-K: Optical densities of NCM (J) and Field L2 (K) Arc expression after novel song exposure, and after WIN pretreatment. Novel song stimulation increases Arc expression by about 90%, but only by about 20% after WIN exposure. Bar in G = 300 μm. Bar in H-I = 30 μm.

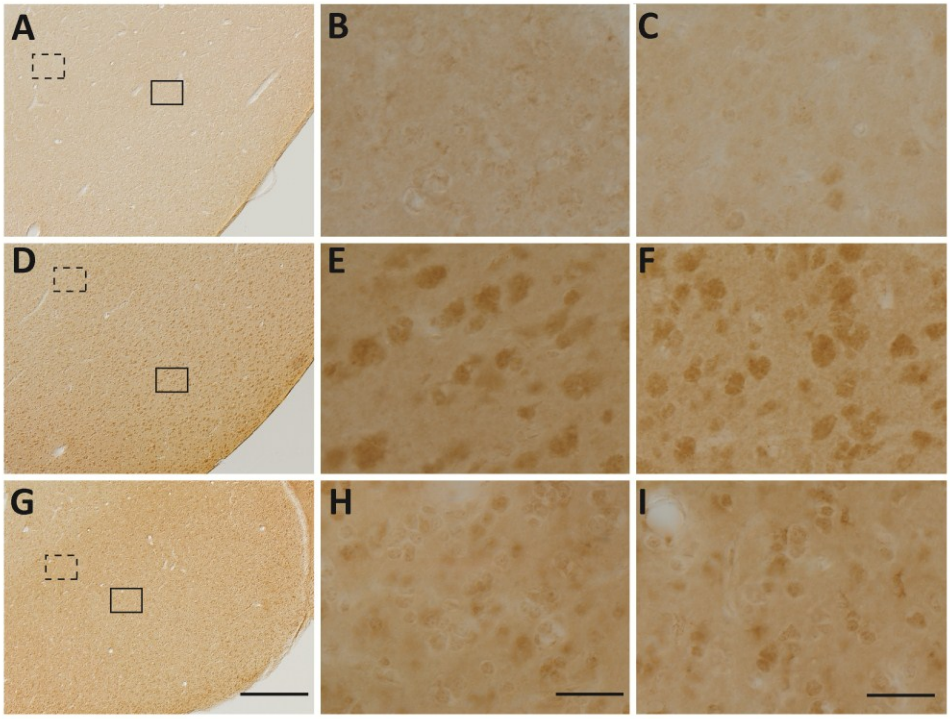
A
B
C
D
E
F
G
H
I

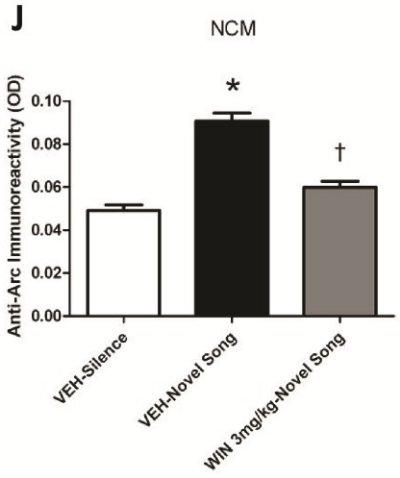
J
NCM
Anti-Arc Immunoreactivity (OD)
0.10
0.08
0.06
0.04
0.02
0.00
*
†
VEH-Silence
VEH-Novel Song
WIN 3mg/kg-Novel Song

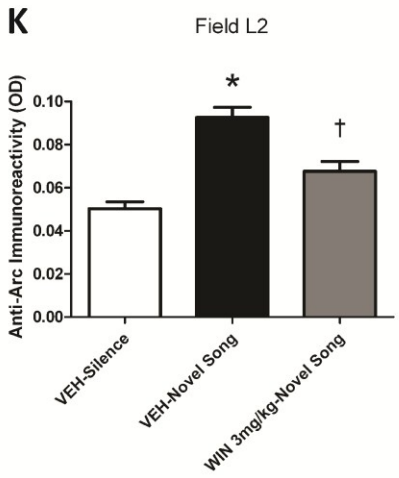
K
Field L2
Anti-Arc Immunoreactivity (OD)
0.10
0.08
0.06
0.04
0.02
0.00
*
†
VEH-Silence
VEH-Novel Song
WIN 3mg/kg-Novel Song

Figure 4.5. Optical densities (G) and immunohistochemical staining (A-F) of Arc expression within Ov in unstimulated controls, after acute novel song exposure, and after pretreatment with WIN. The absence of cannabinoid-mediated effects on Arc expression within this region indicates higher-order involvement of cannabinoid signaling in integrating perceptual information within the auditory telencephalon. Scale Bar in E = 300μm. Scale Bar in F = 30μm.

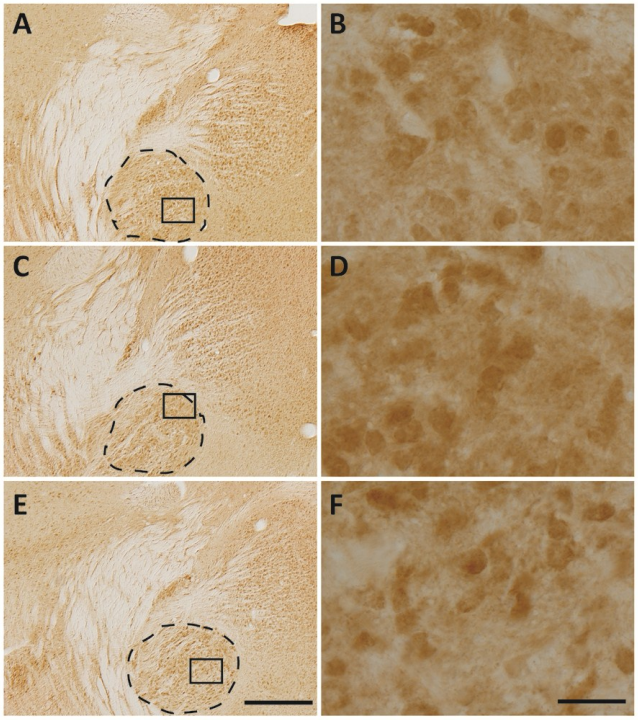
A
B
C
D
E
F

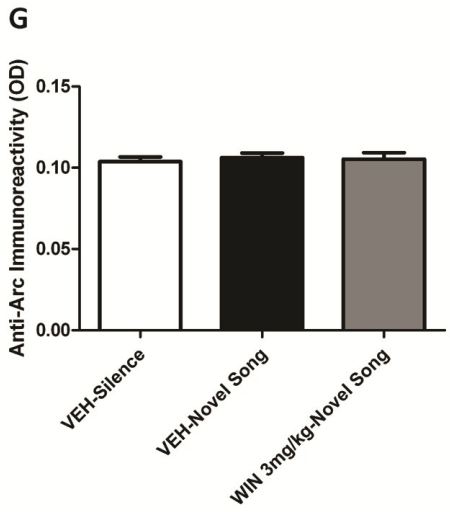
G
Anti-Arc Immunoreactivity (OD)
0.15
0.10
0.05
0.00
VEH-Silence
VEH-Novel Song
WIN 3mg/kg-Novel Song

Figure 4.6. Birds were exposed to the same 30 min song for 3 days. On days 1 and 2, birds received WIN (3 mg/kg), the CB_1-selective antagonist SR141716A (6 mg/kg), or vehicle injections 30 min before song stimulations. On day 3, all groups received vehicle injections prior to song exposure, were euthanized 90 min afterward and brains processed for anti-Arc immunolabeling **(**A-O**). (**G-I**):** Habituation to novel song-induced Arc expression occurs in vehicle treated group as evidenced by a return to baseline levels. WIN exposure disrupts habituation (J-L**)** however, the effect is reversed with the antagonist SR141716A **(**M-O**)**.

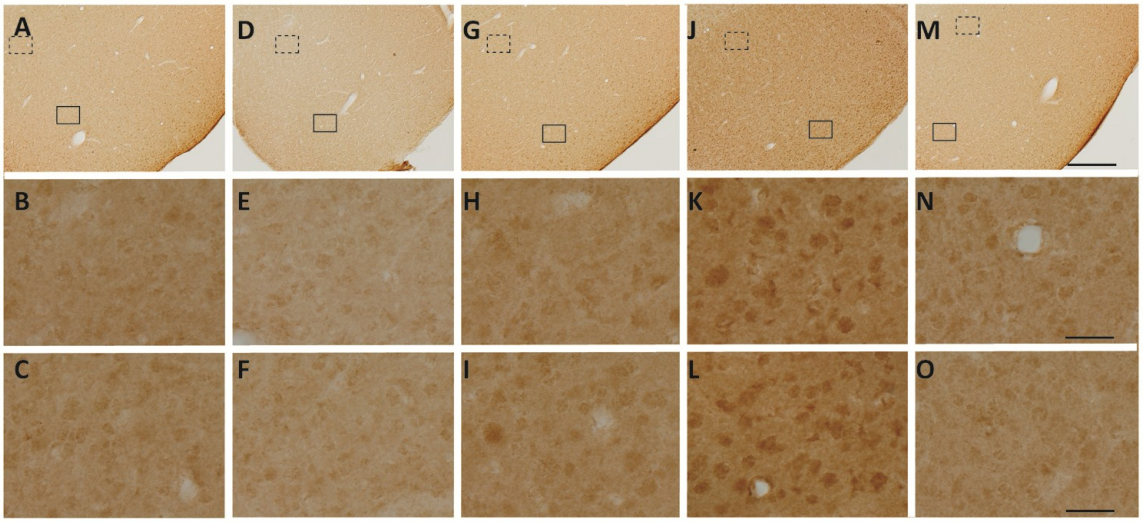
A
D
G
J
M
B
E
H
K
N
C
F
I
L
O

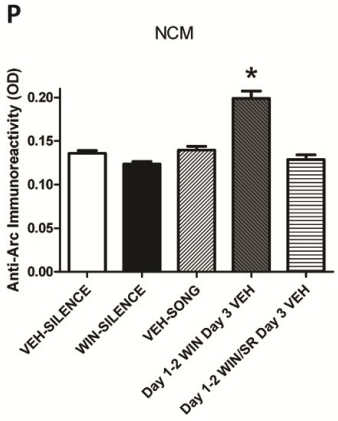
P
NCM
Anti-Arc Immunoreactivity (OD)
0.20
0.15
0.10
0.05
0.00
*
VEH-SILENCE
WIN-SILENCE
VEH-SONG
Day 1-2 WIN Day 3 VEH
Day 1-2 WIN/SR Day 3 VEH

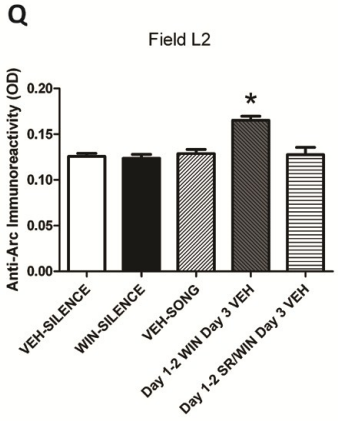
Q
Field L2
Anti-Arc Immunoreactivity (OD)
0.20
0.15
0.10
0.05
0.00
*
VEH-SILENCE
WIN-SILENCE
VEH-SONG
Day 1-2 WIN Day 3 VEH
Day 1-2 SR/WIN Day 3 VEH

Figure 4.7. (A) Representative high power image of an NCM spiny neuron used for analysis. Bar = 30 μm. (B-D) Representative Golgi-Cox impregnated dendrites included in analysis of dendritic spine densities within (B) unstimulated control, (C) 30 min of novel song exposure and (D) cannabinoid-pretreated groups (3 mg/kg WIN 30 min prior to song exposure). (E) Novel song perception results in significant increases in dendritic spine densities within NCM. Note that this effect was produced rapidly after acute auditory exposure (animals were killed 90 min following song exposure). Cannabinoid pretreatment (30 min prior to song exposure) with 3 mg/kg WIN prevents rapid increases in spine densities.

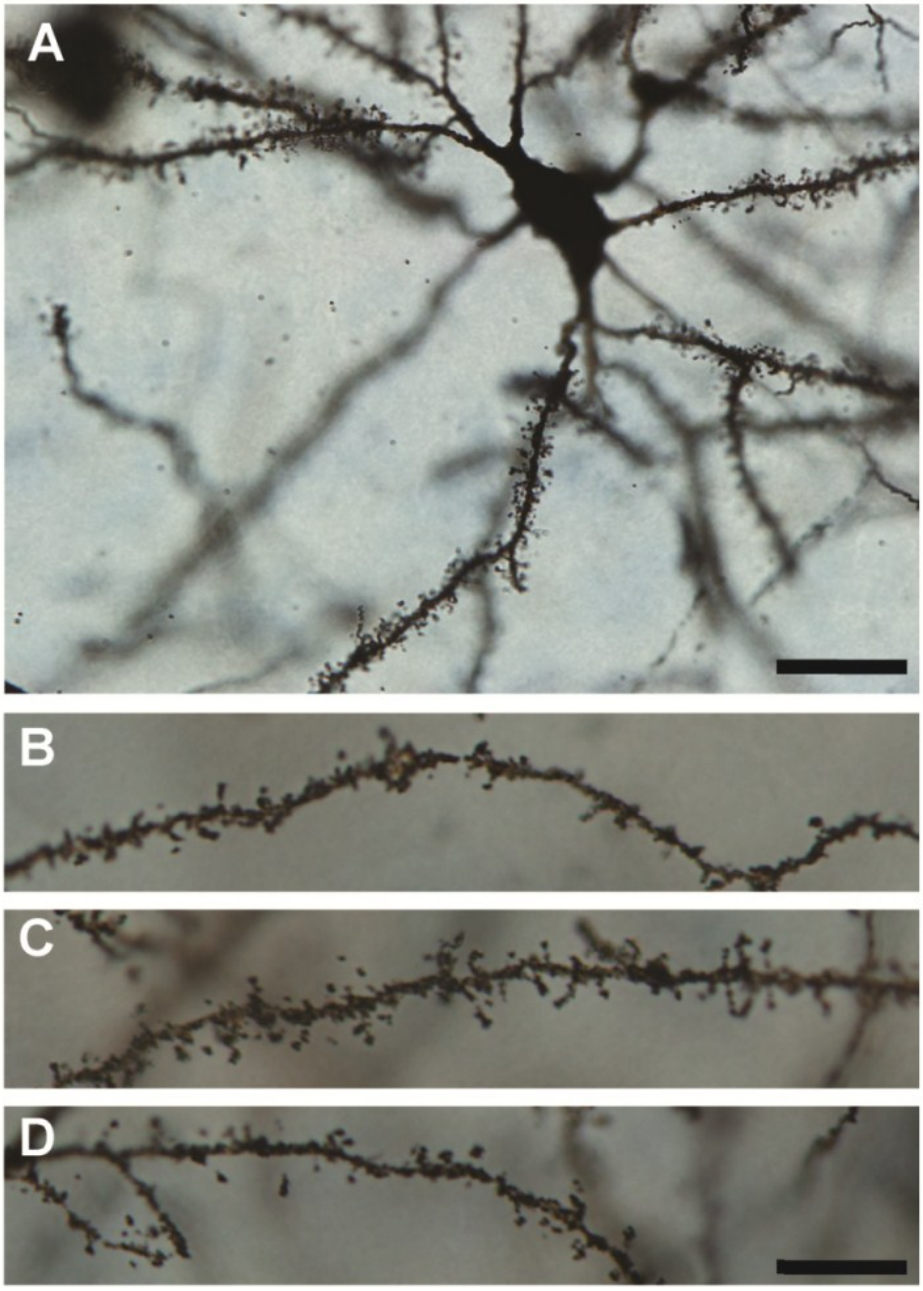
A
B
C
D

CHAPTER 5: GENERAL CONCLUSIONS

INTRODUCTION

Cannabis is the most commonly used illicit substance in the world among teenagers and young adults, and has been demonstrated to clearly possess the potential for addiction in humans (Gardner, 2002). In fact, close to 20% of users who begin during adolescence develop an addiction to these agents, a rate doubling that reported for users that begin in adulthood (Chen et al., 1997; Rubino and Parolaro, 2008). The age of first marijuana use has significantly decreased, which has caused much concern within the healthcare community (Earleywine, 2002). Furthermore, there have been increasing reports of adolescents requiring medical attention as a result of using designer cannabinoid drugs, which on average are 25 times more potent than the organic plant resin. Despite this upward trend in cannabinoid consumption among adolescents, relatively little is known about the lasting neurophysiological consequences of this behavior. It is disturbing to recognize that an agent so widely consumed among individuals of this age group has the potential to alter behavior and neural function in manners that lasts throughout adulthood (Gilbert and Soderstrom, 2011) (Bossong and Niesink, 2010). Adolescence is marked by a period in which several active neuroplastic changes occur that render the organism capable of mature behaviors, including circuit maturation and reorganization, and changes in neurotransmitter system levels. Because of this, it is unsurprising that more than any other period in life, this period of brain development is simultaneously vulnerable to the effects of psychoactive drug exposure, gonadal hormones, and environmental factors (Rubino and Parolaro, 2008). These findings are extended by the fact that most of the persistent changes in behavior

and brain morphology are not produced following similar cannabinoid exposure to adults (Ehrenreich et al., 1999; Wilson et al., 2000). Our laboratory has utilized the zebra finch song learning model because it offers a number of advantages over other systems of drug altered cognitive performance; *Firstly*, zebra finches are one of the few species of animals that undergo vocal learning as humans do. This unique feature allows us to draw very close parallels between what we morphologically observe following persistent cannabinoid-disrupted learning and memory formation, and what is hypothesized to occur in analogous regions of the human telencephalon. *Secondly*, not only is the vocal behavior produced after learning highly stereotyped, and reproducible, but learning takes place during a restricted time period. This feature results in less variability between animal subjects, and offers us more control within experiments. In addition, the restricted time period in which song takes place is adolescence, the time in human postnatal life that possesses the most potential for neuroplasticity, and subsequently is most vulnerable to the effects of exogenous drug consumption. *Lastly*, the density, distribution, and expression patterns of CB_1 receptors are extremely similar to what is seen in humans.

Thus, experiments with the zebra finch model of cannabinoid-altered vocal development have enabled us to study the pharmacological effects of these agents in the context of vocal learning. The fact that drug abuse typically both begins in adolescence and involves *Cannabis*, makes the distinct efficacy of cannabinoids on the CNS during late-postnatal development of particular relevance to the problem of human substance abuse (Fontes et al., 2011).

Our previous experiments determined that once daily developmental cannabinoid agonist treatment during zebra finch adolescent sensorimotor vocal learning reduces numbers of song notes, and causes reduction in song stereotypy – characterized by disordered and repetitive note production (see (Soderstrom and Johnson, 2003)). We also determined that this ability of cannabinoids to alter vocal learning is restricted to development, as treatment of adults already having undergone song learning are rendered ineffective in this manner. Interestingly, developmental cannabinoid exposure produces greater effects on stereotypy when given early in adolescence, and greater effects on note number later (Soderstrom and Tian, 2004). Together these results suggested that the behavioral differences seen might correlate with certain alterations in CNS morphology, in reverse of what is normally seen during postnatal development.

It is a well-known fact that changes in neurophysiology often precede changes in behavior, and as a result, this project sought to identify some of these changes that accompany cannabinoid-altered zebra finch CNS development. Behavior is the result of a great number of physiological processes working in concert to produce responses to our surrounding environment, thus, we aimed to identify three distinct and persistent physiological changes associated with inappropriate CB_1 receptor activation during periadolescent development.

CANNABINOID-ALTERED VOCAL DEVELOPMENT CORRELATES WITH INNAPROPRIATE DENDRITIC SPINE INCREASES

First, and most importantly, we were able to establish a framework for cannabinoid-altered gross morphology within the zebra finch CNS, and gain insight into the extent to which cannabinoid signaling controls dendritic spine and somatic

morphology. CNS gross anatomy is established early in postnatal development, in humans by age five (Giedd et al., 2009). Despite gross similarities between brains of juvenile and adult vertebrates, more subtle developmental changes associated with adolescence also occur. These changes are characterized by increased myelination, decreased grey matter, reduced synapse numbers and dendritic spine densities in adulthood (Rakic et al., 1994).

Zebra finch vocal learning is accompanied by normal decreases in telencephalic dendritic spine densities within regions essential for auditory learning and vocal motor production. Song region spine densities increase rapidly following initial exposure to tutor song during the early auditory learning stage of zebra finch vocal development (Roberts et al., 2010). Similar to the Initial profusion of dendritic spines within song regions are diminished with experience and behavioral maturation. Spine densities normally decrease within some telencephalic song regions from adolescence to adulthood, coincident with vocal practice and auditory feedback associated with sensorimotor learning (Wallhausser-Franke et al., 1995). Coincident spine density changes and normal vocal development led us to test whether cannabinoid-altered vocal development may be attributable to effects on dendritic spines. Cannabinoid treatments that altered vocal development persistently resulted in elevated dendritic spine densities compared to control brains, and suggest that adolescent exposure interferes with normal reductions in dendritic spines (Gilbert and Soderstrom, 2011).

We found that IM injections of WIN intosong-tutored juveniles during sensorimotor learning (50 – 75) days, not only produces the persistently altered song behaviors demonstrated previously (Soderstrom and Johnson, 2003), but results in a

27% increase in dendritic spine densities within Area X, and a 31% increase in spine densities within HVC. In addition, neuronal cell morphology was significantly altered within HVC. Concomitantly, we did not observe any of these morphological differences within the song regions of adult zebra finches that had completed sensorimotor learning. HVC is considered the apex of the zebra finch song system; it is the site where the SMP and AFP converge upon one another (Mooney, 2009a). As stated previously, HVC plays important roles in both song production and sensorimotor learning. The zebra finch brain is organized quite differently than the human brain (instead of having a 6-layered cortex, they possess nucleated regions), but they do possess analogs (Jarvis et al., 2005). HVC is thought to be the avian analog of Broca's area, the brain region that governs speech and language functions; this is supported by a great deal of evidence. Human speech, language acquision and other language-related neural activity display left-sided dominance (Friederici and Alter, 2004; Raboyeau et al., 2010). Moorman and colleagues recently discovered that when zebra finches were exposed to tutor song and novel song, HVC displays identical lateralization to that of Broca's area, regardless of the type of song stimulus presented. Furthermore, like Broca's area, zebra finches display temporal left-sided dominance associated with memory formation early in development (sensory learning) that subsequently fades after memory formation (Moorman et al., 2012). In a striking comparison to the motor/cognitive capabilities of Broca's area, HVC provides sensorimotor integration, and precise movement of the vocal organs. Altered speech-related behavioral manifestations seen in our animal model after developmental cannabinoid administration are very similar to what is seen in aphasiac patients (Hutsler and Zhang, 2010). Additionally, there are correlations

between high dendritic spine densities within Broca's area, and decreased language-related function in other vocal communication- related disorders such as ASD (Hutsler and Zhang, 2010); perhaps these findings are extended to patients with Broca's aphasia as well. Surprisingly, only eight differences exist between the human FOXP2 gene and *Foxp2* in zebra finch, which means these genes share a very high degree of homology (Haesler et al., 2004). FOXP2 is implicated in modulating language-related neural plasticity within the brain, especially Broca's area; mutations in human FOXP2 cause severe deficits in speech and language, and genetic deletion of *Foxp2* in zebra finch Area X result in very similar deficits in vocal learning, an effect that is correlated with increased spine densities within this region (Schulz et al., 2010). The morphological findings in our study may provide evidence for a neurochemical vocal communication network mediated by the cannabinoid system.

VOCAL DEVELOPMENT-ALTERING CANNABINOID EXPOSURE PERSISTENTLY CHANGES EXPRESSION PATTERNS AND DENSITIES OF AXONAL AND DENDRITIC PROTEINS IN ZEBRA FINCH SONG REGIONS

Next, we sought to correlate the behavioral and neuromorphological changes seen previously with changes in levels of proteins related to cell signaling and morphology. During CNS development, CB_1 receptors located on growth cones mediate axonal and dendritic guidance through a $G_{i/O}$-dependent mechanism, by eliciting chemotactic responses (Berghuis et al., 2007) (Vitalis et al., 2008; Watson et al., 2008). These turning responses correlate positively with increased activation of RhoA, an actin-depolymerizing enzyme involved in neurite retraction and growth cone collapse (Gallo and Letourneau, 2004; Tagliaferro et al., 2006). Mechanisms of

cannabinoid regulation of axonal and dendritic differentiation established in vitro are now being studied in the context of developing brain. Embryonic initiation of cortical pyramidal cell axonal outgrowth appears to be promoted by CB_1 activation (Mulder et al., 2008), an effect that suggests that cannabinoid signaling plays opposing roles at different developmental stages, by initially promoting neurite outgrowth, but proceeds to stagnate growth following differentiation (Soderstrom and Gilbert, 2012).

A combination of CB_1 deficient mice and conditional mutants capable of expressing GFP in thalamocortical- and corticothalamic projection neurons, were used by Wu and co-workers to demonstrate that CB_1 activation is critical for appropriate axonal pathfinding and target recognition (Wu et al., 2010). Pathfinding deficits in these developing mice were associated with aberrant migration through the striatocortical boundry. This region is enriched with DAGL, suggesting that appropriate endocannabinoid signaling is critically important for successful axon migration through this region. Compelling evidence also suggests that the endogenous cannabinoid system also functions as a homeostatic mechanism, protecting the CNS from overstimulation by balancing excitatory and inhibitory synaptic input through mechanisms such as DSE and DSI (Marsicano et al., 2003).

Less understood, and more critical, are the physiological consequences of chronically over-stimulating the cannabinoid system during adolescence. Cannabinoids produce lasting changes in synaptic transmission by decreasing the probability of vesicular transmitter release and raising the threshold for depolarization, ultimately decreasing synaptic strength (Domenici et al., 2006; Katona et al., 1999; Kim et al., 2008). These lasting changes are associated with altered neuronal morphologies (Kim

et al., 2008). Altered morphology is associated with significant increases in a number of cytoskeletal proteins and synaptic markers (Tagliaferro et al., 2006). These findings prompted us to investigate whether similar alterations in neuronal cytoarchitecture existed in our model of cannabinoid-altered vocal learning. With the aid of immunohistochemical methods, we examined changes in the anatomy of the neurocytoskeletal network within the four song regions (HVC, RA, lMAN, Area X), thalamic relay regions (Ov, DLM) and cerebellum that occur with prolonged developmental cannabinoid exposure. Specifically, we measured levels of: phosphorylated neurofilament 200 (Nf-200), a protein enriched in axons and MAP2, a prominent dendritic and synaptic marker. We determined that spatial distribution of Nf-200 expression was significantly increased following developmental cannabinoid treatments in all regions examined except for lMAN. Consistent with previous studies, treatment of song-crystallized adults resulted in an almost complete integrity of the axonal cytoarchitecture, as no significant differences were found. We found that the density of dendritic- and synapse-associated protein (MAP2) was significantly elevated within all four song regions, and midbrain auditory region Ov following cannabinoid-induced maintenance of dendritic spines.

CANNABINOID AGONISM ALTERS CNS DEVELOPMENT BY INTERFERING WITH STRUCTURALLY-RELATED IMMEDIATE EARLY GENE EXPRESSION

Cannabinoids influence CNS development by altering gross dendritic morphology; however, it is now becoming clear that in addition to this, CB_1 receptors modulate activity and regulation of structural proteins by influencing activity-induced immediate early gene expression. Immediate-early gene based mediation of synaptic

plasticity plays an important role in the maturation of neural circuits; this suggests a period exists in which the brain is particularly sensitive to these effects. For example, THC exposure during adolescence coincides with lasting deficits in long-term recognition memory, an effect that is coupled with significant long-term reduction in hippocampal expression of several oxidative stress- and cytoskeleton-related proteins (Soderstrom and Gilbert, 2012). These proteins include mortalin/GRP75, important to cellular differentiation and malignant transformation (Quinn et al., 2008; Wadhwa et al., 2002) and NP25, a CNS-specific, F-actin binding protein necessary for actin assembly (Mori et al., 2004). The idea that cannabinoid-altered vocal development is associated with inappropriate maintenance of dendritic spine densities (Gilbert and Soderstrom, 2011) led us to question whether CB_1 regulation of activity-induced effector protein expression may play a role in these structural differences. Such structurally-relevant proteins with established involvement in the zebra finch vocal development model include postsynaptically- restricted caspase-3 (Huesmann and Clayton, 2006) and Arc (Moorman et al., 2011; Velho et al., 2005).

Similar to caspase-3, Arc is an effector-type immediate early gene induced by activity-dependent presynaptic depolarization (Tzingounis and Nicoll, 2006). It has been well-studied in hippocampus and is necessary for LTP, LTD and memory consolidation (Bramham et al., 2008). Arc regulation of synaptic plasticity appears related to promotion of AMPA receptor internalization, which involves an interaction with morphologically-relevant proteins including endofilin, dynamin and cofilin that subsequently modulate F-actin function (Huang et al., 2007; Waung et al., 2008). Our results demonstrate that CB_1 activation effectively prevents novel song-induced Arc

protein expression and habituation to repeated song stimulation to correlate this morphological change in behavior with a CB_1 receptor-mediated aberrant modulation of dendritic spine densities. How does CB_1 receptor activation result in inhibition of auditory perception-related Arc expression? It is hypothesized that CB_1 receptor activation reduces the probability of presynaptic excitatory transmitter release (Elphick and Egertova, 2001a). As Arc expression appears limited to AMPA receptor-containing terminals (Waung et al., 2008), the signaling relationship in zebra finch auditory telencephalon appears similar to that between CB_1-expressing Schaffer collateral terminals that synapse on AMPA receptor-expressing dendrites of hippocampal CA1 pyramidal cells (Hoffman et al., 2010; Soderstrom and Gilbert, 2012). Through DSE, cannabinoid exposure raises the threshold for depolarization-dependent immediate early gene expression. A reduction in postsynaptic excitation also decreases AMPA receptor internalization, increasing sensitivity to later excitatory input (Vazdarjanova et al., 2006). Disregulated glutamatergic sensitivity will disrupt activity-dependent processes important to developmental selective stabilization of neural circuits. This hypothesis, adapted from Changeux and Dehaene, is summarized in Figure 5.1. (Changeux and Dehaene, 1989; Soderstrom and Gilbert, 2012).

NEUROPHYSIOLOGICAL IMPLICATIONS

Given the clear function of the endocannabinoid system in the general reduction of presynaptic neurotransmitter release, we hypothesize that high-level expression of the cannabinoid system during normal adolescent development, likely provides a neuroprotective effect against glutamate-mediated excitotoxic damage resulting from the increased level of synaptic plasticity during this time. Theoretically, if CB_1 receptors

were perpetually activated like in the case of chronic daily cannabinoid consumption, this would compromise the protective effect of the system, and lead to a disturbance of the neuron's delicate LTP/LTD balance by causing excess glutamatergic activation, and consequently, an influx of postsynaptic Ca^{2+}. This scenario could very well lead to either pruning or a lack thereof, of anywhere from the synapse to the dendritic tree. This ultimately results in a persistent perturbance in regional neuronal circuitry and behavior.

Figure 5.1. Diagrammatic models illustrating potential mechanisms responsible for cannabinoid mitigation of neuronal morphological change. Panel A is adapted from the model proposed by Changeux and Dehaene, 1989 for late-postnatal refinement of neural circuitry. Panel B illustrates the potential for CB_1-mediated presynaptic inhibition of glutamate release to prevent activation of structurally-relevant proteins important to zebra finch sensorimotor integration of auditory stimuli [Taken with permission from (Soderstrom and Gilbert, 2012)].

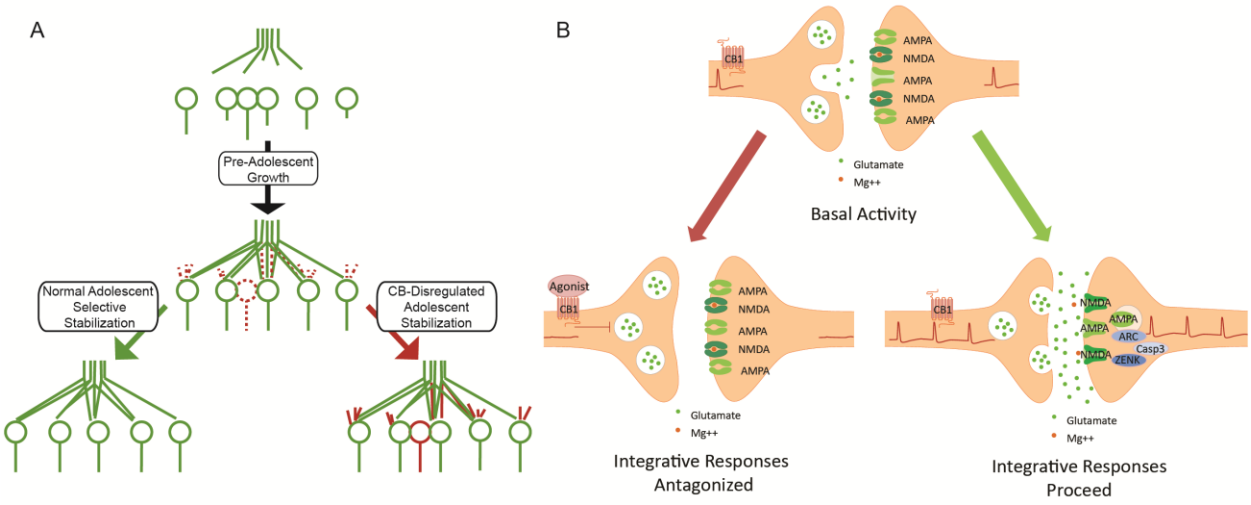
A
Pre-Adolescent Growth
Normal Adolescent Selective Stabilization
CB-Disregulated Adolescent Stabilization
B
CB1
AMPA
NMDA
AMPA
NMDA
AMPA
Glutamate
Mg++
Basal Activity
Agonist
CB1
AMPA
NMDA
AMPA
NMDA
AMPA
Glutamate
Mg++
Integrative Responses Antagonized
CB1
NMDA
AMPA
AMPA
ARC
Casp3
NMDA
zENK
Glutamate
Mg++
Integrative Responses Proceed

LITERATURE CITED

1999. Schedules of controlled substances: rescheduling of the Food and Drug Administration approved product containing synthetic dronabinol [(-) - [DELTA] less than 9 greater than - (trans)-tetrahydrocannabinol] in sesame oil and encapsulated in soft gelatin capsules from schedule II to schedule III. Department of Justice (DOJ), Drug Enforcement Administration (DEA). Final rule. Fed Regist 64(127):35928-35930.

Abel EL. 2005. Jacques Joseph Moreau (1804-1884). Am J Psychiatry 162(3):458.

Abood ME. 2005. Molecular biology of cannabinoid receptors. Handb Exp Pharmacol(168):81-115.

Abush H, Akirav I. 2010. Cannabinoids modulate hippocampal memory and plasticity. Hippocampus 20(10):1126-1138.

Adams R, Cain CK, Loewe S. 1941. Tetrahydrocannabinol Analogs with Marihuana Activity. XI1. Journal of the American Chemical Society 63(7):1977-1978.

Agurell S, Halldin M, Lindgren JE, Ohlsson A, Widman M, Gillespie H, Hollister L. 1986. Pharmacokinetics and metabolism of delta 1-tetrahydrocannabinol and other cannabinoids with emphasis on man. Pharmacol Rev 38(1):21-43.

Airey DC, Kroodsma DE, DeVoogd TJ. 2000. Differences in the complexity of song tutoring cause differences in the amount learned and in dendritic spine density in a songbird telencephalic song control nucleus. Neurobiol Learn Mem 73(3):274-281.

Alberi L, Liu S, Wang Y, Badie R, Smith-Hicks C, Wu J, Pierfelice TJ, Abazyan B, Mattson MP, Kuhl D, Pletnikov M, Worley PF, Gaiano N. 2011. Activity-induced Notch signaling in neurons requires Arc/Arg3.1 and is essential for synaptic plasticity in hippocampal networks. Neuron 69(3):437-444.

Alexanian AR, Maiman DJ, Kurpad SN, Gennarelli TA. 2008. In vitro and in vivo characterization of neurally modified mesenchymal stem cells induced by epigenetic modifiers and neural stem cell environment. Stem Cells Dev 17(6):1123-1130.

Allport DA. 1985. Distributed Memory, Modular Systems and Dysphasia. In: Newman SKaE, R., editor. Current Perspectives in Dysphasia. Edinburgh: Churchill Livingstone.

Ameri A. 1999. The effects of cannabinoids on the brain. Prog Neurobiol 58(4):315-348.

Anavi-Goffer S, Mulder J. 2009. The polarised life of the endocannabinoid system in CNS development. Chembiochem 10(10):1591-1598.

Arseneault L, Cannon M, Witton J, Murray RM. 2004. Causal association between cannabis and psychosis: examination of the evidence. Br J Psychiatry 184:110-117.

Ashmore RC, Wild JM, Schmidt MF. 2005. Brainstem and forebrain contributions to the generation of learned motor behaviors for song. J Neurosci 25(37):8543-8554.

Atkinson HC, Begg EJ, Darlow BA. 1988. Drugs in human milk. Clinical pharmacokinetic considerations. Clin Pharmacokinet 14(4):217-240.

Ausems M, Mesters I, van Breukelen G, De Vries H. 2003. Do Dutch 11-12 years olds who never smoke, smoke experimentally or smoke regularly have different demographic backgrounds and perceptions of smoking? Eur J Public Health 13(2):160-167.

Avraham R, Yarden Y. 2012. Regulation of signalling by microRNAs. Biochem Soc Trans 40(1):26-30.

Azad SC, Monory K, Marsicano G, Cravatt BF, Lutz B, Zieglgansberger W, Rammes G. 2004. Circuitry for associative plasticity in the amygdala involves endocannabinoid signaling. J Neurosci 24(44):9953-9961.

Barnes DW, Sirbasku DA, Sato G. 1984. Methods for preparation of media, supplements, and substrata for serum-free animal cell culture: A.R. Liss.

Basavarajappa BS. 2007. Neuropharmacology of the endocannabinoid signaling system-molecular mechanisms, biological actions and synaptic plasticity. Curr Neuropharmacol 5(2):81-97.

Bellone C, Mameli M. 2012. mGluR-Dependent Synaptic Plasticity in Drug-Seeking. Front Pharmacol 3:159.

Beltramo M, Stella N, Calignano A, Lin SY, Makriyannis A, Piomelli D. 1997. Functional role of high-affinity anandamide transport, as revealed by selective inhibition. Science 277(5329):1094-1097.

Bennett JS. 1974. Le Dain Commission of Inquiry into the Non-Medical Use of Drugs tables fourth and final report. Can Med Assoc J 110(1):105-108.

Berezovska O, McLean P, Knowles R, Frosh M, Lu FM, Lux SE, Hyman BT. 1999. Notch1 inhibits neurite outgrowth in postmitotic primary neurons. Neuroscience 93(2):433-439.

Berezovska O, Xia MQ, Hyman BT. 1998. Notch is expressed in adult brain, is coexpressed with presenilin-1, and is altered in Alzheimer disease. J Neuropathol Exp Neurol 57(8):738-745.

Berghuis P, Rajnicek AM, Morozov YM, Ross RA, Mulder J, Urban GM, Monory K, Marsicano G, Matteoli M, Canty A, Irving AJ, Katona I, Yanagawa Y, Rakic P, Lutz B, Mackie K, Harkany T. 2007. Hardwiring the brain: endocannabinoids shape neuronal connectivity. Science 316(5828):1212-1216.

Bhatt DH, Zhang S, Gan WB. 2009. Dendritic spine dynamics. Annu Rev Physiol 71:261-282.

Bloodgood BL, Sabatini BL. 2007. Ca(2+) signaling in dendritic spines. Curr Opin Neurobiol 17(3):345-351.

Bodor AL, Katona I, Nyiri G, Mackie K, Ledent C, Hajos N, Freund TF. 2005. Endocannabinoid signaling in rat somatosensory cortex: laminar differences and involvement of specific interneuron types. J Neurosci 25(29):6845-6856.

Bolshakov VY, Siegelbaum SA. 1994. Postsynaptic induction and presynaptic expression of hippocampal long-term depression. Science 264(5162):1148-1152.

Bosier B, Muccioli GG, Hermans E, Lambert DM. 2010. Functionally selective cannabinoid receptor signalling: therapeutic implications and opportunities. Biochem Pharmacol 80(1):1-12.

Bossong MG, Niesink RJ. 2010. Adolescent brain maturation, the endogenous cannabinoid system and the neurobiology of cannabis-induced schizophrenia. Prog Neurobiol 92(3):370-385.

Bottjer SW, Miesner EA, Arnold AP. 1984a. Forebrain lesions disrupt development but not maintenance of song in passerine birds. Science 224(4651):901-903.

Bottjer SW, Miesner EA, Arnold AP. 1984b. Forebrain lesions disrupt development but not maintenance of song in passerine birds. Science 224(4651):901-903.

Bouaboula M, Bourrie B, Rinaldi-Carmona M, Shire D, Le Fur G, Casellas P. 1995. Stimulation of cannabinoid receptor CB1 induces krox-24 expression in human astrocytoma cells. J Biol Chem 270(23):13973-13980.

Boylan K, Yang C, Crook J, Overstreet K, Heckman M, Wang Y, Borchelt D, Shaw G. 2009. Immunoreactivity of the phosphorylated axonal neurofilament H subunit (pNF-H) in blood of ALS model rodents and ALS patients: evaluation of blood pNF-H as a potential ALS biomarker. J Neurochem 111(5):1182-1191.

Brainard MS, Doupe AJ. 2000. Auditory feedback in learning and maintenance of vocal behaviour. Nat Rev Neurosci 1(1):31-40.

Bramham CR, Alme MN, Bittins M, Kuipers SD, Nair RR, Pai B, Panja D, Schubert M, Soule J, Tiron A, Wibrand K. 2010. The Arc of synaptic memory. Exp Brain Res 200(2):125-140.

Bramham CR, Worley PF, Moore MJ, Guzowski JF. 2008. The immediate early gene arc/arg3.1: regulation, mechanisms, and function. J Neurosci 28(46):11760-11767.

Bravarenko NI, Onufriev MV, Stepanichev MY, Ierusalimsky VN, Balaban PM, Gulyaeva NV. 2006. Caspase-like activity is essential for long-term synaptic plasticity in the terrestrial snail Helix. Eur J Neurosci 23(1):129-140.

Brown SL. 2005. Relationships between risk-taking behaviour and subsequent risk perceptions. Br J Psychol 96(Pt 2):155-164.

Brugg B, Matus A. 1991. Phosphorylation determines the binding of microtubule-associated protein 2 (MAP2) to microtubules in living cells. J Cell Biol 114(4):735-743.

Bylund DB, Toews ML. 1993. Radioligand binding methods: practical guide and tips. Am J Physiol 265(5 Pt 1):L421-429.

Carlson G, Wang Y, Alger BE. 2002. Endocannabinoids facilitate the induction of LTP in the hippocampus. Nat Neurosci 5(8):723-724.

Carroll FI, Lewin AH, Mascarella SW, Seltzman HH, Reddy PA. 2012. Designer drugs: a medicinal chemistry perspective. Ann N Y Acad Sci 1248:18-38.

Cavuoto P, McAinch AJ, Hatzinikolas G, Janovska A, Game P, Wittert GA. 2007. The expression of receptors for endocannabinoids in human and rodent skeletal muscle. Biochem Biophys Res Commun 364(1):105-110.

Cha YM, Jones KH, Kuhn CM, Wilson WA, Swartzwelder HS. 2007. Sex differences in the effects of delta9-tetrahydrocannabinol on spatial learning in adolescent and adult rats. Behav Pharmacol 18(5-6):563-569.

Chamak B, Fellous A, Glowinski J, Prochiantz A. 1987. MAP2 expression and neuritic outgrowth and branching are coregulated through region-specific neuro-astroglial interactions. J Neurosci 7(10):3163-3170.

Chang MC, Berkery D, Schuel R, Laychock SG, Zimmerman AM, Zimmerman S, Schuel H. 1993. Evidence for a cannabinoid receptor in sea urchin sperm and its role in blockade of the acrosome reaction. Mol Reprod Dev 36(4):507-516.

Changeux JP. 1997. Variation and selection in neural function. Trends Neurosci 20(7):291-293.

Changeux JP, Courrege P, Danchin A. 1973. A theory of the epigenesis of neuronal networks by selective stabilization of synapses. Proc Natl Acad Sci U S A 70(10):2974-2978.

Changeux JP, Dehaene S. 1989. Neuronal models of cognitive functions. Cognition 33(1-2):63-109.

Chen J, Nagayama T, Jin K, Stetler RA, Zhu RL, Graham SH, Simon RP. 1998. Induction of caspase-3-like protease may mediate delayed neuronal death in the hippocampus after transient cerebral ischemia. J Neurosci 18(13):4914-4928.

Chen K, Kandel DB, Davies M. 1997. Relationships between frequency and quantity of marijuana use and last year proxy dependence among adolescents and adults in the United States. Drug Alcohol Depend 46(1-2):53-67.

Chew SJ, Mello C, Nottebohm F, Jarvis E, Vicario DS. 1995. Decrements in auditory responses to a repeated conspecific song are long-lasting and require two periods of protein synthesis in the songbird forebrain. Proc Natl Acad Sci U S A 92(8):3406-3410.

Chew SJ, Vicario DS, Nottebohm F. 1996. A large-capacity memory system that recognizes the calls and songs of individual birds. Proc Natl Acad Sci U S A 93(5):1950-1955.

Childers SR, Deadwyler SA. 1996. Role of cyclic AMP in the actions of cannabinoid receptors. Biochem Pharmacol 52(6):819-827.

Chomczynski P. 1993. A reagent for the single-step simultaneous isolation of RNA, DNA and proteins from cell and tissue samples. Biotechniques 15(3):532-534, 536-537.

Chomczynski P, Sacchi N. 1987. Single-step method of RNA isolation by acid guanidinium thiocyanate-phenol-chloroform extraction. Anal Biochem 162(1):156-159.

Clem RL, Celikel T, Barth AL. 2008. Ongoing in vivo experience triggers synaptic metaplasticity in the neocortex. Science 319(5859):101-104.

Cocchetto DM, Cook LF, Cato AE. 1981. A critical review of the safety and antiemetic efficacy of delta-9-tetrahydrocannabinol. Drug Intell Clin Pharm 15(11):867-875.

Collard JF, Cote F, Julien JP. 1995. Defective axonal transport in a transgenic mouse model of amyotrophic lateral sclerosis. Nature 375(6526):61-64.

Costa RM, Honjo T, Silva AJ. 2003. Learning and memory deficits in Notch mutant mice. Curr Biol 13(15):1348-1354.

Cota D. 2007. CB1 receptors: emerging evidence for central and peripheral mechanisms that regulate energy balance, metabolism, and cardiovascular health. Diabetes Metab Res Rev 23(7):507-517.

D'Souza DC, Perry E, MacDougall L, Ammerman Y, Cooper T, Wu YT, Braley G, Gueorguieva R, Krystal JH. 2004. The psychotomimetic effects of intravenous delta-9-tetrahydrocannabinol in healthy individuals: implications for psychosis. Neuropsychopharmacology 29(8):1558-1572.

Dailey ME, Smith SJ. 1996. The dynamics of dendritic structure in developing hippocampal slices. J Neurosci 16(9):2983-2994.

Daniel H, Rancillac A, Crepel F. 2004. Mechanisms underlying cannabinoid inhibition of presynaptic Ca2+ influx at parallel fibre synapses of the rat cerebellum. J Physiol 557(Pt 1):159-174.

Dekker N, Smeerdijk AM, Wiers RW, Duits JH, van Gelder G, Houben K, Schippers G, Linszen DH, de Haan L. 2010. Implicit and explicit affective associations towards cannabis use in patients with recent-onset schizophrenia and healthy controls. Psychol Med 40(8):1325-1336.

DeLuca JG. 2010. Kinetochore-microtubule dynamics and attachment stability. Methods Cell Biol 97:53-79.

Demuth DG, Molleman A. 2006. Cannabinoid signalling. Life Sci 78(6):549-563.

Denault JB, Eckelman BP, Shin H, Pop C, Salvesen GS. 2007. Caspase 3 attenuates XIAP (X-linked inhibitor of apoptosis protein)-mediated inhibition of caspase 9. Biochem J 405(1):11-19.

Devane WA, Hanus L, Breuer A, Pertwee RG, Stevenson LA, Griffin G, Gibson D, Mandelbaum A, Etinger A, Mechoulam R. 1992. Isolation and structure of a brain constituent that binds to the cannabinoid receptor. Science 258(5090):1946-1949.

Devoogd TJ, Nixdorf B, Nottebohm F. 1985. Synaptogenesis and changes in synaptic morphology related to acquisition of a new behavior. Brain Res 329(1-2):304-308.

Di Marzo V, Melck D, Bisogno T, De Petrocellis L. 1998. Endocannabinoids: endogenous cannabinoid receptor ligands with neuromodulatory action. Trends Neurosci 21(12):521-528.

Diana MA, Levenes C, Mackie K, Marty A. 2002. Short-term retrograde inhibition of GABAergic synaptic currents in rat Purkinje cells is mediated by endogenous cannabinoids. J Neurosci 22(1):200-208.

Diana MA, Marty A. 2004. Endocannabinoid-mediated short-term synaptic plasticity: depolarization-induced suppression of inhibition (DSI) and depolarization-induced suppression of excitation (DSE). Br J Pharmacol 142(1):9-19.

Dickstein DL, Kabaso D, Rocher AB, Luebke JI, Wearne SL, Hof PR. 2007. Changes in the structural complexity of the aged brain. Aging Cell 6(3):275-284.

Dinh TP, Carpenter D, Leslie FM, Freund TF, Katona I, Sensi SL, Kathuria S, Piomelli D. 2002. Brain monoglyceride lipase participating in endocannabinoid inactivation. Proc Natl Acad Sci U S A 99(16):10819-10824.

Domenici MR, Azad SC, Marsicano G, Schierloh A, Wotjak CT, Dodt HU, Zieglgansberger W, Lutz B, Rammes G. 2006. Cannabinoid receptor type 1 located on presynaptic terminals of principal neurons in the forebrain controls glutamatergic synaptic transmission. J Neurosci 26(21):5794-5799.

Doupe AJ, Kuhl PK. 1999. Birdsong and human speech: common themes and mechanisms. Annu Rev Neurosci 22:567-631.

Duan H, Wearne SL, Rocher AB, Macedo A, Morrison JH, Hof PR. 2003. Age-related dendritic and spine changes in corticocortically projecting neurons in macaque monkeys. Cereb Cortex 13(9):950-961.

Dur EAM, Imran M, Gul A. 2011. Calcium dynamics in dendritic spines: A link to structural plasticity. Math Biosci 230(2):55-66.

Earleywine M. 2002. Understanding Marijuana: A New Look at the Scientific Evidence: Oxford University Press, USA.

Egertova M, Elphick MR. 2000. Localisation of cannabinoid receptors in the rat brain using antibodies to the intracellular C-terminal tail of CB. J Comp Neurol 422(2):159-171.

Ehrenreich H, Rinn T, Kunert HJ, Moeller MR, Poser W, Schilling L, Gigerenzer G, Hoehe MR. 1999. Specific attentional dysfunction in adults following early start of cannabis use. Psychopharmacology (Berl) 142(3):295-301.

El Manira A, Kyriakatos A. 2010. The role of endocannabinoid signaling in motor control. Physiology (Bethesda) 25(4):230-238.

Elphick MR. 2002. Evolution of cannabinoid receptors in vertebrates: identification of a CB(2) gene in the puffer fish Fugu rubripes. Biol Bull 202(2):104-107.

Elphick MR, Egertova M. 2001a. The neurobiology and evolution of cannabinoid signalling. Philos Trans R Soc Lond B Biol Sci 356(1407):381-408.

Elphick MR, Egertova M. 2001b. The neurobiology and evolution of cannabinoid signalling. Philos Trans R Soc Lond B Biol Sci 356(1407):381-408.

ElSohly MA. 2006. Marijuana and the Cannabinoids: Humana Press.

Farah CA, Leclerc N. 2008. HMWMAP2: new perspectives on a pathway to dendritic identity. Cell Motil Cytoskeleton 65(7):515-527.

Fee MS, Goldberg JH. 2011. A hypothesis for basal ganglia-dependent reinforcement learning in the songbird. Neuroscience 198:152-170.

Feldman DE. 2009. Synaptic mechanisms for plasticity in neocortex. Annu Rev Neurosci 32:33-55.

Fernandez-Ruiz J, Hernandez M, Ramos JA. 2010. Cannabinoid-dopamine interaction in the pathophysiology and treatment of CNS disorders. CNS Neurosci Ther 16(3):e72-91.

Fernandez-Ruiz JJ, Berrendero F, Hernandez ML, Romero J, Ramos JA. 1999. Role of endocannabinoids in brain development. Life Sci 65(6-7):725-736.

Fernberger SW. 1939. Review of Marihuana: America's new drug problem. Psychological Bulletin 36(4):300-301.

Fontes MA, Bolla KI, Cunha PJ, Almeida PP, Jungerman F, Laranjeira RR, Bressan RA, Lacerda AL. 2011. Cannabis use before age 15 and subsequent executive functioning. Br J Psychiatry 198(6):442-447.

Fosnaugh JS, Bhat RV, Yamagata K, Worley PF, Baraban JM. 1995. Activation of arc, a putative "effector" immediate early gene, by cocaine in rat brain. J Neurochem 64(5):2377-2380.

Fowler CJ. 2012. Anandamide uptake explained? Trends Pharmacol Sci 33(4):181-185.

Franklin JL, Berechid BE, Cutting FB, Presente A, Chambers CB, Foltz DR, Ferreira A, Nye JS. 1999. Autonomous and non-autonomous regulation of mammalian neurite development by Notch1 and Delta1. Curr Biol 9(24):1448-1457.

Frey KA, Albin RL. 2001. Receptor binding techniques. Curr Protoc Neurosci Chapter 1:Unit1 4.

Friederici AD, Alter K. 2004. Lateralization of auditory language functions: a dynamic dual pathway model. Brain Lang 89(2):267-276.

Fujimoto T, Tanaka H, Kumamaru E, Okamura K, Miki N. 2004. Arc interacts with microtubules/microtubule-associated protein 2 and attenuates microtubule-associated protein 2 immunoreactivity in the dendrites. J Neurosci Res 76(1):51-63.

Funabiki Y, Funabiki K. 2009. Factors limiting song acquisition in adult zebra finches. Dev Neurobiol 69(11):752-759.

Gallo G, Letourneau PC. 2004. Regulation of growth cone actin filaments by guidance cues. J Neurobiol 58(1):92-102.

Galloway PG, Mulvihill P, Siedlak S, Mijares M, Kawai M, Padget H, Kim R, Perry G. 1990. Immunochemical demonstration of tropomyosin in the neurofibrillary pathology of Alzheimer's disease. Am J Pathol 137(2):291-300.

Galve-Roperh I, Aguado T, Rueda D, Velasco G, Guzman M. 2006. Endocannabinoids: a new family of lipid mediators involved in the regulation of neural cell development. Curr Pharm Des 12(18):2319-2325.

Gao Y, Vasilyev DV, Goncalves MB, Howell FV, Hobbs C, Reisenberg M, Shen R, Zhang MY, Strassle BW, Lu P, Mark L, Piesla MJ, Deng K, Kouranova EV, Ring RH, Whiteside GT, Bates B, Walsh FS, Williams G, Pangalos MN, Samad TA, Doherty P. 2010. Loss of retrograde endocannabinoid signaling and reduced adult neurogenesis in diacylglycerol lipase knock-out mice. J Neurosci 30(6):2017-2024.

Gaoni Y, Mechoulam R. 1964. Isolation, Structure, and Partial Synthesis of an Active Constituent of Hashish. Journal of the American Chemical Society 86(8):1646-1647.

Garcia DE, Brown S, Hille B, Mackie K. 1998. Protein kinase C disrupts cannabinoid actions by phosphorylation of the CB1 cannabinoid receptor. J Neurosci 18(8):2834-2841.

Gardner EL. 2002. Addictive potential of cannabinoids: the underlying neurobiology. Chem Phys Lipids 121(1-2):267-290.

Ge X, Hannan F, Xie Z, Feng C, Tully T, Zhou H, Zhong Y. 2004. Notch signaling in Drosophila long-term memory formation. Proc Natl Acad Sci U S A 101(27):10172-10176.

Gertsch J, Pertwee RG, Di Marzo V. 2010. Phytocannabinoids beyond the Cannabis plant - do they exist? Br J Pharmacol 160(3):523-529.

Giedd JN, Lalonde FM, Celano MJ, White SL, Wallace GL, Lee NR, Lenroot RK. 2009. Anatomical brain magnetic resonance imaging of typically developing children and adolescents. J Am Acad Child Adolesc Psychiatry 48(5):465-470.

Gilbert MT, Soderstrom K. 2011. Late-postnatal cannabinoid exposure persistently elevates dendritic spine densities in area X and HVC song regions of zebra finch telencephalon. Brain Res 1405:23-30.

Greene LA, Tischler AS. 1976. Establishment of a noradrenergic clonal line of rat adrenal pheochromocytoma cells which respond to nerve growth factor. Proc Natl Acad Sci U S A 73(7):2424-2428.

Groot PC, Mager WH, Henriquez NV, Pronk JC, Arwert F, Planta RJ, Eriksson AW, Frants RR. 1990. Evolution of the human alpha-amylase multigene family through unequal, homologous, and inter- and intrachromosomal crossovers. Genomics 8(1):97-105.

Grotenhermen F. 2003. Pharmacokinetics and pharmacodynamics of cannabinoids. Clin Pharmacokinet 42(4):327-360.

Grotenhermen F. 2007. The toxicology of cannabis and cannabis prohibition. Chem Biodivers 4(8):1744-1769.

Guindon J, Hohmann AG. 2009. The endocannabinoid system and pain. CNS Neurol Disord Drug Targets 8(6):403-421.

Guliaeva NV. 2004. "Apoptotic" mechanisms in normal brain plasticity: caspase-3 and long-term potentiation. Zh Vyssh Nerv Deiat Im I P Pavlova 54(4):437-447.

Gulyaeva NV, Kudryashov IE, Kudryashova IV. 2003. Caspase activity is essential for long-term potentiation. J Neurosci Res 73(6):853-864.

Guzowski JF, Lyford GL, Stevenson GD, Houston FP, McGaugh JL, Worley PF, Barnes CA. 2000. Inhibition of activity-dependent arc protein expression in the rat hippocampus impairs the maintenance of

long-term potentiation and the consolidation of long-term memory. J Neurosci 20(11):3993-4001.

Guzowski JF, McNaughton BL, Barnes CA, Worley PF. 2001. Imaging neural activity with temporal and cellular resolution using FISH. Curr Opin Neurobiol 11(5):579-584.

Guzowski JF, Timlin JA, Roysam B, McNaughton BL, Worley PF, Barnes CA. 2005. Mapping behaviorally relevant neural circuits with immediate-early gene expression. Curr Opin Neurobiol 15(5):599-606.

Haddara M. 1956. A quantitative study of the postnatal changes in the packing density of the neurons in the visual cortex of the mouse. J Anat 90(4):494-501.

Haesler S, Wada K, Nshdejan A, Morrisey EE, Lints T, Jarvis ED, Scharff C. 2004. FoxP2 expression in avian vocal learners and non-learners. J Neurosci 24(13):3164-3175.

Hall W. 2006. Dissecting the causal anatomy of the link between cannabis and other illicit drugs. Addiction 101(4):472-473; discussion 474-476.

Ham RG, McKeehan WL. 1979. Media and growth requirements. Methods Enzymol 58:44-93.

Hanson KL, Winward JL, Schweinsburg AD, Medina KL, Brown SA, Tapert SF. 2010. Longitudinal study of cognition among adolescent marijuana users over three weeks of abstinence. Addict Behav 35(11):970-976.

Harder S, Rietbrock S. 1997. Concentration-effect relationship of delta-9-tetrahydrocannabiol and prediction of psychotropic effects after smoking marijuana. Int J Clin Pharmacol Ther 35(4):155-159.

Harris KM, Kater SB. 1994. Dendritic spines: cellular specializations imparting both stability and flexibility to synaptic function. Annu Rev Neurosci 17:341-371.

Hasbani MJ, Schlief ML, Fisher DA, Goldberg MP. 2001. Dendritic spines lost during glutamate receptor activation reemerge at original sites of synaptic contact. J Neurosci 21(7):2393-2403.

Heerlein A, Richter P. 1991. [Discrepancy between clinical depression and psychometric depression]. Acta Psiquiatr Psicol Am Lat 37(4):317-323.

Hemphill JK, Turner JC, Mahlberg PG. 1980. Cannabinoid Content of Individual Plant Organs From Different Geographical Strains of Cannabis sativa L. Journal of Natural Products 43(1):112-122.

Herkenham M, Lynn AB, Johnson MR, Melvin LS, de Costa BR, Rice KC. 1991. Characterization and localization of cannabinoid receptors in rat brain: a quantitative in vitro autoradiographic study. J Neurosci 11(2):563-583.

Herkenham M, Lynn AB, Little MD, Johnson MR, Melvin LS, de Costa BR, Rice KC. 1990. Cannabinoid receptor localization in brain. Proc Natl Acad Sci U S A 87(5):1932-1936.

Hoffman AF, Laaris N, Kawamura M, Masino SA, Lupica CR. 2010. Control of cannabinoid CB1 receptor function on glutamate axon terminals by endogenous adenosine acting at A1 receptors. J Neurosci 30(2):545-555.

Hollister LE. 1969. Criminal laws and the control of drugs of abuse. An historical view of the law (or, it's the lawyer's fault). J Clin Pharmacol J New Drugs 9(6):345-348.

Holthoff K, Tsay D, Yuste R. 2002. Calcium dynamics of spines depend on their dendritic location. Neuron 33(3):425-437.

Howlett A, Shim JY. 2000. Cannabinoid Receptors and Signal Transduction. Madame Curie Bioscience Database [Internet]. Austin, TX: Landes Bioscience.

Howlett AC. 2005. Cannabinoid receptor signaling. Handb Exp Pharmacol(168):53-79.

Huang F, Chotiner JK, Steward O. 2007. Actin polymerization and ERK phosphorylation are required for Arc/Arg3.1 mRNA targeting to activated synaptic sites on dendrites. J Neurosci 27(34):9054-9067.

Huesmann GR. 2005. Is It Memory or Is It Death? Caspase-3 and Memory Formation [Dissertation]. Urbana: University of Illinois, Urbana-Champaign. 179 p.

Huesmann GR, Clayton DF. 2006. Dynamic role of postsynaptic caspase-3 and BIRC4 in zebra finch song-response habituation. Neuron 52(6):1061-1072.

Huestis MA. 2007. Human cannabinoid pharmacokinetics. Chem Biodivers 4(8):1770-1804.

Huppertz B, Frank HG, Kaufmann P. 1999. The apoptosis cascade--morphological and immunohistochemical methods for its visualization. Anat Embryol (Berl) 200(1):1-18.

Hutsler JJ, Zhang H. 2010. Increased dendritic spine densities on cortical projection neurons in autism spectrum disorders. Brain research 1309:83-94.

Iribarne C, Berthou F, Baird S, Dreano Y, Picart D, Bail JP, Beaune P, Menez JF. 1996. Involvement of cytochrome P450 3A4 enzyme in the N-demethylation of methadone in human liver microsomes. Chem Res Toxicol 9(2):365-373.

Iversen L. 2003. Cannabis and the brain. Brain 126(Pt 6):1252-1270.

Izumi Y, Zorumski CF. 2012. NMDA receptors, mGluR5, and endocannabinoids are involved in a cascade leading to hippocampal long-term depression. Neuropsychopharmacology 37(3):609-617.

Jackson SJ, Pryce G, Diemel LT, Cuzner ML, Baker D. 2005. Cannabinoid-receptor 1 null mice are susceptible to neurofilament damage and caspase 3 activation. Neuroscience 134(1):261-268.

Jarvis ED, Gunturkun O, Bruce L, Csillag A, Karten H, Kuenzel W, Medina L, Paxinos G, Perkel DJ, Shimizu T, Striedter G, Wild JM, Ball GF, Dugas-Ford J, Durand SE, Hough GE, Husband S, Kubikova L, Lee DW, Mello CV, Powers A, Siang C, Smulders TV, Wada K, White SA, Yamamoto K, Yu J, Reiner A, Butler AB. 2005. Avian brains and a new understanding of vertebrate brain evolution. Nat Rev Neurosci 6(2):151-159.

Johnson M, Devane W, Howlett A, Melvin L, Milne G. 1988. Structural studies leading to the discovery of a cannabinoid binding site. NIDA Res Monogr 90:129-135.

Johnston LD, O'Malley, P.M., Bachman, J.G., Schulenbert, J.E. 2012. Monitoring the Future National Survey Results on Drug Use, 1975 - 2011. Volume I: Secondary School Students. . Ann Arbor: Institute for Social Research, The University of Michigan. 760 p.

Jones EG. 1994. Santiago Ramon y Cajal and the Croonian Lecture, March 1894. Trends Neurosci 17(5):190-192.

Julien JP, Mushynski WE. 1998. Neurofilaments in health and disease. Prog Nucleic Acid Res Mol Biol 61:1-23.

Kalant H. 2001. Medicinal use of cannabis: history and current status. Pain Res Manag 6(2):80-91.

Kalant OJ. 1971. Ludlow on cannabis: a modern look at a nineteenth century drug experience. Int J Addict 6(2):309-322.

Kandel DB. 1984. Marijuana users in young adulthood. Arch Gen Psychiatry 41(2):200-209.

Kapitein LC, Yau KW, Hoogenraad CC. 2010. Microtubule dynamics in dendritic spines. Methods Cell Biol 97:111-132.

Kaplan J. 1969. Criminal laws and the control of drugs of abuse. The special case of marijuana (or, it's the doctor's fault). J Clin Pharmacol J New Drugs 9(6):349-351.

Kapur A, Yeckel MF, Gray R, Johnston D. 1998. L-Type calcium channels are required for one form of hippocampal mossy fiber LTP. J Neurophysiol 79(4):2181-2190.

Katona I, Freund TF. 2012. Multiple functions of endocannabinoid signaling in the brain. Annu Rev Neurosci 35:529-558.

Katona I, Sperlagh B, Sik A, Kafalvi A, Vizi ES, Mackie K, Freund TF. 1999. Presynaptically located CB1 cannabinoid receptors regulate GABA release from axon terminals of specific hippocampal interneurons. J Neurosci 19(11):4544-4558.

Kenakin T. 2007. Functional selectivity through protean and biased agonism: who steers the ship? Mol Pharmacol 72(6):1393-1401.

Kim H, Binder LI, Rosenbaum JL. 1979. The periodic association of MAP2 with brain microtubules in vitro. J Cell Biol 80(2):266-276.

Kim HJ, Waataja JJ, Thayer SA. 2008. Cannabinoids inhibit network-driven synapse loss between hippocampal neurons in culture. J Pharmacol Exp Ther 325(3):850-858.

Kinsey SG, O'Neal ST, Long JZ, Cravatt BF, Lichtman AH. 2011. Inhibition of endocannabinoid catabolic enzymes elicits anxiolytic-like effects in the marble burying assay. Pharmacol Biochem Behav 98(1):21-27.

Koch C, Zador A. 1993. The function of dendritic spines: devices subserving biochemical rather than electrical compartmentalization. J Neurosci 13(2):413-422.

Kogan NM, Mechoulam R. 2007. Cannabinoids in health and disease. Dialogues Clin Neurosci 9(4):413-430.

Kozorovitskiy Y, Saunders A, Johnson CA, Lowell BB, Sabatini BL. 2012. Recurrent network activity drives striatal synaptogenesis. Nature 485(7400):646-650.

Kreuz DS, Axelrod J. 1973. Delta-9-tetrahydrocannabinol: localization in body fat. Science 179(4071):391-393.

Kristensen K, Cadenhead KS. 2007. Cannabis abuse and risk for psychosis in a prodromal sample. Psychiatry Res 151(1-2):151-154.

Krutzfeldt NO, Logerot P, Kubke MF, Wild JM. 2010. Connections of the auditory brainstem in a songbird, Taeniopygia guttata. II. Projections of nucleus angularis and nucleus laminaris to the superior olive and lateral lemniscal nuclei. J Comp Neurol 518(11):2135-2148.

Laky K, Fowlkes BJ. 2008. Notch signaling in CD4 and CD8 T cell development. Curr Opin Immunol 20(2):197-202.

Lambert DM. 2001. [Medical use of cannabis through history]. J Pharm Belg 56(5):111-118.

Lanahan A, Worley P. 1998. Immediate-early genes and synaptic function. Neurobiol Learn Mem 70(1-2):37-43.

Landmesser LT. 1998. Synaptic plasticity: keeping synapses under control. Curr Biol 8(16):R564-567.

Lardelli M, Williams R, Lendahl U. 1995. Notch-related genes in animal development. Int J Dev Biol 39(5):769-780.

Lauay C, Komorowski RW, Beaudin AE, Devoogd TJ. 2005. Adult female and male zebra finches show distinct patterns of spine deficits in an auditory area and in the song system when reared without exposure to normal adult song. J Comp Neurol 487(2):119-126.

Law B, Mason PA, Moffat AC, Gleadle RI, King LJ. 1984. Forensic aspects of the metabolism and excretion of cannabinoids following oral ingestion of cannabis resin. J Pharm Pharmacol 36(5):289-294.

Lehmann R, Jiménez F, Dietrich U, Campos-Ortega JA. 1983. On the phenotype and development of mutants of early neurogenesis in<i>Drosophila melanogaster</i&gt. Development Genes and Evolution 192(2):62-74.

Lemberger L, Silberstein SD, Axelrod J, Kopin IJ. 1970. Marihuana: studies on the disposition and metabolism of delta-9-tetrahydrocannabinol in man. Science 170(3964):1320-1322.

Leonardo A, Fee MS. 2005. Ensemble coding of vocal control in birdsong. J Neurosci 25(3):652-661.

Letourneau PC. 1975. Possible roles for cell-to-substratum adhesion in neuronal morphogenesis. Dev Biol 44(1):77-91.

Li H-L. 1973. An archaeological and historical account of cannabis in China. Economic Botany 28(4):437-448.

Lieshoff C, Bischof HJ. 2003. The dynamics of spine density changes. Behav Brain Res 140(1-2):87-95.

Lin J, Wang C, Wu Z. 2010. [Preliminary study on effects of human brain-derived neurotrophic factor gene-modified bone marrow mesenchymal stem cells by intravenous transplantation on

structure and function of rat injured spinal cord]. Zhongguo Xiu Fu Chong Jian Wai Ke Za Zhi 24(8):982-987.

Lindwall G, Cole RD. 1984. Phosphorylation affects the ability of tau protein to promote microtubule assembly. J Biol Chem 259(8):5301-5305.

Lipton MA, DiMascio A, Killam KF, Neuropsychopharmacology ACo. 1979. Psychopharmacology: a generation of progress: Raven Press.

Liu JP, Chang LR, Gao XL, Wu Y. 2008. Different expression of caspase-3 in rat hippocampal subregions during postnatal development. Microsc Res Tech 71(9):633-638.

Liu ZJ, Shirakawa T, Li Y, Soma A, Oka M, Dotto GP, Fairman RM, Velazquez OC, Herlyn M. 2003. Regulation of Notch1 and Dll4 by vascular endothelial growth factor in arterial endothelial cells: implications for modulating arteriogenesis and angiogenesis. Mol Cell Biol 23(1):14-25.

Lovinger DM. 2008. Presynaptic modulation by endocannabinoids. Handb Exp Pharmacol(184):435-477.

Lyford GL, Yamagata K, Kaufmann WE, Barnes CA, Sanders LK, Copeland NG, Gilbert DJ, Jenkins NA, Lanahan AA, Worley PF. 1995. Arc, a growth factor and activity-regulated gene, encodes a novel cytoskeleton-associated protein that is enriched in neuronal dendrites. Neuron 14(2):433-445.

Maccarrone M, Finazzi-Agro A. 2002. Endocannabinoids and their actions. Vitam Horm 65:225-255.

MacGrogan D, Luna-Zurita L, de la Pompa JL. 2011. Notch signaling in cardiac valve development and disease. Birth Defects Res A Clin Mol Teratol 91(6):449-459.

Mackie K. 2005. Distribution of cannabinoid receptors in the central and peripheral nervous system. Handb Exp Pharmacol(168):299-325.

Mackie K. 2008. Cannabinoid receptors: where they are and what they do. J Neuroendocrinol 20 Suppl 1:10-14.

Mackie K, Lai Y, Westenbroek R, Mitchell R. 1995. Cannabinoids activate an inwardly rectifying potassium conductance and inhibit Q-type calcium currents in AtT20 cells transfected with rat brain cannabinoid receptor. J Neurosci 15(10):6552-6561.

Mackowiak M, Chocyk A, Dudys D, Wedzony K. 2009. Activation of CB1 cannabinoid receptors impairs memory consolidation and hippocampal polysialylated neural cell adhesion molecule expression in contextual fear conditioning. Neuroscience 158(4):1708-1716.

Margoliash D. 1997. Functional organization of forebrain pathways for song production and perception. J Neurobiol 33(5):671-693.

Marler P, Tamura M. 1964. Culturally Transmitted Patterns of Vocal Behavior in Sparrows. Science 146(3650):1483-1486.

Marroyo Gordo JM, Nombela Beltran P, de las Mozas Lillo R, Gomez-Escalonilla Lorenzo B, Gomez-Escalonilla Lorenzo S. 2012. [Perception of the risk of drugs consumption in teenagers of our environment]. Rev Enferm 35(5):16-21.

Marsicano G, Goodenough S, Monory K, Hermann H, Eder M, Cannich A, Azad SC, Cascio MG, Gutierrez SO, van der Stelt M, Lopez-Rodriguez ML, Casanova E, Schutz G, Zieglgansberger W, Di Marzo V, Behl C, Lutz B. 2003. CB1 cannabinoid receptors and on-demand defense against excitotoxicity. Science 302(5642):84-88.

Martin BR, Compton DR, Thomas BF, Prescott WR, Little PJ, Razdan RK, Johnson MR, Melvin LS, Mechoulam R, Ward SJ. 1991. Behavioral, biochemical, and molecular modeling evaluations of cannabinoid analogs. Pharmacol Biochem Behav 40(3):471-478.

Martin SJ, Grimwood PD, Morris RG. 2000. Synaptic plasticity and memory: an evaluation of the hypothesis. Annu Rev Neurosci 23:649-711.

Massey PV, Bashir ZI. 2007. Long-term depression: multiple forms and implications for brain function. Trends Neurosci 30(4):176-184.

Mato S, Del Olmo E, Pazos A. 2003. Ontogenetic development of cannabinoid receptor expression and signal transduction functionality in the human brain. Eur J Neurosci 17(9):1747-1754.

Matsuda LA, Bonner TI, Lolait SJ. 1992. Cannabinoid receptors: which cells, where, how, and why? NIDA Res Monogr 126:48-56.

Mattson MP, Keller JN, Begley JG. 1998. Evidence for synaptic apoptosis. Exp Neurol 153(1):35-48.

McKeehan WL, Ham RG. 1976. Stimulation of clonal growth of normal fibroblasts with substrata coated with basic polymers. J Cell Biol 71(3):727-734.

McNaughton BL. 2003. Long-term potentiation, cooperativity and Hebb's cell assemblies: a personal history. Philos Trans R Soc Lond B Biol Sci 358(1432):629-634.

Mechoulam R, Ben-Shabat S, Hanus L, Ligumsky M, Kaminski NE, Schatz AR, Gopher A, Almog S, Martin BR, Compton DR, et al. 1995. Identification of an endogenous 2-monoglyceride, present in canine gut, that binds to cannabinoid receptors. Biochem Pharmacol 50(1):83-90.

Melck D, Rueda D, Galve-Roperh I, De Petrocellis L, Guzman M, Di Marzo V. 1999. Involvement of the cAMP/protein kinase A pathway and of mitogen-activated protein kinase in the anti-proliferative effects of anandamide in human breast cancer cells. FEBS Lett 463(3):235-240.

Mello CV, Clayton DF. 1994. Song-induced ZENK gene expression in auditory pathways of songbird brain and its relation to the song control system. J Neurosci 14(11 Pt 1):6652-6666.

Mello CV, Velho TA, Pinaud R. 2004. Song-induced gene expression: a window on song auditory processing and perception. Ann N Y Acad Sci 1016:263-281.

Mello CV, Vicario DS, Clayton DF. 1992. Song presentation induces gene expression in the songbird forebrain. Proc Natl Acad Sci U S A 89(15):6818-6822.

Mikuriya TH. 1969. Marijuana in medicine: past, present and future. Calif Med 110(1):34-40.

Mikuriya TH. 1973. Marijuana: medical papers, 1839-1972.

Mooney R. 1999. Sensitive periods and circuits for learned birdsong. Curr Opin Neurobiol 9(1):121-127.

Mooney R. 2009a. Neural mechanisms for learned birdsong. Learn Mem 16(11):655-669.

Mooney R. 2009b. Neurobiology of song learning. Curr Opin Neurobiol 19(6):654-660.

Moore NL, Greenleaf AL, Acheson SK, Wilson WA, Swartzwelder HS, Kuhn CM. 2010. Role of cannabinoid receptor type 1 desensitization in greater tetrahydrocannabinol impairment of memory in adolescent rats. J Pharmacol Exp Ther 335(2):294-301.

Moorman S, Gobes SM, Kuijpers M, Kerkhofs A, Zandbergen MA, Bolhuis JJ. 2012. Human-like brain hemispheric dominance in birdsong learning. Proceedings of the National Academy of Sciences of the United States of America 109(31):12782-12787.

Moorman S, Mello CV, Bolhuis JJ. 2011. From songs to synapses: molecular mechanisms of birdsong memory. Molecular mechanisms of auditory learning in songbirds involve immediate early genes, including zenk and arc, the ERK/MAPK pathway and synapsins. Bioessays 33(5):377-385.

Moreau JJ. 1973. Hashish and mental illness: Lippincott Williams & Wilkins.

Mori K, Muto Y, Kokuzawa J, Yoshioka T, Yoshimura S, Iwama T, Okano Y, Sakai N. 2004. Neuronal protein NP25 interacts with F-actin. Neurosci Res 48(4):439-446.

Moser MB. 1999. Making more synapses: a way to store information? Cell Mol Life Sci 55(4):593-600.

Mulder J, Aguado T, Keimpema E, Barabas K, Ballester Rosado CJ, Nguyen L, Monory K, Marsicano G, Di Marzo V, Hurd YL, Guillemot F, Mackie K, Lutz B, Guzman M, Lu HC, Galve-Roperh I, Harkany T. 2008. Endocannabinoid signaling controls pyramidal cell specification and long-range axon patterning. Proc Natl Acad Sci U S A 105(25):8760-8765.

Munro S, Freeman M. 2000. The notch signalling regulator fringe acts in the Golgi apparatus and requires the glycosyltransferase signature motif DXD. Curr Biol 10(14):813-820.

Murphy N, Cowley TR, Blau CW, Dempsey CN, Noonan J, Gowran A, Tanveer R, Olango WM, Finn DP, Campbell VA, Lynch MA. 2012. The fatty acid amide hydrolase inhibitor URB597 exerts anti-

inflammatory effects in hippocampus of aged rats and restores an age-related deficit in long-term potentiation. J Neuroinflammation 9:79.

Musto DF. 1972. The Marihuana Tax Act of 1937. Arch Gen Psychiatry 26(2):101-108.

Nahas GG. 1984. Marihuana in science and medicine: Raven Press.

Nations U. 2012. World Drug Report 2012: United Nations Publications.

Nixdorf-Bergweiler BE. 2001. Lateral magnocellular nucleus of the anterior neostriatum (LMAN) in the zebra finch: neuronal connectivity and the emergence of sex differences in cell morphology. Microsc Res Tech 54(6):335-353.

Norrholm SD, Ouimet CC. 2001. Altered dendritic spine density in animal models of depression and in response to antidepressant treatment. Synapse 42(3):151-163.

Nottebohm F, Alvarez-Buylla A, Cynx J, Kirn J, Ling CY, Nottebohm M, Suter R, Tolles A, Williams H. 1990. Song learning in birds: the relation between perception and production. Philos Trans R Soc Lond B Biol Sci 329(1253):115-124.

Nottebohm F, Kelley DB, Paton JA. 1982. Connections of vocal control nuclei in the canary telencephalon. J Comp Neurol 207(4):344-357.

Ohlsson A, Lindgren JE, Wahlen A, Agurell S, Hollister LE, Gillespie HK. 1980. Plasma delta-9 tetrahydrocannabinol concentrations and clinical effects after oral and intravenous administration and smoking. Clin Pharmacol Ther 28(3):409-416.

Okuno H. 2011. Regulation and function of immediate-early genes in the brain: beyond neuronal activity markers. Neurosci Res 69(3):175-186.

Osei-Hyiaman D, DePetrillo M, Pacher P, Liu J, Radaeva S, Batkai S, Harvey-White J, Mackie K, Offertaler L, Wang L, Kunos G. 2005. Endocannabinoid activation at hepatic CB1 receptors stimulates fatty acid synthesis and contributes to diet-induced obesity. J Clin Invest 115(5):1298-1305.

Oudin MJ, Hobbs C, Doherty P. 2011. DAGL-dependent endocannabinoid signalling: roles in axonal pathfinding, synaptic plasticity and adult neurogenesis. Eur J Neurosci 34(10):1634-1646.

Pagotto U, Marsicano G, Cota D, Lutz B, Pasquali R. 2006. The emerging role of the endocannabinoid system in endocrine regulation and energy balance. Endocr Rev 27(1):73-100.

Pastuzyn ED, Chapman DE, Wilcox KS, Keefe KA. 2011. Altered Learning and Arc-Regulated Consolidation of Learning in Striatum by Methamphetamine-Induced Neurotoxicity. Neuropsychopharmacology.

Patel NA, Moldow RL, Patel JA, Wu G, Chang SL. 1998. Arachidonylethanolamide (AEA) activation of FOS proto-oncogene protein immunoreactivity in the rat brain. Brain Res 797(2):225-233.

Perez-Reyes M, Wall ME. 1982. Presence of delta9-tetrahydrocannabinol in human milk. N Engl J Med 307(13):819-820.

Pertwee RG. 1997. Pharmacology of cannabinoid CB1 and CB2 receptors. Pharmacol Ther 74(2):129-180.

Pertwee RG. 2006a. Cannabinoid pharmacology: the first 66 years. Br J Pharmacol 147 Suppl 1:S163-171.

Pertwee RG. 2006b. The pharmacology of cannabinoid receptors and their ligands: an overview. Int J Obes (Lond) 30 Suppl 1:S13-18.

Pertwee RG, Howlett AC, Abood ME, Alexander SP, Di Marzo V, Elphick MR, Greasley PJ, Hansen HS, Kunos G, Mackie K, Mechoulam R, Ross RA. 2010. International Union of Basic and Clinical Pharmacology. LXXIX. Cannabinoid receptors and their ligands: beyond CB(1) and CB(2). Pharmacol Rev 62(4):588-631.

Pettit DA, Harrison MP, Olson JM, Spencer RF, Cabral GA. 1998. Immunohistochemical localization of the neural cannabinoid receptor in rat brain. J Neurosci Res 51(3):391-402.

Pinaud R, Terleph TA. 2008. A songbird forebrain area potentially involved in auditory discrimination and memory formation. J Biosci 33(1):145-155.

Pini A, Mannaioni G, Pellegrini-Giampietro D, Passani MB, Mastroianni R, Bani D, Masini E. 2012. The Role of Cannabinoids In Inflammatory Modulation of Allergic Respiratory Disorders, Inflammatory Pain and Ischemic Stroke. Curr Drug Targets.

Piomelli D. 2003. The molecular logic of endocannabinoid signalling. Nat Rev Neurosci 4(11):873-884.

Plath N, Ohana O, Dammermann B, Errington ML, Schmitz D, Gross C, Mao X, Engelsberg A, Mahlke C, Welzl H, Kobalz U, Stawrakakis A, Fernandez E, Waltereit R, Bick-Sander A, Therstappen E, Cooke SF, Blanquet V, Wurst W, Salmen B, Bosl MR, Lipp HP, Grant SG, Bliss TV, Wolfer DP, Kuhl D. 2006. Arc/Arg3.1 is essential for the consolidation of synaptic plasticity and memories. Neuron 52(3):437-444.

Ploski JE, Pierre VJ, Smucny J, Park K, Monsey MS, Overeem KA, Schafe GE. 2008. The activity-regulated cytoskeletal-associated protein (Arc/Arg3.1) is required for memory consolidation of pavlovian fear conditioning in the lateral amygdala. J Neurosci 28(47):12383-12395.

Poindron P, Piguet P, Förster E. 2005. New Methods For Culturing Cells From Nervous Tissues: Karger.

Presente A, Boyles RS, Serway CN, de Belle JS, Andres AJ. 2004. Notch is required for long-term memory in Drosophila. Proc Natl Acad Sci U S A 101(6):1764-1768.

Ptacek JM, Fagan-Dubin L. 1974. Developmental changes in neuron size and density in the visual cortex and superior colliculus of the postnatal golden hamster. J Comp Neurol 158(3):237-242.

Puck TT, Cieciura SJ, Robinson A. 1958. Genetics of somatic mammalian cells. III. Long-term cultivation of euploid cells from human and animal subjects. J Exp Med 108(6):945-956.

Purves D. 2011. Neuroscience: Sinauer Associates.

Q. Ashton Acton PD. Issues in Biological and Life Sciences Research: 2011 Edition: ScholarlyEditions.

Quinn HR, Matsumoto I, Callaghan PD, Long LE, Arnold JC, Gunasekaran N, Thompson MR, Dawson B, Mallet PE, Kashem MA, Matsuda-Matsumoto H, Iwazaki T, McGregor IS. 2008. Adolescent rats find repeated Delta(9)-THC less aversive than adult rats but display greater residual cognitive

deficits and changes in hippocampal protein expression following exposure. Neuropsychopharmacology 33(5):1113-1126.

Raboyeau G, Marcotte K, Adrover-Roig D, Ansaldo AI. 2010. Brain activation and lexical learning: the impact of learning phase and word type. Neuroimage 49(3):2850-2861.

Rakic P, Bourgeois JP, Goldman-Rakic PS. 1994. Synaptic development of the cerebral cortex: implications for learning, memory, and mental illness. Prog Brain Res 102:227-243.

Rausch G, Scheich H. 1982. Dendritic spine loss and enlargement during maturation of the speech control system in the mynah bird (Gracula religiosa). Neurosci Lett 29(2):129-133.

Razdan RK. 1986. Structure-activity relationships in cannabinoids. Pharmacol Rev 38(2):75-149.

Realini N, Vigano D, Guidali C, Zamberletti E, Rubino T, Parolaro D. 2011. Chronic URB597 treatment at adulthood reverted most depressive-like symptoms induced by adolescent exposure to THC in female rats. Neuropharmacology 60(2-3):235-243.

Redmond L, Oh SR, Hicks C, Weinmaster G, Ghosh A. 2000. Nuclear Notch1 signaling and the regulation of dendritic development. Nat Neurosci 3(1):30-40.

Reggio PH. 1987. Molecular determinants for cannabinoid activity: refinement of a molecular reactivity template. NIDA Res Monogr 79:82-95.

Reggio PH. 2008. The Cannabinoid Receptors: Humana Press.

Richards DA, De Paola V, Caroni P, Gahwiler BH, McKinney RA. 2004. AMPA-receptor activation regulates the diffusion of a membrane marker in parallel with dendritic spine motility in the mouse hippocampus. J Physiol 558(Pt 2):503-512.

Rickhag M, Teilum M, Wieloch T. 2007. Rapid and long-term induction of effector immediate early genes (BDNF, Neuritin and Arc) in peri-infarct cortex and dentate gyrus after ischemic injury in rat brain. Brain Res 1151:203-210.

Roberts TF, Tschida KA, Klein ME, Mooney R. 2010. Rapid spine stabilization and synaptic enhancement at the onset of behavioural learning. Nature 463(7283):948-952.

Rodriguez de Fonseca F, Del Arco I, Bermudez-Silva FJ, Bilbao A, Cippitelli A, Navarro M. 2005. The endocannabinoid system: physiology and pharmacology. Alcohol Alcohol 40(1):2-14.

Rodriguez de Fonseca F, Ramos JA, Bonnin A, Fernandez-Ruiz JJ. 1993. Presence of cannabinoid binding sites in the brain from early postnatal ages. Neuroreport 4(2):135-138.

Romero J, Garcia L, Fernandez-Ruiz JJ, Cebeira M, Ramos JA. 1995. Changes in rat brain cannabinoid binding sites after acute or chronic exposure to their endogenous agonist, anandamide, or to delta 9-tetrahydrocannabinol. Pharmacol Biochem Behav 51(4):731-737.

Ross RA. 2009. The enigmatic pharmacology of GPR55. Trends Pharmacol Sci 30(3):156-163.

Rubino T, Parolaro D. 2008. Long lasting consequences of cannabis exposure in adolescence. Mol Cell Endocrinol 286(1-2 Suppl 1):S108-113.

Rubino T, Realini N, Braida D, Alberio T, Capurro V, Vigano D, Guidali C, Sala M, Fasano M, Parolaro D. 2009a. The depressive phenotype induced in adult female rats by adolescent exposure to THC is associated with cognitive impairment and altered neuroplasticity in the prefrontal cortex. Neurotox Res 15(4):291-302.

Rubino T, Realini N, Braida D, Guidi S, Capurro V, Vigano D, Guidali C, Pinter M, Sala M, Bartesaghi R, Parolaro D. 2009b. Changes in hippocampal morphology and neuroplasticity induced by adolescent THC treatment are associated with cognitive impairment in adulthood. Hippocampus 19(8):763-772.

Ruiz-Canada C, Ashley J, Moeckel-Cole S, Drier E, Yin J, Budnik V. 2004. New synaptic bouton formation is disrupted by misregulation of microtubule stability in aPKC mutants. Neuron 42(4):567-580.

Russo D, Castellani G, Chiocchetti R. 2012. Expression of high-molecular-mass neurofilament protein in horse (Equus caballus) spinal ganglion neurons. Microsc Res Tech 75(5):626-637.

Russo EB. 2007. History of cannabis and its preparations in saga, science, and sobriquet. Chem Biodivers 4(8):1614-1648.

Sagar SM, Sharp FR, Curran T. 1988. Expression of c-fos protein in brain: metabolic mapping at the cellular level. Science 240(4857):1328-1331.

Sakai T, Kitamoto T. 2006. [Recent development of research on long-term memory in Drosophila]. Seikagaku 78(1):38-41.

Samat A, Tomlinson B, Taheri S, Thomas GN. 2008. Rimonabant for the treatment of obesity. Recent Pat Cardiovasc Drug Discov 3(3):187-193.

Sambrook J, Russell DW. 2001. Molecular Cloning: A Laboratory Manual: Cold Spring Harbor Laboratory Press.

Sanchez C, Diaz-Nido J, Avila J. 2000. Phosphorylation of microtubule-associated protein 2 (MAP2) and its relevance for the regulation of the neuronal cytoskeleton function. Prog Neurobiol 61(2):133-168.

Saraceno GE, Ayala MV, Badorrey MS, Holubiec M, Romero JI, Galeano P, Barreto G, Giraldez-Alvarez LD, Kolliker-Fres R, Coirini H, Capani F. 2012. Effects of perinatal asphyxia on rat striatal cytoskeleton. Synapse 66(1):9-19.

Schneider M. 2008. Puberty as a highly vulnerable developmental period for the consequences of cannabis exposure. Addict Biol 13(2):253-263.

Schneider M, Koch M. 2003. Chronic pubertal, but not adult chronic cannabinoid treatment impairs sensorimotor gating, recognition memory, and the performance in a progressive ratio task in adult rats. Neuropsychopharmacology 28(10):1760-1769.

Schulz SB, Haesler S, Scharff C, Rochefort C. 2010. Knockdown of FoxP2 alters spine density in Area X of the zebra finch. Genes Brain Behav 9(7):732-740.

Schulze DR, Carroll FI, McMahon LR. 2012. Interactions between dopamine transporter and cannabinoid receptor ligands in rhesus monkeys. Psychopharmacology (Berl).

Scotto-Lomassese S, Rochefort C, Nshdejan A, Scharff C. 2007. HVC interneurons are not renewed in adult male zebra finches. Eur J Neurosci 25(6):1663-1668.

Segal I, Korkotian I, Murphy DD. 2000. Dendritic spine formation and pruning: common cellular mechanisms? Trends Neurosci 23(2):53-57.

Segal M. 2005. Dendritic spines and long-term plasticity. Nat Rev Neurosci 6(4):277-284.

Sestan N, Artavanis-Tsakonas S, Rakic P. 1999. Contact-dependent inhibition of cortical neurite growth mediated by notch signaling. Science 286(5440):741-746.

Shaw G, Yang C, Ellis R, Anderson K, Parker Mickle J, Scheff S, Pike B, Anderson DK, Howland DR. 2005. Hyperphosphorylated neurofilament NF-H is a serum biomarker of axonal injury. Biochem Biophys Res Commun 336(4):1268-1277.

Sheng M, Greenberg ME. 1990. The regulation and function of c-fos and other immediate early genes in the nervous system. Neuron 4(4):477-485.

Shepherd JD, Bear MF. 2011. New views of Arc, a master regulator of synaptic plasticity. Nat Neurosci 14(3):279-284.

Smith PB, Compton DR, Welch SP, Razdan RK, Mechoulam R, Martin BR. 1994. The pharmacological activity of anandamide, a putative endogenous cannabinoid, in mice. J Pharmacol Exp Ther 270(1):219-227.

Soderstrom K, Gilbert MT. 2012. Cannabinoid mitigation of neuronal morphological change important to development and learning: Insight from a zebra finch model of psychopharmacology. Life Sci.

Soderstrom K, Johnson F. 2000. CB1 cannabinoid receptor expression in brain regions associated with zebra finch song control. Brain Res 857(1-2):151-157.

Soderstrom K, Johnson F. 2001. Zebra finch CB1 cannabinoid receptor: pharmacology and in vivo and in vitro effects of activation. J Pharmacol Exp Ther 297(1):189-197.

Soderstrom K, Johnson F. 2003. Cannabinoid exposure alters learning of zebra finch vocal patterns. Brain Res Dev Brain Res 142(2):215-217.

Soderstrom K, Luo B. 2010. Late-postnatal cannabinoid exposure persistently increases FoxP2 expression within zebra finch striatum. Dev Neurobiol 70(3):195-203.

Soderstrom K, Poklis JL, Lichtman AH. 2011. Cannabinoid exposure during zebra finch sensorimotor vocal learning persistently alters expression of endocannabinoid signaling elements and acute agonist responsiveness. BMC Neurosci 12:3.

Soderstrom K, Tian Q. 2004. Distinct periods of cannabinoid sensitivity during zebra finch vocal development. Brain Res Dev Brain Res 153(2):225-232.

Soderstrom K, Tian Q. 2006. Developmental pattern of CB1 cannabinoid receptor immunoreactivity in brain regions important to zebra finch (Taeniopygia guttata) song learning and control. J Comp Neurol 496(5):739-758.

Soderstrom K, Tian Q. 2008. CB(1) cannabinoid receptor activation dose dependently modulates neuronal activity within caudal but not rostral song control regions of adult zebra finch telencephalon. Psychopharmacology (Berl) 199(2):265-273.

Soderstrom K, Tian Q, Valenti M, Di Marzo V. 2004. Endocannabinoids link feeding state and auditory perception-related gene expression. J Neurosci 24(44):10013-10021.

Sohrabji F, Nordeen EJ, Nordeen KW. 1990. Selective impairment of song learning following lesions of a forebrain nucleus in the juvenile zebra finch. Behav Neural Biol 53(1):51-63.

Solowij N, Michie PT. 2007. Cannabis and cognitive dysfunction: parallels with endophenotypes of schizophrenia? J Psychiatry Neurosci 32(1):30-52.

Song ZH, Bonner TI. 1996. A lysine residue of the cannabinoid receptor is critical for receptor recognition by several agonists but not WIN55212-2. Mol Pharmacol 49(5):891-896.

Stripling R, Volman SF, Clayton DF. 1997. Response modulation in the zebra finch neostriatum: relationship to nuclear gene regulation. J Neurosci 17(10):3883-3893.

Sugiura T, Kobayashi Y, Oka S, Waku K. 2002. Biosynthesis and degradation of anandamide and 2-arachidonoylglycerol and their possible physiological significance. Prostaglandins Leukot Essent Fatty Acids 66(2-3):173-192.

Sugiura T, Kondo S, Sukagawa A, Nakane S, Shinoda A, Itoh K, Yamashita A, Waku K. 1995. 2-Arachidonoylglycerol: a possible endogenous cannabinoid receptor ligand in brain. Biochem Biophys Res Commun 215(1):89-97.

Tagliaferro P, Javier Ramos A, Onaivi ES, Evrard SG, Lujilde J, Brusco A. 2006. Neuronal cytoskeleton and synaptic densities are altered after a chronic treatment with the cannabinoid receptor agonist WIN 55,212-2. Brain Res 1085(1):163-176.

Tahir SK, Trogadis JE, Stevens JK, Zimmerman AM. 1992. Cytoskeletal organization following cannabinoid treatment in undifferentiated and differentiated PC12 cells. Biochem Cell Biol 70(10-11):1159-1173.

Takahashi N, Ishizuka B. 2012. The involvement of neurofilament heavy chain phosphorylation in the maturation and degeneration of rat oocytes. Endocrinology 153(4):1990-1998.

Teramitsu I, Poopatanapong A, Torrisi S, White SA. 2010. Striatal FoxP2 is actively regulated during songbird sensorimotor learning. PLoS One 5(1):e8548.

Terleph TA, Mello CV, Vicario DS. 2007. Species differences in auditory processing dynamics in songbird auditory telencephalon. Dev Neurobiol 67(11):1498-1510.

Thompson JA, Johnson F. 2007. HVC microlesions do not destabilize the vocal patterns of adult male zebra finches with prior ablation of LMAN. Dev Neurobiol 67(2):205-218.

Tischmeyer W, Grimm R. 1999. Activation of immediate early genes and memory formation. Cell Mol Life Sci 55(4):564-574.

Touw M. 1981. The religious and medicinal uses of Cannabis in China, India and Tibet. J Psychoactive Drugs 13(1):23-34.

Tschida K, Mooney R. 2012. The role of auditory feedback in vocal learning and maintenance. Curr Opin Neurobiol 22(2):320-327.

Turner CE, Hadley K, Fetterman PS. 1973. Constituents of Cannabis sativa L. VI. Propyl homologs in samples of known geographical origin. J Pharm Sci 62(10):1739-1741.

Turu G, Hunyady L. 2010. Signal transduction of the CB1 cannabinoid receptor. J Mol Endocrinol 44(2):75-85.

Tzingounis AV, Nicoll RA. 2006. Arc/Arg3.1: linking gene expression to synaptic plasticity and memory. Neuron 52(3):403-407.

Varga K, Wagner JA, Bridgen DT, Kunos G. 1998. Platelet- and macrophage-derived endogenous cannabinoids are involved in endotoxin-induced hypotension. FASEB J 12(11):1035-1044.

Vazdarjanova A, Ramirez-Amaya V, Insel N, Plummer TK, Rosi S, Chowdhury S, Mikhael D, Worley PF, Guzowski JF, Barnes CA. 2006. Spatial exploration induces ARC, a plasticity-related immediate-early gene, only in calcium/calmodulin-dependent protein kinase II-positive principal excitatory and inhibitory neurons of the rat forebrain. J Comp Neurol 498(3):317-329.

Velho TA, Pinaud R, Rodrigues PV, Mello CV. 2005. Co-induction of activity-dependent genes in songbirds. Eur J Neurosci 22(7):1667-1678.

Verdurand M, Nguyen V, Stark D, Zahra D, Gregoire MC, Greguric I, Zavitsanou K. 2011. Comparison of Cannabinoid CB(1) Receptor Binding in Adolescent and Adult Rats: A Positron Emission Tomography Study Using [F]MK-9470. Int J Mol Imaging 2011:548123.

Vincze T, Posfai J, Roberts RJ. 2003. NEBcutter: A program to cleave DNA with restriction enzymes. Nucleic Acids Res 31(13):3688-3691.

Vitalis T, Laine J, Simon A, Roland A, Leterrier C, Lenkei Z. 2008. The type 1 cannabinoid receptor is highly expressed in embryonic cortical projection neurons and negatively regulates neurite growth in vitro. Eur J Neurosci 28(9):1705-1718.

Wadhwa R, Taira K, Kaul SC. 2002. An Hsp70 family chaperone, mortalin/mthsp70/PBP74/Grp75: what, when, and where? Cell Stress Chaperones 7(3):309-316.

Wall ME, Sadler BM, Brine D, Taylor H, Perez-Reyes M. 1983. Metabolism, disposition, and kinetics of delta-9-tetrahydrocannabinol in men and women. Clin Pharmacol Ther 34(3):352-363.

Wallhausser-Franke E, Nixdorf-Bergweiler BE, DeVoogd TJ. 1995. Song isolation is associated with maintaining high spine frequencies on zebra finch 1MAN neurons. Neurobiol Learn Mem 64(1):25-35.

Walton R. 1938. Marihuana, America's new drug problem. Oxford, England: Lippincott. ix, 223 p.

Wang Y, Chan SL, Miele L, Yao PJ, Mackes J, Ingram DK, Mattson MP, Furukawa K. 2004. Involvement of Notch signaling in hippocampal synaptic plasticity. Proc Natl Acad Sci U S A 101(25):9458-9462.

Watson S, Chambers D, Hobbs C, Doherty P, Graham A. 2008. The endocannabinoid receptor, CB1, is required for normal axonal growth and fasciculation. Mol Cell Neurosci 38(1):89-97.

Waung MW, Pfeiffer BE, Nosyreva ED, Ronesi JA, Huber KM. 2008. Rapid translation of Arc/Arg3.1 selectively mediates mGluR-dependent LTD through persistent increases in AMPAR endocytosis rate. Neuron 59(1):84-97.

Weisshaar B, Doll T, Matus A. 1992. Reorganisation of the microtubular cytoskeleton by embryonic microtubule-associated protein 2 (MAP2c). Development 116(4):1151-1161.

Welberg L. 2008. Synaptic plasticity: Learning through continuing potentiation. Nat Rev Neurosci 9(2):82-83.

Wenger T, Gerendai I, Fezza F, Gonzalez S, Bisogno T, Fernandez-Ruiz J, Di Marzo V. 2002. The hypothalamic levels of the endocannabinoid, anandamide, peak immediately before the onset of puberty in female rats. Life Sci 70(12):1407-1414.

Wharton KA, Johansen KM, Xu T, Artavanis-Tsakonas S. 1985. Nucleotide sequence from the neurogenic locus notch implies a gene product that shares homology with proteins containing EGF-like repeats. Cell 43(3 Pt 2):567-581.

White MK, Amini S, Khalili K, Kogan M, Donaldson K, Darbinian N. 2008. Development of a bidirectional caspase-3 expression system for the induction of apoptosis. Cancer Biol Ther 7(6):945-954.

Whitney O, Soderstrom K, Johnson F. 2003. CB1 cannabinoid receptor activation inhibits a neural correlate of song recognition in an auditory/perceptual region of the zebra finch telencephalon. J Neurobiol 56(3):266-274.

Wigstrom H, Gustafsson B. 1986. Postsynaptic control of hippocampal long-term potentiation. J Physiol (Paris) 81(4):228-236.

Williams DW, Kondo S, Krzyzanowska A, Hiromi Y, Truman JW. 2006. Local caspase activity directs engulfment of dendrites during pruning. Nat Neurosci 9(10):1234-1236.

Williams PL, Moffat AC. 1980. Identification in human urine of delta 9-tetrahydrocannabinol-11-oic acid glucuronide: a tetrahydrocannabinol metabolite. J Pharm Pharmacol 32(7):445-448.

Wilson W, Mathew R, Turkington T, Hawk T, Coleman RE, Provenzale J. 2000. Brain morphological changes and early marijuana use: a magnetic resonance and positron emission tomography study. J Addict Dis 19(1):1-22.

Wirth MJ, Brun A, Grabert J, Patz S, Wahle P. 2003. Accelerated dendritic development of rat cortical pyramidal cells and interneurons after biolistic transfection with BDNF and NT4/5. Development 130(23):5827-5838.

Woelkart K, Salo-Ahen OM, Bauer R. 2008. CB receptor ligands from plants. Curr Top Med Chem 8(3):173-186.

Woolley CS, McEwen BS. 1993. Roles of estradiol and progesterone in regulation of hippocampal dendritic spine density during the estrous cycle in the rat. J Comp Neurol 336(2):293-306.

Wu CS, Zhu J, Wager-Miller J, Wang S, O'Leary D, Monory K, Lutz B, Mackie K, Lu HC. 2010. Requirement of cannabinoid CB(1) receptors in cortical pyramidal neurons for appropriate development of corticothalamic and thalamocortical projections. Eur J Neurosci 32(5):693-706.

Xu T, Yu X, Perlik AJ, Tobin WF, Zweig JA, Tennant K, Jones T, Zuo Y. 2009. Rapid formation and selective stabilization of synapses for enduring motor memories. Nature 462(7275):915-919.

Yamamoto T, Takada K. 2000. Role of cannabinoid receptor in the brain as it relates to drug reward. Jpn J Pharmacol 84(3):229-236.

Yavin E, Yavin Z. 1974. Attachment and culture of dissociated cells from rat embryo cerebral hemispheres on polylysine-coated surface. J Cell Biol 62(2):540-546.

Ye B, Zhang Y, Song W, Younger SH, Jan LY, Jan YN. 2007. Growing dendrites and axons differ in their reliance on the secretory pathway. Cell 130(4):717-729.

Yenjerla M, Lopus M, Wilson L. 2010. Analysis of dynamic instability of steady-state microtubules in vitro by video-enhanced differential interference contrast microscopy with an appendix by Emin Oroudjev. Methods Cell Biol 95:189-206.

Zaretsky MD. 1978. A new auditory area of the songbird forebrain: a connection between auditory and song control centers. Exp Brain Res 32(2):267-273.

Zevin JD, Seidenberg MS, Bottjer SW. 2004. Limits on reacquisition of song in adult zebra finches exposed to white noise. J Neurosci 24(26):5849-5862.

Zhang F, Hong S, Stone V, Smith PJ. 2007. Expression of cannabinoid CB1 receptors in models of diabetic neuropathy. J Pharmacol Exp Ther 323(2):508-515.

Zhang Q, Ma P, Iszard M, Cole RB, Wang W, Wang G. 2002. In vitro metabolism of R(+)-[2,3-dihydro-5-methyl-3-[(morpholinyl)methyl]pyrrolo [1,2,3-de]1,4-benzoxazinyl]-(1-naphthalenyl) methanone mesylate, a cannabinoid receptor agonist. Drug Metab Dispos 30(10):1077-1086.

Zhang Y, Fukushima H, Kida S. 2011. Induction and requirement of gene expression in the anterior cingulate cortex and medial prefrontal cortex for the consolidation of inhibitory avoidance memory. Mol Brain 4:4.

Zhuang SY, Bridges D, Grigorenko E, McCloud S, Boon A, Hampson RE, Deadwyler SA. 2005. Cannabinoids produce neuroprotection by reducing intracellular calcium release from ryanodine-sensitive stores. Neuropharmacology 48(8):1086-1096.

Zuardi AW. 2006. History of cannabis as a medicine: a review. Rev Bras Psiquiatr 28(2):153-157.

Zuo Y, Lin A, Chang P, Gan WB. 2005. Development of long-term dendritic spine stability in diverse regions of cerebral cortex. Neuron 46(2):181-189

Appendix A: Animal Use Approval Letter

East Carolina University

Animal Care and
Use Commitee
212 Ed Warren Life
Sciences Building
East Carolina University
Greenville, NC 27834

252-744-2436 office
252-744-2355 fax

April 15, 2011

Ken Soderstrom, Ph.D.
Department of Pharmacology
Brody 6S-10
ECU Brody School of Medicine

Dear Dr. Soderstrom:

Your Animal Use Protocol entitled, "Cannabinoid-Altered Vocal Development" (AUP #W190c) was reviewed by this institution's Animal Care and Use Committee on 4/15/11. The following action was taken by the Committee:

"Approved as submitted"

Please contact Dale Aycock at 744-2997 prior to hazard use

A copy is enclosed for your laboratory files. Please be reminded that all animal procedures must be conducted as described in the approved Animal Use Protocol. Modifications of these procedures cannot be performed without prior approval of the ACUC. The Animal Welfare Act and Public Health Service Guidelines require the ACUC to suspend activities not in accordance with approved procedures and report such activities to the responsible University Official (Vice Chancellor for Health Sciences or Vice Chancellor for Academic Affairs) and appropriate federal Agencies.

Sincerely yours,

Scott E. Gordon, Ph.D.
Chairman, Animal Care and Use Committee

SEG/jd

enclosure

Animal Care and Use Committee
East Carolina University
212 Ed Warren Life Sciences Building
Greenville, NC 27834
252-744-2436 office • 252-744-2355 fax

April 17, 2008

Ken Soderstrom, Ph.D.
Department of Pharmacology
Brody 6S-10
ECU Brody School of Medicine

Dear Dr. Soderstrom:

Your Animal Use Protocol entitled, "Cannabinoid-Altered Vocal Development," (AUP #W190b) was reviewed by this institution's Animal Care and Use Committee on 4/17/08. The following action was taken by the Committee:

"Approved as submitted"

A copy is enclosed for your laboratory files. Please be reminded that all animal procedures must be conducted as described in the approved Animal Use Protocol. Modifications of these procedures cannot be performed without prior approval of the ACUC. The Animal Welfare Act and Public Health Service Guidelines require the ACUC to suspend activities not in accordance with approved procedures and report such activities to the responsible University Official (Vice Chancellor for Health Sciences or Vice Chancellor for Academic Affairs) and appropriate federal Agencies.

Sincerely yours,

Robert G. Carroll, Ph.D.
Chairman, Animal Care and Use Committee

RGC/jd

enclosure

Appendix B: PC12 experiments

Introduction

Cannabinoid receptor stimulation plays an essential role in the regulation of neurotransmitter release, thus acting to dramatically reduce neuronal plasticity in the CNS. It is generally agreed upon that the endogenous cannabinoid system is considered one of the brain's homeostatic, de-novo mechanisms to protect itself from overstimulation by reducing excitatory synaptic input (Marsicano et al., 2003), but the physiological consequences of chronically overstimulating the cannabinoid system itself are not fully understood. Results from numerous studies indicate that periadolescents (including humans) exposed once daily to the cannabinoid agonist WIN during postnatal brain maturation and sensorimotor learning exhibit persistently altered patterns in learning and behavior. Furthermore, it is becoming increasingly clear that many of these observations regarding daily periadolescent cannabinoid exposure extend more directly to consequences such as persistently impaired CNS morphology and sensorimotor gating that last throughout adulthood (Tahir et al., 1992). For example, in the periadolescent zebra finch, we recently discovered that this development-altering cannabinoid treatment leads to an inappropriate maintenance in dendritic spine densities in a subset of brain regions responsible for vocal learning, an effect that is strongly associated with a marked decrease in production of learned stereotyped song (Gilbert and Soderstrom, 2011). In a CHO cell culture model, cannabinoid treatment is associated with a drastic reorganization of microfilaments and microtubules, both major factors in the control of neuronal shape and growth (Tahir et al., 1992). In the hippocampus, cannabinoid receptor stimulation is associated with a tonic autoinhibition

of a population of GABAergic neurons, and causes a decrease in glutamate release in principal neurons (Domenici et al., 2006; Katona et al., 1999; Kim et al., 2008). These lasting changes in transmission alter cellular morphologies in many instances (Kim et al., 2008).

Although mechanisms behind periadolescent cannabinoid altered learning and CNS development largely remain uninvestigated, a few studies recently indicated a number of potential neural targets that may be affected by inappropriate cannabinoid receptor activation. In particular, Tagliaferro et al. reported significant increases in a number of cytoskeletal proteins and synaptic markers with respect to chronic WIN treatment of adolescent Wistar rats (Tagliaferro et al., 2006). These findings prompted us to investigate our hypothesis of whether similar alterations in neuronal cytoarchitecture can be identified in our model of cannabinoid-altered vocal learning as well, and if so, whether these morphological changes persist throughout adulthood.

In order to identify potential cannabinoid-induced morphological changes in real time, a neuronal cell culture model that adequately expresses CB1 receptor is necessary. The previously observed morphological changes in zebra finch telencephalon following cannabinoid treatment promped us to consider cannabinoid effects on synaptic loss, neurite outgrowth and neurogenesis on the PC12 cell culture system. This cell line is a well-characterized system which can be induced to form neurites upon stimulation with nerve growth factor. This aspect is advantageous, as neuronal differentiation in this model heavily depends on the controlled reorganization of the cytoskeleton, a characteristic that cannabinoids are known to significantly disrupt in other systems. After assessing whether this cell line can endogenously express

functional CB_1 receptors, we discovered that when in a low-glucose environment, CB_1 expression in these cells is undetectable, which allows heterologous expression of the zebra finch CB_1 receptor in a neuronal system with a virtual “clean slate” in this respect. In order to begin to assess mechanisms involved in cannabinoid-altered gross neuronal morphology, we constructed a functionally expressing zebra finch CB_1 HIV-based lentivector for stable infection of PC12 cells. These experiments will be performed on both pre-differentiated and undifferentiated PC12 cells in an effort to access the cannabinoid effects on processes related to neurite formation and regression, such as neurite length, number of branches per process (arborization), number of spines per process per neuron (spine densities), and cell densities as compared to a control group).

Materials and Methods

Materials

All materials and reagents were purchased from Sigma (St. Louis, MO), or VWR International (Radnor, PA). Disposable plasticware was purchased from Corning (Corning, NY). cDNA synthesis, PCR, and reagents used for molecular cloning the zebra finch CB_1 receptor were purchased from Invitrogen Laboratories (Grand Island, NY). HIV-based lentiviral packaging vectors and system were purchased from Systems Biosciences (Mountain View, NY). RNA isolation solution was purchased from Fluka Chemicals (St. Louis, MO). Radiolabeled full CB_1 agonist [^{3}H] CP 55,940 was purchased from Perkin Elmer (Boston, MA). Equithesin was prepared from reagents (40 % propylene glycol, 10 % ETOH, 5 % chloral hydrate, 1 % pentobarbital). The synthetic

cannabinoid agonist WIN was suspended in vehicle from concentrated DMSO stocks (10 mM). Vehicle consisted of a suspension of 1:1:18 DMSO:Alkamuls EL-620 (Rhodia, Cranberry, NJ):phosphate-buffered saline.

Preparation of Zebra Finch Synaptosomal Membranes

Washed P2 synaptosomal membranes were prepared from 50-day old male zebra finches as described in the Materials and Methods section, and as previously described in (Soderstrom and Johnson, 2000).

Radiolabeled Receptor Binding of CB_1

Radioligand binding experiments were conducted according to protocols developed by (Soderstrom and Johnson, 2001). The ^{3}H-labeled synthetic cannabinoid agonist CP-55,940 (180 Ci/mmol) was used in these experiments because it possesses a higher specific activity than many other radioligands, and because it has been used in the past to characterize cannabinoid receptors in the zebra finch and other species (Pertwee, 1997; Soderstrom and Johnson, 2001). Binding reactions were conducted in a final volume of 200 µl solution containing 50 mM Tris/ 10 mM $MgCl_2$, 5 mg/ml BSA, and 0.1 % DMSO. A total of 100 µg of zebra finch P2 membrane protein, and 100 µg of PC12 cell lysate were used in each replicate for saturation isotherms. Nonspecific binding was defined as binding of ^{3}H-labeled CP-55,940 to other receptor sites and adsorption to the membranes in the presence of a vast molar excess of drug (1µM WIN, diluted from a 10X stocks). Specific binding was calculated as the difference between the total binding and nonspecific binding. Saturation binding experiments were conducted in a 24-well format, incubated at 30° C for 90 minutes, and terminated by rapid filtration over GF/C glass fiber filters (Brandel Incorporated, Gaithersburg MD).

Filters were washed immediately after termination with 50 mM Tris/10 mM $MgCl_2$, at 4° C. Following this, filters were dried for 1 hour, and then quantified using a Packard 2200CA Tri-Carb liquid scintillation analyzer (Perkin Elmer, Boston MA). Tritium efficiency was approximately 50 %. Radioligand binding data were analyzed using GraphPad Prism 5.0 software (San Diego, CA). The relative appropriateness of one-site binding models was compared with two-site binding models was compared through *F* tests, in order to determine if additional parameters improve the fit of the data to more complex equations (Bylund and Toews, 1993; Frey and Albin, 2001).

Cell Culture

PC12 cells were maintained and propagated in complete RPMI 1640 media, and HEK-293TN cells were maintained and propagated in complete DMEM media. Both cell lines were incubated at 37° C supplemented, with 5 % CO_2 and subcultured as described in the Materials and Methods section.

Cloning of CB_1 and Transfection of PC12 Cells

A zebra finch CB1-expressing mammalian vector was first constructed in pcDNA 3.1+ for transient lipid-based transfection of PC-12 cells. Molecular cloning methods used were as described in the Materials and Methods section (Chapter number)? The forward primer 5'-ATGAAGCTTAGTC ATGAAGTCAATTCTAGATG and reverse primer 5'-ATGCTCGAGTTACAACGCTTCAGCTGT were designed based on the complete coding sequence provided to GenBank by (Soderstrom and Johnson 2001), Accession number AF255388. The restriction sites XhoI and HindIII were incorporated into the design of the primers. Standard PCR procedures were performed with an annealing

temperature of 72°C. The amplified PCR product was then TA-subcloned into vector PCR 2.1, and used to transform DH5α E.Coli cells using protocols listed in the Materials and Methods section. Inserts were digested and sequenced, 3130 Genetic Analyser (Applied Biosystems, Carlsbad CA) then inserted into the mammalian expression vector pcDNA 3.1+ for further use.

Because PC12 cells are notoriously difficult to transfect, and are extremely vulnerable to cytotoxicity during transfection. We attempted to transfect cells with the more gentle Lipofectamine LTX and Plus reagent. Approximately 1 µg of DNA was used per reaction, and transfection methods were performed as described in the Materials and Methods section.

Transfection of HEK-293TN Cells

Production of a high-titer of lentiviral particles was accomplished by simultaneous transfection with lentiviral expression and packaging plasmids into the HEK-293TN packaging cell line. Transfection protocols were adapted from instructions provided by Systems Biosciences (Mountain View, CA), and infections were adapted from methods used by (Soderstrom and Johnson, 2000). One day prior to transfection, cells were counted and approximately 8.0 x 10^6 cells seeded into a sterile T75 flask, in DMEM containing 10 % FBS with no antibiotics/antimycotics. The next day, when cells reached 17 % confluency, cells were transfected with the lentivector pCDH-CMV-MCS (Systems Biosciences Cat# CD500B-1), containing cDNA encoding the zebra finch CB_1 receptor. Breifly, 1.6 ml of serum free DMEM was added to 4.5 µg of plasmid DNA, and mixed with 40 µl of Lipofectamine™ reagent, and mixed gently by pipetting. This mixture was

incubated for 30 minutes at room temperature in order to allow DNA-Lipofectamine™ complexes to form. Following this, the DMEM-plasmid-Lipofectamine™ mixture was added drowpise to the T75 flask, and swirled around in order to ensure even distribution throughout the plate. Cells were returned to a quarantined incubator supplemented with 5 % CO_2 at 37° C. At approximately 72 hours after transfection, media was collected and centrifuged at 3000 x g, and stored at - 80° C until use. pseudoviral titers were determined by transduction of PC12 cells with the lentivirus, followed by microscopic analysis.

Lentiviral Infections

The day before infection, undifferentiated PC12 cells were seeded in 6-well plates at a confluency of 50%, and differentiated PC12 cells were subcultured into 6-well plates at a confluency of approximately 30%. The next day, culture medium was removed via serological pipetting, and 2 ml of complete DMEM culture media containing viral suspension and 5 µg/ ml of Polybrene was added to each well. To determine the effect of viral incubation time on CB_1 receptor expression, cells were incubated in viral media for varying time periods, then fixed and subjected to immunostaining described below. If applicable, media was replaced every 12 hours. Cultures co-transfected with EGFP-expressing vector were used as controls.

Drug Treatments

The day following transfections, cultures will be treated with various concentrations of WIN (0, 1, 3, 10, 30, 100 nM) for four days, with fresh drug-containing

media replaced daily. Morphological measures (neurite length, number of branches per process, number of spines per process per neuron and cell densities) will be recorded.

Immunostaining of Infected Cells

In an effort to immunostain cells for CB_1, cultures were grown on 22 x 22 mm glass coverslips. Cells were briefly rinsed with warm PBS, and then treated with 1ml of ice-cold methanol per well, and incubated at -20° C for 10 minutes. Cells were then blocked with a solution containing 5% BSA in PBS for 30 minutes with gentle agitation. Culture dishes containing the glass coverslips were incubated in a primary antibody mixture (1:1000) containing anti-CB_1 antibody in the 5 % BSA/PBS solution overnight at 4° C. The next day, cells were washed three times with ice-cold PBS, and then incubated in FITC-conjugated goat anti-rabbit secondary antibody (1:1000) for thirty minutes at room temperature, for 1 hour in the dark. Finally, coverslips were washed three times with PBS-T, then wet-mounted on slides using an anti-fade fluorescent mounting medium (Invitrogen, Grand Island NY). Slides were stored in the dark at -20° C for extended use.

Results

Radioligand Binding

Saturation binding experiments were performed in order to determine the densities of zebra finch CB_1 binding sites within PC12 membranes. Experiments involving saturation binding of zebra finch P2 membranes were used as a positive control for radioligand binding techniques (Soderstrom and Johnson, 2001). Results revealed that in control experiments, zebra finch binding site density (B_{max} = 1800

fmol/mg protein, 95% CI, 1626 - 2161) These results confirm previous findings presented by Soderstrom et al., who in their hands, determined that B_{max} = 2100 fmol/mg of protein; 95% CI, 1917–2283) and affinity (K_d = 1.51 ± 0.14 nM). For PC12 cell membranes, B_{max} was significantly lower than control B_{max}, (B_{max} = 433 fmol/mg protein, 95% CI, -376 - 1615). These results are discussed below.

Transfection of PC12 Cell Line

Transfection of the PC12 cell line with $ZFCB_1$ using Lipofectamine LTX and Plus reagent did not yield intended results. We witnessed both a significantly reduced PC12 cell viability by about 75% following transfection when using this method. This reduction in cell count severely limited the growth of the viable cells still left in the dish. It appears as though the low seeding density caused the cells to grow very slowly and then detach from the bottom of the dish. This effect was presumably due to a concentration of secreted growth factors in the medium that was too low to thrive on. In addition, we also found that PC12 cells had a transfection efficiency of about 20 %. Although a low efficiency was expected on some level because of the nature of this cell line, these results were deemed unsuitable for our experiments.

Infection of PC12 Cell Line with HIV-Based Lentiviral Vector

Because of the lack of results experienced with transfection agents, we decided to try a more stable method of delivery provided by the lentivirus. In an order to access functional expression of the zebra finch CB_1 receptor delivered by the virus, PC12 cells were grown in complete medium to 70 % confluence on glass coverslips in 6-well plates, and infected with a predetermined concentration of lentivirus. Exactly 48 hours

after infection, cells were fixed, treated with anti-CB_1 antibody, and subjected to immunofluorescent analysis via laser-scanning confocal microscopy. Microscopic analysis revealed that under the conditions the PC12 cells were grown in, the CB_1 receptor was not trafficked to the cell membrane or neurite surface. Therefore, pharmacological experiments aimed to examine the functionality of the CB_1 receptor could not be completed. However, we did find that the CB_1 receptor is robustly expressed within the cytoplasm.

Discussion

In this study, we aimed to investigate the gross morphological changes conferred to neurons by various doses of cannabinoids in real-time, using a PC12 neuronal cell model heterologously-expressing zebra finch CB_1. We originally predicted that similar to most other cell lines, PC12 cells constitutively express a certain density of CB_1 receptors possessing a high affinity for WIN, regardless of culturing conditions. Unfortunately, a quick literature review of this subject led us to understand that the current consensus regarding whether this cell line actually expresses a functional CB_1 receptor is very unclear.

Figure AB1. Results of PC12 radioligand binding experiments, using zebra finch membranes as a control. For PC12 membranes, B_{max} was significantly lower than B_{max} of control saturation experiments.

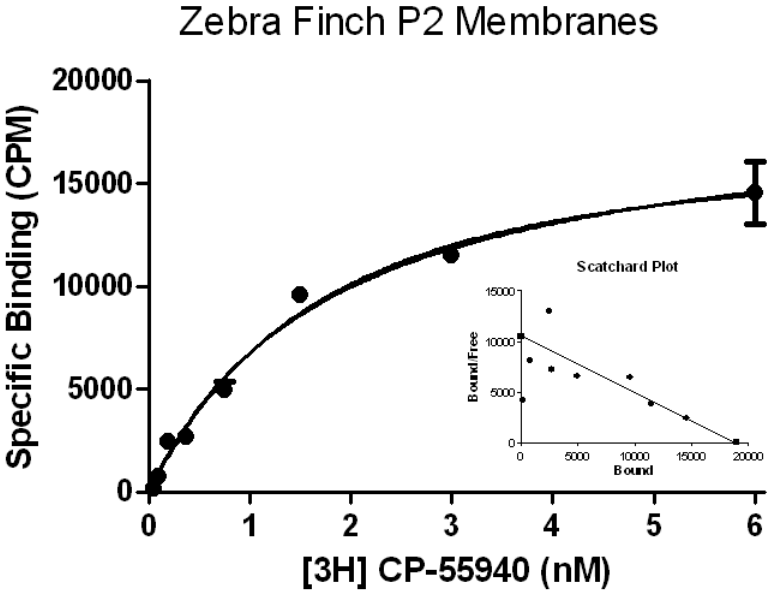
Zebra Finch P2 Membranes
Specific Binding (CPM)
20000
15000
10000
5000
0
0
1
2
3
4
5
6
[3H] CP-55940 (nM)
Scatchard Plot
Bound/Free
15000
10000
5000
0
0
5000
10000
15000
20000
Bound

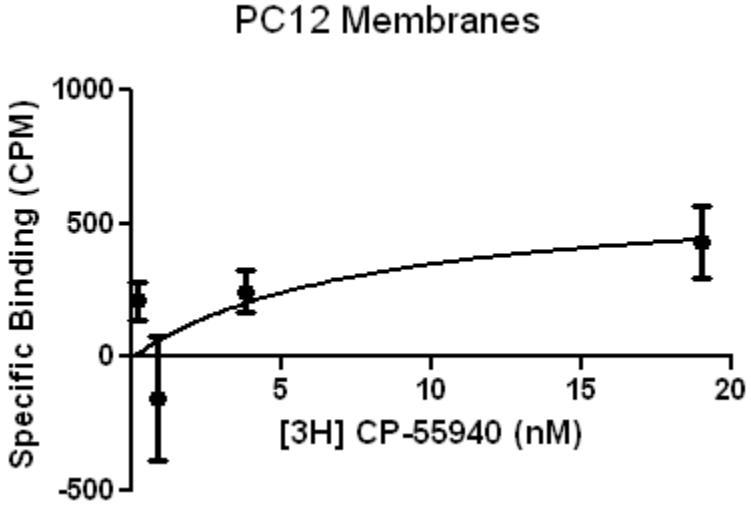
PC12 Membranes
Specific Binding (CPM)
1000
500
0
-500
5
10
15
20
[3H] CP-55940 (nM)

In an effort to confirm our hypothesis, we proceeded to characterize the CB_1 receptor in these cells by examining the density of functional CB_1 receptors within the membrane as well as their affinity for an agonist ([^{3}H] CP-55940). In order to determine B_{max} for PC12 cells, saturation binding experiments were performed with PC12 cell lysates using zebra finch P2 membranes as a control. We found that binding was significantly low in experimental groups, which led to a series of possible scenarios: either (1) either the PC12 cells assayed possessed a very low CB_1 receptor density, but a comparable affinity (low K_d) to the zebra finch CB_1 receptor, or (2) these cells possessed a considerable CB_1 receptor density, however these receptors possessed an extremely low affinity for the ligands used. After reviewing the generated data in its entirety, we concluded that the former of the two scenarios had taken place. At first consideration, we found these data to be quite contradictory to our predictions, but recent studies regarding a novel role for CB_1 in diabetic neuropathy shed light on this issue. In these studies, researchers determined that within PC12 cells, the CB_1 receptor is selectively expressed under certain cell culturing conditions. In high-glucose conditions, CB_1 becomes internalized, as evident by a lack of protein expression on the neuronal membrane (Zhang et al., 2007). In contrast, low concentrations of glucose, which is needed in order to differentiate PC12 cells into neurons, were associated with an increase in CB_1 receptor expression. We were unable to utilize this cell line without a method of controlling CB_1 receptor expression in the presence of different culturing conditions, so we made preparations to create a heterogolously-expressing zebra finch CB_1/PC12 cell line.

We were successful in constructing a zebra finch CB_1-expressing mammalian vector (in pcDNA3.1+) for transient lipid-based transfection of PC12 cells, and subsequently a HIV-based CB_1 lentiviral vector for stable infections. Pharmacological experiments were intended to be performed on pre-differentiated (with 50 ug/ml nerve growth factor for 3 days) and differentiating PC12 cells to assess effects on processes of neurite formation and regression, and immunochemical measures of PSD-95, MAP2, NF-200, and synaptotagmin were to be taken in separate cultures however, a number of setbacks occurred that prevented us from pursuing this study further. Unfortunately, the CB_1 receptor failed to express at the PC12 cell membrane surface, so experiments were not moved forward (Figure AB2).

Figure AB2. A) Immunofluorescent confocal image of PC12 cells heterologously expressing CB1 receptor. Note the lack of expression on the cell membrane surface, and the high levels of expression within the cytoplasm. B) DIC darkfield image of the same cell field as pictured in A. C) Control PC12 cells infected with GFP-expressing lentivirus.

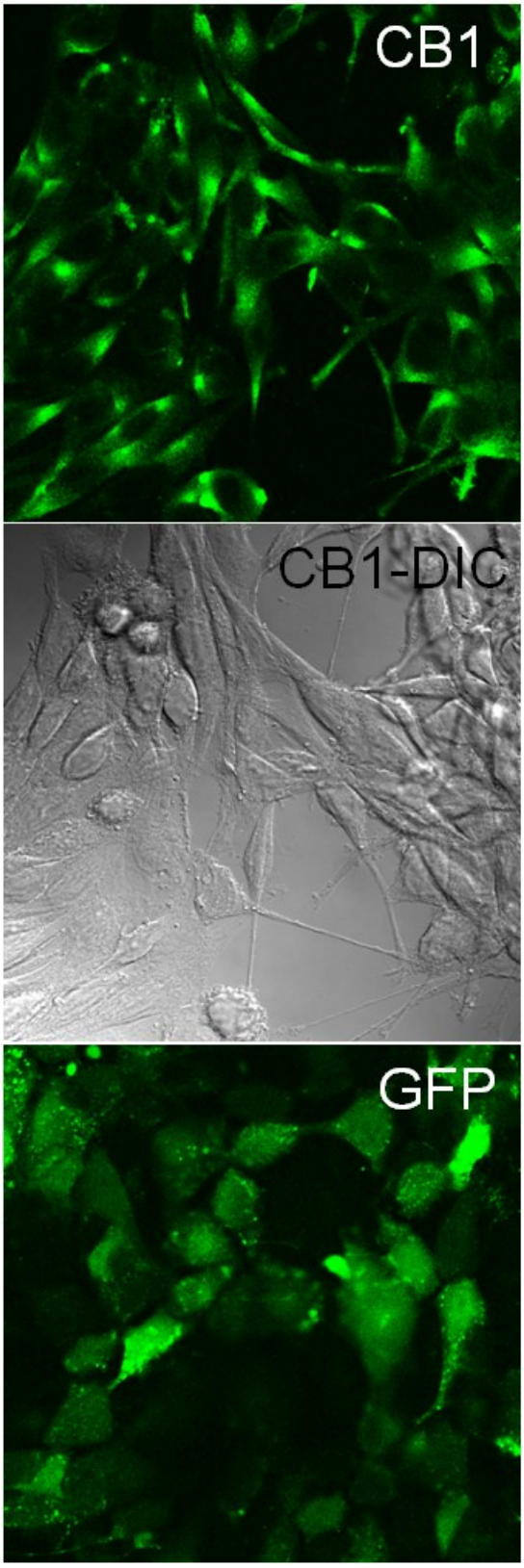
CB1
CB1-DIC
GFP

A number of mechanistic factors could have contributed to this issue. Firstly, It could be possible that within the PC12 cell line, cell signaling mechanisms that govern receptor internalization and recycling (such as cell anchoring cascades, microRNAs) are expressed more readily than those that govern CB1 receptor expression (Avraham and Yarden, 2012). Furthermore, it may be the case that this CPCR will only function as a homo/heterodimer in the PC12 cell line, and the adhesion molecules necessary for this to take place are not present, or are in low number within the cell. Also, it is possible tht the expression of other GPCRs may hinder factors and mocular machinery necessary for expression. Future experiments will aim to determine this caus

APPENDIX C: Caspase-3 Experiments

INTRODUCTION

Cannabinoids, the active constituents of marijuana, are known to produce an array of behavioral changes in most vertebrate species, including disruptions in learning and memory formation, reductions in locomotor activity, and various psychoactive effects. The central actions of these compounds have been attributed to activation of the cannabinoid receptor 1 (CB1). CB1 receptors are enriched in various forebrain areas, including the cerebellum, hippocampus, forebrain, and basal ganglia which correlates with well-documented influences on locomotor coordination, anxiolysis, and increases in reward-like behaviors present in models of drug addiction (El Manira and Kyriakatos, 2010; Fernandez-Ruiz et al., 2010; Kinsey et al., 2011).

More intriguing, and less understood, are the effects of cannabinoids on the neural aspects of learning and memory formation. It is thought that cannabinoids influence the acquisition and consolidation of sensory stimuli, though the precise specifics remain unclear. Recent observations have led to the hypothesis that caspase-3 likely plays a role in at least one form of cannabinoid-induced disruption of cognitive function. It has been shown that the cysteine-aspartic protease caspase-3, a terminal mediator in a major cascade that leads to programmed cell death, plays a non-apoptotic role in healthy neural tissue during postnatal development, growth, and adulthood (Chen et al., 1998; Liu et al., 2008). Throughout the scientific community the role of caspase-3 in the cell is most widely studied in the context of global apoptosis. When cells undergo caspase- dependent apoptosis, 32 kDa pro-caspase 3 is processed by

caspases 8, 9, and 10 into 17 kDa and 12kDa subunits, which ultimately lead to the formation of an activated caspase-3 complex when assembled as a tetramer (Huppertz et al., 1999; White et al., 2008). At this point, activated caspase-3 cleaves a site on caspase 9 that is usually bound by XIAP in a non-apoptotic state, which in turn prevents this inhibitor from sequestering caspase 9. Under these conditions, caspase-3 is free to destroy a number of proteins necessary for survival, and the cell is irreversibly committed to death (Denault et al., 2007; Huppertz et al., 1999). However, studies have indicated that caspase-3 plays a major regulatory role in neuronal development, signaling, remodeling, and forms of learning and memory acquisition. For example, in *Drosophila*, descrete, localized caspase-3 activity has been shown to direct the phagocytic engulfment of severed dendritic spines during pruning (Williams et al., 2006). Administration of Z-DEVD-FMK, an inhibitor of caspase-3, inhibits long-term potentiation in rat hippocampal slices, and long term sensitization in the terrestrial snail helix (Bravarenko et al., 2006; Guliaeva, 2004; Gulyaeva et al., 2003). By examining the role of caspase-3 in the song-specific *zenk* habituation response of the adult zebra finch, Huesmann and Clayton suggest a mechanism by which caspase-3 is tightly controlled at specific synaptic sites in an effort to regulate neuronal plasticity (Huesmann and Clayton, 2006). In this model, hearing a novel conspecific song stimulus causes a robust induction in the immediate early gene *zenk* in NCM, a forebrain region involved in higher order processing of auditory stimuli (Chew et al., 1996; Mello and Clayton, 1994; Mello et al., 1992). However, after repeated presentations of the same song, the *zenk* response habituates, thus creating a molecular representation of context-specific memory (Chew et al., 1995; Stripling et al.,

1997). They effectively demonstrated that activated caspase-3 is constitutively present, but sequestered, in postsynaptic neurons, and is thought to be locally released upon demand. This activation was required in order to facilitate the *zenk*-induced long-term habituation response to song. In accordance with this data, it has been recently shown that cannabinoid administration reduces *zenk* mRNA levels in the NCM by almost 60% following novel song presentation, and blocks the *zenk* habituation response after repeated stimulus presentation (Whitney et al., 2003).

The studies presented herein were conducted in order to test the hypothesis that the cannabinoid reduction of long term song habituation in zebra finch NCM involves a direct inhibition of activated caspase-3, which in turn blocks the emergence of the zenk response.

EXPERIMENTAL PROCEDURE

Materials

Except where noted, all materials and reagents were purchased from Sigma (St. Louis, MO), or Fisher Scientific (Pittsburgh, PA). The synthetic cannabinoid agonist WIN55212-2 (WIN) used for injections was suspended in vehicle from concentrated DMSO stocks (30 mM). Vehicle consisted of a suspension of 1:1:18 DMSO:Alkamuls EL-620 (Rhodia, Cranberry, NJ):saline.

Animals

Adult male zebra finches aged over 110 days old were used in these experiments. Birds were obtained from our breeding aviary, and caged with free access to grit, water, mixed seeds (Sunseed VitaFinch), and cuttlebone, and provided multiple perches.

Animals were maintained on a 14:10 light/dark cycle, and ambient temperature was maintained at 78° F. Birds were housed from 25-50 days of age with an adult male tutor, and then moved to a flight cage containing 12 adult males. Birds used in individual experiments were removed from adult flight cages and housed in visual isolation, in soundproof recording chambers in order to acclimate to the environment. Birds were cared for and experiments conducted according to protocols approved by East Carolina University's Animal Care and Use Committee.

Activation of Caspase-3 in Zebra Finch NCM

An established protocol was adapted(Whitney et al., 2003) in an effort to determine whether cannabinoid exposure interfered with caspase-3 activation in zebra finch NCM following novel song exposure. Two birds were exposed to song, while one bird was exposed to continued silence. Birds were injected with either 3mg/kg WIN 55212-2 (WIN) or vehicle in the morning, thirty minutes before lights on. Naïve animals were exposed to a 10 minute song playback loop consisting of 15 seconds of a 5 second novel birdsong bout played three times back-to-back, followed by 45 seconds of recorded silence. This presentation was repeated for a total of 10 times. Immediately after 10 minutes of song exposure, birds were quickly anesthesized with an Equithesin overdose (0.05ml), and brains perfused with buffered saline, followed by 4% paraformaldehyde. Brains were submerged and left overnight in 4% paraformaldehyde, and stored in a 20% sucrose solution.

Activated Caspase-3 Immunohistochemistry

An antibody directed against the large fragment of caspase-3 resulting from cleavage (17 kDa) was purchased from Cell Signaling Technology (Danvers, MA). All serums,

secondary antibodies, and reagents used for immunohistochemistry were purchased from Vector Laboratories (Burbank, CA). The telencephalon was blocked at its lateral edge and sectioned at 30um, using a vibrating blade microtome (Leica Microsystems, Newcastle United Kingdom). Tissue was incubated in a 1% H_2O_2 solution for 30 minutes, followed by a 35 minute block with 5% normal goat serum in 0.3% Triton-X-100, and incubated overnight in antibody (1:3000 dilution). Tissues were rinsed in PBS the following day, and incubated in biotinylated secondary antibody solution (1:3000 dilution). Avidin/Biotin-HRP solutions were prepared as indicated by the instructions (Vector ABC *elite*), and reactivity was visualized with DAB solution. Tissue was mounted onto slides coated with 0.3% bovine gelatin, and allowed to dry. Slides were dehydrated in graded concentrations of ethanol (70%, 95%, and 100%) for 30 seconds each, followed by incubation in xylenes for 1 minute. Coverslips were immediately placed on slides with Permount.

Optical Density Measurements and Statistical Analyses

Punctate and neuropil staining was visualized using an Olympus BX51 microscope; Images were captured with a Spot Insight QE digital camera and Image-Pro Plus software (Media Cybernetics, Silver Spring MD) under identical exposure conditions. Using Image-Pro Plus software, these images were converted to 8-bit grayscale, and areas of interest were traced manually. Data pertaining to Field L, a primary auditory region were reported as a ratio of mean optical densities in Field L, as compared to mean optical densities in tissue adjacent to this area (NCM). The optical densities of treatment groups were reported relative to both vehicle and untreated animals +/- standard error of the mean. Data pertaining to NCM were reported as the mean number

of reactive nuclei per mm^2 of NCM; these data were compared across all 3 treatment groups as well. All labeling quantification was made without knowledge of experimental treatments. Data analyses were performed using Graph Pad Prism and Microsoft Excel PC software.

RESULTS

Under the treatment conditions, statistical analyses failed to detect significant differences between the numbers of immunoreactive nuclei in the NCM of either untreated, vehicle or cannabinoid treated groups. However, a one way ANOVA revealed that disparities between measured optical densities in Field L and NCM of untreated animals were significantly greater than differences between Field L and NCM of both vehicle and cannabinoid-treated groups ($F_{(2,114)} = 40.71$, $p = 0.0001$). Mean optical densities decreased from 1.070, $p < 0.05$ for untreated groups, to 1.018 and 1.012, $p<0.05$ for vehicle and WIN treated groups, respectively.

DISCUSSION

Overall, our results strongly suggest that the methods employed in these experiments are not reliable for accurately assessing whether cleaved activated caspase-3 is induced to levels comparable to previous reports in the NCM following 10 minutes of stimulation with a novel song (Huesmann and Clayton, 2006). While we acknowledge that a portion of data collected bore weak statistical significance, we speculate these differences between antibody staining intensities in auditory Field L of untreated and treated groups are most likely due to differences in tissue handling. Concomitantly, the

hypothesized manner in which cannabinoids may interact with activated caspase-3 to decrease song-induced habituation in zebra finches remains to be seen.

It is likely that following one or a combination of several procedures in this study that differed from previously reported methods used to obtain similar data has led to deviations from expected results. Foremost, selection of more appropriate controls for our experiments will lead to the means to make more accurate comparisons. Adding a negative control group, in which naïve birds are exposed to 10 minutes of silence during the time in which birds in treatment groups are exposed to song will allow us to accurately assess whether 10 minutes of song exposure induces activated caspase-3 levels above the baseline in our hands, as is reported in the literature. In addition, creating a more "novel" song recording may increase the probability of inducing adequate levels of caspase-3 expression. A number of researchers report using novel song recordings consisting of 5 seconds of song from three different conspecific males, played in sequence. The duration of this presentation is 15 seconds, separated by 45 seconds of silence, and thus each 1 minute of presentation corresponds to 15 seconds of song. Although currently there is little criteria available for determining the novelty of perceived song in each individual case this method may in turn decrease the likelihood that the animals will habituate to recorded song loops early. Activation of caspase-3 levels in NCM following song stimulation is a transient event. Prolonged maintenance of cytoplasmic caspase-3 levels is presumably self-destructive to the neuron, thus rapid, local activation, followed by deactivation via sequestration is a necessary event (Mattson et al., 1998). During sessions in which animals are exposed to song, activated caspase-3 levels begin to rise significantly at 2 minutes, peak at 10 minutes, and then

rapidly decline to baseline levels around 20 minutes. Our procedure mandated that birds be anesthetized, and perfused with buffered saline followed by 4% paraformaldehyde. With this approach, starting from the moment at which animals received Equithtesin injections, brain processing time averaged around 30 minutes, thus likely preventing us from capturing peak levels of enzyme activation. Perhaps utilizing more rapid techniques for capturing/processing tissue, such as using a gaseous mixture of 5 % isofluorane mixed with 95 % oxygen, or quickly decapitating the bird, dissecting the tissue of interest, and snap-freezing in cold ethanol will allow for better preservation of the signal (Huesmann, 2005). In our experiments, an antibody directed against active caspase-3 was used in an attempt to directly measure signal induction in NCM; however, several problems with this method have been reported. Due to the nucleated structure of the avian forebrain, especially the NCM, neurons are anatomically organized into clusters, or “micro-nuclei” that can make visually distinguishing between labeled and non-labeled cells extremely challenging. For example, Huesmann et al. report that upon titratrating the antibody to obtain optimal concentrations and observing a significant difference between groups, an unusually high amount of background staining was still present in the region. Alternatively, the authors used a biotinylated amino-acid short peptide (biotin-DEVD-cho) known to specifically bind to the substrate recognition pocket of cleaved activated caspase-3 in its tertiary folded form, and observed significantly lower background staining(Huesmann and Clayton, 2006). Perhaps applying this method of epitope detection in concert with the aforementioned strategies will aid in yielding more accurate results in our future experiments.

APPENDIX D: Notch1 Experiments

ABSTRACT

Traditionally, Notch receptor signaling is regarded as among the most essential constituents of mechanisms known to regulate vertebrate CNS development. However, because of significant advances in genetic and molecular neuroscience, it is becoming increasingly clear that Notch signaling possesses more integrative roles in controlling adult neural morphology and synaptic plasticity than previously thought of. Notch1 is dynamically regulated by the immediate-early gene Arc in response to changes in activity at the synapse induced by novel stimulus learning; this action is required for the synaptic plasticity necessary for memory formation. Through previous work in adult zebra finches, we identified a strong causal relationship between acute cannabinoid reduction in dendritic spine density changes that normally occur during learning, and a proportional acute cannabinoid-reduction in activity-induced Arc protein expression after presentation of a novel song stimulus. While both studies suggest clear roles for context-dependent Notch1 signaling and CB_1 in events necessary for sensorimotor learning and proper memory acquisition, it remains unclear whether these two proteins interact with Arc or other known plasticity genes that disrupts learning-related dendritic spine plasticity. Using the zebra finch song-stimulus auditory habituation model, we aim to determine whether activity-induced Notch1 signaling is required for plastic changes within NCM neurons during novel stimulus learning. Furthermore, we aim to explore whether a relationship exists between the morphological and behavioral effects of inappropriate cannabinoid receptor agonism, and the consequences of cannabinoid-disruption of Notch1 activity during auditory stimulus presentation.

INTRODUCTION

Normal brain development is a multi-faceted process that requires precise timing of neural growth and differentiation programs, and Notch signaling is a well-known master regulator of these events. Originally discovered and cloned from *Drosophila Melanogaster,* the Notch locus is categorized within as a neurogenic gene, a homozygous mutation that results in hyperproliferation of neural tissue required to determine neural fate, along with Notch ligands *Delta,* and *Jagged* (Lehmann et al., 1983; Wharton et al., 1985). In evolutionary terms, the Notch signaling pathway is a highly-conserved system present in almost all multicellular organisms, known for mediating communication in events including regulation of angiogenesis, cardiac valve homeostasis, the transformation of common lymphoid precursors to active T-cells, and many others (Laky and Fowlkes, 2008; Liu et al., 2003; MacGrogan et al., 2011). Spanning the cell membrane in a single pass, these integral membrane receptors possess the uncommon ability to communicate via juxtacrine signaling, and consist of a Notch extracellular domain (NECD) and a Notch intracellular domain (NICD) that function primarily as two distinct functional entities. In more specific terms, these receptors possess a mechanism of action in which the extracellular domain acts as a regulatory element involved in ligand binding; the action of ligand binding to the receptor triggers proteolysis of the intracellular domain (the “business end” of the receptor), which eventually enters the cell nucleus and alters gene expression (Lardelli et al., 1995; Munro and Freeman, 2000).

In the literature, Notch receptor signaling has been mostly regarded in the context of cell fate specification, and progenitor cell regulation during early prenatal

development. However, a growing body of evidence has also identified a non-canonical role for at least one receptor subtype, Notch receptor type 1 (Notch1) in postnatal and adult nervous systems (Groot et al., 1990). These include such frequently occurring events as compartmentalized dendritic spine plasticity in mature neurons following integration of sensory stimuli, and long term memory formation (Ge et al., 2004; Presente et al., 2004; Sakai and Kitamoto, 2006). Based on previous evidence that Notch1 regulates axon outgrowth, and that it continues to be expressed at high levels in adult neurons, many have speculated that Notch1 may regulate dendritic extension as well (Berezovska et al., 1998). Accordingly, a recent series of exciting studies have emerged within the literature that confirm that in addition to nuclear expression, both Notch1 receptor and ligands are densely expressed within postsynaptic densities of CNS neurons (Franklin et al., 1999). In young developmental cortical cells, Notch1 receptor signaling has been shown to mediate dendritic arborization and outgrowth (Costa et al., 2003; Wang et al., 2004). However, up-regulation of Notch1 results in a decrease in dendritic growth in these cells (Berezovska et al., 1999; Redmond et al., 2000; Sestan et al., 1999). In addition, mature cortical neurons that heavily express Notch1 exhibit very little dendritic growth, and pharmacological inhibition of these receptors promotes dendritic extension (Redmond et al., 2000; Sestan et al., 1999). Based on this data, a number of labs have begun to alter their view of Notch signaling in mature neurons as a potential molecular regulator of communication between individual synapses; indeed, several manipulation experiments of Notch1 have shown that Notch receptor signaling is heavily involved in neuronal circuit maturation during LTP and LTD, and suggest that Notch1 signaling in mature cortical neurons promotes dendritic

branching while simultaneously inhibiting dendritic extension (Redmond et al., 2000). Taken together, this information demonstrates a regulatory role for Notch signaling in CNS plasticity throughout life; it appears that in mature neurons, activity-induced formation of new synapses between dendritic spines up-regulates Notch activity while acting as a tonic inhibitor of dendritic growth.

Continuing with the notions that Notch1 is localized at postsynaptic densities of mature postnatal neurons, and that Notch1 signaling is involved in mediating plastic changes at this level, others have since begun to explore the relationship between Notch1 signaling and the expression of induced immediate-early genes in response to direct synaptic activation. Using an antibody that recognizes the cleaved intracellular domain of Notch1 (NICD1, S3 fragment), researchers were able to demonstrate that activated Notch1 receptors and the immediate-early gene Arc are present at the same activated synapses within layer V of the rat somatosensory cortex (Alberi et al., 2011). Not only does Arc positively regulate γ-secretase-mediated cleavage of Notch1 NICD from NECD in somatosensory neuronal cultures, (a significant reduction of NICD1, S3 fragment was observed in Arc mutants), but it is required for the activity-induced recruitment of Notch1 signaling at the synapse (Alberi et al., 2011). Furthermore, activity-induced Notch1 signaling promotes plasticity-associated spine density increases on hippocampal CA1 pyramidal dendrites, and the genetic deletion of Notch1 during postnatal development leads to altered CA1 dendritic spine morphology, and a 25% reduction in spine densities of the very same neurons (Alberi et al., 2011).

In essence, the Notch pathway is often regarded as an early prenatal developmental pathway, but many components of Notch signaling are expressed and

active in the postnatal and adult brain. Similar to what is seen in studies in which CB_1 receptor activity is altered, both genetic and pharmacological manipulation of Notch1 receptor signaling results in persistently altered neuronal morphology and behavior that parallel in comparison; specifically, in instances where CNS CB_1 receptor activity is inappropriately increased, or postsynaptic Notch1 receptor activity is decreased, short-term memory is spared, whereas long-term memory remains persistently impaired. In vitro and in vivo, pharmacological activation of central CB_1 receptors and inactivation of Notch1 receptors during postnatal development negatively impacts dendritic spine densities and morphology through Arc-dependent mechanisms (Alberi et al., 2011; Gilbert and Soderstrom, 2011). Given that activity-regulated neuronal Notch1 signaling is heavily dependent upon Arc expression, and that acute cannabinoid administration disrupts Arc-dependent changes in dendritic spine densities during sensory integration, we have hypothesized that in a cascade disruptive to learning-related dendritic spine plasticity. By virtue of these facts, we have developed the hypothesis that cannabinoid administration disrupts novel song-induced Notch1 receptor activity and neuronal morphology within zebra finch NCM through an Arc-dependent mechanism, as indicated by a significantly reduced expression of NICD1 S3 fragment, and a lack of change in dendritic spine densities that persists following novel stimulus exposure. We also hypothesize that proper functioning and interaction of these two receptors, given their ubiquitous nature, is essential to normal neuronal development and performance throughout life. This theory was tested through the experiments listed below.

MATERIALS AND METHODS

Reagents

Except where noted, all materials and reagents were purchased from Sigma (St. Louis, MO), or Fisher Scientific (Pittsburgh, PA). RNA isolation solution was purchased from Fluka Chemicals (St. Louis, MO). cDNA synthesis, molecular cloning and PCR reagents were purchased from Invitrogen Laboratories (Grand Island, NY). Equithesin was prepared from reagents (40 % propylene glycol, 10 % ETOH, 5 % chloral hydrate, 1 % pentobarbital). The synthetic cannabinoid agonist WIN and antagonist SR141716A were suspended in vehicle from concentrated DMSO stocks (10 mM). Vehicle consisted of a suspension of 1:1:18 DMSO:Alkamuls EL-620 (Rhodia, Cranberry, NJ):phosphate-buffered saline.

Animals

As with the Arc protein expression experiments, the subjects to be used in these experiments will be adult male zebra finches bred and raised in our aviary. Before the start of behavioral experiments, animals will be singly housed with free access to water, grit, mixed seeds (Sunseed VitaFinch) and provided multiple perches. Animals will be maintained on a 14:10 light/dark cycle, and room temperature was maintained at 78° F.

Cloning of Zebra Finch Notch1 Receptor

No known reports of sequenced Notch1 gene in zebra finches exist thus far, so we attempted to clone a cDNA fragment of Notch1 from whole male zebra finch brain RNA using degenerate primers, and reverse transcriptase-polymerase chain reaction (RT-PCR). Whole zebra finch brain RNA was lysed and purified using a denaturation solution for the isolation of RNA (Fluka Chemicals, St. Louis, MO). Following this, we used a SuperScript III First-Strand Synthesis System for RT-PCR to prime isolated RNA

with Oligo$(dT)_{20}$ in an effort to select for mRNA with poly-A 3' tails; this product was then reverse transcribed into cDNA. The mixture was then incubated at 50° C for 50 minutes, and then reaction terminated at 85° C for 5 minutes. 1 µl of RNAse H was added to the mixture, and allowed to incubate for another 20 minutes at 37° C. The zebra finch Notch1 gene was amplified by using a mixture of two sets of degenerate primers to conserved regions of the known coding sequences from human, rat, chicken, and African Tree frog in the NCBI protein database (accession numbers NP_060087.3, NP_001099191.1, XP_415420.2, and NP_001090757 respectively). The forward oligo DNA primers were named "ZFN15A" (5'-ATGGAATTCATGGAYGAYAAYCAR-3'), "ZFN15B" (5'- ATGGAATTCCARTGGACNCARCARCAW-3'), "ZFN13A" (5'-ACDATRTCSTGSTGCATAAGCTTCAT-3'), and "ZFN13B" (5'-TTRTTYTGCATRTCYTTAAGCTTCAT-3'). PCR thermocycling conditions were performed in tubes containing 1X PCR buffer as follows: PCR initialization at 95° C for 4 minutes, and then the following three steps were repeated in sequence for a total of 25 times: denaturation at 95° C for 45 seconds, annealing at 50° C for 1 minute, and extension/elongation at 72° C for 25 seconds. The PCR reaction was then exposed to a final elongation at 72° C for 7 minutes, and then held at 4° C until further use. A portion of the PCR products were examined on 1.75% agarose-TAE gels to confirm product existence and sizes. Following this, PCR products were subcloned into the pCR 2.1 TOPO plasmid, and transformed into chemically-competent One-Shot TOP10 E.coli cells. Plasmid minipreps were performed to isolate DNA, and the inserted cDNA sequence was sequenced from the 5' and 3' ends by the East Carolina University Genome Sequencing Core Laboratory. In order to confirm what had been cloned,

sequences were BLAST searched against other known Notch1 sequences within the NCBI Nucleotide database, however little homology was found.

The following experiments are to be performed once the zebra finch Notch1 receptor has been cloned:

Acute and Chronic Behavioral Experiments

Three days prior to the start of experiments, birds will be housed singly in visual and auditory isolation in soundproof recording chambers. Since it has been shown that in cortical neurons, activity-induced Notch1 signaling requires the induction of Arc, the method that will be used to promote activity-induced Notch1 receptor activity (cleavage of NICD1, S3 fragment) within zebra finch auditory telencephalon will be similar to that employed for Arc mRNA induction. In order to explore the kinetics of Notch1 activation, animals will be exposed to a tape recording of thirty minutes of novel conspecific song, and killed after varying survival intervals. The novel song used consists of a collection of five second song bouts from three adult male birds whose song will be unrecognizable to experimental animals. Song playbacks will be presented in a fifteen-second medley, followed by forty-five seconds of silence, for a total of a one minute block. This procedure will be repeated for a total of thirty times. Un-stimulated control groups will be exposed to silence, and killed after varying survival intervals that parallel with experimental conditions.

In experiments that involve drug injections, because of the pharmacodynamic properties of WIN within the zebra finch, treatments will be administered thirty minutes prior to the playback of song stimuli. A similar protocol previously established during experiments

involving Arc protein induction will be used here in an effort to determine whether WIN treatment would acutely disrupt activity-induced Notch1 receptor activity and molecular habituation to repeated presentations of the same song over the course of three days. Animals will be scheduled to receive a single intramuscular injection of WIN (3mg/kg), SR141716a (6mg/kg), or vehicle via intramuscular injection, thirty minutes before the start of song presentation. Silent controls will be exposed to the same drug regimen. On the third day, all groups will be given a single intramuscular injection of vehicle. Animals will be exposed to the same survival intervals as in the acute experiments above, and given an overdose of Equithesin (50 µl), and brains prepared for in-situ hybridization experiments.

Developmental Treatments

In order to determine whether daily exposure to a cannabinoid agonist during sensorimotor learning will enduringly influence Notch1 receptor activity after novel song presentation later in adulthood, once daily 50 µl injections of either vehicle or WIN (1mg/kg) will be administered into the pectoralis muscle in the morning, thirty minutes before lights on for 25 consecutive days, starting at 50 days of age, and ending at 75 days. We have previously demonstrated that these daily cannabinoid treatments given during the zebra finch sensorimotor learning period from 50 to 75 days persistently alter vocal development and stereotyped song production (Soderstrom and Johnson, 2003). Following the completion of experiments, animals will be allowed to mature to at least 110 days of age in visual isolation. In order to further validate previous findings of persistently altered song in the developmental WIN-treated animals, single birds will be isolated in soundproof chambers, and then recorded. Ten complete song bouts from

each treatment unit (WIN/50-75 days, vehicle/50-75 days) were randomly selected from a collection of recordings taken over the course of seven days. After recordings, animals will be killed by Equithesin overdose, and brains prepared for immunohistochemistry. After analysis of this developmental experiment, and determination of a significant treatment effect, a second experiment will be performed using adult animals, in order to assess the developmental dependence of treatment effects. The adult experiment will be done employing the same regiment of 25 daily treatments given to adult animals that had already learned song.

In-Situ Hybridizations

After behavioral treatments, animals will be transcardially perfused with 1x PBS, followed by phosphate-buffered 4 % paraformaldehyde [pH = 7.0]. Birds will then be decapitated, brains dissected and transferred to an ice-cold solution of phosphate-buffered 4 % paraformaldehyde overnight. Brains will be blocked down the midline and sectioned immediately using a Vibratome. Sections will be collected into an ice-cold 2X SCC solution (0.3 M NaCl, and 0.03 M $Na_3C_6H_5O_7$) prepared with DEPC-treated water. Sections will then be re-suspended in pre-hybridization buffer (50% formamide, 10% Dextran Sulfate, 2X SSC, 1X Denhardt's Solution, 0.5M DTT, and 0.5mg/ml denatured salmon sperm DNA) and incubated for one hour at 48°C. radiolabeled riboprobes synthesized from cloned cDNA fragments will be added to hybridization reactions, and reactions incubated overnight at 48C°. The following morning, sections will be washed in decreasing concentrations of 1X SSC. Negative controls will contain the experimental reactions, but will have an additional 100 µg of RNase A added. In order to detect signal, slide mounted sections will be coated with a photographic emulsion

(Hypercoat LM-1 from Amersham BioSciences), and allowed to incubate at 4° C, for a total of three weeks. After developing with Ilford Hypam fixer and Phenisol developer (AEH Business Solutions), the autoradiograms are to be counterstained with 0.1% thionin and coverslipped with Permount. Mounted tissues will be examined by microscopy, as performed in immunohistochemical experiments.

Optical Density Measurements

Hybridization reactions are to be examined in various brain regions at 40X, 100X, and 1000X using an Olympus BX51 microscope with Nomarski DIC optics. Images will be captured using a Spot Insight QE digital camera, and Image-Pro plus 5.0 software (MediaCybernetics, Silver Spring, MD). It is important to note that images may not be captured under identical, calibrated exposure conditions, due to the fact that with in-situ hybridization techniques, not every photon that reaches the camera can be converted into measurable output. In order to mitigate this issue, images will be background corrected, converted to 8-bit gray scale, an optical density measurements acquired for each region of interest. These measurements will then be transformed into percentages of the maximal mean optical densities determined across all age groups and brain regions examined.

RESULTS

Cloning of the Zebra Finch Notch 1 Receptor

A 963 base-pair fragment of the zebra finch Notch1 receptor was successfully amplified via polymerase chain reaction with primers ZFN15A and ZFN13A (see Figure

AD1.). We are currently working to subclone this fragment into the PCR 2.1 TOPO vector in an effort to verify sequence integrity.

Figure AD1. Electrophoretic analysis of PCR products generated in an effort to clone ZFN1.

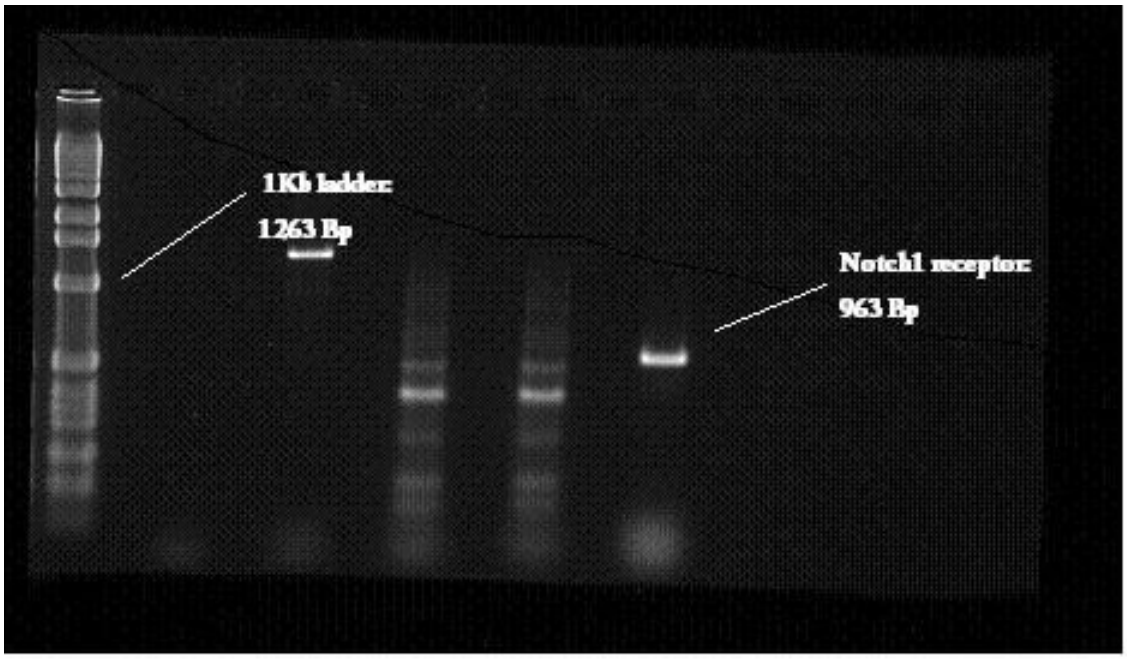
1Kb ladder
1263 Bp
Notch1 receptor
963 Bp

APPENDIX E: General Materials and Methods

In-Silico Cloning

In an attempt to isolate cDNA sequences contained within genes of interest, specific zebra finch ESTs were located within Genbank by accessing the Nucleotide database, or for cases where cDNA sequences were unknown, the Protein database (http://www.ncbi.nlm.nih.gov/). Following this, the ESTs were BLASTed against the zebra finch genome, and the genomes of other species (specifically human, rat, and chicken) in order to determine an adequate level of specific alignment and sequence homology (usually between 85 % -100 % sequence homology).

Following this procedure, NEBcutter V2.0 was used to locate all non-overlapping ORFs within the target sequence (http://tools.neb.com/NEBcutter2/). The program included the genetic sequence of E.Coli with our chosen oligonucleotide sequence, and used all commercially available type II restriction endonucleases to cut the resulting product wherever possible (Vincze et al., 2003). Only type II restriction endonucleases available from New England Biolabs were used by the program to cut oligonucleotide sequences, so special care was taken to only use restriction endonucleases from New England Biolabs (Beverly, MA) to physically digest DNA products. Sequences that proved interesting after these in-silico procedures were then physically cloned at the bench.

Gene-Specific Primer Design

A target segment of DNA was chosen from the zebra finch genome to amplify. Primers were designed in an effort to clone into mammalian expression plasmid vectors (either PCDNA 3.1+ or p Tracer cmv/bsd), and so the following steps were taken: Type II restriction endonuclease sites were selected from those sites available within the multiple cloning site designed within the vector that were not present in the target cDNA coding sequences (i.e., those restriction endonucleases identified as present within the cDNA sequence by the NEBcutter V2.0 program were NOT chosen). When designing 5' end cDNA primers, a Kozak consensus sequence was added to the first 19 bases chosen from the 5' end of the target sequence segment. Following this, a spacer and a restriction site were added to the beginning of the new 5' end. To make 3' end cDNA primers, the last 19 or so bases were chosen from the 3' end of the target sequence segment to be cloned. Due to primer ordering requirements, and the fact that all sequences are read from 5' to 3' end, the corresponding complement of this sequence was reverted, and both a restriction site and a spacer were added to the new 5' end. What resulted were to primer sequences that resembled this pattern:

Forward: 5'-SPACER-RESTRICTION SITE-KOZAK-19 BASE cDNA TARGET SEQUENCE-3'

Reverse: 5'-SPACER-RESTRICTION SITE-18 BASE REVERTED COMPLEMENT of cDNA TARGET SEQUENCE-3'

Traditional RACE Cloning

Total RNA Isolation

The following methods were adapted from protocols provided by Life Technologies (Grand Island, NY), and methods derived by Chomczynski (1993), and colleagues (Chomczynski, 1993; Chomczynski and Sacchi, 1987). All products and plasticware used were either cleaned with RNAse Away (Sigma), rinsed with DEPC-

treated water, or were RNase/DNase-free as purchased. Zebra finches were anesthetized, decapitated, and brains rapidly dissected. Distinct regions of interest were quickly isolated on an ice-cold weighing tray, weighed, and added to a polypropylene centrifuge tube. 1 ml of denaturation solution for the isolation of RNA, or TRIzol reagent per 50 mg of tissue sample. Tissue was then ground on ice to homogeneity using a glass and Teflon homogenizer. Since brain tissues isolated contained a high content of fat, additional measures were taken to remove all insoluble material from the samples. Following homogenization, the samples were microcentrifuged at *12,000 x g* at 4 ° C for 10 minutes. This results in a separation of the sample into three distinct layers: A pellet containing the extracellular matrix, polysaccharides, and high-molecular weight DNA, a clear supernatant containing RNA nucleoprotein complexes, and a fatty layer above the supernatant. Special care was taken not to disrupt the layers as the middle clear supernatant was pipette out, and placed into fresh DNAse/RNAse-free microcentrifuge tubes. In order to commence phase separation, the supernatant was incubated for 5 minutes at room temperature, in order to permit complete dissociation of the nucleoprotein complexes. 0.2 ml of chloroform per 1 ml of denaturation solution for the isolation of RNA used for homogenization was added to the mix, and tubes were sealed tightly and vortexed for a minimum of 30 seconds. The mixture was allowed to incubate at room temperature for an additional 3 minutes, and then was centrifuged at *12,000 x g* for 15 minutes at 4° C. Of the three phases the mixture separated into (a lower reddish organic phenol-chloroform phase, an opaque interphase, and a colorless upper aqueous phase), the RNA-containing upper aqueous phase was drawn out, all while being careful not to disrupt the other phases. The aqueous phase was then placed into

a fresh DNase/RNase free microcentrifuge tube. An equal volume of 100 % isopropyl alcohol was added to the aqueous phase (approximately 0.5 ml of isopropanol per 1ml of reagent used for homogenization); this mixture was shaken vigorously, and then allowed to incubate at room temperature for 10 minutes. Following this, the mixture was again microcentrifuged at *12,000 x g* at 4° C for 10 minutes. At this stage, the RNA formed a gel-like pellet inside the bottom of the tube. Supernatant was discarded and the resulting pellet was washed in 1 ml of 75% EtOH/DEPC-treated water per 1ml of reagent used for initial homogenization. The sample was vortexed briefly, microcentrifuged at *7500 x g* at 4° C for 5 minutes, and wash discarded. This process was repeated a total of 3 times. The resulting washed pellet was air dried for 10 minutes and either resuspended in a known volume of RNase-free water, or stored as a 100 % EtOH precipitate at -80° C. RNA yield was determined by spectrophotometric analysis at an absorbance value of 263 nm.

First Strand cDNA Synthesis

The following method was adapted from protocols provided by the Invitrogen SuperScript™ III First-Strand Synthesis System for RT-PCR (Cat. No. 18080-051), and molecular cloning handbooks (Sambrook and Russell, 2001). In all cases, isolated total RNA preparations were used to synthesize first-strand cDNA. The following reagents were mixed, briefly centrifuged, and combined in a 0.5 ml tube:

Component	Amount Per Reaction
5 µg of total RNA	*Volume varies with RNA yield*

50 μM oligo$(dT)_{20}$ OR	1 μl
50 ng/μl random hexamers	
10 mM dNTPs	1 μl
DEPC-treated water	QS to 10 μl

Centrifuge tubes were incubated at 65° C for 5 minutes, and then placed on ice for at least 1 minute, while the following components were mixed together to create 10μl cDNA synthesis mix. Special care was taken to ensure each component was added in the following order:

Component	Per Reaction	Per 5 Reactions
10X RT buffer	2 μl	10 μl
25 mM $MgCl_2$	4 μl	20 μl
0.1 M DTT	2 μl	10 μl
RNaseOUT™ (40 U/ μl)	1 μl	5 μl
SuperScript™ III Reverse Transcriptase (200 U/ μl)	1 μl	5 μl
Total:	10 μl	50 μl

10 µl of cDNA synthesis mix was added to each RNA/primer mixture, mixed gently, and collected by brief centrifugation. Oligo$(dT)_{20}$-primed mixtures were then incubated at 50 ° C for 50 minutes, and reactions terminated by incubating at 85° C for 5 minutes. Random hexamer-primed mixtures were incubated at 25° C for 10 minutes, then at 50° C incubation for 50 minutes, followed by reaction termination at 85° C for 5 minutes. After reaction termination, tubes were chilled on ice. After ice-cold, reactions were collected by brief centrifugation, and 1 µl of RNase H was added to each tube, and incubated for 20 minutes at 37° C. cDNA synthesis reactions were then either used for PCR immediately, or stored at -20° C for later use. Occasionally, unexpected issues arose using this method of cDNA synthesis, so the following steps were taken to troubleshoot/correct the problem(s):

Problem	Solution
No bands after electrophoretic analysis of PCR products	Use positive control RNA to verify the efficiency of the reaction
Inhibitors of reverse transcriptase present	Remove possible inhibitors by 70 % EtOH/DEPC-treated water wash, followed by 100 % EtOH precipitation of RNA preparation. Resuspend in RNase-free water.

PCR Amplification of DNA

PCR reactions were performed in 0.2 ml RNase/DNase-free tubes, in a total volume of 50 µl. Oligonucleotide primers were synthesized by Invitrogen (Grand Island, NY). Primers were reconstituted in sterilized 10mM Tris, pH = 8.0 at a final working

concentration of 10 µM. For every combination of forward and reverse primers run as a sample reaction, a positive control reaction (template cDNA + primers demonstrated to amplify target sequence), and a negative control reaction (forward and reverse primers included in the sample reaction, no template cDNA) were included. The following components were mixed together to create PCR reactions. Special care was taken to ensure each component was added in the following order:

Reagent	Negative Control (-)	Positive Control (+)	Reaction ($R_{1,2...x}$)
Sterile water	40.5 µl	40 µl	40 µl
10X Polymerase Buffer	5 µl	5 µl	5 µl
dNTPs	1 µl	1 µl	1 µl
Forward (5') primer	0.5 µl	0.5 µl	0.5 µl
Reverse (3') primer	0.5 µl	0.5 µl	0.5 µl
cDNA template	----	0.5 µl	0.5 µl
$MgCl_2$*	2 µl	2 µl	2 µl
Polymerase -*Taq* -*Vent***	0.5 µl	0.5 µl	0.5 µl
Total:	50 µl	50 µl	50 µl

* The efficiency/success of many of my PCR reactions have been contingent upon the concentration of divalent cations (here seen in the form of $MgCl_2$) used in the PCR reaction. I found it advantageous to perform a quick $MgCl_2$ concentration optimization in half-log units (from 0.3mM to 3mM).

** When sequence fidelity was of the upmost importance, Vent polymerase was preferred for use over Taq/Platinum Taq; not only does Vent possess a 5X higher fidelity than Taq/Platinum Taq, but these polymerases possess 5' → 3' exonuclease activity, whereas Vent possesses 3' → 5' proofreading activity.

Reactions were synthesized on ice, immediately placed into a prewarmed thermocycler (set at 94° C), and reactions run for an indicated amount of time dictated by the number and length of each cycle. When using Vent to amplify DNA products for TA subcloning, an additional step was added to the PCR procedure. As amplification with Vent produces blunt ended PCR products, 1 µl of Taq was added to each reaction, and reactions were allowed to incubate at 72° C for an additional 15 minutes in a final A-tailing step before returning to the holding temperature of 4° C.

Occasionally, unexpected issues arose during PCR amplification, so the following steps were taken to troubleshoot/correct the problem(s):

Problem	Solution
Annealing Temperature sub-optimal	Run a temperature gradient in 2° C increments
dNTP stocks degraded	dNTPs are very susceptible to freeze-thawing. Use fresh aliquots only, and discard after one-time use.

PCR reaction contamination	Always check negative control for bands
cDNA template degraded	Aliquot cDNA to minimize freeze-thawing. Run an aliquot on an agarose gel to check integrity.

TA cloning of Taq-Amplified PCR Products

TOPO Cloning Reaction

Taq-amplified PCR products were subcloned into a linearized vector containing single overhanging 3'-deoxythymidine residues covalently bonded to Topoisomerase I. This modification allows PCR product inserts with A-tails to efficiently ligate into the vector (Puck et al., 1958). A total of 6 µl of TOPO cloning reaction was set up for eventual transformation into chemically-competent DH5-α E. coli cells. Reagents were mixed together in a clean 0.5 ml centrifuge tube at room temperature.

The reaction was gently mixed, and allowed to incubate for an additional 15 minutes at room temperature. The reaction was then placed on ice, until ready to be transformed into chemically competent cells. NOTE: reactions were never stored at -20° C overnight, for further use.

Transforming Chemically-Competent DH5-α E. coli Cells

Vials of One Shot™ Chemically-Competent DH5-α E. Coli Cells were retrieved from -80° C, and thawed on ice. A total of 2 µl of the TOPO cloning reaction (see above) was added to a pre-chilled 1.7 ml microcentrifuge tube, and a 25 µl aliquot of chemically-competent cells were gently pipetted onto the reaction, while taking special care to keep the reaction ice-cold. Optimal transformation conditions were set up such

that the TOPO cloning reaction was ~10 % of the total volume. A 25 µl aliquot of chemically-competent cells transformed with pUC 19 DNA served as a positive transformation control, and a 25 µl aliquot of chemically-competent cells incubated without the TOPO cloning reaction served as a negative transformation control in these experiments. Following reaction setup, the cells were incubated on ice for an additional 30 minutes. Next, the reactions were heat shocked in a 42° C water bath for a total of 30 seconds, then returned to ice for 2 minutes. Then, 200 µl of room temperature S.O.C medium was added to reactions, tubes capped tightly, and reactions then shaken horizontally at 200 rpm at 37° C for 1 hour. While reactions were shaking, LB/Amp-agar plates were pre-warmed in a hybridization oven at 37° C. Just before reactions were finished shaking, pre-warmed plates were spread with 40 µl of X-Gal (40 mg/ml, dissolved in N, N-Dimethylformamide) until dry, to allow for blue/white screening. Following this, entire ~200 µl reactions were spread evenly with a sterile cell spreader onto the pre-warmed selective plates until dry. Plates were incubated in the pre-warmed hybridization oven at 37° C overnight (or for a minimum of 12 hours). Efficient TOPO cloning reactions produced several hundred colonies per plate. The next morning, 2-4 well-separated white colonies were picked with sterile pipette tips for analysis.

Isolation of Plasmid DNA from Bacterial Cultures

The following methods were adapted from Sambrook et al. (2001). Well-separated bacterial colonies picked for sequence analysis were cultured overnight at 37° C, and shaken horizontally at 250 rpm in 1.5 ml of LB broth, containing 50 µg/ml ampicillin (Amresco Biochemicals, Solon, OH). Cultures were decanted into 1.7 ml

microcentrifuge tubes, and spun at *15,000 x g* for 1 minute. Following this, supernatants were carefully decanted into a sterile beaker containing 10 % bleach, and microcentrifuge tubes were inverted onto paper towels to drain and remove drops. Next, pellets were resuspended by pipette in 100 µl of Miniprep Solution I. Special care was taken to ensure no pellet clumps remained. After this, cells were lysed by adding 200 µl of Miniprep Solution II. Microcentrifuge tube caps were closed tightly, and tubes inverted several times to thoroughly mix and create a viscous solution. This solution was allowed to incubate at room temperature for 5 minutes. Next, protein and chromosomal DNA was precipitated from solution by adding 150 µl of Miniprep Solution III. These mixtures were again inverted several times, and then taped to a horizontal shaker and shaken for at least 5 minutes. The suspensions were microcentrifuged at room temperature for 5 minutes at *15,000 x g*, and supernatants removed into a clean 1.7 ml tube, while taking special care to avoid fluffy white precipitate. Microcentrifuge tubes were then placed on ice. Following this, plasmid DNA was precipitated out of solution by adding 2.5 volumes of ice-cold EtOH (approximately 900 µl) to each microcentrifuge tube, mixed vigorously, then placed on ice. Tubes were centrifuged at *15,000 x g* at 4° C, for 10 minutes, and supernatants decanted. Resulting pellets were then washed with two volumes of 70 % EtOH, tubes inverted over a paper towel, and pellets allowed to dry. Pellets were either resuspended in 50 µl of sterile 10 mM Tris, pH = 8.0 containing 30 µg/ml of RNase A, or nuclease-free water. Isolated plasmid DNA was then either stored at 4° C for short-term use, or -20° C for later use.

Restriction Digestion of DNA

Restriction digests of DNA were used for plasmid DNA mapping (to confirm that isolated DNA plasmids were recombinant) and liberation of cloned insert products from vectors in preparation for insert-DNA gel purification. Firstly, the multiple cloning site of the plasmid vector, and specifications used during primer design were used was used to determine which restriction enzymes would liberate cDNA inserts. 20 µl restriction digest reactions were prepared by placing reagents in 0.5 ml microcentrifuge tubes in the following order:

Reagent	Uncut Control	Plasmid + Restriction Endonuclease A	Plasmid + Restriction Endonuclease B	Plasmid + Restriction Endonuclease A and B
Water	14.5 µ	13.5 µl	13.5 µ	12.5 µl
10X RE Buffer	2 µl	2 µl	2 µl	2 µl
BSA*	0.5 µl	0.5 µl	0.5 µl	0.5 µl
R. Endonuclease A	---	1 µl	---	1 µl
R. Endonuclease B	---	---	1 µl	1 µl

Plasmid Vector	3 µl	3 µl	3 µl	3 µl
Total:	20 µl	20 µl	20 µl	20 µl

Reagents were incubated in a hybridization oven at 37° C for at least 1 hour. Restriction digests mixed with 10 % loading dye were run on a 1.5 % agarose/TAE gel with ethidium bromide, and sizes of vector and insert bands were determined by comparison to migration of molecular weight markers (either lambda BST EII marker, or 1 KB DNA ladder (Invitrogen)).

Dephosphorylation of Linearized Plasmid

In instances were the same restriction endonuclease was used to free the DNA insert on both ends of the vector, removal of the terminal 5' phosphate groups on the ends of linearized fragments were used to suppress self-ligation and circularization of plasmid DNA. By removing the 5' phosphate residues from both termini of the plasmid with CIAP, recircularization of DNA is substantially minimized (Sambrook and Russell, 2001). Therefore, in cases where this technique was needed, 4 µl of CIAP was added to every 20 µl of restriction digest reaction, and incubated in the hybridization oven as usual. An additional incubation at 85° C was included at the end of incubation time in order to deactivate CIAP enzymes. This was followed by phenol/chloroform extraction of DNA.

Phenol/Chloroform Extraction of DNA

Occasionally, the DNA isolation methods used would render DNA that was not of a level of purity for restriction digestion analysis. To mitigate this issue, we utilized the properties of polar solvents (water), and non-polar solvents (phenol, chloroform) to separate nucleic acids in solution from protein and cell lysate debris not purified from DNA isolation. Equal amounts of a Phenol:Chloroform:Isoamyl alcohol (25:24:1 v/v) solution was added to the microcentrifuge tube containing a known volume of DNA in water or 10 mM Tris buffer, pH = 8.0. This mixture was emulsified by vortexing for at least 1 minute, followed by a 2 minute centrifugation at room temperature at 14,000 rpm. The mixture separated into three phases, and the upper aqueous layer (aqueous phase) was drawn out, and pipetted into a new tube. DNA was precipitated out of solution by creating a high-salt environment within the aqueous solution in order to disrupt the dissolving properties of water. This was accomplished by adding a volume of 3M NaOAC equal to 10 % of the total solution volume to the aqueous phase, shaking vigorously, adding an additional 2.5 volumes of ice-cold EtOH to the centrifuge tube, then shaking again. This mixture was incubated at -20° C for 1 hour. Following this, the mixture was spun at 4° C for 30 minutes at 14,000 rpm. The resulting pellet was decanted of EtOH, and carefully washed 2 times in 70 % EtOH, at room temperature. Finally, tubes inverted over a paper towel, and pellets allowed to dry. Pellets were either resuspended in 50 µl of sterile 10 mM Tris, pH = 8.0 containing 30 µg/ml of RNase A, or nuclease-free water. Isolated plasmid DNA was then either stored at 4° C for short-term use, or -20° C for later use.

DNA Purification from Agarose Gels

Using an 18 gauge needle, single holes were poked through the lid and base of a 0.5 ml microcentrifuge tube. These tubes were then placed into larger 1.7 ml microcentrifuge tubes in which lids had been removed, and filled 1/3 of the way with a paper slurry filter (made of shredded chromatography paper in sterile 10 mM Tris buffer, pH = 8.0). In order to remove extra buffer, tubes were spun at 14,000 rpm for 3-4 minutes, and residual buffer collected in the larger tube removed and discarded. DNA bands isolated from agarose gel under minimum UV exposure conditions were placed in the tubes containing the paper slurry mixture, and spun for 4 minutes at 14,000 rpm. The resulting eluted DNA was used to transform chemically-competent E.Coli cells, or ligate into linearized plasmid vectors.

Ligation of Target DNA Inserts into Linearized Vectors

The ligations were synthesized at 4° C, in 10 µl reactions. Reagents were added to 0.5 ml microcentrifuge tubes in the following order:

Reagent	Positive Control (+)	Negative Control (-)	Ligation Rxn ($R_{1,2...X}$)
Water	QS to 10 µl	QS to 10 µl	QS to 10 µl
5X T4 DNA Ligase Buffer	2 µl	2 µl	2 µl
Linearized Vector Ratio	1	2 µl	1

Insert Ratio	5	---	5
T4 DNA Ligase	1 unit (sticky ends) 5 units (blunt ends)	1 unit (sticky ends) 5 units (blunt ends)	1 unit (sticky ends) 5 units (blunt ends)
Total:	10 µl	10 µl	10 µl

Reactions were incubated in a 16° C water bath for 24 hours, then placed on ice the following day. Ligated plasmids were then transformed into chemically-competent E.Coli cells.

DNA Sequencing of Results

Plasmid minipreps were performed to isolate DNA, and the inserted cDNA sequence was sequenced from the 5' and 3' ends by the East Carolina University Genome Sequencing Core Laboratory.

Receptor Protein Analysis

Cell Culture

All cell culture dishes/media flasks contained the following components:

- Culture media- designed to allow cells to maintain their normal function. The type of culture media varied depending on the particular cell line.
- Fetal Bovine Serum- Used as a supplement to cell culture media, as it provided a broad spectrum of macromolecules, carrier proteins for lipoid substances and

trace elements, attachment and spreading factors, low molecular weight nutrients, hormones and growth factors cells need in order grow and divide.

- Penicillin/Streptomycin- Used to keep prokaryotic organisms and contamination out of cell culture dishes. Special care was taken to used only the specified amount, as inappropriate levels may kill or alter cell growth.
- Amphotericin B- Antimycotic; Special care was taken to used only the specified amount, as inappropriate levels are known kill or alter cell growth.
- Sodium Bicarbonate- Used as a buffer in cell culture media, as it improved the pH control of cell culture media (cells were incubated in a CO_2 atmosphere that sometimes varied between 5 and 10 %). Sodium bicarbonate was also used as a non-toxic means to provide cells with carbonate ions to aid in general metabolic functions.
- Sodium Pyruvate- Added to cell culture media as an additional source of energy, and to protect against inappropriately high levels of hydrogen peroxide.

The PC12 cell line required the following additional component:

- Coating with either PDL or PLL- Used to enhance cell attachment to plastic and glass surfaces. The tissue culture plastic used in these experiments had a net negative surface charge produced by plasma treatment of the polystyrene (i.e., TC-treated surface). We empirically determined that these cells will grow in suspension without this additional step, but overall, PC12 cultures were dramatically improved by coating the culture surface with positively-charged polymers. In addition to promoting cell adhesion, PLL and PDL is known to enhance the adsorption of serum or extracellular matrix proteins to the culture

substrate (Barnes et al., 1984; Ham and McKeehan, 1979; Letourneau, 1975; McKeehan and Ham, 1976; Poindron et al., 2005; Yavin and Yavin, 1974).

Preparing Cell Culture Media

All media was prepared and cells cultured according to American Tissue Culture Collection guidelines. The following reagents were used to prepare cell culture media for the cell lines used:

Reagent	[Conc.]	Cho-K1	PC12	PC12-Adh	HEK-TN
Culture Media	1X	F-12K, 500 ml	RPMI-1640, 500 ml	F-12K, 500 ml	DMEM, 500 ml
FBS	1X	50 ml	25 ml	12.5 ml	50 ml
Horse Serum	1X	---	50 ml	---	---
HI-Horse Serum	1X	---	---	75 ml	---
HEPES-Buffered Saline (1 M)	1x	---	5 ml	---	10 ml
L-Glutamine (200 mM)	100X	10 ml	10 ml	10 ml	---
P/S	100X	5 ml	5 ml	5 ml	5 ml
Antimycotic	100X	5 ml	5 ml	5 ml	5 ml
Sodium Pyruvate (100	100X	2.5ml	2.5 ml		---

mM)					
Sodium Bicarbonate	1X	---	0.75 g	---	---
Total:		572.5 ml	602.5 ml	607.5 ml	570 ml

Media was prepared before subculturing, and stored at 4° C for a maximum of 1 month, and immediately discarded upon accidental contamination.

Preparing for Subculturing Cells

Thirty minutes prior to the start of subculturing, negative-pressure hoods cell culture dishes, and disposable plasticware were exposed to UV radiation. Cell culture media bottles were incubated at 37° C in a hot water bath. Immediately before subculturing, all materials and reagent bottles were disinfected by wiping down with ample 70 % 2-propanol, and fresh Kimwipes® , lint-free disposable towelettes, and placed under the negative-pressure hood.

Subculturing Cho-K1 Cells

Culture medium was removed and discarded by vacuum filtration. Cell culture flasks were briefly rinsed with 2.0 ml of 0.25 % (w/v) Trypsin- 0.53 mM EDTA solution in order to remove all traces of serum, which contained trypsin inhibitor. Following this, 3.0 ml of Trypsin-EDTA solution was added to the flask, and visualized under an inverted microscope for approximately 3 minutes, until cell monolayer became detached. Occasionally, when cell detachment seemed difficult to facilitate, flasks were placed into a 37° C incubator supplemented with 5 % CO_2 for 4 minutes or until detachment occurred. Following this step, flasks were banged against a hard surface 6

or 7 times, and cells allowed to collect at the bottom of the flask. A known volume of complete growth medium was added to the flask, cells aspirated by gentle pipetting, and then counted using a hemacytometer. Appropriate aliquots of cell suspension were added to new culture vessels (usually at a subcultivation ratio of 1:4), and cultures were returned to incubate at 37° C, supplemented with 5 % CO_2. Medium was renewed every 2 days (Puck et al., 1958).

Subculturing PC12 Cells

Cell suspension was transferred to a sterile centrifuge tube, and remaining cells adhered to the bottom of the plate were removed with 2 ml of Trypsin-EDTA solution. These cells were added to the centrifuge tube as well, and cells centrifuged at *225 x g* for 10 minutes at room temperature. During this time, fresh plates were prepared by adding media to dishes pre-coated with PLL. Afterwards, cell debris and supernatant was discarded by vacuum filtration, and the resulting pellet was resuspended in a known volume of fresh medium by rapid aspiration with a sterile 20 gauge needle, and counted using a hemacytometer. Aliquots of cell suspension were pipette into coated dishes, and swirled carefully to ensure even distribution (usually at a subcultivation ratio of 1:2, or 1:3). Cells were returned to incubate at 37° C, supplemented with 5 % CO_2. Medium was renewed every 3 days, and cells were subcultured when densities reached 4 x 10^6 cells per 1 ml of medium (Greene and Tischler, 1976).

Subculturing PC12-Adh Cells

Old culture medium was removed and discarded by vacuum filtration, starting from the top edge of the media working down, taking care not to scrape the bottom of the flask. Following this, 10 ml of fresh medium, and 1 ml of Trypsin-EDTA solution was

pipetted over the cell sheet, and scraped with a disposable cell scraper. Next, cells were aspirated with a small bore serological pipette to break up clusters and counted using a hemacytometer. Appropriate aliquots of cell suspension were added to either Corning CellBIND® dishes, or dishes manually coated with a hydrophilic, negatively-charged amino acid layer. Cells were seeded at a subcultivation ratio of 1:3, twice weekly. Cells were returned to incubate at 37° C, supplemented with 5 % CO_2.

Subculturing HEK-293TN Cells

Medium was removed from cells, and discarded via vacuum filtration. Cells were briefly rinsed with Trypsin-EDTA solution, in order to remove traces of serum containing trypsin inhibitors. Next, 3.0 ml of Trypsin-EDTA solution was added to the flask, and observed under an inverted microscope for 10 minutes, or until cell layer was dispersed. Trypsin-EDTA solution was aspirated via vacuum filtration, and 10 ml of complete growth medium was added before aspirating cells by gently pipetting. Appropriate aliquots were added to new culture vessels; cells were seeded at a subcultivation ratio of 1:8, and medium was renewed every 3 days.

Cryogenic Preservation of Cell Lines

Media and cell debris were removed from viable cells, either by spinning at *225 x g*, or trypsinizing (see subculturing methods). Cells were resuspended in fresh media, and DMSO was added to the cell suspension to equal a final concentration of 10 %. Cells were counted using a hemacytometer, and suspensions were quickly pipetted into 2 ml cryogenic tubes, depending on the densities desired. Cells were initially frozen at -20° C for 1 hour, then -80° C overnight. The following day, cryogenic vials were transferred to liquid nitrogen vapor phase for future use.

General Guidelines for Culturing Cells in Various-Sized Vessels:

Flask Size	Media Volume	Trypsin Volume	Suspension Volume
35 mm dish	2-3ml	200ul	40,000 cells
60 mm dish	4-5ml	500ul	40,000 cells
100mm dish	10ml	1ml	50-100ul cells
T75 Flask	20ml	3-5ml	100ul cells
T150 Flask	30-45ml	10ml	200-400ul cells
T225 Flask	45ml	10ml	1 ml cells

Transfection of Plasmid DNA into Cultured Cells

DNA and Lipofectamine optimizations were performed before the start of every experiment. The day before transfections were to occur, cells were removed from dishes and counted. Following this, cells were plated at a density of 4×10^4 cells per well (24-well plate) in 0.5 ml of complete growth medium, as it was essential that cells were transfected during the exponential growth phase. The next morning, cells were observed to be 50-80 % confluent before starting procedures. For each well of cells that were transfected, 0.5 µg of DNA was diluted per 100 µl of reduced serum medium without serum. For cell lines more sensitive to transfection reagents, PLUS™ Reagent was added in a 1:1 ratio to DNA, directly to the DNA. This mixture was gently incubated for 10 minutes at room temperature before being added to the medium. For each well of cells, 0.75-1.75 µl of Lipofectamine LTX was diluted into the DNA/medium solution, gently mixed, and incubated for 25 minutes at room temperature, in an effort to allow for the formation of DNA-Lipofectamine complexes. After this, growth medium was

removed from cells, and replaced with 0.5 ml of complete growth medium. Exactly 100 µl of the DNA-Lipofectamine complexes were directly added to each well containing cells, and gently mixed by rocking the plate back and forth. Finally, cells were incubated at 37° C in a CO_2 incubator for 24 hours before being used in other assays for transgene expression.

Scaling Transfections

Occasionally, cultured cells required transfection in various tissue culture formats, and so the amounts of DNA, cells, and transfection reagents were altered relative to the surface area of the culture vessel. The following was used as a general guideline when scaling transfections:

Vessel	Media Volume	Cells/ Well	DNA	Volume Dilution Media	Lipofectamine	PLUS™
96-well	100 µl	8×10^3	100 ng	20 µl	0.15 – 0.35 µl	0.1 µl
48-well	200 µl	2×10^4	200 ng	40 µl	0.3 – 0.7 µl	0.2 µl
24-well	500 µl	4×10^4	500 ng	100 µl	0.75 – 1.75 µl	0.5 µl
12-well	1 ml	8×10^4	1 µg	200 µl	1.5 – 3.5 µl	1 µl
6-well	2 ml	2×10^5	2.5 µg	500 µl	3.75 – 8.75 µl	2.5 µl

Pseudoviral Particle Production

The day before procedure was scheduled to begin, HEK293TN cells were cultured in complete medium, supplemented with 10 % FBS and antibiotics. The following day, when cells reached 70 % confluence, cells were transfected with an HIV-based packaging plasmid and DNA construct as described above. After 48 hours of incubation, viral supernatant was collected under a BL-3 culture hood into a sterile 50 ml conical tube, and centrifuged at 3000 rpm for 15 minutes at room temperature, in order to pellet cell debris. Following centrifugation, viral supernatant was transferred and aliquoted into sterile 1.7 ml microcentrifuge tubes.

HIV-Based Lentiviral Infections

Complete culture medium was aspirated from cells that have reached 70% confluence. A mixture of complete medium with polybrene was prepared at a final concentration of 5 µg/ml. Old culture medium was discarded, and replaced with 10 ml of polybrene/media mixture. Cells were infected by adding a 1:1 medium:pseudoviral stock mixture to the flasks. Cells were then incubated at 37° C supplemented with 5 % CO_2 overnight. The following day, culture medium was removed, and replaced with 1 ml of complete medium.

Immunocytofluorescence

Because cells are cultured in a monolayer, immunocytofluorescence was performed over a 1 day period. Cells were removed from the incubator, and washed three times with 1X PBS. Next, cells were fixed with ice-cold methanol, and incubated at -20° C for 10 minutes. Cells were washed again three times with 1X PBS, and blocked in 3% BSA in PBS for 30 minutes. Following this, cells were incubated in a 3%

BSA/PBS mixture containing primary antibody for 30 minutes, followed by a 0.3% Tri-X wash. Then, fluorescent conjugated secondary antibody in a 3% BSA/PBS mixture was added to cells (1:100), and washed three times with 0.3% Tri-X, in the dark. Finally, cells were mounted on slides with an anti-fade aqueous mounting medium, and allowed to dry in the dark at 4° C.

Receptor Protein Analysis

Preparation of P2 Membranes

Zebra finches were overdosed with Equithesin, and brains were removed and placed into a glass and Teflon grinder containing 25 volumes of ice-cold 0.32 M sucrose in 5 mM Tris, pH = 7.4. After tissue was ground to homogeneity on ice, homogenate was transferred to clean centrifuge tubes, and spun at *1000 X g* at 4° C for 15 minutes. Pellets were discarded, and supernatant was carefully removed to a separate tube. Next, supernatant was centrifuged at *20,000 X g* at 4° C, for 60 minutes. Following this, resulting pellets were snap-frozen overnight at -80° C, thawed on ice, and resuspended in 150 volumes of 50 mM Tris, 10 mM EDTA, pH = 7.4. Membranes were incubated for 2 hours at 4° C, in order to allow endogenous cation chelating and dissociation of ligand from membrane-bound GPCRs. Next, membranes were centrifuged at *20,000 X g* for 60 minutes, re-homogenized, and washed in 150 volumes of 50 mM Tris, 5 mM $MgCl_2$. Protein concentrations were determined by the Bradford method.

APPENDIX F: Permission Letters

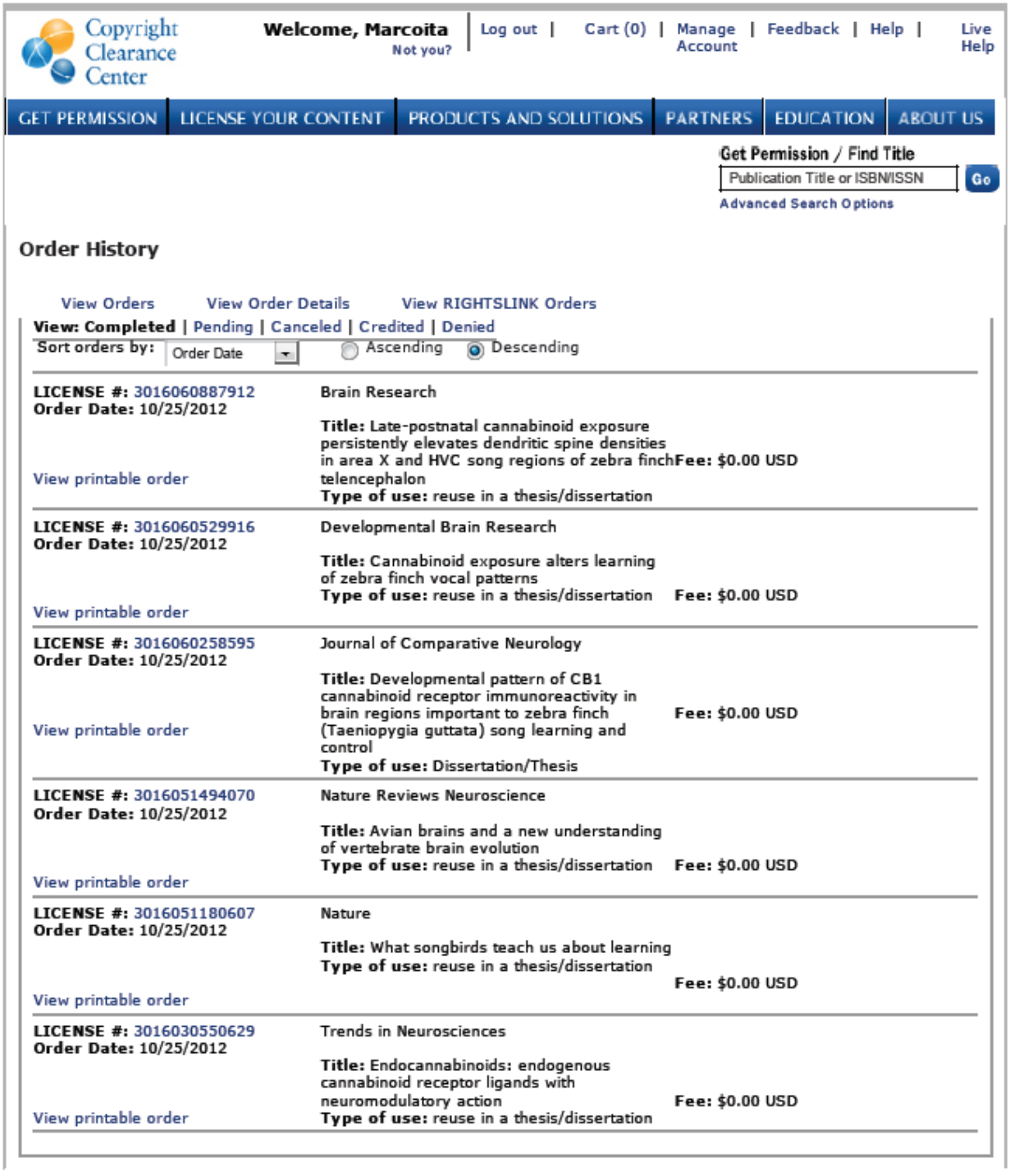

Copyright Clearance Center

Welcome, Marcoita
Not you?

Log out | Cart (0) | Manage Account | Feedback | Help | Live Help

GET PERMISSION | LICENSE YOUR CONTENT | PRODUCTS AND SOLUTIONS | PARTNERS | EDUCATION | ABOUT US

Get Permission / Find Title
Publication Title or ISBN/ISSN Go
Advanced Search Options

Order History

View Orders | View Order Details | View RIGHTSLINK Orders

View: Completed | Pending | Canceled | Credited | Denied

Sort orders by: Order Date | Ascending | Descending

LICENSE #: 3016060887912 **Order Date:** 10/25/2012 View printable order	Brain Research **Title:** Late-postnatal cannabinoid exposure persistently elevates dendritic spine densities in area X and HVC song regions of zebra finch telencephalon **Type of use:** reuse in a thesis/dissertation	**Fee:** $0.00 USD
LICENSE #: 3016060529916 **Order Date:** 10/25/2012 View printable order	Developmental Brain Research **Title:** Cannabinoid exposure alters learning of zebra finch vocal patterns **Type of use:** reuse in a thesis/dissertation	**Fee:** $0.00 USD
LICENSE #: 3016060258595 **Order Date:** 10/25/2012 View printable order	Journal of Comparative Neurology **Title:** Developmental pattern of CB1 cannabinoid receptor immunoreactivity in brain regions important to zebra finch (Taeniopygia guttata) song learning and control **Type of use:** Dissertation/Thesis	**Fee:** $0.00 USD
LICENSE #: 3016051494070 **Order Date:** 10/25/2012 View printable order	Nature Reviews Neuroscience **Title:** Avian brains and a new understanding of vertebrate brain evolution **Type of use:** reuse in a thesis/dissertation	**Fee:** $0.00 USD
LICENSE #: 3016051180607 **Order Date:** 10/25/2012 View printable order	Nature **Title:** What songbirds teach us about learning **Type of use:** reuse in a thesis/dissertation	**Fee:** $0.00 USD
LICENSE #: 3016030550629 **Order Date:** 10/25/2012 View printable order	Trends in Neurosciences **Title:** Endocannabinoids: endogenous cannabinoid receptor ligands with neuromodulatory action **Type of use:** reuse in a thesis/dissertation	**Fee:** $0.00 USD

Get Permission | License Your Content | Products & Solutions | Partners | Education | About CCC
Privacy Policy | Terms & Conditions

PT62T@NIH.gov

Attachments:

drugfactshsyt3.jpg (178 KB)

Sent Items

Thursday, October 11, 2012 11:23 AM

Hello,

My name is Marcoita Gilbert, a graduating Ph.D student from the department of Pharmacology and Toxicology at East Carolina University. I am in the process of writing a general literature review for my dissertation, and came across a very helpful figure depicting nationwide drug trends across age groups.

http://www.drugabuse.gov/publications/drugfacts/nationwide-trends

I would like to ask for permission to use this figure for educational purposes; all material obtain will be properly cited. If you should have additional questions, please do not hesitate to contact me. I look forward to hearing from you soon.

Thank you,

Marcoita

Marcoita T. Gilbert
Doctoral Candidate
Departments of Pharmacology and Toxicology/IDPBS
East Carolina University
6S-36 Brody School of Medicine
Greenville, NC 27834
Gilbertm02@students.ecu.edu
Telephone:252-744-2750

Dear Marcoita Gilbert,

With reference to your kind email asking for permission to use one of the images on CNSforum.com.

Permission is granted to download the image(s) and use them as you wish, including in presentations, articles and publications, provided that the copyright notice on the images is not hidden nor removed.

If used on other websites, the images must also link to this website: www.cnsforum.com

Good luck with your studies!

Kind regards

Gitte Handlos

From: Gilbertm02@students.ecu.edu [mailto:Gilbertm02@students.ecu.edu]

Sent: Thursday, October 11, 2012 6:35 PM

To: cnsforum@cnsforum.com

Subject: Message sent from Contact Us form on CNSforum

A mail has been received from the "Contact Us" form on CNSforum.com

Name: Marcoita Gilbert

Email: Gilbertm02@students.ecu.edu

Subject: Permission to use a figure in dissertation

Message:

Hello,

My name is Marcoita Gilbert, a graduating Ph.D student in the department of Pharmacology at East Carolina University, USA. East Carolina University. I am in the process of writing a general literature review for my dissertation, and came across a very helpful figure depicting the molecular mechanisms of cannabinoid receptor signaling:

http://www.cnsforum.com/imagebank/item/MOA_cannab/default.aspx

I would like to ask for permission to use this figure for educational purposes; all material obtain will be properly cited. If you should have additional questions, please do not hesitate to contact me. I look forward to hearing from you soon.

Thank you,

Marcoita Gilbert

Marcoita T. Gilbert

Doctoral Candidate

Departments of Pharmacology and Toxicology/IDPBS

East Carolina University

6S-36 Brody School of Medicine

Greenville, NC 27834

Gilbertm02@students.ecu.edu

Telephone:252-744-2750

Permissions Europe/NL [Permissions.Dordrecht@springer.com]

Inbox

Wednesday, October 31, 2012 9:56 AM

Dear Sir,

With reference to your request (copy herewith) to reprint material on which Springer Science and Business Media controls the copyright, our permission is granted, free of charge, for the use indicated in your enquiry.

This permission
- allows you non-exclusive reproduction rights throughout the World.
- permission includes use in an electronic form, provided that content
  * is password protected;
  * at intranet;
  * not separately downloadable

- excludes use in any other electronic form. Should you have a specific project in mind, please reapply for permission

- requires a full credit (Springer/Kluwer Academic Publishers book/journal title, volume, year of publication, page, chapter/article title, name(s) of author(s), figure number(s), original copyright notice) to the publication in which the material was originally published, by adding: with kind permission of Springer Science and Business Media.

The material can only be used for the purpose of defending your dissertation, and with a maximum of 100 extra copies in paper.

Permission free of charge on this occasion does not prejudice any rights we might have to charge for reproduction of our copyrighted material in the future.

Kind regards,

Nel van der Werf (Ms)
Rights and Permissions/Springer

Van Godewijckstraat 30 | P.O. Box 17
3300 AA Dordrecht | The Netherlands
tel +31 (0) 78 6576 298
fax +31 (0)78 65 76-377

Nel.vanderwerf @springer.com
www.springer.com

Gilbert, Marcoita Terreen

Actions

To:

permissions.dordrecht@springer.com

Sent Items

Thursday, October 25, 2012 3:40 PM

Hello,

I am writing this email in order to request permission from Springer Publishing group to use a figure of the molecular structure of the Cannabinoid Receptor 1 from a book source.

This figure (Figure 1) was published in a chapter titled "Cannabinoid Receptors and Signal Transduction", by Howlett AC, Shim J-Y. This chapter can be found in the book "Cannabinoids." by V. Di Marzo published in 2004 (ISBN 978-0-306-48228-1) and is a part to the Neuroscience Intellegence Unit series.

This figure will be used in the introduction portion of my dissertation, and will be used for academic purposes only. My dissertation, titled "CHANGES IN ZEBRA FINCH NEURONAL MORPHOLOGY FOLLOWING DEVELOPMENTAL CANNABINOID EXPOSURE" will be available in both print and electronic form via ProQuest, the dissertation distributing company.

If I can provide further information to you, please let me do not hesitate to contact me. I look forward to your reply.

Thanks,

Marcoita T. Gilbert
Doctoral Candidate
Departments of Pharmacology and Toxicology/IDPBS
East Carolina University
6S-36 Brody School of Medicine
Greenville, NC 27834
Gilbertm02@students.ecu.edu
Telephone: 252-744-2750

Celeste Carlton [celeste@landesbioscience.com]

Inbox

Thursday, October 25, 2012 2:24 PM

Dear Marcoita Gilbert:

We grant you our non-exclusive permission to reproduce Figure 1 in your dissertation, provided the following:

1) Since this book is co-published you will also need to obtain permission from Springer (who now owns Kluwer). You may use the following websites:

http://www.springerlink.com/content/
Search for the chapter, then click on "permissions and reprints".

http://www.springer.com/rights?SGWID=0-122-0-0-0

2) Give the following citation in the figure legend:

Reproduced with copyright permission from: Howlett AC, Shim J-Y. Cannabinoid receptors and signal transduction. In: Di Marzo V, ed. Cannabinoids. Austin/New York: Landes Bioscience/Kluwer Academic / Plenum Publishers, 2004:85-98.

Or, if the above citation is given in complete form in a reference list, you may instead include the following citation in the figure legend:

Reproduced from reference XX, with copyright permission from Landes Bioscience and Kluwer Academic / Plenum Publishers.

This permission includes both print and electronic versions.

Sincerely,
Celeste Carlton

Production Manager
Book Department
Landes Bioscience
1806 Rio Grande
Austin, TX 78701
512.637.6050 Phone
512.637.6079 FAX
1.800.736.9948
celeste@landesbioscience.com
http://www.LandesBioscience.com

Gilbert, Marcoita Terreen

Sent Items

Thursday, October 25, 2012 1:42 PM

Hello, I am writing in order to request permission to use a figure in the Landes Bioscience Madame Curie Bioscience Database. The figure will be used in the introduction portion of my dissertation, which will be electronically available. The figure, of the molecular structure of the Cannabinoid Receptor 1, can be found here:
http://www.landesbioscience.com/curie/chapter/1446/

and also here in the NIH pubmed database:
Bookshelf ID: NBK6154, "Cannabinoid Receptors and Signal Transduction", Allyn Howlett (2000)

If I can provide further information to you, please let me do not hesitate to contact me. I look forward to your reply.

Sincerely,

Marcoita T. Gilbert

Doctoral Candidate

Departments of Pharmacology and Toxicology/IDPBS

East Carolina University

6S-36 Brody School of Medicine

Greenville, NC 27834

Gilbertm02@students.ecu.edu

Telephone: 252-744-2750